



Copyright

By

Stephanie Unruh

2016

**Diagenesis and Reservoir Quality of the Oligocene  
Vedder Sandstones, of the Rio Bravo Oil Field,  
Kern County, California**

**By**

**Stephanie Unruh**

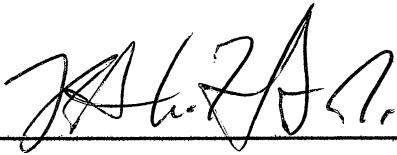
**A Thesis Submitted to the Department of Geological Sciences  
California State University, Bakersfield  
In Partial Fulfillment of the Degree of  
Master of Science**

**Spring 2016**

Diagenesis and Reservoir Quality of the Oligocene Vedder Sandstones, of the Rio  
Bravo Oil Field, Kern County, California

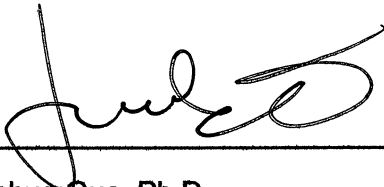
Stephanie Unruh  
Department of Geological Sciences  
California State University, Bakersfield  
9001 Stockdale Hwy, Bakersfield, CA 93311

This thesis has been accepted on behalf of the Department of Geological Sciences by their  
supervisory committee:



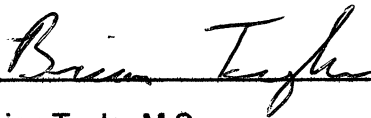
---

Robert Horton, Jr., Ph.D.  
Committee Chair



---

Junhua Guo, Ph.D.



---

Brian Taylor M.S.

## TABLE OF CONTENTS

ABSTRACT.....	i
INTRODUCTION .....	1
GEOLOGIC AND TECTONIC SETTING .....	3
STRUCTURE.....	7
STRATIGRAPHY .....	9
METHODS.....	11
RESULTS .....	13
Detrital Composition.....	13
DETRITAL MINEROLOGY.....	17
Quartz .....	17
Potassium Feldspar .....	17
Plagioclase.....	17
Rock Fragments.....	20
Accessory Minerals .....	20
Fossils.....	20
AUTHIGENIC MATERIAL .....	21
Glauconite.....	21
Phosphate .....	22
Pyrite .....	23
Rutile .....	24
Clays .....	25
Chlorite.....	27
Illite .....	29
Kaolinite .....	30
Dolomite .....	32
Calcite.....	34
Zeolite .....	36
Albite .....	37
Potassium Feldspar .....	39
Quartz .....	40
Pseudomatrix .....	42
Barite.....	43
Anhydrite .....	44
Hydrocarbons.....	45
Compaction and Fractures.....	46

Porosity .....	49
Mass Balance .....	50
DISCUSSION.....	54
SUMMARY .....	69
ACKNOWLEDGMENTS.....	71
REFERENCES .....	72
APPENDIX I – Point Count Data.....	81
APPENDIX II – Contact Index and Tight-Packing Index.....	84
APPENDIX III – Mass Balance Data .....	86
APPENDIX IV – Sandstone Petrography Data.....	88

## TABLE OF FIGURES

Figure 1: General location map showing the study area within the San Joaquin basin. Modified from sjvgeology.org.....	2
Figure 2: General location map showing the geologic and tectonic setting within the San Joaquin basin. Modified from MacPherson (1978). .....	3
Figure 3: General map of the San Joaquin basin showing the locations of the arches and subbasins. Modified from sjvgeology.org.....	4
Figure 4: Contour map on top of Rio Bravo Sandstone with the location of wells Fink-1, Geisinger-2, Kernco 61-34, Mandell-3, Rudnick-1, Ruhl-1, Pacific States, and Weber shown. Modified California Division of Oil and Gas (1941). .....	8
Figure 5: Generalized stratigraphic column of the Rio Bravo oil field. Based on data in Sullivan and Weddle (1960). .....	10
Figure 6: QFRf ternary diagram (Pettijohn et al., 1987) for Vedder Sandstones. ....	14
Figure 7: QFL ternary diagram (Dickinson, 1985) for Vedder Sandstones. The arrow heads represent the present composition, the arrow tails represent compositions reconstructed following Harris (1989). .....	15
Figure 8: Typical texture of the Vedder Sandstones. The sample shows porosity stained blue. Well: Ruhl, depth: 11,437 ft (3,486 m). ....	15
Figure 9: Atypical texture of the Vedder Sandstones with pseudomatrix occluding pore space. Well: Ruhl, depth: 11,574 ft (3,528 m). ....	16
Figure 10: Detrital quartz grains showing evidence of compaction by long ( $C_L$ ) and sutured contact ( $C_S$ ) grains. Point contact ( $C_P$ ) is also present. Well: Fink, depth: 11,387 ft (3,471 m). ...	16
Figure 11: K,Na,Ca ternary diagram of detrital and authigenic feldspars. ....	18
Figure 12: (a-c) Plots of feldspars vs. depth, N = 65. ....	19
Figure 13: Unidentified fossil. Well: Ruhl, depth: 11,574 ft (3,528 m). ....	20
Figure 14: Partially dissolved glauconite (Gl) grain along a partially dissolved plagioclase (Pl) grain contact. Hydrocarbons (Hy) fill fractures in the glauconite (red arrows) grain as well as the intragranular pore in the plagioclase grain. Well: Kernco 61-34, depth 11,410 ft (3,478 m). ....	21
Figure 15: <b>(a)</b> Individual rounded phosphate (P) peloid in carbonate cement. Well: Ruhl 1, Depth: 11,502 ft (3,505 m). <b>(b)</b> SEM-BSE image of phosphate (P) replacing plagioclase (Pl) grain (red arrows). Well: Mandell 3, depth: 11,436 ft (3,486 m). ....	22

Figure 16: **(a)** SEM-BSE image of framboidal pyrite (Py). Well: Kernco 61-34, depth: 11,490 ft (3,502 m) **(b)** SEM-BSE image of pyrite (Py) that formed along biotite cleavage planes. Well: Ruhl 1, depth: 11,437 ft (3,486 m) **(c)** Transmitted light photomicrograph of hydrocarbon (Hy) (yellow arrows) Well: Kernco 61-34, depth: 11,410 ft (3,478 m) **(d)** Reflected light photomicrograph of the same area as figure 16c showing pyrite (Py) (red arrows) that formed within hydrocarbon (Hy) (yellow arrows) in oversized pore. Well: Kernco 61-34, depth: 11,410 ft (3,478 m). .....23

Figure 17: SEM-BSE image of rutile (Ru) (yellow arrows) that formed in a round oversize pore with pyrite (Py) (red arrows). Well: Kernco 61-34, depth: 11,410 ft (3,478 m).....24

Figure 18: Mixture of grains that have been altered to clay and squeezed into surrounding pore spaces. Well: Rudnick 1, depth: 11,400 ft (3,475 m). .....25

Figure 19: Clay coatings (red arrows) surround detrital grains in pokilotopic calcite (C) cement. Well: Pacific States 21, depth 11,543 ft (3,518 m).....26

Figure 20: Remnant clay coating (red arrows) from detrital grain that was dissolved. Well: Ruhl 1, depth: 11,437 ft (3,486 m). .....26

Figure 21: **(a)** Chlorite occurring along fractures within the grain (red arrows). Well: Pacific States 21, depth: 11,549 ft (3,520 m). **(b)** Chlorite occurring as a thin coating on a detrital grain (red arrows). Well: Pacific States 21, depth: 11,549 ft (3,520 m).....27

Figure 22: Biotite grain that is partially altered to chlorite (Cl) with pyrite (Py) crystals. Well: Pacific States 21, depth: 11,549 ft (3,520 m).....28

Figure 23: Chlorite cement (red arrows) filling pores. Well: Mandell 3, depth: 11,436 ft (3,489 m). .....28

Figure 24: Pore-lining illite/smectite or illite/chlorite (red arrows) with relic detrital grains (G<sub>R</sub>). Well: Mandell 3, depth: 11,436 ft (3,486 m).....29

Figure 25: Illite/smectite or illite/chlorite is present between a dissolved feldspar (F<sub>D</sub>) grain. Well: Mandell 3, depth: 11.436 ft (3,486 m).....30

Figure 26: SEM-BSE image of kaolinite showing booklets and associated microporosity (red arrows). Well: Ruhl 1, depth: 11,437 ft (3,486 m). .....31

Figure 27: Kaolinite occluding pore spaces adjacent to partially dissolved grains (red arrows). Well: Pacific States 21, depth: 11,554 ft (3,522 m).....31

Figure 28: SEM-BSE image of zoned dolomite (Do), calcite (C), and zeolite (Z) cemented sandstone. Well: Kernco 61-34, depth: 11,450 ft (3,490 m).....32

Figure 29: Diamond-shaped hollow core from dissolution of dolomite rhomb (D<sub>O</sub>). Well: Ruhl 1, depth: 11,437 ft (3,486 m). .....33

Figure 30: Dolomite (D<sub>o</sub>) that has replaced a plagioclase (P) grain. Chlorite (C) is present as pore-filling cement. Well: Kernco 61-34, depth: 11,450 (3,490 m). .....33

Figure 31: Dolomite (D<sub>o</sub>) between biotite cleavage planes. Well: Ruhl 1, depth: 11,437 ft (3,486 m). .....34

Figure 32: Calcite that partially replaced a plagioclase grain (red arrow) and quartz grain (Q). Hydrocarbon is present within the fractures of the calcite. Geisinger 2, depth: 11,443 ft (3,488). .....35

Figure 33: Through-going fracture filled with poikilotopic calcite (red arrows). Well: Rudnick 1, depth: 11,400 ft (3,475). .....35

Figure 34: SEM-BSE image of poikilotopic zeolite (Z) cement. Plagioclase (Pl) grains exhibit K-feldspar overgrowths (K<sub>o</sub>) (red arrows) surrounded by zeolite cement. Dolomite (Do) rhomb is surrounded by zeolite (Z) cement. Zeolite cement shows partial dissolution (Z<sub>D</sub>). Well: Kernco 61-34, depth: 11,410 ft (3,478 m). .....36

Figure 35: SEM-BSE image of authigenic albitization (Ab) (red arrows), along fractures within a detrital plagioclase (Pl) grain. Well: Weber, depth: 11,445 ft (3,488 m). .....37

Figure 36: **(a)** SEM-BSE image of plagioclase (Pl) grains that are albitized (Ab). **(b)** CL image reveals authigenic albite is non-luminescent **(c)** Composite image of SEM-BSE and CL images reveals authigenic albite is non-luminescent. Well: Mandell 3, depth: 11,436 ft. ....38

Figure 37: SEM-BSE image of albitized (Ab) plagioclase (Pl) exhibiting K-feldspar infilled (K<sub>i</sub>) fractures along with K-feldspar overgrowth (K<sub>o</sub>) in zeolite (Z) cement. K-feldspar overgrowth shows partial dissolution (K<sub>D</sub>). Well: Kernco 61-34, depth: 11,410 ft (3,478 m). .....39

Figure 38: Overgrowth with euhedral termination on detrital quartz grain. The red arrows point to the detrital grain edge. Well: Rudnick 1, depth: 11,413 ft (3,479 m). .....40

Figure 39: **(a)** SEM-BSE image of fractured (Fr) quartz (Q) and quartz overgrowth (Q<sub>o</sub>) on quartz grain. **(b)** CL image reveals quartz overgrowth (Q<sub>o</sub>) on a quartz grain (red arrows) and healed fractures (yellow arrows) are non-luminescent. **(c)** Composite image of SEM-BSE and CL images reveals quartz overgrowth (Q<sub>o</sub>) on a quartz grain (red arrows) and healed fractures (yellow arrows). Well: Mandell 3, depth: 11,436 ft. ....41

Figure 40: Pseudomatrix (red arrows) formed by deformation of labile volcanic fragments. Well: Rudnick 1, depth: 11,413 ft (3,478 m). .....42

Figure 41: SEM-BSE image of barite (Ba) cement present within secondary porosity. Barite (Ba) is also present as either replacing an albitized (Ab) plagioclase grain or as cement filling secondary pore space in plagioclase. Well: Mandell 3, depth: 11,436 ft (3,486 m). .....43

Figure 42: Anhydrite (An) coating on dolomite (D<sub>o</sub>) cement. Well: Ruhl 1, depth: 11,512 ft (3,509 m). .....44

Figure 43: Partially dissolved plagioclase grain showing varying degrees of alteration to clay or sericite with hydrocarbons (Hy) present in secondary pore space. Well: Rudnick 1, depth: 11,413 ft (3,479 m).....	45
Figure 44: <b>(a)</b> Contact index <b>(b)</b> and tight-packing index of the Vedder Sandstones. ....	47
Figure 45: Twin lamellae in plagioclase grain offset along fracture (yellow arrow). Well: Pacific States 21, depth: 11,502 ft (3,505 m). ....	48
Figure 46: Intensely fractured feldspar grains (red arrows). Well: Kernco 61-34, depth: 11,410 ft (3,478 m). ....	48
Figure 47: Plot of total porosity vs. depth (feet) for samples with less than a 15% combination of calcite, dolomite, clay, and ductile grains. ....	49
Figure 48: Plot of total porosity vs. depth (feet) comparing cemented and uncemented sandstone porosity. ....	50
Figure 49: Plot of actual percent kaolinite vs. expected percent kaolinite assuming a microporosity of 0% according to the classification of examined Vedder Sandstones. ....	52
Figure 50: Plot of actual percent kaolinite vs. expected percent kaolinite assuming a microporosity of 0% according to each Rio Bravo well examined. ....	52
Figure 51: Plot of actual percent kaolinite vs. expected percent kaolinite assuming a microporosity of 40% according to the classification of examined Vedder Sandstones. ....	53
Figure 52: Plot of actual percent kaolinite vs. expected percent kaolinite assuming a microporosity of 40% according to each Rio Bravo well examined. ....	53
Figure 53: Paragenetic sequence for the Vedder Sandstones.....	55
Figure 54: Ternary diagram showing Ca-Mg-Fe composition of carbonate cements (electron microprobe analysis). ....	58
Figure 55: Quartz grain showing effects of dissolution along the grain's edge. Well: Fink 1, depth: 11,387 ft (3,471 m). ....	64
Figure 56: Partially dissolved K-feldspar (K) grain. Dissolution occurs parallel to cleavage plains. Well: Pacific States 21, depth: 11,382 ft (3,469 m). ....	64
Figure 57: QKP ternary diagram plotted for the Vedder sandstones following the methodology of Harris (1989). The arrow heads indicate the present composition, the arrow tails show the reconstructed compositions.....	65
Figure 58: Plot of percent dissolved plagioclase volume vs. depth in feet. ....	66

Figure 59: Plot of percent dissolved K-feldspar volume vs. depth in feet.....66

## TABLES

Table 1: Point count data for Well: Fink.....	82
Table 2: Point count data for Well: Geisinger .....	82
Table 3: Point count data for Well: Kernco .....	82
Table 4: Point count data for Well: Mandell .....	82
Table 5: Point count data for Well: Pacific States .....	83
Table 6: Point count data for Well: Rudnick.....	83
Table 7: Point count data for Well: Ruhl .....	83
Table 8: Point count data for Well: Weber .....	83
Table 9: Contact index and tight-packing index of the Vedder sandstones.....	85
Table 10: Mass balance data of the Vedder Sandstones .....	87

## **ABSTRACT**

The Rio Bravo oil field is located about fifteen miles northwest of Bakersfield, California. The zone of importance is the Vedder Sandstone, which is about 1,250 ft (380 m) in thickness. The thin (<100 ft, 30 m) Miocene Rio Bravo sandstone, which unconformably overlies the Vedder Sandstone, is included in the main Vedder reservoir. Burial depths range from approximately 10,750 ft (3,277 m) to 12,450 ft (3795 m), with reservoir temperature at 248°F (120°C). These sandstones are presumed to be at or very near their deepest burial depths based upon temperature and burial comparisons of similar oil fields located on the east side of the San Joaquin basin. The mineralogy and lithology of Oligocene sandstones of the Rio Bravo oil field were examined using a petrographic microscope and a scanning electron microscope equipped with an energy dispersive x-ray spectrometer (SEM-EDS) and a cathode luminescence imaging system (SEM-CL).

The Vedder Sandstones are medium-to fine-grain, subangular to subround, very poorly to well-sorted arkosic to lithic arenites deposited as shallow marine sandstones. Accessory minerals of the Vedder Formation include biotite, muscovite, zircon, hornblende, rutile, garnet, epidote, and magnetite/titanomagnetite. The diagenetic features affecting reservoir quality of the Vedder Sandstones include compaction, cementation, deformation, dissolution, recrystallization, and replacement of minerals.

Porosity within the Vedder Sandstones is controlled mainly by compaction and dissolution of framework-grains. Compaction decreased porosity through ductile deformation of shale clasts, micas, and volcanics, which commonly were squeezed into adjacent pores to form pseudomatrix. Rotation and slippage of grains and fracturing of brittle grains were also widespread. Dissolution of framework-grains and carbonate cements created oversized and elongate pores and altered quartz:feldspar:rock fragments, and quartz:feldspar:lithics ratios.

Albitization occurred extensively along fractures in plagioclase and potassium feldspar grains. Precipitation of potassium feldspars occurred as overgrowths on and in fractures within detrital feldspar grains. Plagioclase shows varying degrees of alteration to clay or sericite. Biotite has been altered to chlorite and pyrite. Cements include: clays (kaolinite, chlorite, and mixed-layer illite/smectite or illite/chlorite), and carbonates. Kaolinite occurs as pore-filling cement, commonly associated with feldspar dissolution. Carbonates include calcite and dolomite. Calcite cement occurs within some through going fractures. Both late-stage calcite and dolomite have partially to completely replaced framework-grains.

Textural relationships of the Vedder Sandstones diagenetic minerals delineate the following paragenetic sequence: (1) glauconite; (2) phosphate; (3) burial and alteration of detrital biotite, feldspars, and volcanics; (4) early pyrite cement; (5) biotite altering to chlorite; (6) early grain dissolution; (7) precipitation of rutile; (8) early pore-lining clays coatings; (9) early dolomite cement; (10) anhydrite cement; (11) early calcite cement; (12) compaction; (13) fracturing; (14) grain/cement dissolution; (15) albitization; (16) late pore-lining and pore-filling clays; (17) potassium feldspar overgrowths; (18) quartz overgrowths; (19) zeolite cement; (20) precipitation of barite; (21) hydrocarbon migration; (19) late pyrite cement.

## INTRODUCTION

The ability to accurately predict reservoir quality in sandstones (as controlled by porosity and permeability) is one of the most important responsibilities facing a petroleum geologist during hydrocarbon exploration and production. Often, reservoir quality is largely controlled by diagenesis—the chemical, physical, and biological processes that occur subsequent to deposition (Ali, 1981; Pettijohn et al., 1987; Boggs, 1992). Diagenetic processes include compaction, cementation, deformation, dissolution, recrystallization, and replacement of minerals (Hayes, 1979). These processes can significantly alter the reservoir quality by reducing porosity through compaction and cementation or enhancing porosity through dissolution. Understanding the diagenetic history of a reservoir is important because it can reduce the risks when searching for new hydrocarbons and it can also facilitate in the success of enhanced-recovery methods (Ali, 1981; Taylor, 2007).

The Rio Bravo oil field, located about fifteen miles northwest of the city of Bakersfield, California and three miles south of the town of Shafter (Figure 1), has been producing hydrocarbons since their discovery in 1937. Production comes mainly from the Oligocene Vedder Sandstones. Burial depths of the Vedder Sandstones range from approximately 10,750 ft (3,276 m) to 12,450 ft (3,794 m).

The Vedder Sandstones of the Rio Bravo oil field have been identified for potential carbon capture and sequestration (CCS) (Gillespie, 2011). Before CCS can occur the mineralogy and reservoir properties must be evaluated. To date there have been no detailed studies published about the mineralogy, lithology or porosity/permeability of the Vedder Sandstones at the Rio Bravo oil field. This research sets out to determine the mineralogy and lithology of Oligocene Vedder Sandstones of the Rio Bravo oil field, and to interpret the diagenetic processes that have affected reservoir quality by altering porosity and permeability (Pettijohn et al., 1987; Boggs, 1992; Horton et al., 2009). Such information will be crucial in

evaluating enhanced-recovery methods for continuing future oil production. It will also be essential for determining the feasibility for subsurface CO<sub>2</sub> sequestration in these strata (Gillespie, 2011).

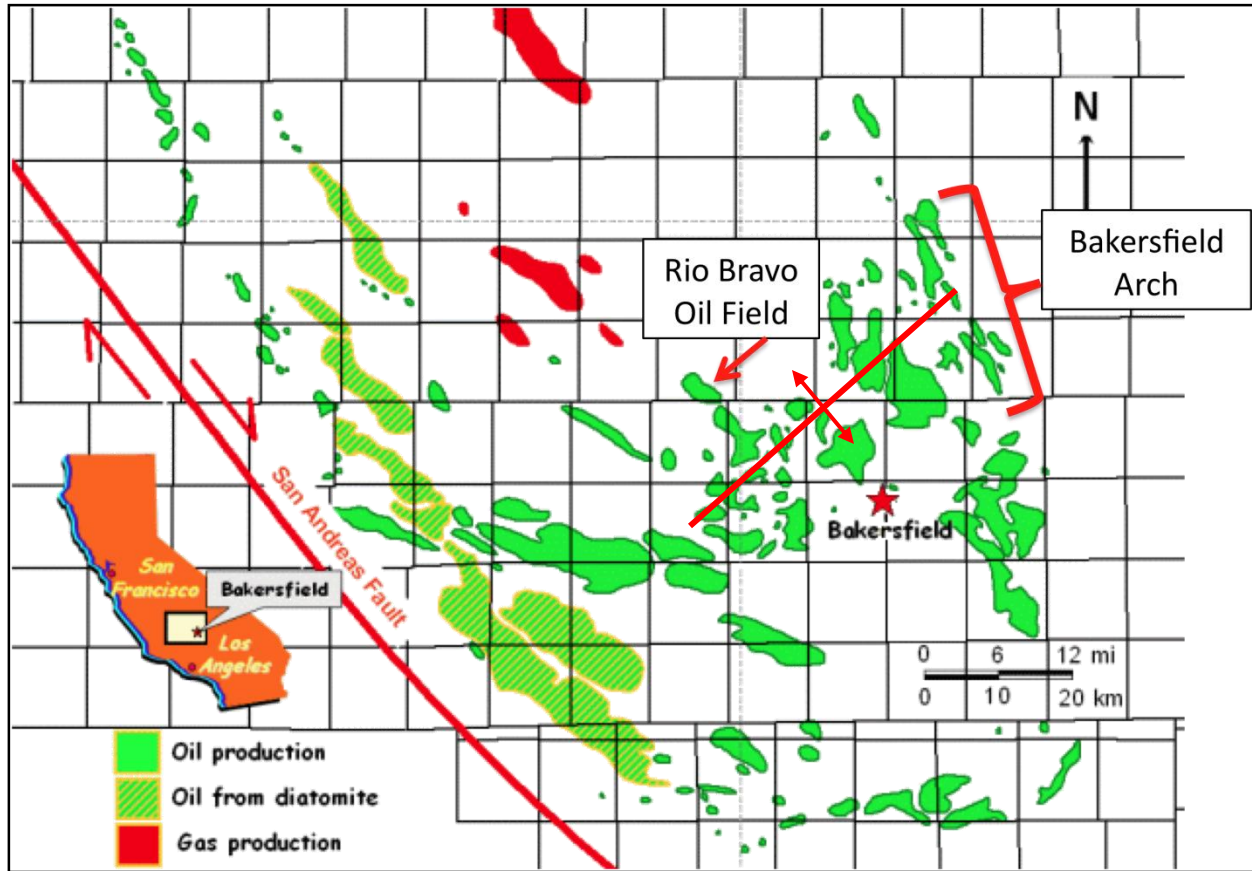


Figure 1: General location map showing the study area within the San Joaquin basin. Modified from [sjgeology.org](http://sjgeology.org).

## GEOLOGIC AND TECTONIC SETTING

The San Joaquin basin is an asymmetric, sediment-filled (upper Mesozoic and Cenozoic sediments) forearc basin in the central portion of California (Bartow, 1991; Moxon, 1988). The basin is bound by the California Coast Ranges (Diablo and Tumbler Ranges) to the west, the Sierra Nevada plutonic complex to the east, and the Transverse Ranges (San Emigdio-Tehachapi Ranges) to the south (Figure 2) (Fischer & Surdam, 1988). The Stockton arch to the north separates the San Joaquin basin from the Sacramento basin. The Bakersfield arch (Figures 1, 3), a NE-SW trending anticline, divides the basin into two sub-basins: the Tejon sub-basin (Figure 3) to the south, and the Buttonwillow sub-basin (Figure 3) to the north (Fischer & Surdam, 1988).

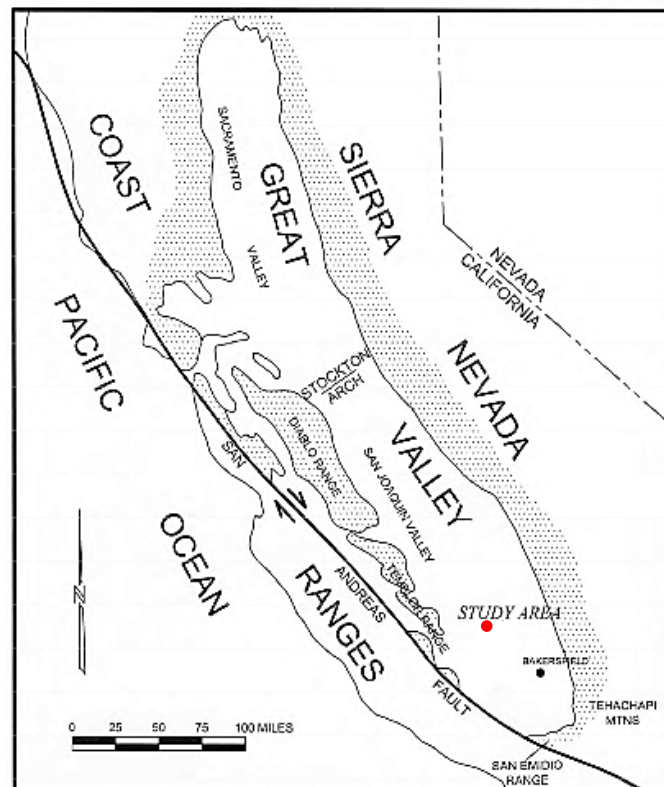


Figure 2: General location map showing the geologic and tectonic setting within the San Joaquin basin. Modified from MacPherson (1978).

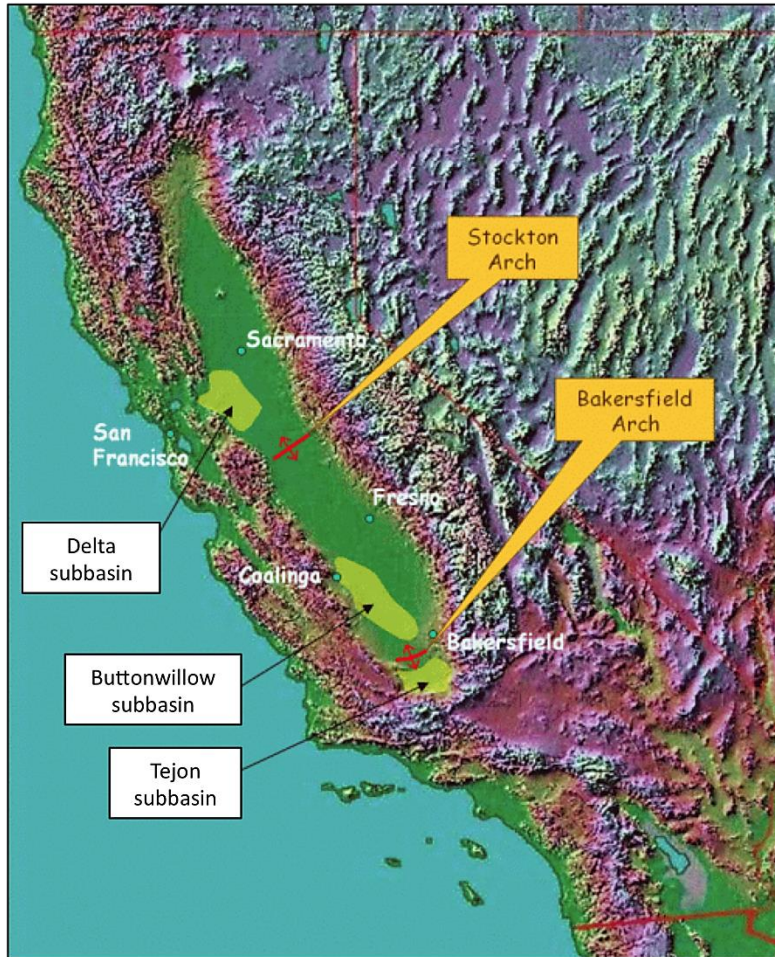


Figure 3: General map of the San Joaquin basin showing the locations of the arches and subbasins. Modified from sjvgeology.org.

The San Joaquin basin is characterized by a complex history of sedimentation and tectonics (Fischer & Surdam, 1988). During Late Jurassic and Cretaceous time, the San Joaquin basin formed the southern part of an extensive forearc basin (Bartow, 1991; Graham, 1987). During the Cretaceous the Sierra Nevada arc developed as the Pacific plate subducted beneath the North American plate (Fischer & Surdam, 1988; Reid, 1988). The San Joaquin basin continued to evolve during the Tertiary as the East Pacific Rise collided with the subduction zone along the western margin of the North American plate (Atwater & Molnar, 1973). This consequently created right-lateral strike-slip movement along a fault system termed

the “proto-San Andreas fault” (Nilsen and Clarke, 1975; Bent, 1988). These events transformed the western margin of the San Joaquin basin from convergent-margin tectonics to wrench-style transform-margin tectonics (Bent, 1988). The changing stress regimes and resulting tectonic changes along the western margin of the basin are reflected in fold and thrust faults, which parallel the San Andreas Fault (Figure 2) (Bartow, 1991; Fischer & Surdam, 1988; Harding, 1976; Simonson, 1955; Wilcox et. al 1973). Most of the east-central San Joaquin basin lacks significant structural features other than normal faults concentrated in the area of the Bakersfield arch (Bartow, 1991).

Tertiary sedimentary sequences consist of deep-marine, shallow-marine, and continental deposits which thicken from east to west across the basin (Fischer & Surdam, 1988). The Vedder Sandstones are shallow marine and were deposited on a marine shelf during the Oligocene (Olson, 1988). The Vedder Sandstones contain several thin shale beds between the major sand bodies, and also contain a “grit” zone occurring around 11,315 ft (3,449 m) to 11,325 ft (3,452 m); this consists of a conglomerate of black pebbles with matrix of poorly-sorted and well-cemented sand (Kasline, 1941; Olson, 1988). The “grit” zone may represent small transgressive lags, followed by muddy silty embayment or lagoonal deposits, and capped by shallow-marine sands (Olson, 1988). Evidence from outcrops of the Vedder Sandstones provides support of a depositional environment ranging from inner shelf to the foreshore area (Olson, 1988).

Most known oil accumulations within the Vedder Sandstones are believed to have been sourced from shale of the Kreyenhagen Formation (Isaacson & Blueford, 1984; Lillis & Magoon, 2007), one of the major sources of oil and gas in the San Joaquin Valley. The Kreyenhagen Formation is a thermally mature, transgressive-unit in the Buttonwillow depocenter that covered most of the San Joaquin basin in the Late Eocene (Bartow, 1991; Gautier & Scheirer, 2007a; Gautier & Scheirer, 2007b; Isaacson and Blueford, 1984). The Kreyenhagen Formation is thickest on the west side of the San Joaquin basin and thins to the east (Isaacson & Blueford,

1984). The Eocene Tumey Formation may have also produced and expelled oil in the Vedder Sands (Gautier & Scheirer, 2007a; Gautier & Scheirer, 2007b; Reid, 1988). Both formations are composed of mostly deep-marine shale, with minor siltstone and sandstone interbeds (Isaacson & Blueford, 1984; Reid 1988).

## STRUCTURE

The Rio Bravo-Vedder pool at the Rio Bravo oil field consists of an elongated asymmetrical dome trending generally northwest-southeast. It is located on the north flank, just off the crest, of the Bakersfield arch (Figure 1, 3) (Hiatt & Gallagher, 1975; Sullivan & Weddle, 1960). This anticlinal fold extends a distance of 20 miles (32 km), from the Greeley to Wasco oil field. Dips along the southwestern and southern flanks are slight ranging from four to eight degrees, while the northeastern and northern flanks are much steeper at twelve to fifteen degrees. Oil accumulation in the Vedder Sandstones is controlled by structural traps, with stratigraphic traps playing a very minor role (Richardson, 1966). The Rio Bravo oil field also includes several faults (Figure 4). The most important fault runs along the eastern edge of the field and through the center of Section 35. This fault is a continuation of the Greeley fault (south of the Rio Bravo field), which forms the updip closure in the Greeley oil field, and determines the southeastern limits of production for the Rio Bravo oil field. This fault has a vertical displacement of about 250 ft (76 m) (Sullivan & Weddle, 1960). A northern normal fault, downthrown to the east, with vertical displacements from 0 in the south to over 225 ft (69 m) in the north, passes through the northern end of the dome along the eastern border of Section 28. North-west of the former, a third fault trends almost due north-south with vertical displacement ranging from 0 in the south to 140 ft (43 m) in the north. A fourth parallel fault is downthrown to the east and displaces the Rio Bravo Sandstones by approximately 20 ft (6 m). The minor faults are documented as not affecting production, which leads to the hypothesis that the faults formed after the oil was in place (Sullivan & Weddle, 1960).

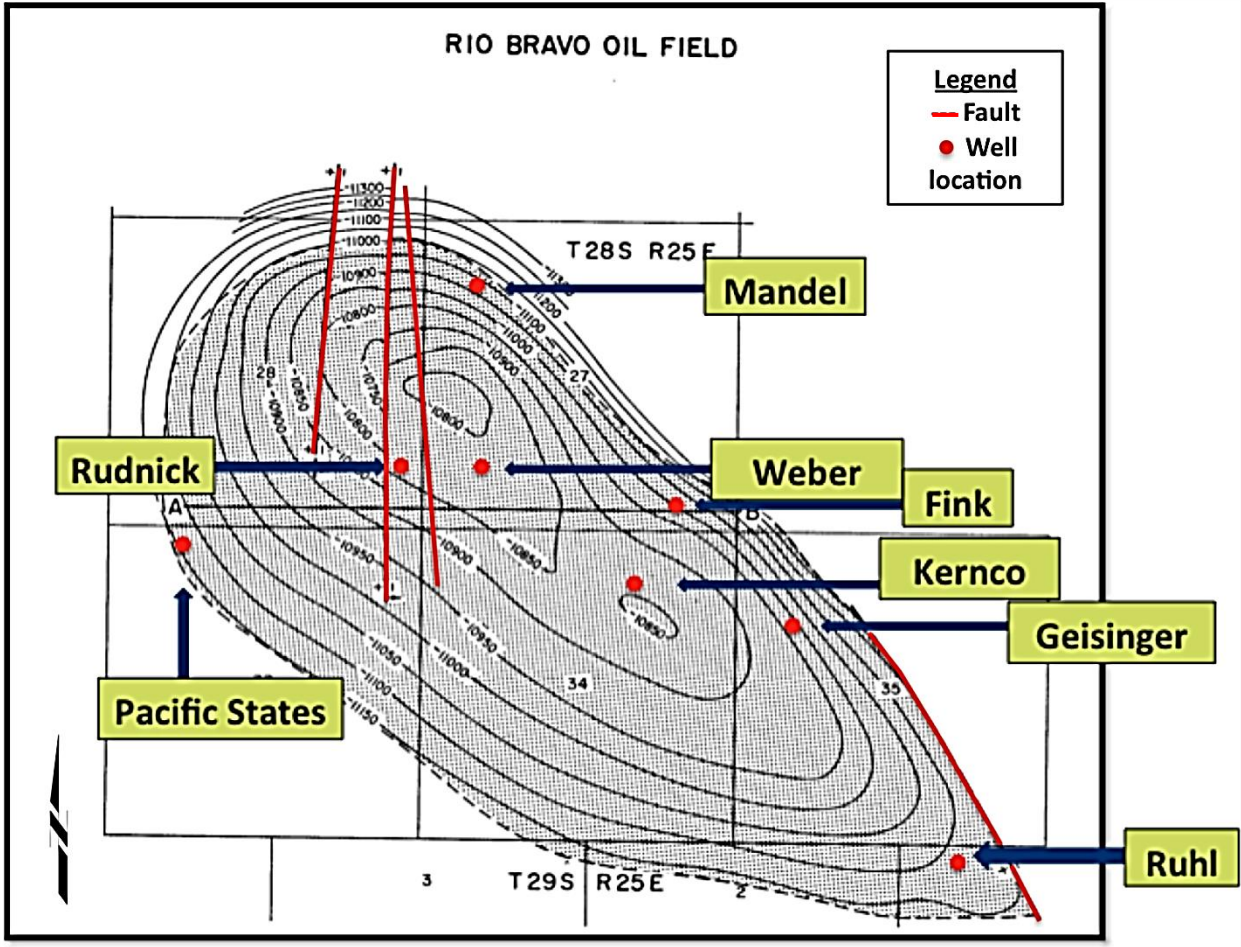


Figure 4: Contour map on top of Rio Bravo Sandstone with the location of wells Fink-1, Geisinger-2, Kernco 61-34, Mandell-3, Rudnick-1, Ruhl-1, Pacific States, and Weber shown. Modified California Division of Oil and Gas (1941).

## **STRATIGRAPHY**

The Vedder Sandstones are widespread in the southeastern San Joaquin basin and range up to 1,246 ft (380 m) in thickness. The Vedder Sandstones crop out as a narrow sand lense ranging up to approximately 260 ft (79 m) thick north of Poso Creek where they are composed of light gray, well-sorted fine- to medium-grain sandstone and dark brown shales (Bartow & McDougall, 1984). In general, the Vedder Sandstones increase in thickness from the outcrop belt on the east toward the west as they dip into the San Joaquin basin (Olson, 1988). In the subsurface the marine Vedder Sandstones disconformably overlie and interfinger with the non-marine sandstones of the Walker Formation, which most likely resulted from eustatic oscillation (Olson, 1988). Included within the upper portion of the Vedder Sandstones are three important oil producing zones: Main Vedder, Osborn, and Helbling. The marine Rio Bravo Sandstone unconformably overlies the three upper Vedder Sandstones and is bound above by deep-marine shales of the Freeman-Jewett Formation (Figure 5) (Sullivan & Weddle, 1960).

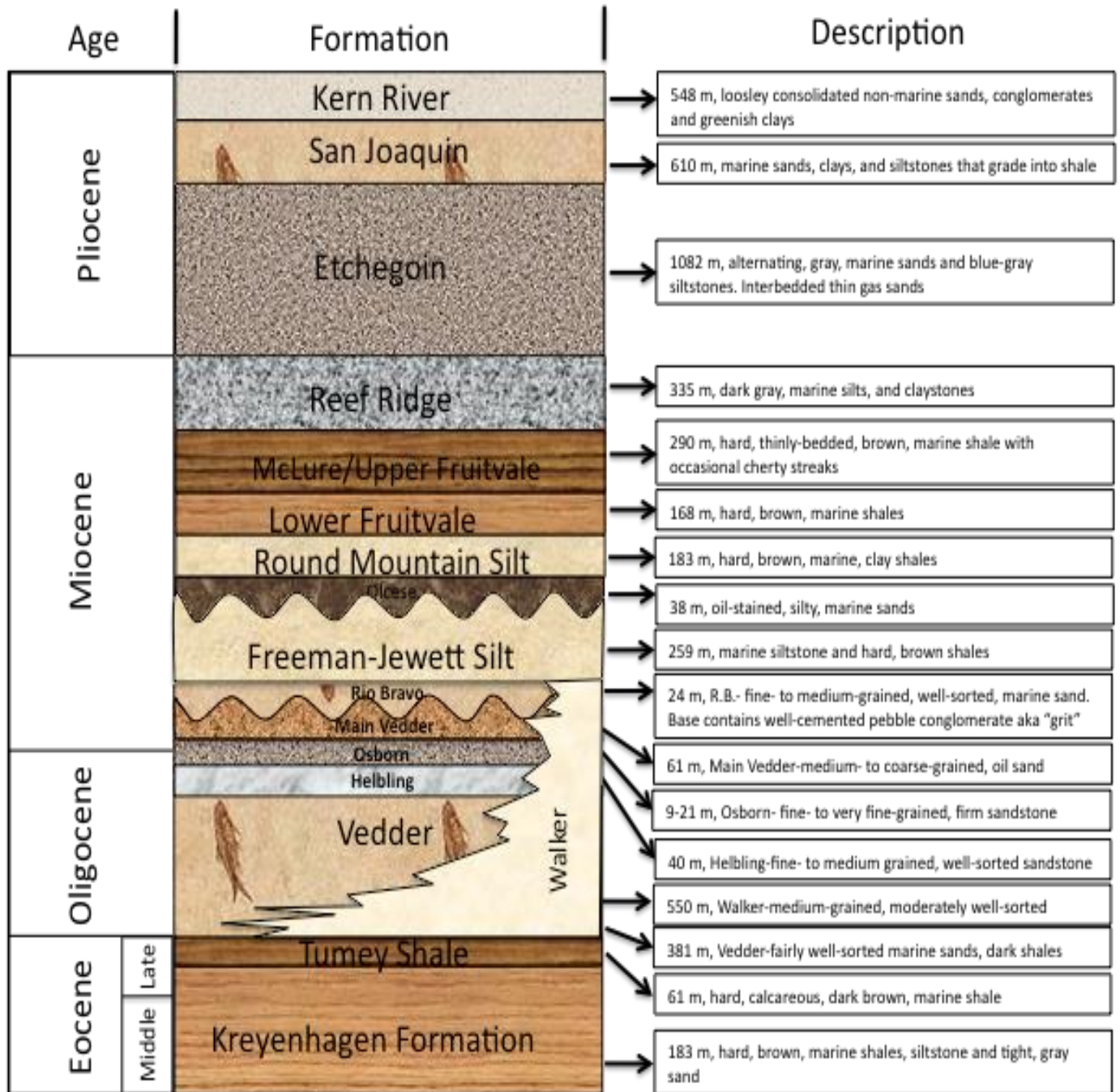


Figure 5: Generalized stratigraphic column of the Rio Bravo oil field. Based on data in Sullivan and Weddle (1960).

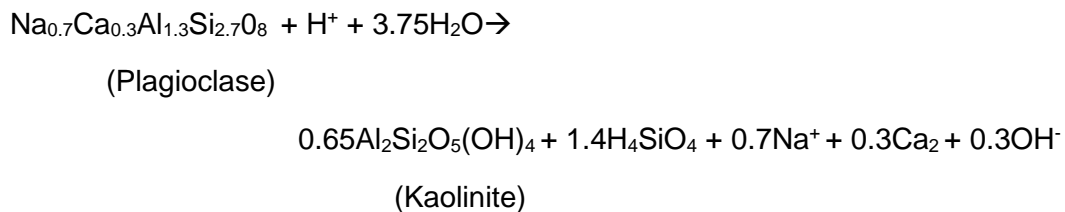
## METHODS

Research was conducted using samples of the Vedder Sandstones from eight Rio Bravo oil field wells: Fink-1, Geisinger-2, Kernco 61-34, Mandell-3, Rudnick-1, Ruhl-1, Pacific States, Weber (Figure 4). These samples were obtained from the California Well Sample Repository. Samples were taken from depths between 11,380 (3,469 m) to 11,580 ft (3,530 m). Sixty-five (65) thin sections were point-counted (300 points per thin section) using a petrographic microscope. All thin sections were impregnated with a blue epoxy in order to show porosity. Some of the thin sections were stained yellow for potassium. For each thin section the mineralogy, grain size, roundness, and sorting were recorded. Diagenetic features such as cementation, alteration, dissolution, and compaction were also recorded. The methodologies of Schmidt and McDonald (1979) and Shanmugam (1985) were used to distinguish secondary porosity from primary porosity. The petrographic criteria used for recognition of secondary sandstone porosity included: (1) partial dissolution; (2) molds; (3) inhomogeneity of packing and floating grains; (4) oversized pores; (5) elongate pores; (6) corroded grains; (7) honeycombed grains; and (8) fractured grains. Selected thin sections were analyzed using a Hitachi S-3400 scanning electron microscope (SEM) equipped with a back-scattered electron (BSE) imaging and Gatan cathode luminescence (CL) systems, as well as an Oxford INCA energy-dispersive x-ray spectrometer (EDS). The SEM-EDS analytical system supplied the chemical components of the minerals while the SEM-BSE and SEM-CL systems supplied the textural relationships between the cements, detrital grains, and fractures. Each chemical analysis was normally acquired using the SEM in single spot mode with an electron-interaction area of approximately 10 $\mu$ m in diameter.

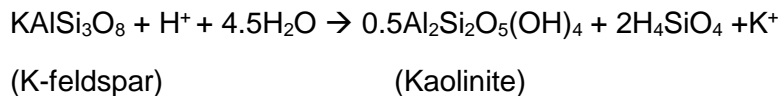
Quantitative analysis of compaction of the Vedder Sandstones were documented using the contact index (CI) and tight-packing index (TPI) following the methodologies of Wilson and McBride (1998). Sandstone data gathered from petrographic analysis were plotted on three

ternary diagrams following schemes of Dickinson (1970), Dott (1964) as modified by Pettijohn et al. (1987), and Harris (1989).

Mass transfer of aluminum was calculated from point-counted volumes of leached feldspars and authigenic kaolinite. Hayes and Boles (1992) initial average composition of  $\text{Na}_{0.7}\text{Ca}_{0.3}\text{Al}_{1.3}\text{Si}_{2.7}\text{O}_8$  ( $\text{An}_{30}$ ) for plagioclase from the Sierra Nevada was assumed. Assuming all  $\text{Al}^{3+}$  liberated during feldspar dissolution and precipitated as kaolinite, for each mole of  $\text{An}_{30}$  plagioclase dissolved, 0.65 mole of kaolinite could have precipitated:



For each mole of K-feldspar dissolved, 0.5 mole of kaolinite could have precipitated:



Clays other than kaolinite as well as zeolites in the Vedder Sandstones represent potential aluminum sinks, however, they are volumetrically minor and have minimal impact on the aluminum mass balance (Hayes and Boles, 1992). A potential source of error when calculating mass-balance is secondary porosity for which the dissolved mineral could not be identified. Therefore, the mass-balance calculations of the Vedder Sandstones are conservative.

## RESULTS

### Detrital Composition

The Vedder Sandstones at the Rio Bravo oil field are arkosic to lithic arenites (Figure 6) and plot mostly in the basement uplift and dissected arc region of the QFL diagram (Figure 7). Samples that contained significant amounts of pseudomatrix were further classified as arkosic wackes (Pettijohn et al., 1987). The sandstones are composed of quartz, K-feldspar (orthoclase, microcline, perthite), plagioclase, and rock fragments. The mean value for the Vedder Sandstones is  $Q_{44}F_{41}Rf_{15}$ .

Framework-grain size of the Vedder Sandstones ranges from fine to medium sand (Figures 8, 9), with wacke grain size typically smaller (Figure 9). The Vedder Sandstones are generally moderately to well sorted with framework grains that vary from angular to subround. Some of the samples are tightly packed as indicated by long (Figure 10), concavo-convex, and sutured grain contacts (Figure 10), as well as brittle-grain fracturing. Ductile minerals such as biotite and volcanic rock fragments are commonly deformed and squeezed into surrounding pore spaces due to compaction.

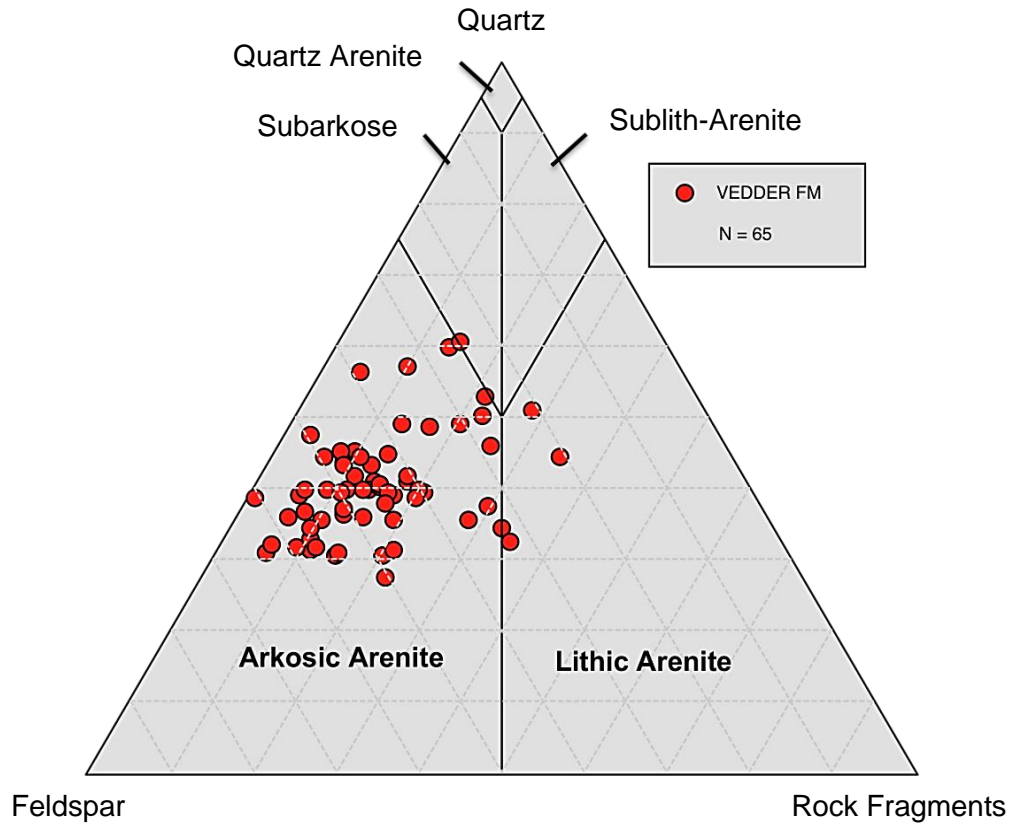


Figure 6: QFRf ternary diagram (Pettijohn et al., 1987) for Vedder Sandstones.

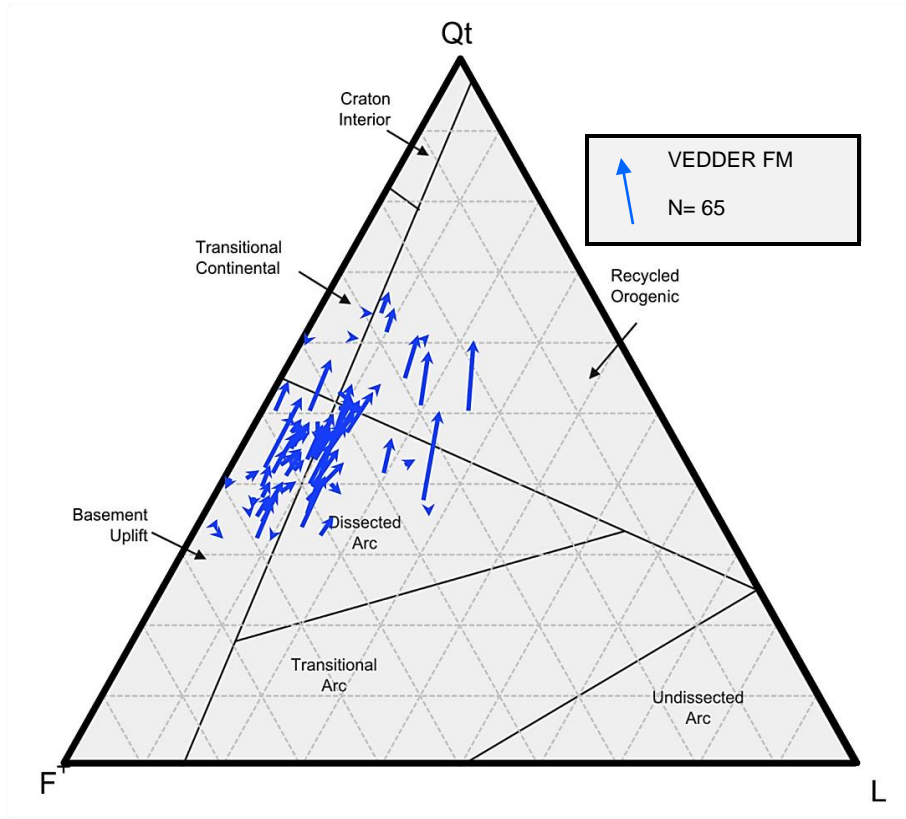


Figure 7: QFL ternary diagram (Dickinson, 1985) for Vedder Sandstones. The arrow heads represent the present composition, the arrow tails represent compositions reconstructed following Harris (1989).

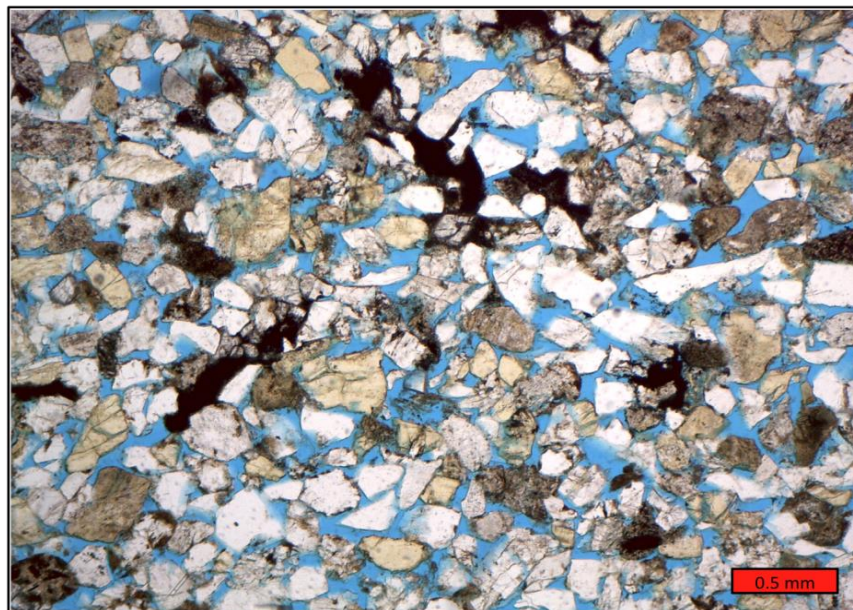


Figure 8: Typical texture of the Vedder Sandstones. The sample shows porosity stained blue. Well: Ruhl, depth: 11,437 ft (3,486 m).



Figure 9: Atypical texture of the Veddler Sandstones with pseudomatrix occluding pore space. Well: Ruhl, depth: 11,574 ft (3,528 m).

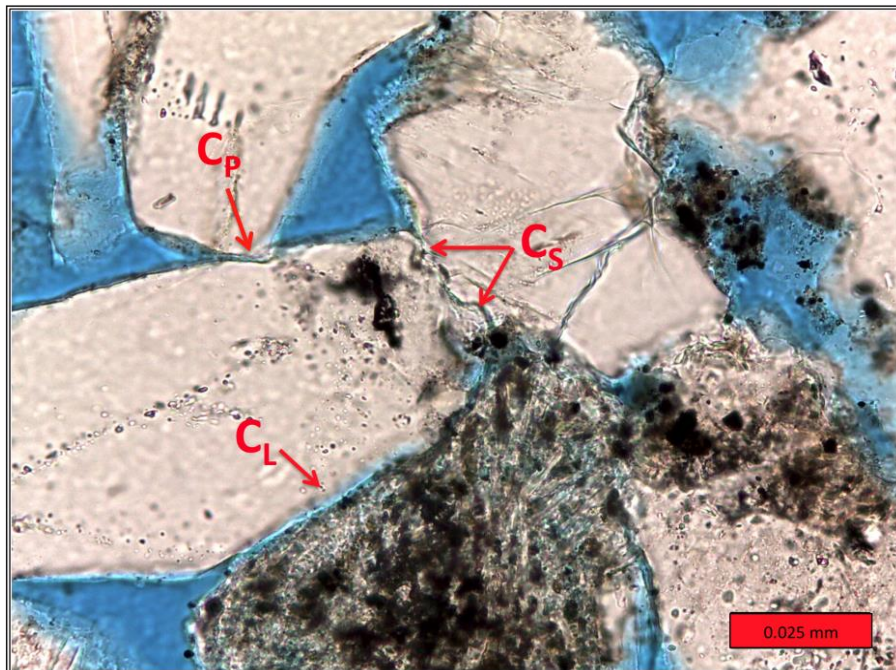


Figure 10: Detrital quartz grains showing evidence of compaction by long (C<sub>L</sub>) and sutured contact (C<sub>S</sub>) grains. Point contact (C<sub>P</sub>) is also present. Well: Fink, depth: 11,387 ft (3,471 m).

## **DETRITAL MINEROLOGY**

### **Quartz**

Quartz is generally monocrystalline and is the most common type of detrital grain in the Vedder Sandstones. Quartz grains range anywhere from 12 to 43% of the rock volume, averaging 23%. Detrital quartz luminesces blue. Other characteristics quartz grains exhibit within the Vedder Sandstones are undulose extinction patterns, cloudy appearances, fracturing, grain-edge dissolution, pressure-induced dissolution, and some vacuoles; however, most quartz grains are free of inclusions.

### **Potassium Feldspar**

Detrital potassium feldspars range from 2 to 16% of the total rock volume and luminesce pink and blue under SEM-CL analysis. Most potassium feldspar grains consist of orthoclase, however, small amounts of perthite and microcline are present in most samples. SEM-EDS analyses indicates potassium feldspar compositions in the Vedder Sandstones range from Or<sub>83</sub> to Or<sub>98</sub> (Figure 11). Some grains contain small amounts of barium. Figure 12a shows that total feldspars decrease with depth. Figure 12b is a plot of potassium feldspar vs. depth suggesting a slight decrease in potassium feldspar with increasing depth.

### **Plagioclase**

Detrital plagioclase feldspars range from 5 to 26% of the total rock volume and luminesce pink under SEM-CL analysis. Plagioclase grains were affected by fracturing, alteration, replacement by calcite, and abritization. SEM-EDS analyses indicates detrital plagioclase ranges from An<sub>53</sub> to An<sub>5</sub> (Figure 11). Figure 12c is a plot of plagioclase feldspar vs. depth indicating a general decrease in plagioclase grains with increasing depth. Plagioclase decreases at a higher rate compared to potassium feldspars (Figure 12a-c).

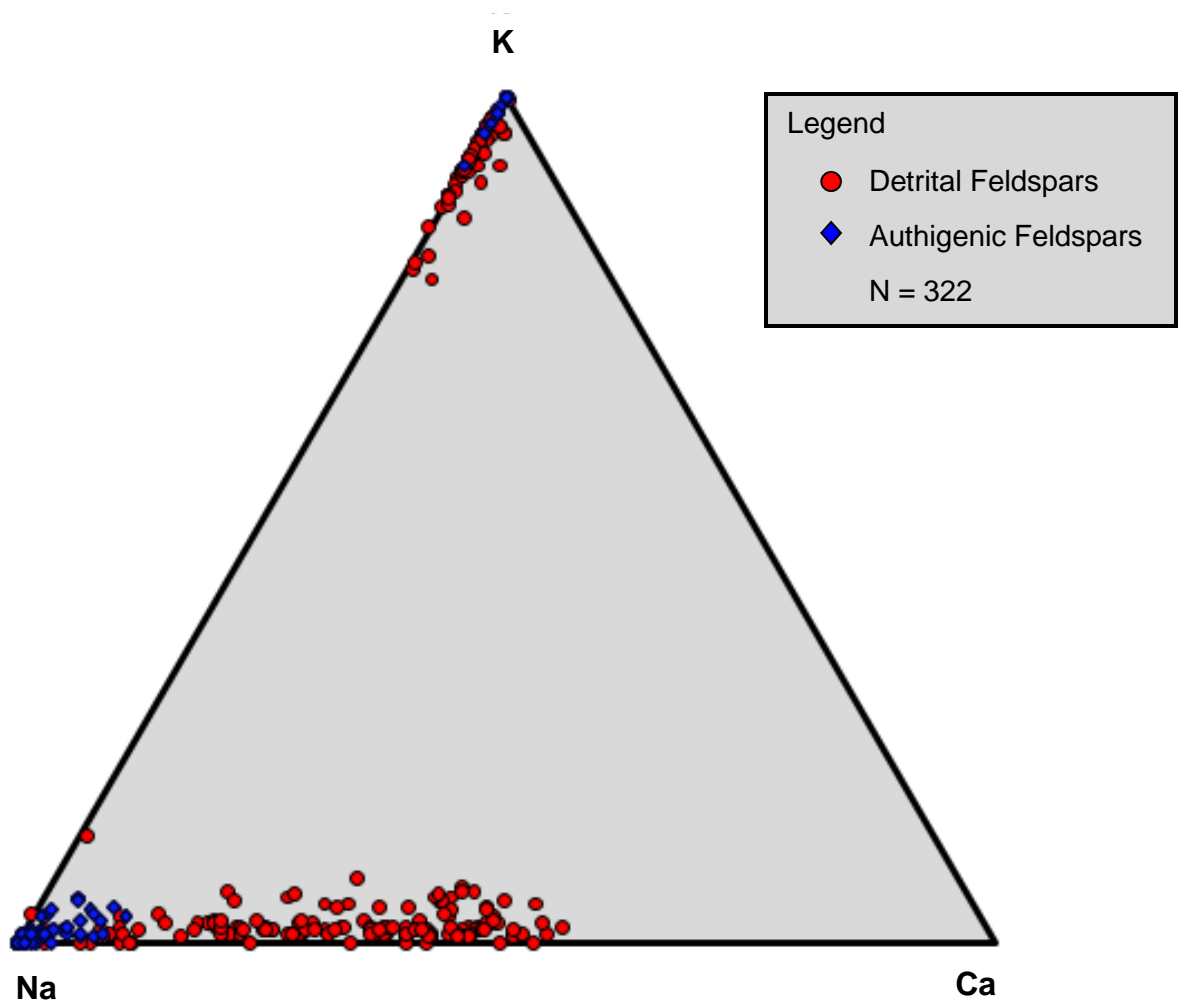


Figure 11: K,Na,Ca ternary diagram of detrital and authigenic feldspars.

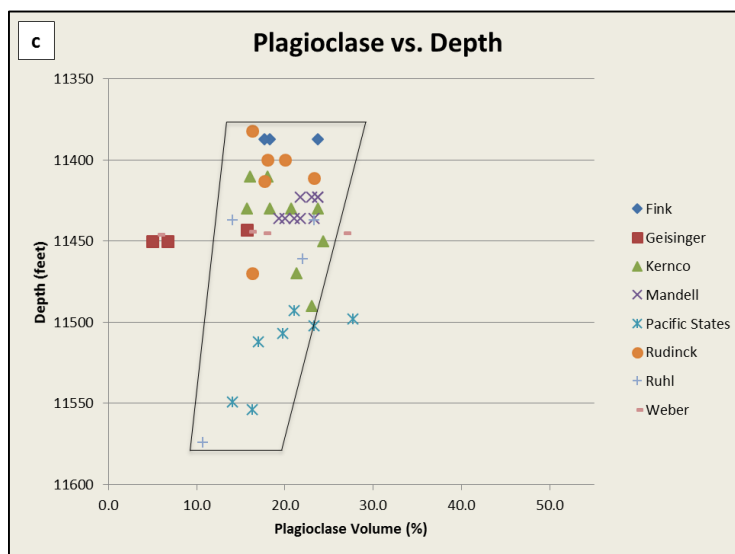
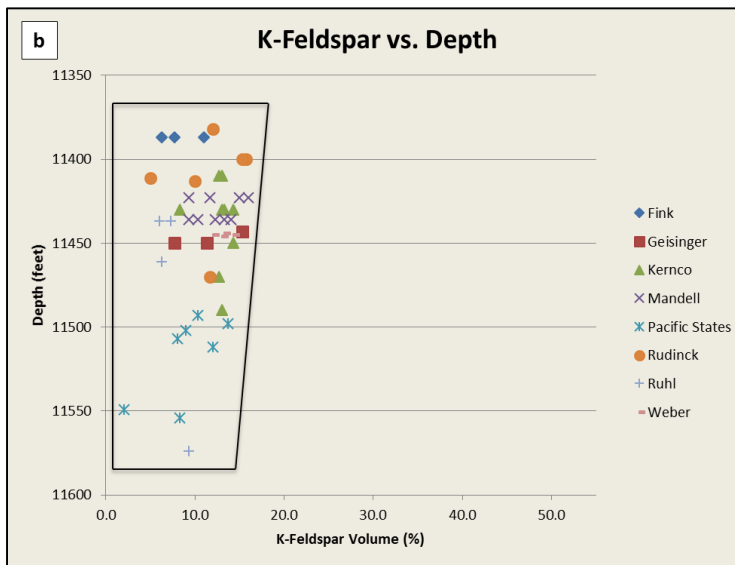
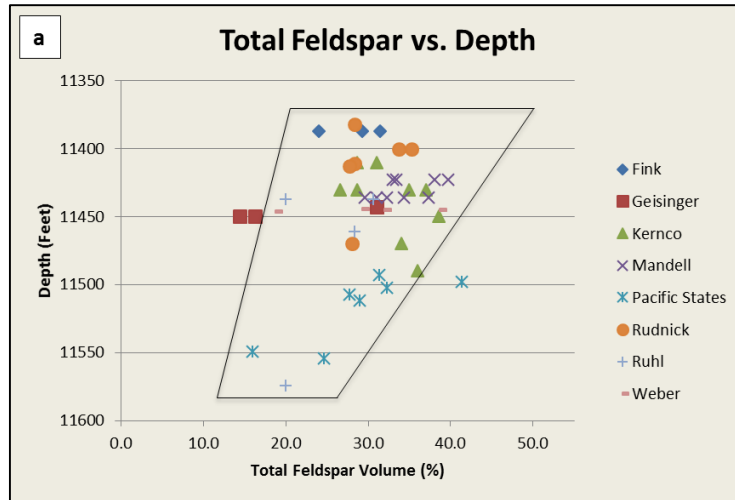


Figure 12: (a-c) Plots of felspars vs. depth, N = 65.

## **Rock Fragments**

Rock fragments range from 2 to 20% of the rock volume in the Vedder sandstones and are generally volcanic in origin with minor amounts of sedimentary (shale clasts, chert, siltstone), metamorphic (quartzite, schist), and igneous (microphanaritic) rock fragments. Many of the volcanic grains have undergone alteration and deformation to form pseudomatrix and clays.

## **Accessory Minerals**

Accessory minerals range from traces to 17% of the rock volume. Biotite is the most common accessory mineral and is present in almost all of the samples. Other detrital minerals include muscovite, zircon, hornblende, rutile, garnet, epidote, and magnetite/titanomagnetite.

## **Fossils**

Fossils are present in some samples (Figure 13), however, no attempt was made to identify them.

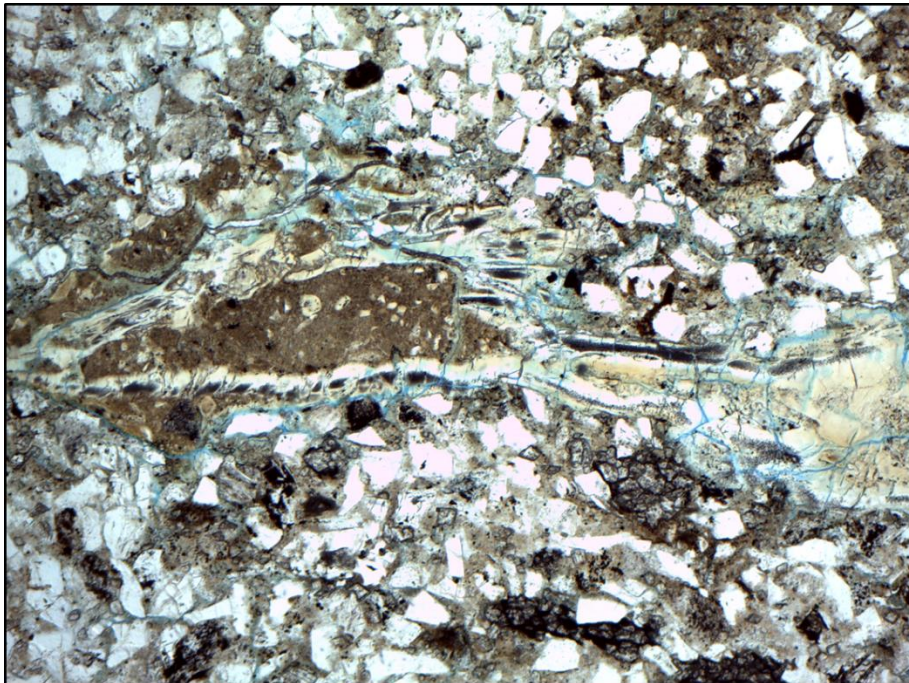


Figure 13: Unidentified fossil. Well: Ruhl, depth: 11,574 ft (3,528 m).

## AUTHIGENIC MATERIAL

### Glaucanite

Glaucanite grains occur as dark green round peloids and are present as trace amounts in most samples. However, some samples contain up to 6% glaucanite. Glaucanite grains commonly were deformed by compaction and squeezed into surrounding pore space. Additionally, glaucanite partially to completely replaced gains along grain boundaries, especially in feldspars (Figure 14).

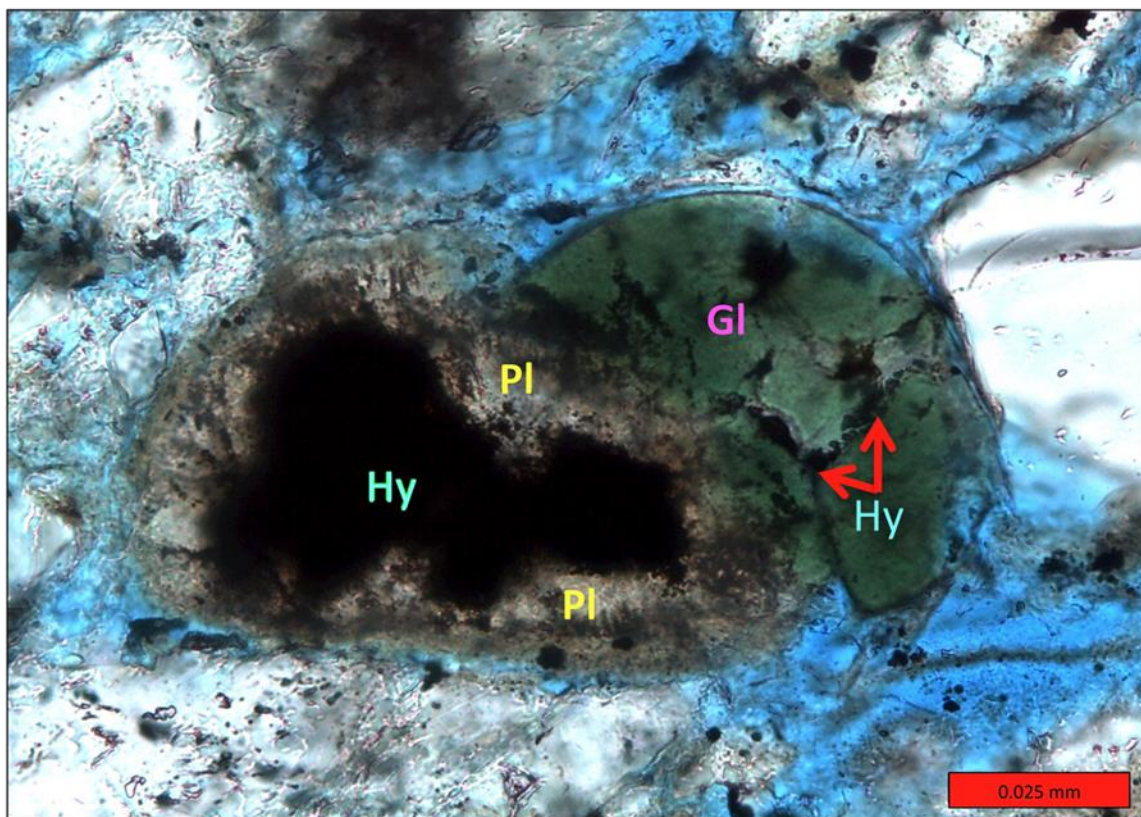


Figure 14: Partially dissolved glaucanite (GI) grain along a partially dissolved plagioclase (PI) grain contact. Hydrocarbons (Hy) fill fractures in the glaucanite (red arrows) grain as well as the intragranular pore in the plagioclase grain. Well: Kernco 61-34, depth 11,410 ft (3,478 m).

## Phosphate

Phosphate is generally associated with glauconite and occurs as round dark brown peloids (Figure 15a), coatings on framework grains, and cement. It is present in trace amounts in most samples. Phosphate replaced glauconite, feldspars, and quartz both within the grains and along grain boundaries (Figure 15b).

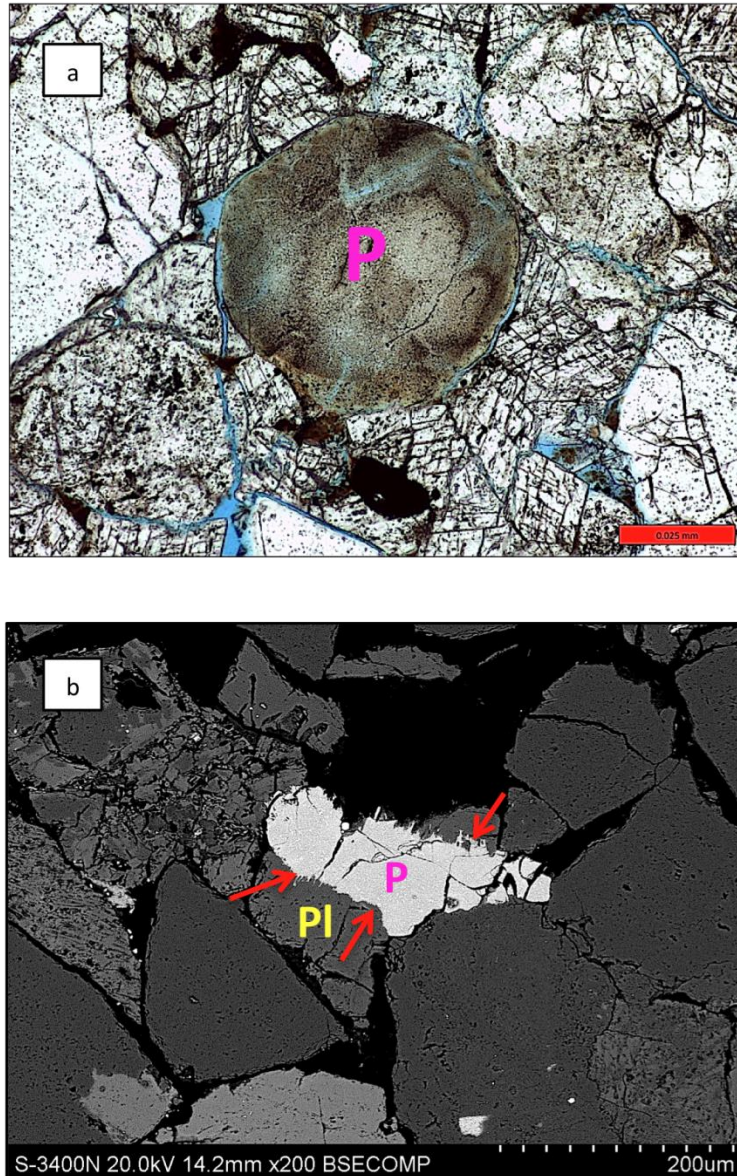


Figure 15: **(a)** Individual rounded phosphate (P) peloid in carbonate cement. Well: Ruh1 1, Depth: 11,502 ft (3,505 m). **(b)** SEM-BSE image of phosphate (P) replacing plagioclase (Pl) grain (red arrows). Well: Mandell 3, depth: 11,436 ft (3,486 m).

## Pyrite

Authigenic pyrite occurs throughout the sandstones as scattered crystals, cement, or small framboidal masses (Figure 16a), and ranges up to 10% of the rock volume. Pyrite crystals range in size from  $< 1$  to  $4 \mu\text{m}$ . Pyrite formed along biotite cleavage planes (Figure 16b), within chloritized biotite, and within hydrocarbon-filled pores (Figure 16c, 16d), and it occurs in association with glauconite.

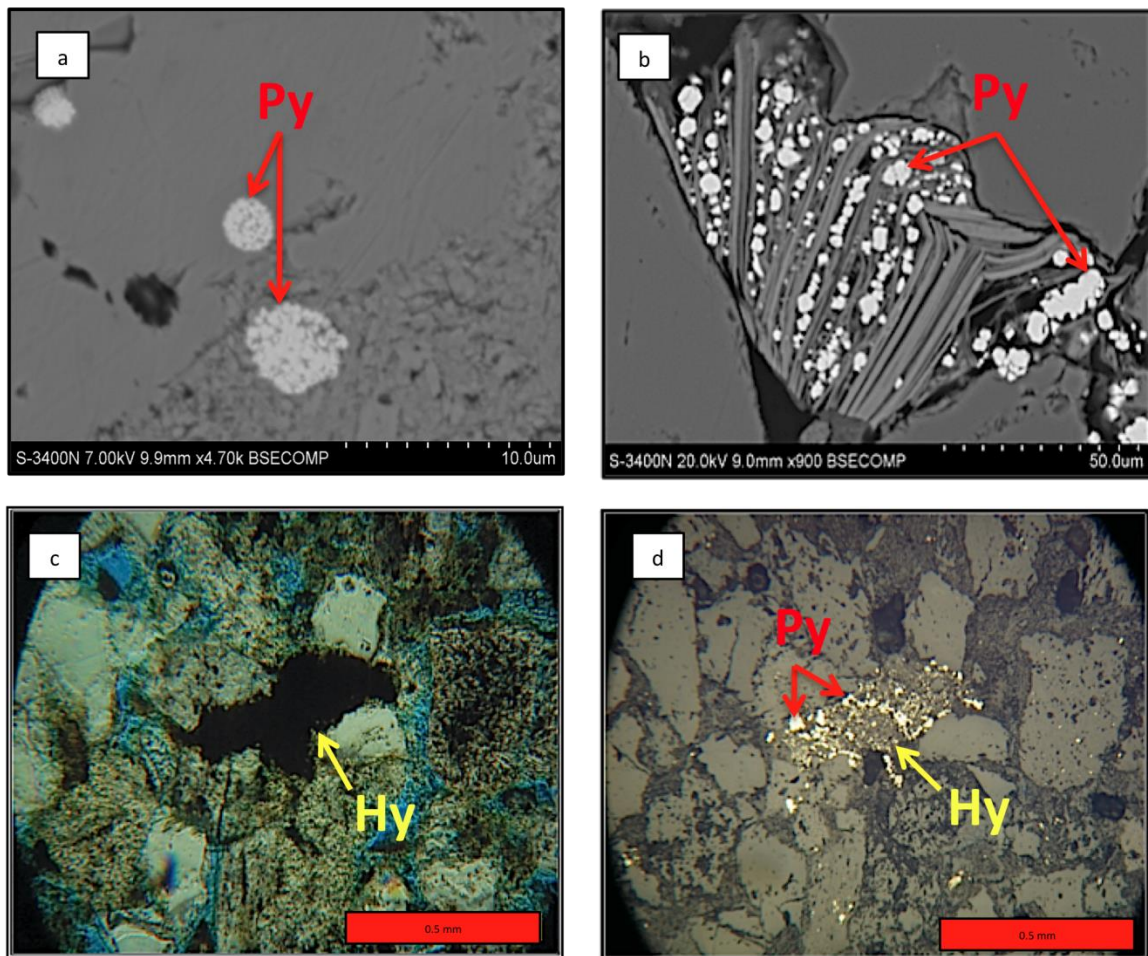


Figure 16: **(a)** SEM-BSE image of framboidal pyrite (Py). Well: Kernco 61-34, depth: 11,490 ft (3,502 m) **(b)** SEM-BSE image of pyrite (Py) that formed along biotite cleavage planes. Well: Ruhl 1, depth: 11,437 ft (3,486 m) **(c)** Transmitted light photomicrograph of hydrocarbon (Hy) (yellow arrows) Well: Kernco 61-34, depth: 11,410 ft (3,478 m) **(d)** Reflected light photomicrograph of the same area as figure 16c showing pyrite (Py) (red arrows) that formed within hydrocarbon (Hy) (yellow arrows) in oversized pore. Well: Kernco 61-34, depth: 11,410 ft (3,478 m).

## Rutile

Diagenetic rutile crystals occur in minor amounts, typically in coarser samples. These crystals occur in association with pyrite and clay (Figure 17).

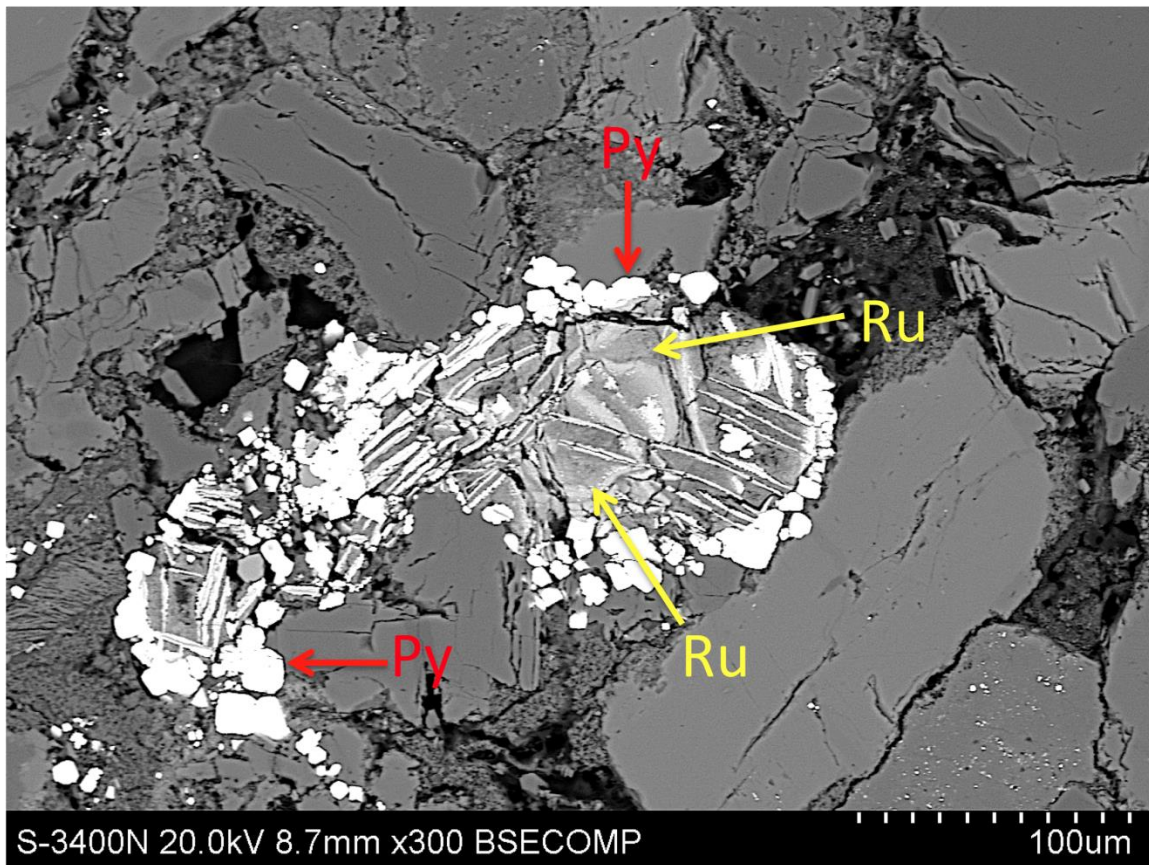


Figure 17: SEM-BSE image of rutile (Ru) (yellow arrows) that formed in a round oversize pore with pyrite (Py) (red arrows). Well: Kernco 61-34, depth: 11,410 ft (3,478 m).

## Clays

Authigenic clays occur as alteration products (Figure 18), pore-linings, clay-coatings (Figure 19, Figure 20) and pore-filling cements. Chlorite, kaolinite, and mixed-layer illite/smectite or illite/chlorite is present throughout the Vedder Sandstones identified through petrographic and SEM-EDS analysis. Clay minerals range from trace amounts up to 18% of the rock volume (Table 1). Most clays in these sandstones occurred as a pseudomatrix from alteration of feldspars and rock fragments (Figure 18).

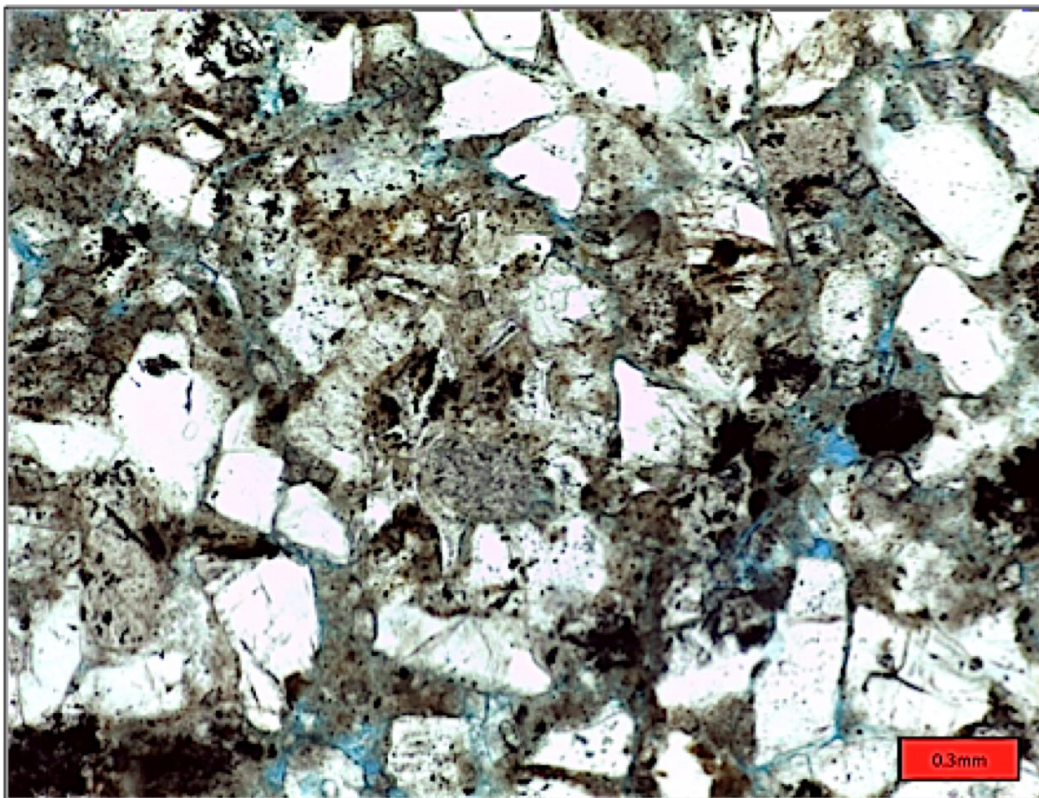


Figure 18: Mixture of grains that have been altered to clay and squeezed into surrounding pore spaces. Well: Rudnick 1, depth: 11,400 ft (3,475 m).

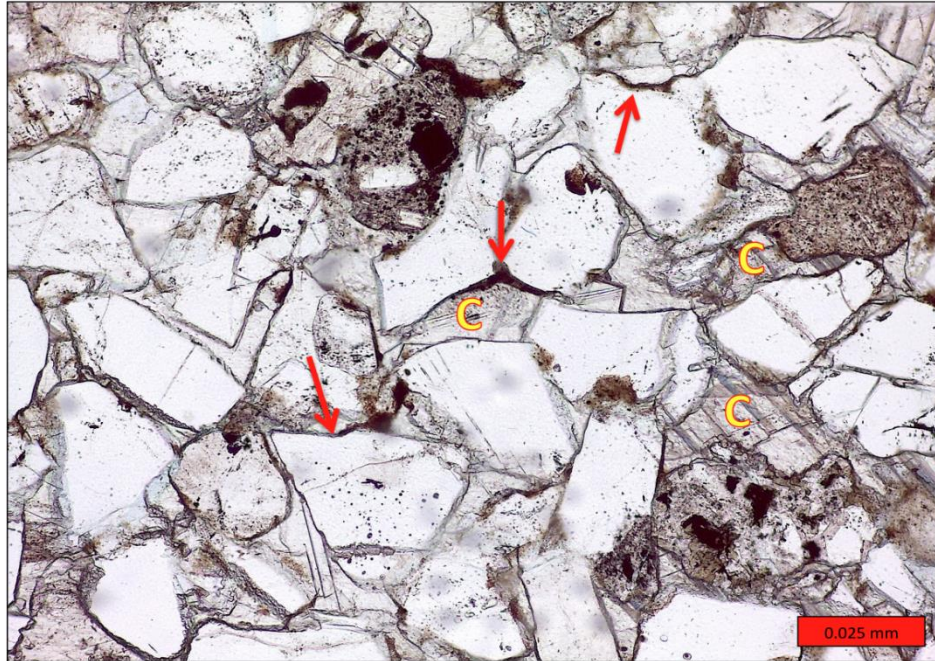


Figure 19: Clay coatings (red arrows) surround detrital grains in pokilotic calcite (C) cement. Well: Pacific States 21, depth 11,543 ft (3,518 m).

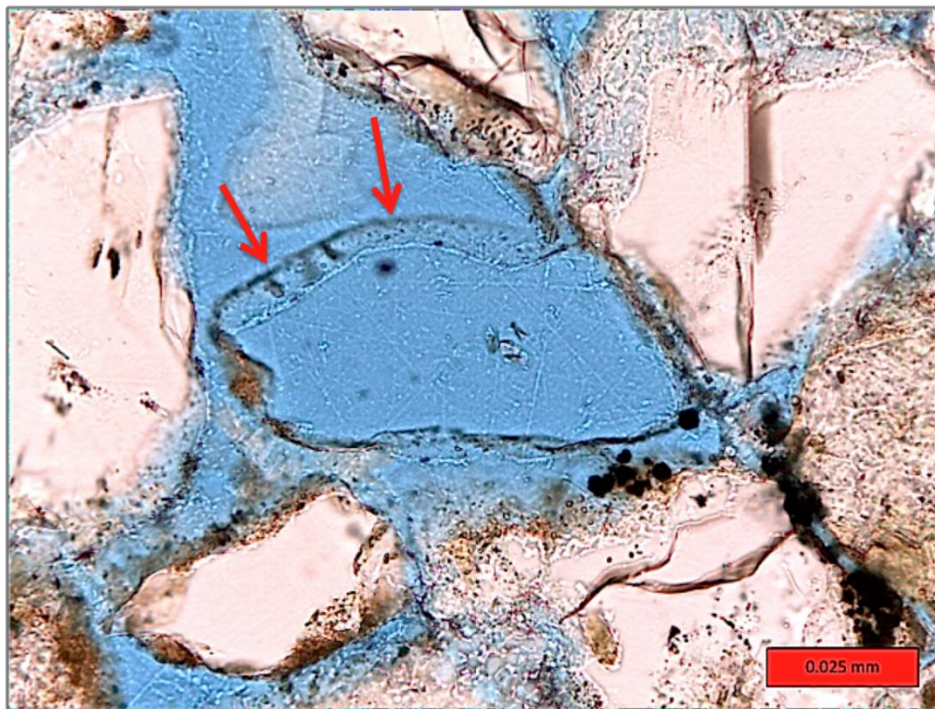


Figure 20: Remnant clay coating (red arrows) from detrital grain that was dissolved. Well: Ruhl 1, depth: 11,437 ft (3,486 m).

## Chlorite

Chlorite is present in small amounts in most samples. It occurs along fractures within detrital grains (Figure 21a), as thin coatings on detrital grains (Figure 21b), as a product of alteration of biotite (Figure 22) and volcanic grains, and as cement filling nearby pores (Figure 23).

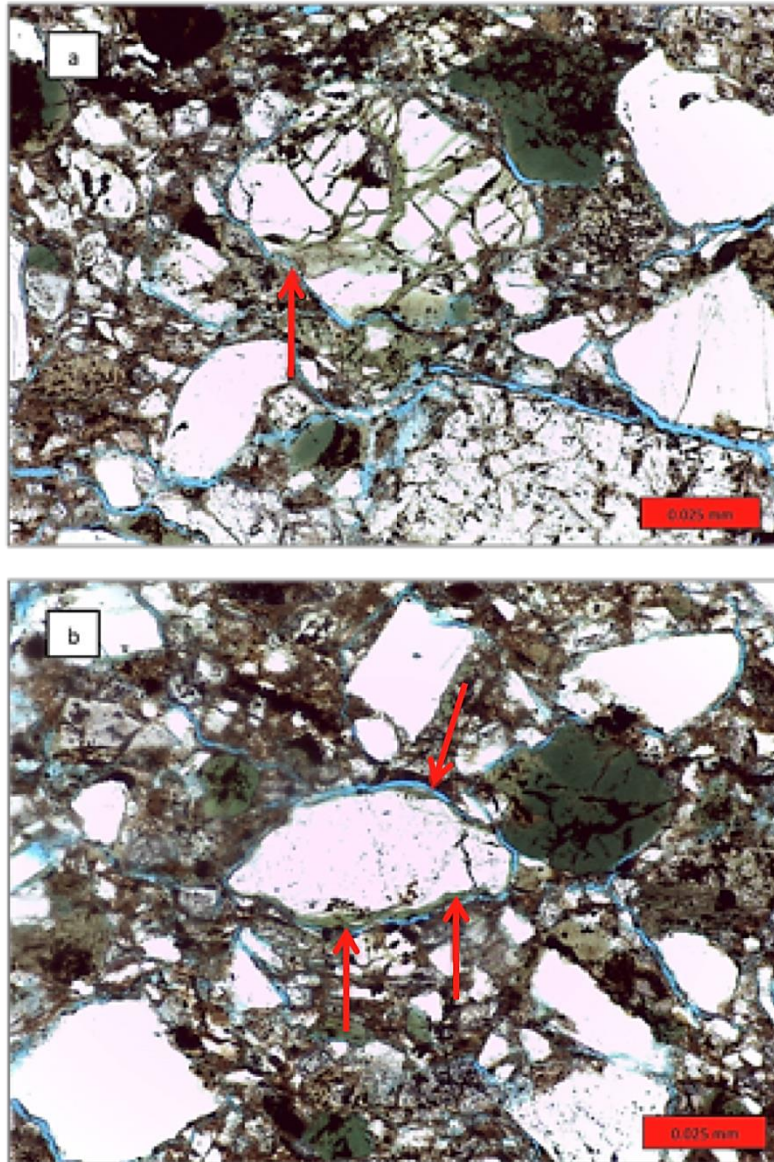


Figure 21: (a) Chlorite occurring along fractures within the grain (red arrows). Well: Pacific States 21, depth: 11,549 ft (3,520 m). (b) Chlorite occurring as a thin coating on a detrital grain (red arrows). Well: Pacific States 21, depth: 11,549 ft (3,520 m).

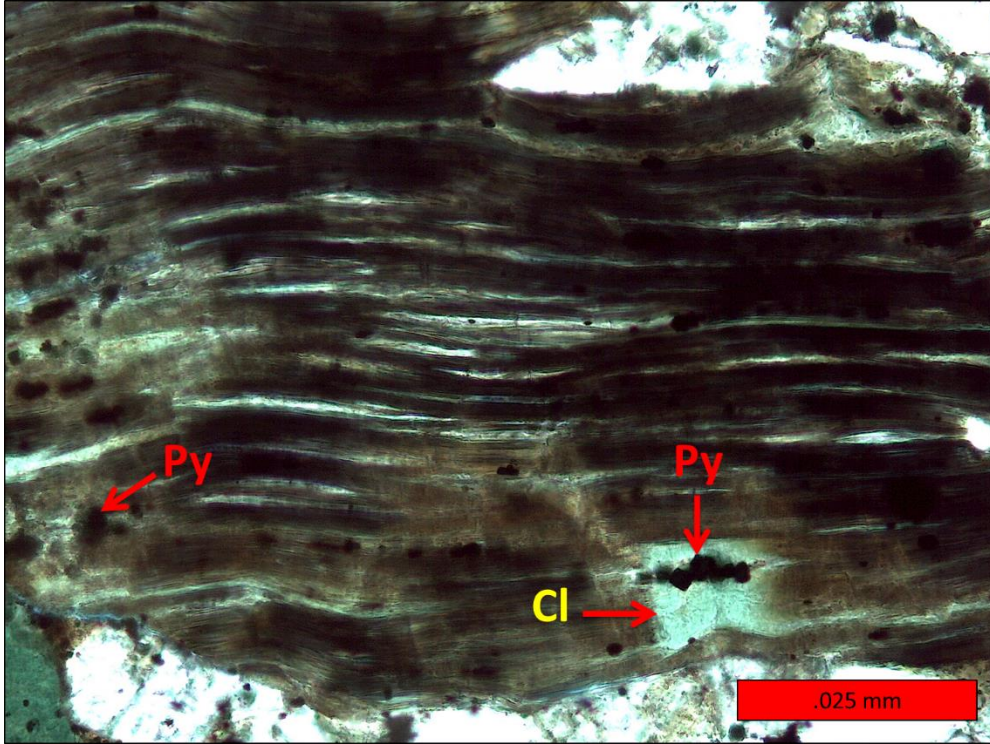


Figure 22: Biotite grain that is partially altered to chlorite (Cl) with pyrite (Py) crystals. Well: Pacific States 21, depth: 11,549 ft (3,520 m).

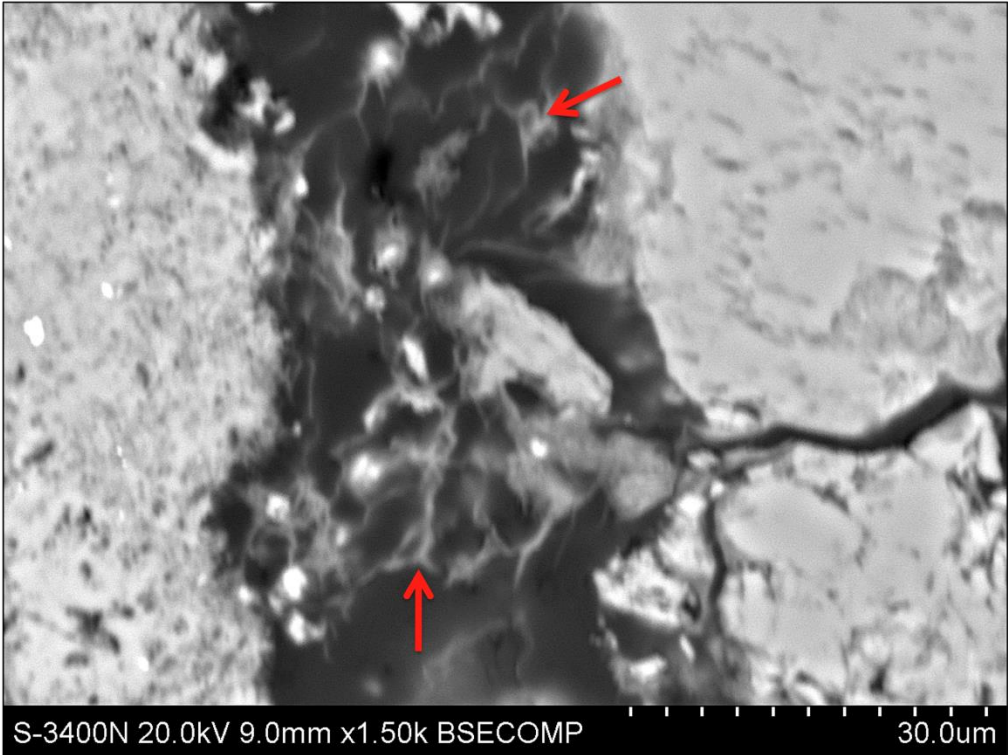


Figure 23: Chlorite cement (red arrows) filling pores. Well: Mandell 3, depth: 11,436 ft (3,489 m).

## Illite

Mixed-layer illite/smectite or illite/chlorite occur within shards of feldspar grains (Figure 24) and as pore-linings or coatings (Figure 25). SEM-EDS analyses show that this material contains small amounts of calcium, iron, sodium, and magnesium. Mixed-layer illitic clays range from trace amounts to 28%.

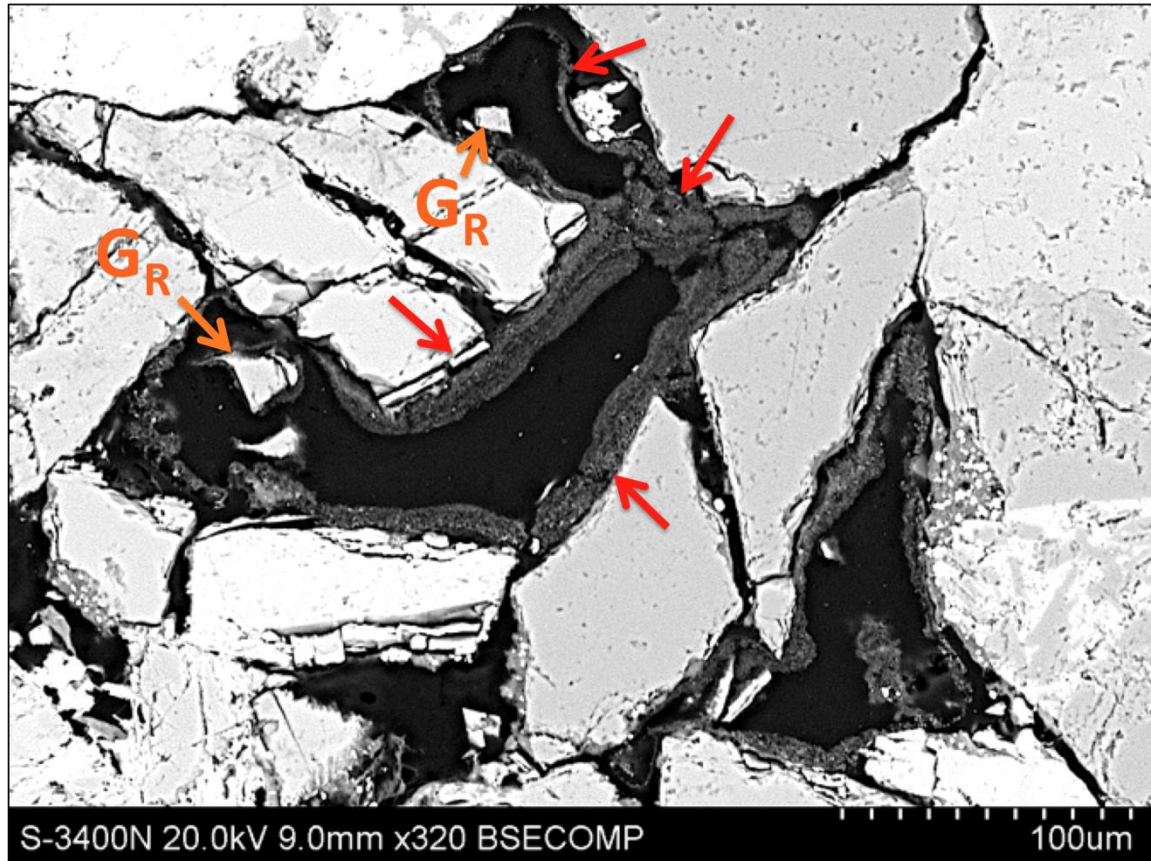


Figure 24: Pore-lining illite/smectite or illite/chlorite (red arrows) with relic detrital grains (G<sub>R</sub>). Well: Mandell 3, depth: 11,436 ft (3,486 m).

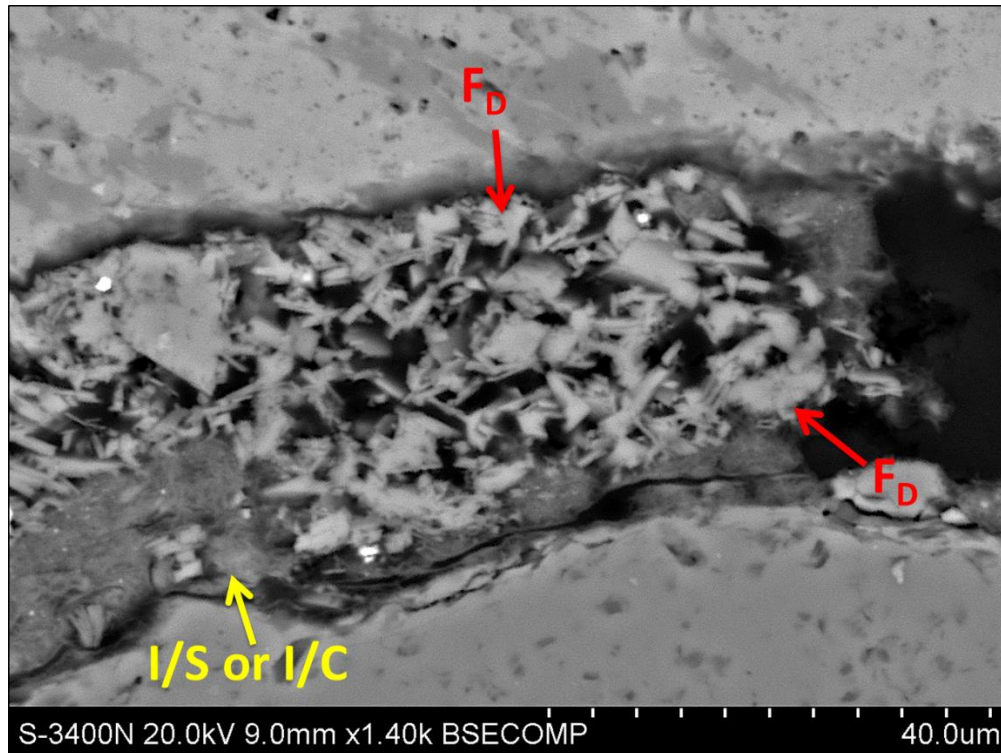


Figure 25: Illite/smectite or illite/chlorite is present between a dissolved feldspar (F<sub>D</sub>) grain. Well: Mandell 3, depth: 11.436 ft (3,486 m).

### **Kaolinite**

Kaolinite is present in the majority of samples and occurs as pore-lining and pore-filling cement with a rock volume ranging from trace to 6%. Kaolinite commonly occurs as well developed booklets of micron-size crystals that partially to completely fill intergranular pores (Figure 26). Kaolinite cement in the Rio Bravo Vedder Sandstones contains an estimated microporosity of 40%. Kaolinite often formed adjacent to dissolved feldspars (Figure 27). Occasionally kaolinite replaced volcanic rock fragments.

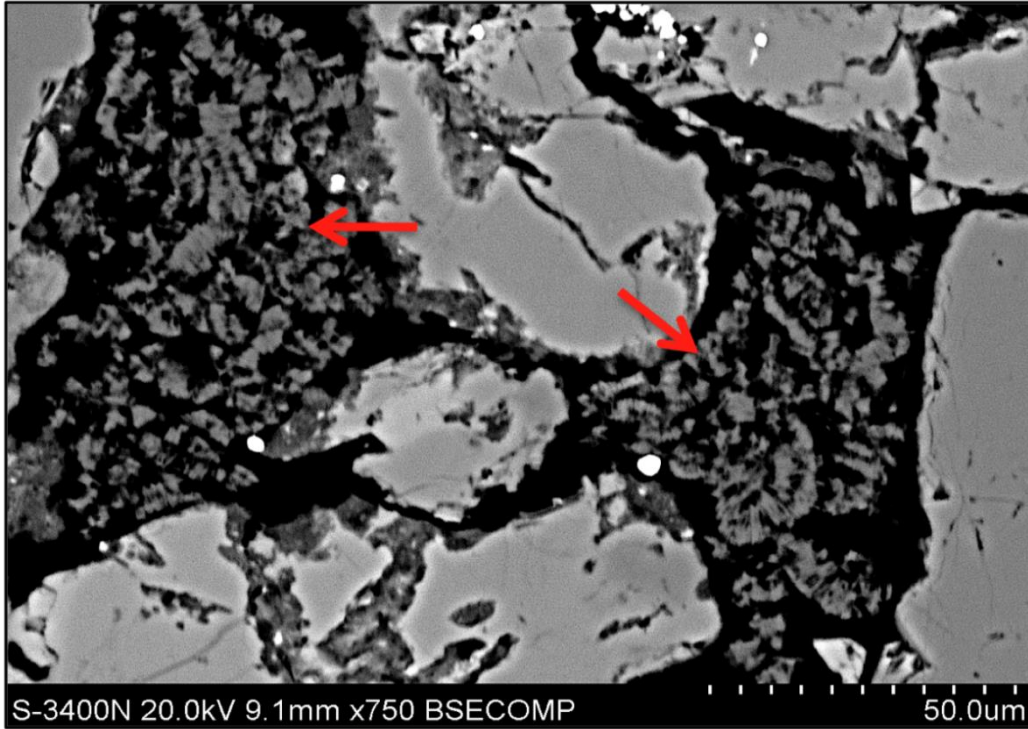


Figure 26: SEM-BSE image of kaolinite showing booklets and associated microporosity (red arrows). Well: Ruhl 1, depth: 11,437 ft (3,486 m).

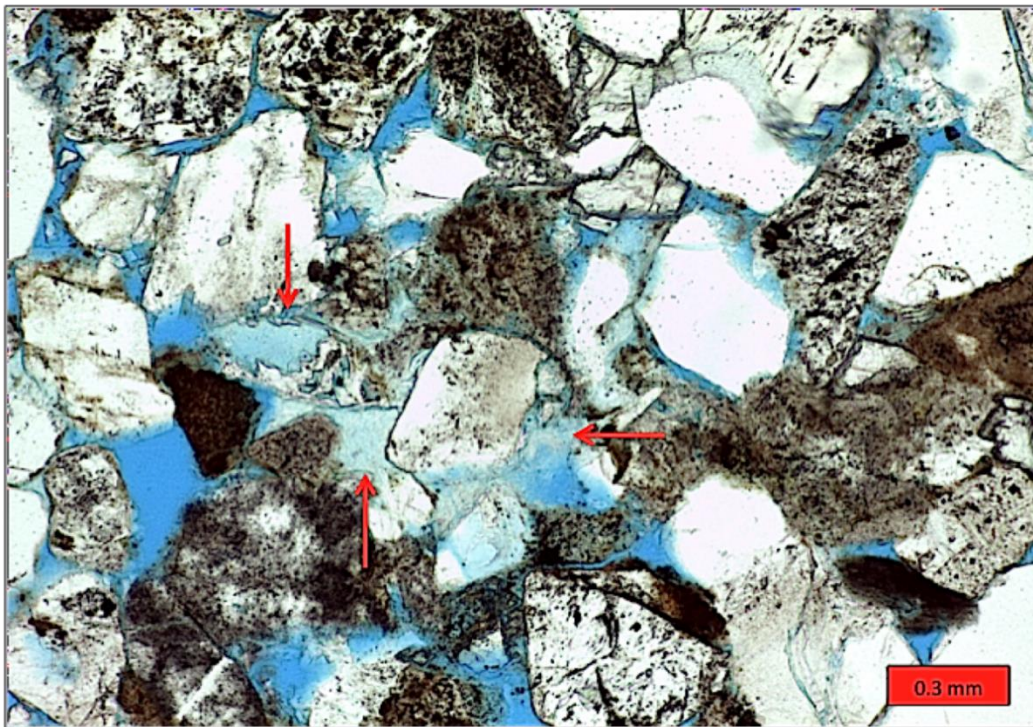


Figure 27: Kaolinite occluding pore spaces adjacent to partially dissolved grains (red arrows). Well: Pacific States 21, depth: 11,554 ft (3,522 m).

## Dolomite

Dolomite cement ranges from trace amounts to 52%. It is present as pore-filling cement and as euhedral rhombic crystals (Figure 28). Compositional zoning is common in the crystals where some samples display thin iron-rich zones (Figure 28). Some dolomite crystals have dissolved cores (Figure 29). Dolomite occurs as a replacement of detrital feldspars (Figure 30) and between biotite cleavage planes (Figure 31).

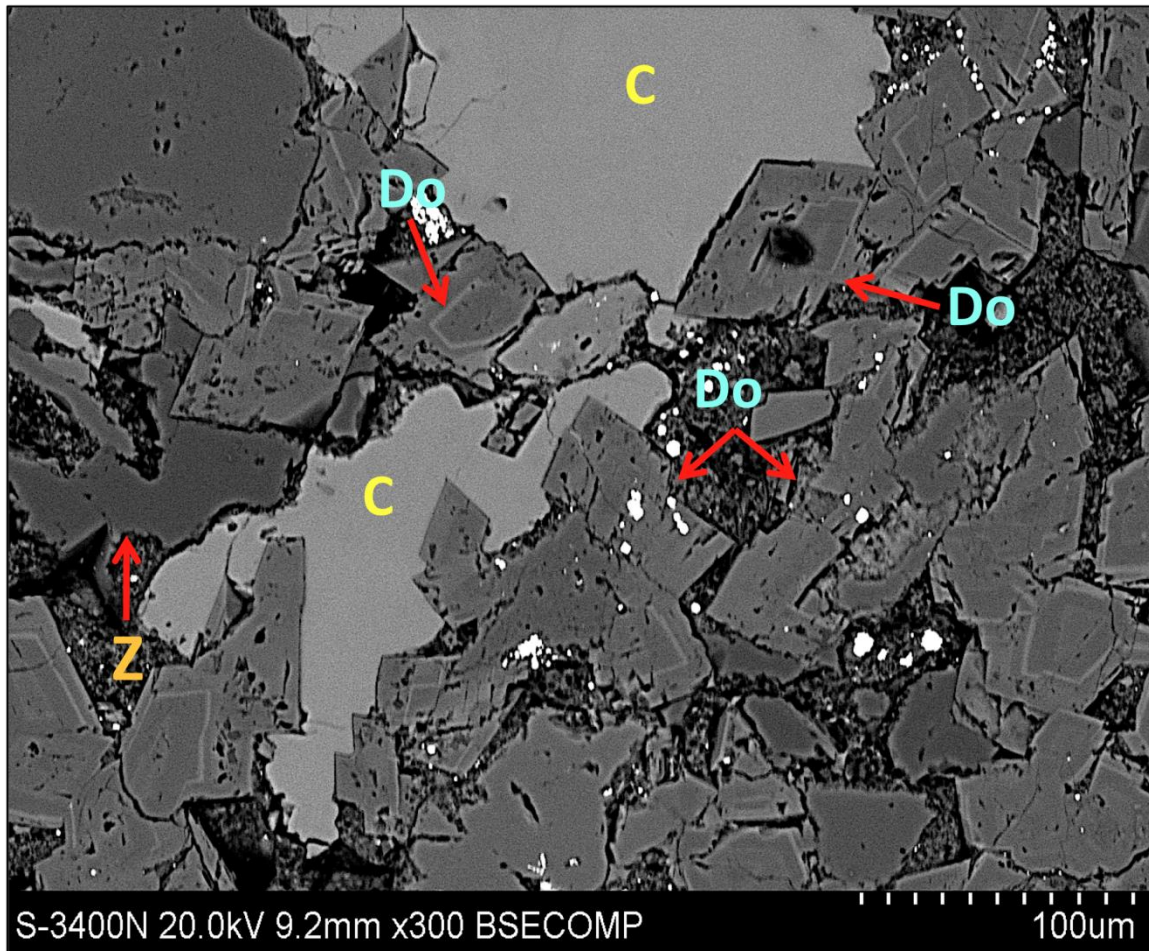


Figure 28: SEM-BSE image of zoned dolomite (Do), calcite (C), and zeolite (Z) cemented sandstone. Well: Kernco 61-34, depth: 11,450 ft (3,490 m).

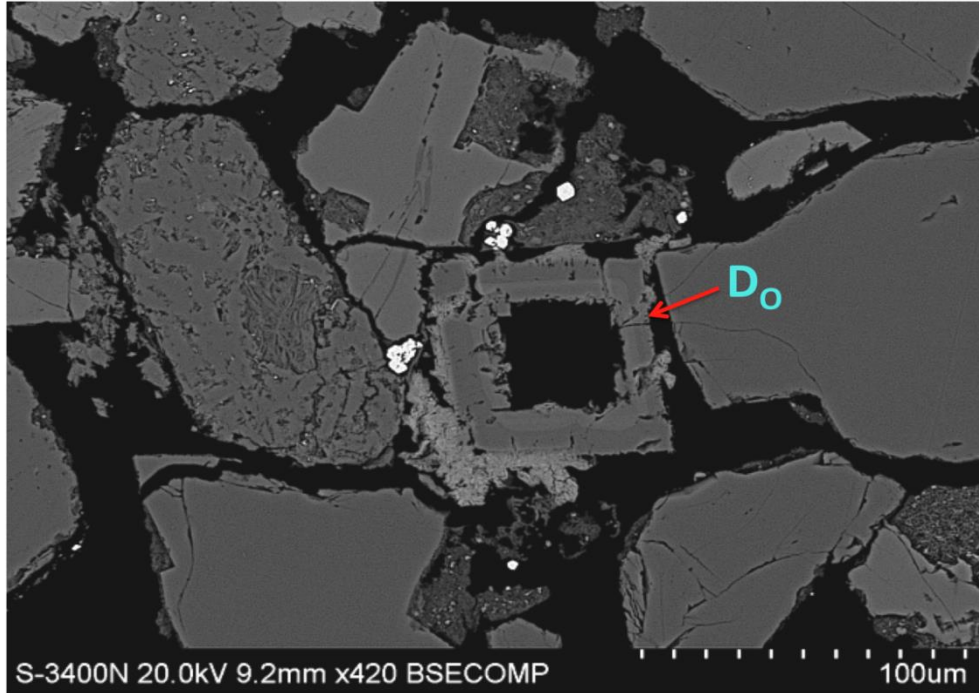


Figure 29: Diamond-shaped hollow core from dissolution of dolomite rhomb (D<sub>0</sub>). Well: Ruhl 1, depth: 11,437 ft (3,486 m).

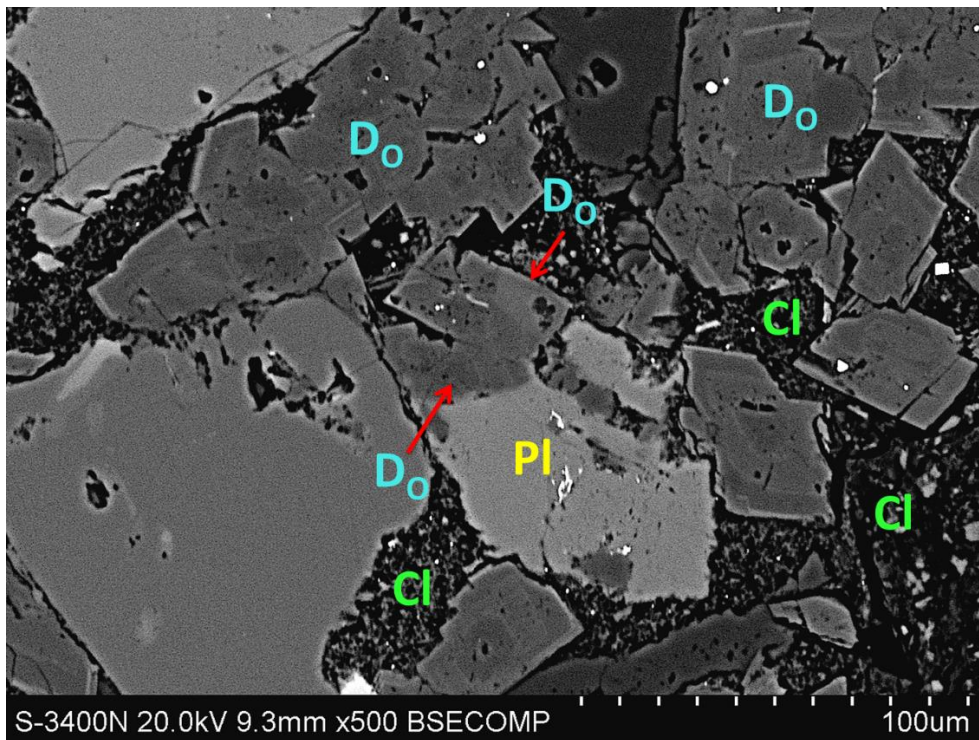


Figure 30: Dolomite (D<sub>0</sub>) that has replaced a plagioclase (P) grain. Chlorite (C) is present as pore-filling cement. Well: Kernco 61-34, depth: 11,450 (3,490 m).

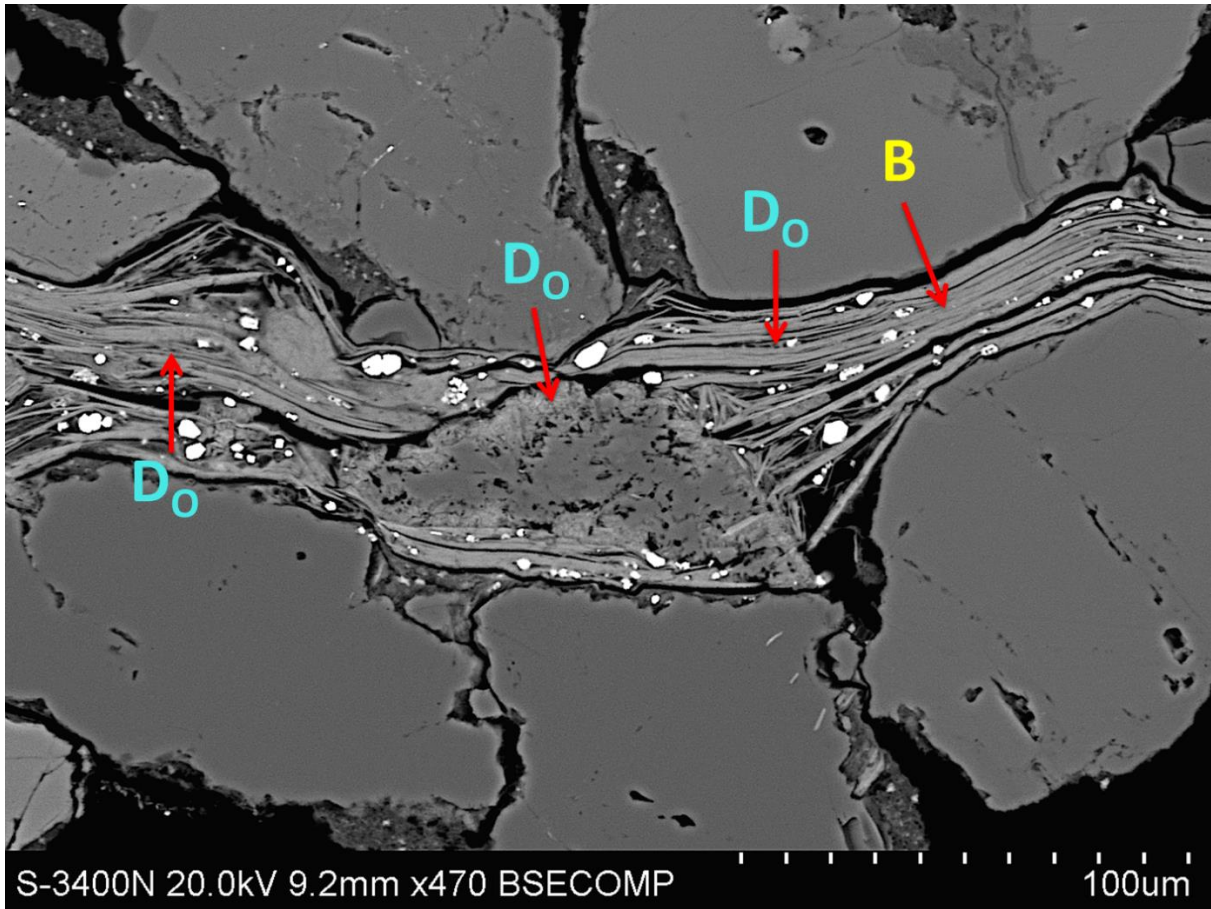


Figure 31: Dolomite (D<sub>0</sub>) between biotite cleavage planes. Well: Ruhl 1, depth: 11,437 ft (3,486 m).

### Calcite

Calcite cement occurs in the majority of samples from trace amounts to 55%. Early-stage calcite forms as poikilotopic pore-filling cement (Figure 19) in large intergranular spaces where little to no porosity exists. Some samples show evidence of early clay coatings surrounding the detrital grains in the calcite cement (Figure 19). Grains in cemented sands are less altered than in non-cemented sands. Authigenic overgrowths were not observed in sandstones cemented by early poikilotopic calcite. A later stage of calcite cementation occurred in which calcite also replaced grains, including quartz, plagioclase (Figure 32), K-feldspars, and volcanics. Late-stage calcite also occurs within through-going fractures (Figure 33).

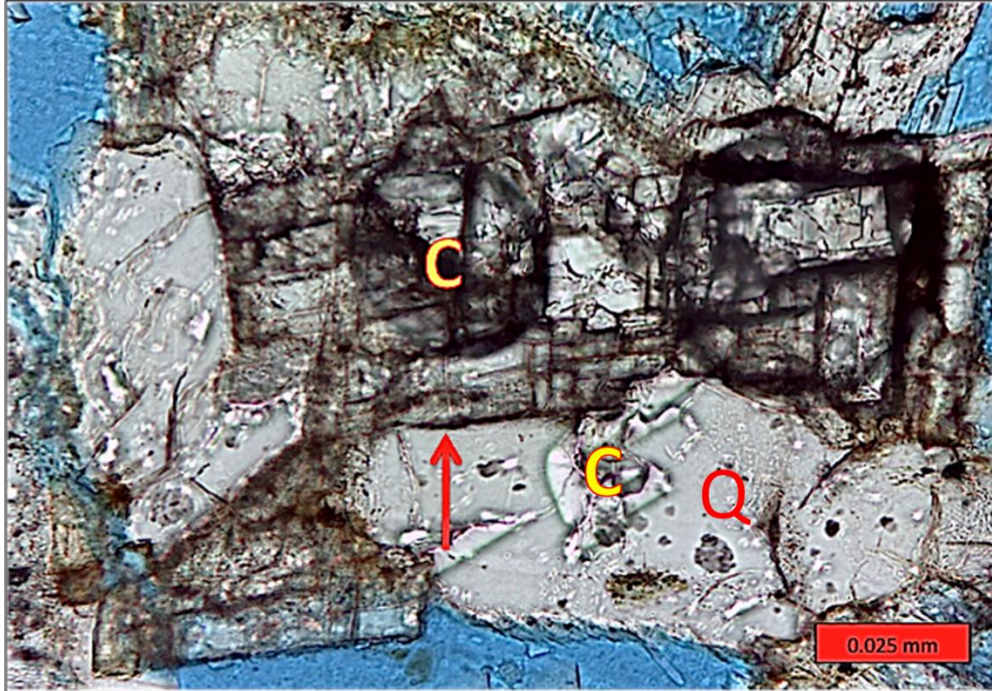


Figure 32: Calcite that partially replaced a plagioclase grain (red arrow) and quartz grain (Q). Hydrocarbon is present within the fractures of the calcite. Geisinger 2, depth: 11,443 ft (3,488).

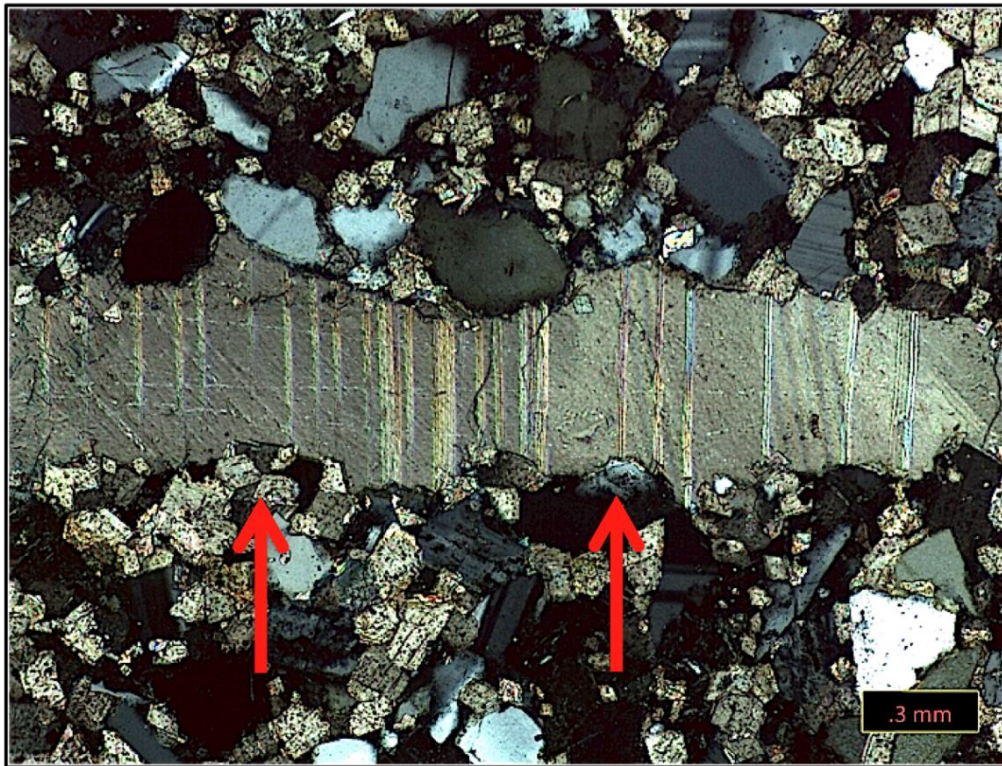


Figure 33: Through-going fracture filled with poikilotopic calcite (red arrows). Well: Rudnick 1, depth: 11,400 ft (3,475).

## Zeolite

Zeolite cement occurs as poikilotopic pore-filling cement (Figure 34). Zeolite cement is common among many of the samples containing significant volcanic grains. The most abundant amounts of zeolite cement are found in samples from well Kernco 61-34. SEM-EDS analyses indicate that zeolite cement is sodium rich.

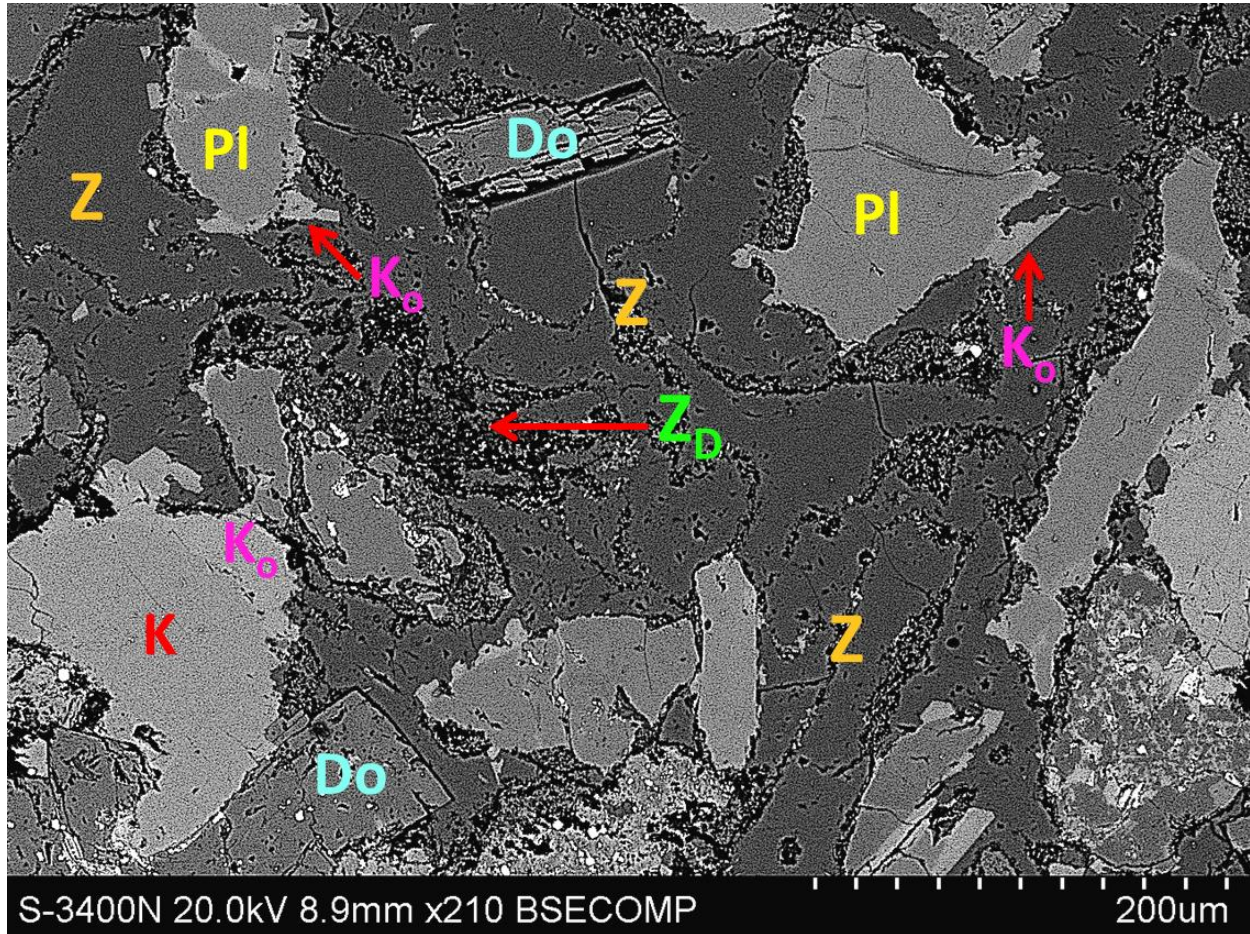


Figure 34: SEM-BSE image of poikilotopic zeolite (Z) cement. Plagioclase (PI) grains exhibit K-feldspar overgrowths ( $K_o$ ) (red arrows) surrounded by zeolite cement. Dolomite (Do) rhomb is surrounded by zeolite (Z) cement. Zeolite cement shows partial dissolution ( $Z_D$ ). Well: Kernco 61-34, depth: 11,410 ft (3,478 m).

## Albite

Authigenic albite is present in the majority of samples and partially to completely replaced plagioclase and K-feldspar grains. The average composition for albite in samples is  $Ab_{98.9}An_{0.7}Or_{0.4}$ . Albitization of detrital feldspars occurred along cleavage planes and fractures (Figure 35). Authigenic albite is non-luminescent (Figure 36).

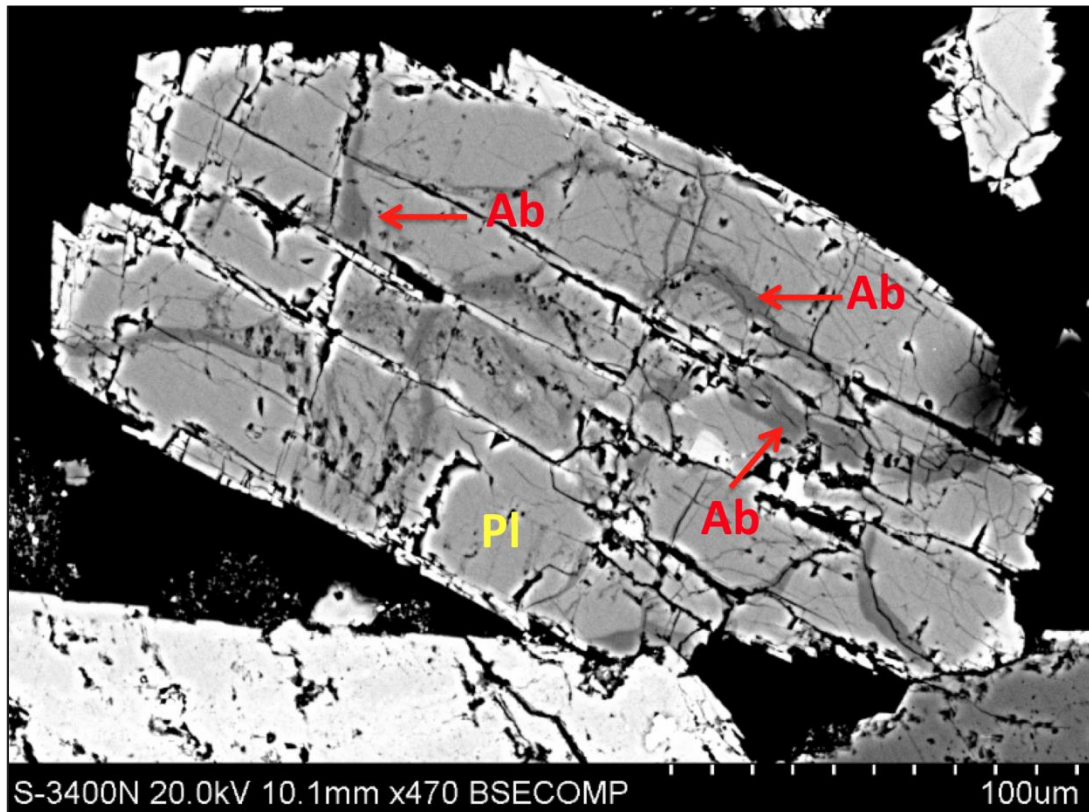


Figure 35: SEM-BSE image of authigenic albitization (Ab) (red arrows), along fractures within a detrital plagioclase (Pl) grain. Well: Weber, depth: 11,445 ft (3,488 m).

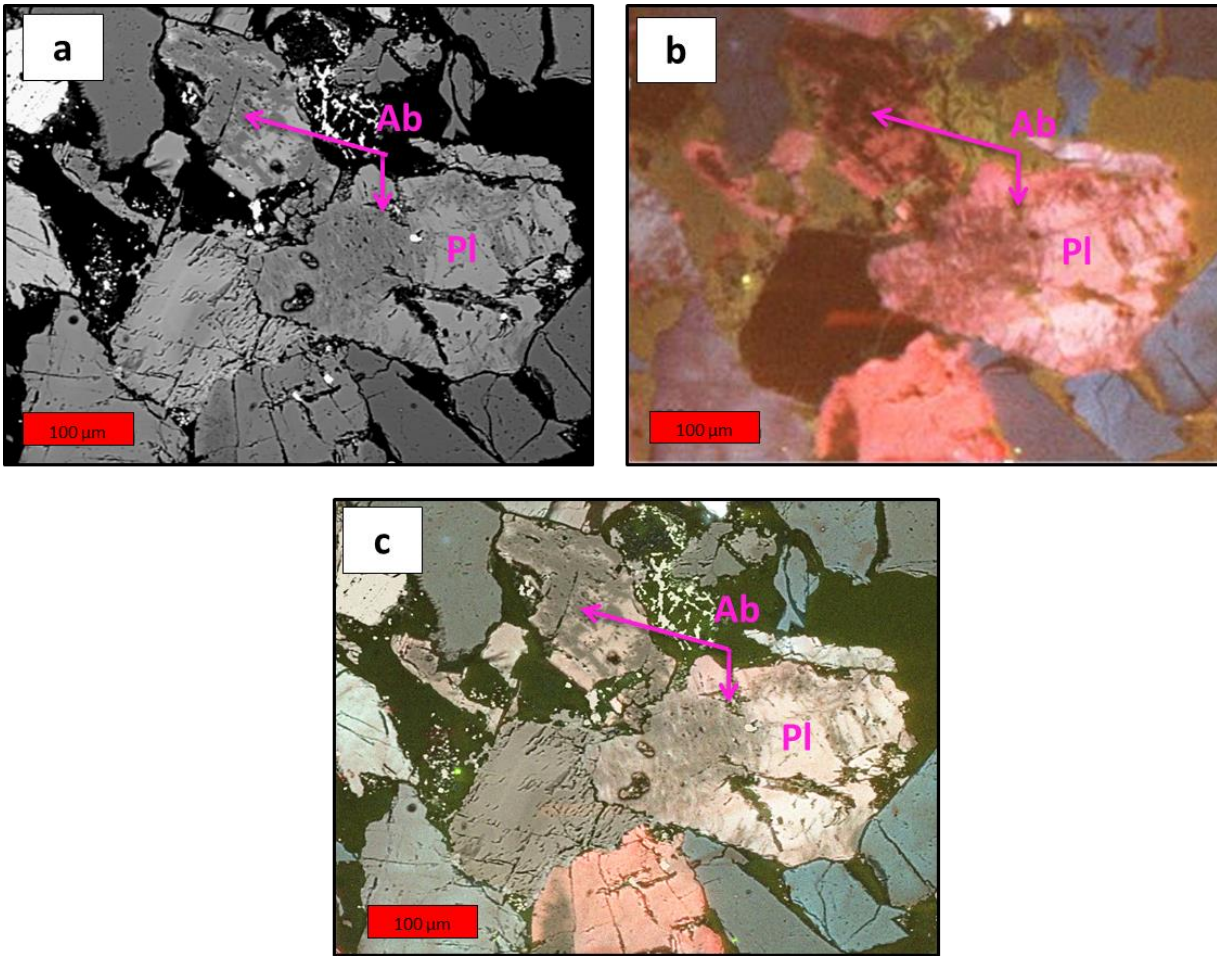


Figure 36: **(a)** SEM-BSE image of plagioclase (Pl) grains that are albitized (Ab). **(b)** CL image reveals authigenic albite is non-luminescent **(c)** Composite image of SEM-BSE and CL images reveals authigenic albite is non-luminescent. Well: Mandell 3, depth: 11,436 ft.

## Potassium Feldspar

Authigenic K-feldspar (Average:  $Or_{97.5}Ab_{2.5}An_{0.0}$ ) occurs as overgrowths and within fractures in plagioclase and K-feldspar grains. In some cases potassium feldspar overgrowths have formed along fractures in authigenic albite (Figure 37). Some potassium feldspar overgrowths exhibit partial dissolution (Figure 37). Overgrowths were not observed in sandstones cemented by poikilotopic calcite. Authigenic potassium feldspar is non-luminescent.

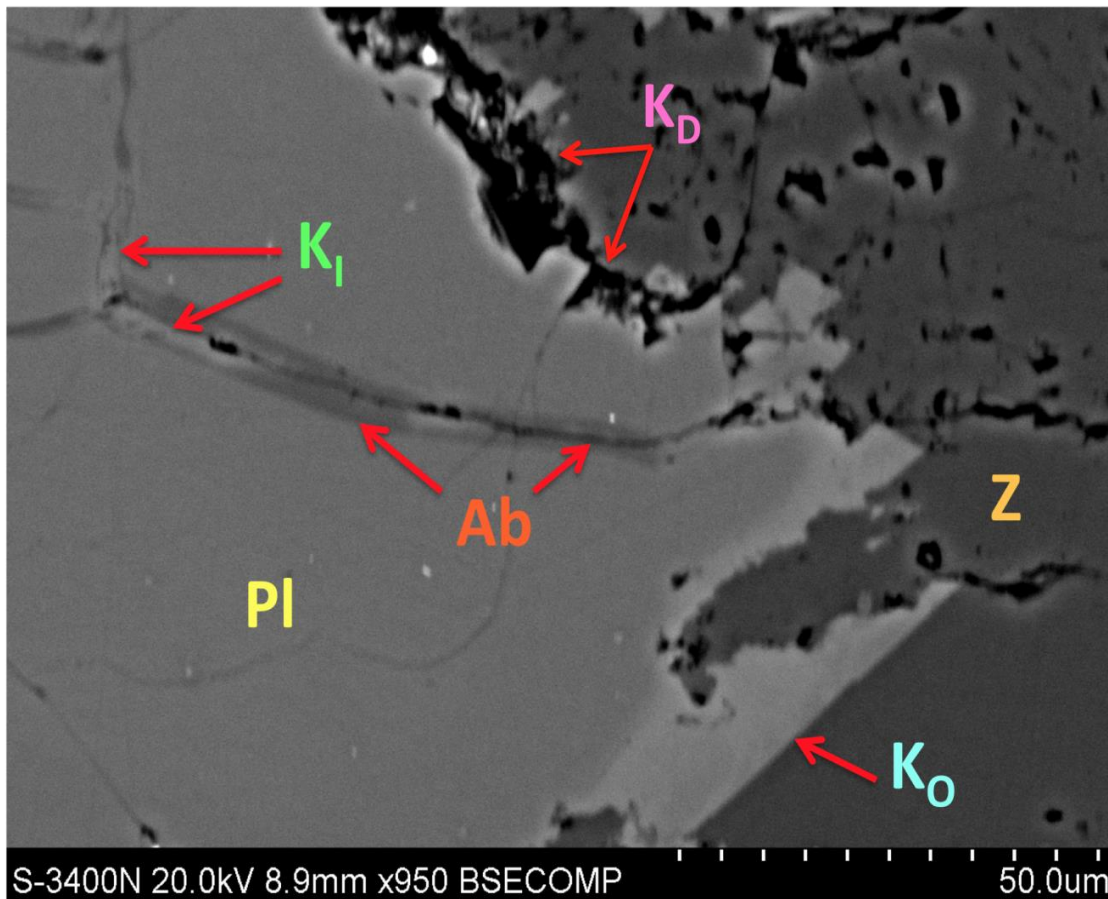


Figure 37: SEM-BSE image of albitized (Ab) plagioclase (Pl) exhibiting K-feldspar infilled (K<sub>I</sub>) fractures along with K-feldspar overgrowth (K<sub>O</sub>) in zeolite (Z) cement. K-feldspar overgrowth shows partial dissolution (K<sub>D</sub>). Well: Kernco 61-34, depth: 11,410 ft (3,478 m).

## Quartz

Authigenic quartz developed mostly as overgrowths on detrital quartz grains (Figure 38, 39) and makes up less than 1% of the rock volume. Authigenic quartz also fills fractures within detrital quartz grains (Figure 39). Authigenic quartz often cannot be identified under the petrographic microscope because it is optically continuous with the detrital grain. In some instances the authigenic overgrowths are separated from the detrital grains by clay coatings that delineate the grain boundaries (Figure 38). In other instances where clay coatings are absent authigenic overgrowths can be recognized by the presence of euhedral crystal shapes where they are fully developed. SEM-CL images reveal that authigenic quartz overgrowths and healed fractures are non-luminescent (Figure 39)

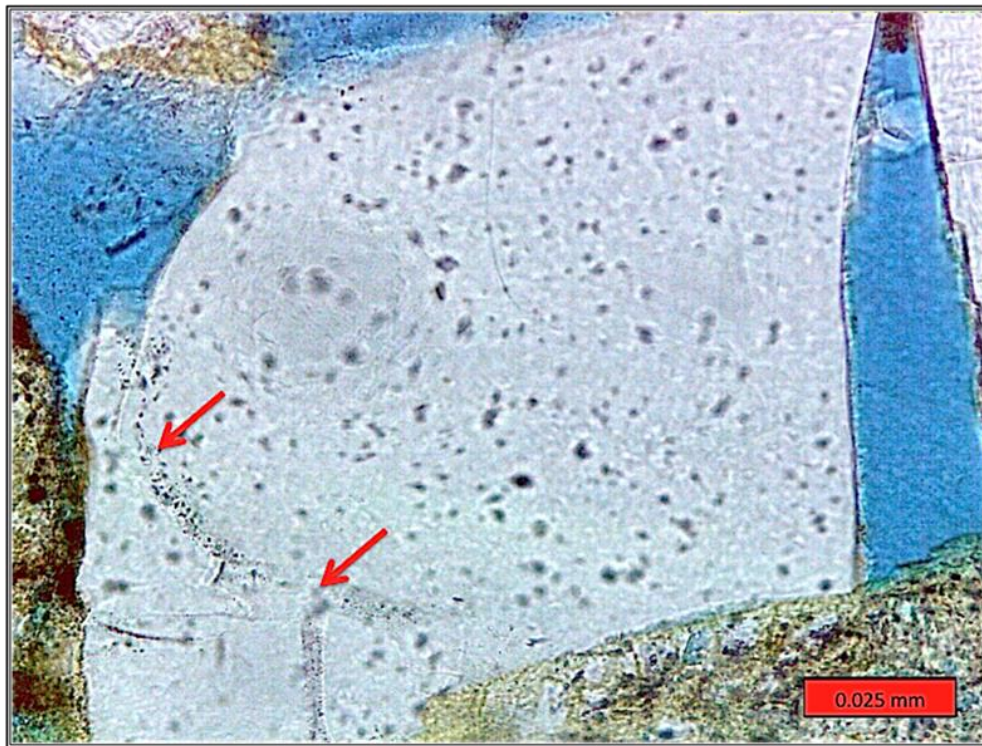


Figure 38: Overgrowth with euhedral termination on detrital quartz grain. The red arrows point to the detrital grain edge. Well: Rudnick 1, depth: 11,413 ft (3,479 m).

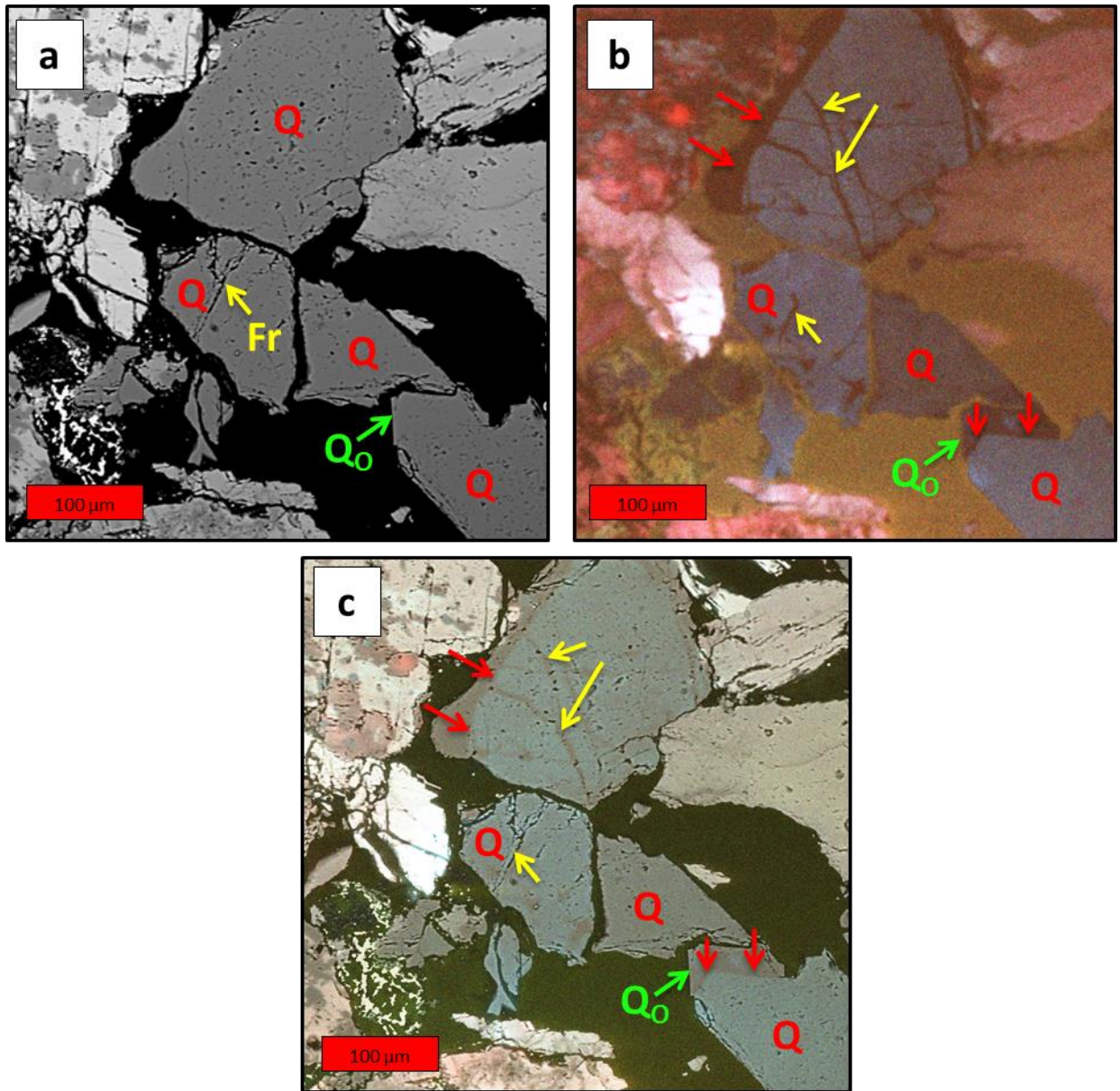


Figure 39: **(a)** SEM-BSE image of fractured (Fr) quartz (Q) and quartz overgrowth (Q<sub>o</sub>) on quartz grain. **(b)** CL image reveals quartz overgrowth (Q<sub>o</sub>) on a quartz grain (red arrows) and healed fractures (yellow arrows) are non-luminescent. **(c)** Composite image of SEM-BSE and CL images reveals quartz overgrowth (Q<sub>o</sub>) on a quartz grain (red arrows) and healed fractures (yellow arrows). Well: Mandell 3, depth: 11,436 ft.

## Pseudomatrix

Pseudomatrix is abundant in over half of the samples ranging from 0 to 27% of the rock volume. Pseudomatrix formed by mechanical compaction and squeezing of ductile grains such as micas and rock fragments into intergranular pores. Pseudomatrix is most common in sandstones containing significant amounts of volcanic rock fragments (Figure 18, 40).

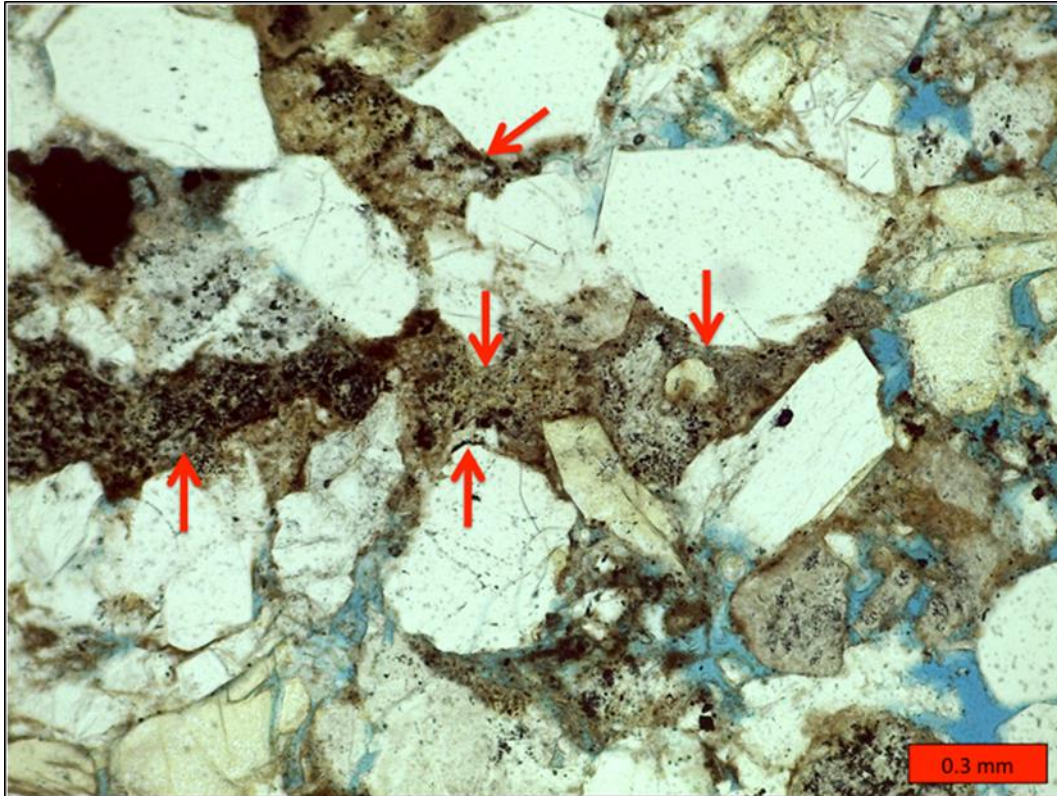


Figure 40: Pseudomatrix (red arrows) formed by deformation of labile volcanic fragments. Well: Rudnick 1, depth: 11,413 ft (3,478 m).

## Barite

Barite is present in small amounts throughout the Vedder Sandstones. It occurs as poikilotopic cement, occupies secondary pore spaces, and possibly replaces feldspar grains (Figure 41).

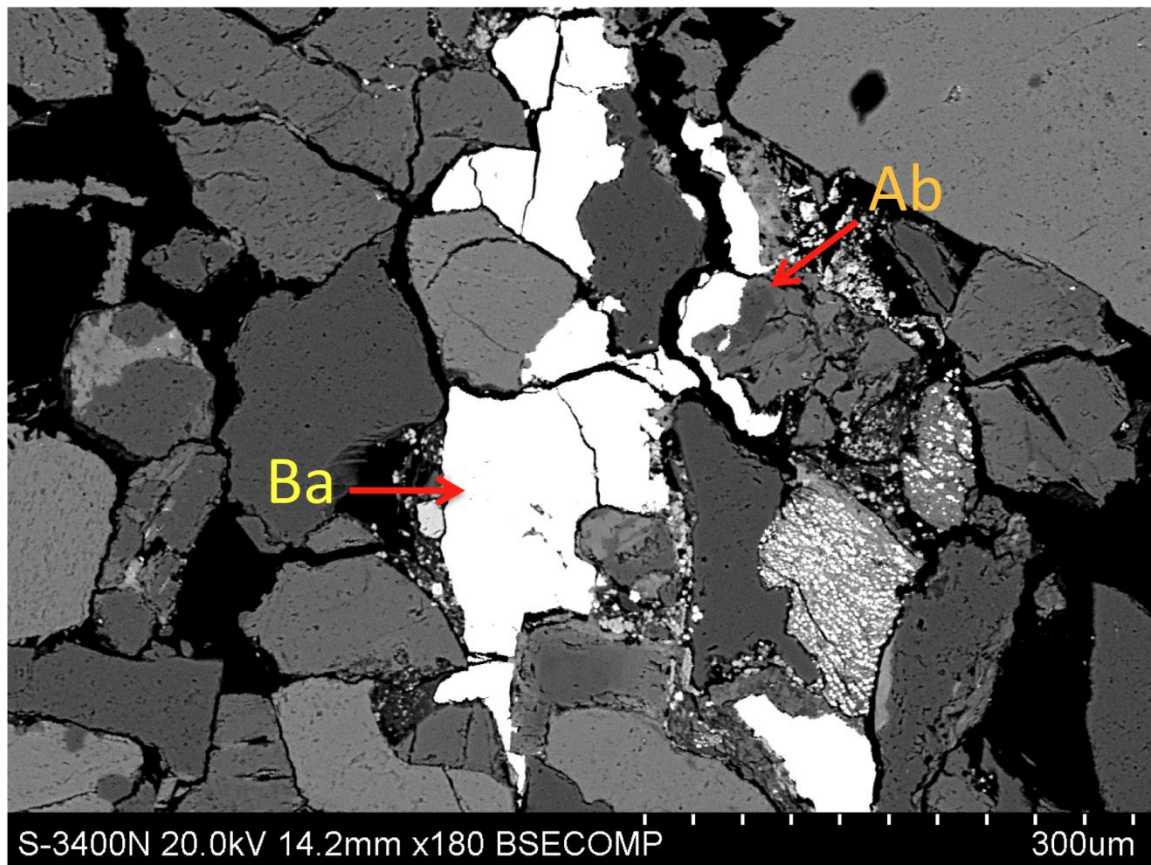


Figure 41: SEM-BSE image of barite (Ba) cement present within secondary porosity. Barite (Ba) is also present as either replacing an albitized (Ab) plagioclase grain or as cement filling secondary pore space in plagioclase. Well: Mandell 3, depth: 11,436 ft (3,486 m).

## Anhydrite

Anhydrite cement was identified using SEM-EDS analysis. It is present in minor amounts in samples that contain dolomite cement and occurs as thin coatings surrounding the dolomite rhombohedra (Figure 42). However, the petrographic thin sections were prepared using water, which could have dissolved some anhydrite. Therefore, the actual amount of anhydrite is unknown.

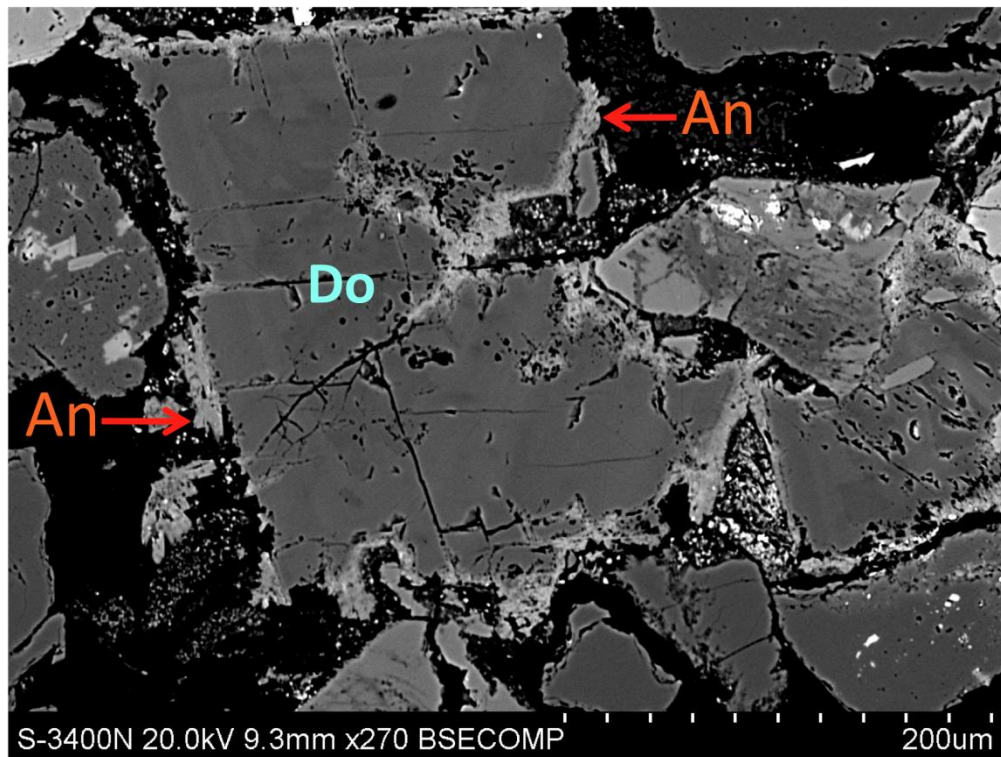


Figure 42: Anhydrite (An) coating on dolomite (Do) cement. Well: Ruhl 1, depth: 11,512 ft (3,509 m).

## Hydrocarbons

During the manufacturing of the thin sections most hydrocarbons were removed, however, small amounts of hydrocarbons still remain. The residual hydrocarbons reside in pores containing clays that could have interfered with the removal process (Figure 43). No attempt was made to further characterize the hydrocarbons due to the instability of the old cores.

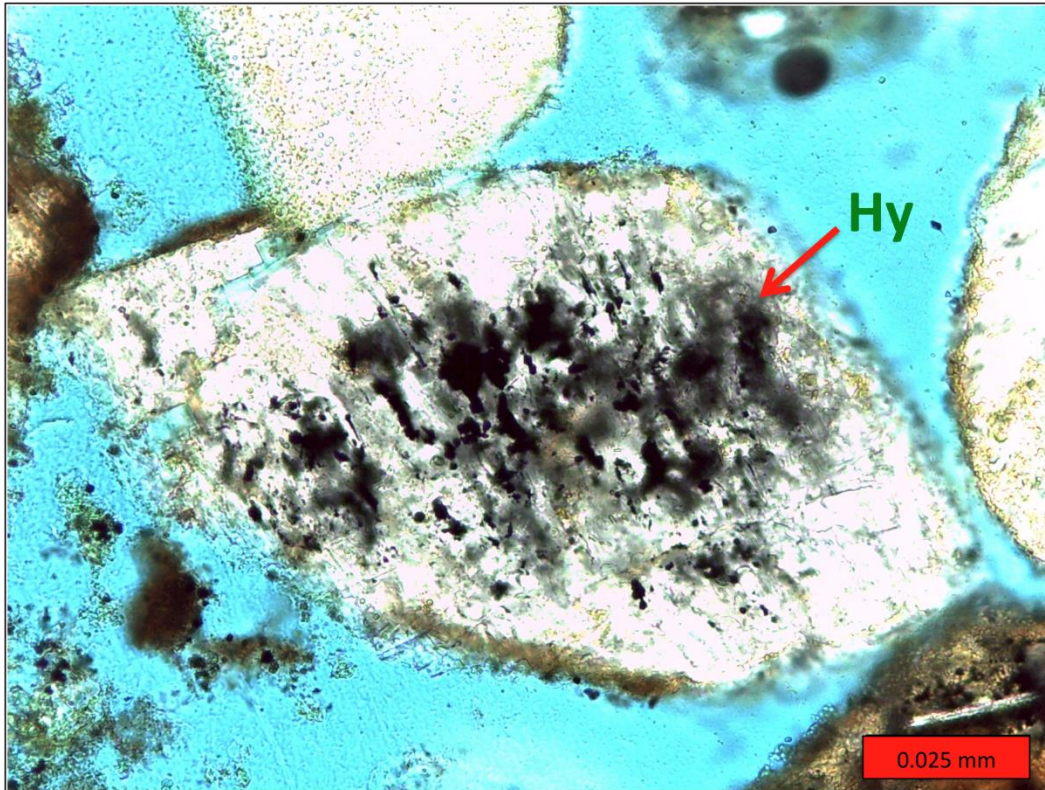


Figure 43: Partially dissolved plagioclase grain showing varying degrees of alteration to clay or sericite with hydrocarbons (Hy) present in secondary pore space. Well: Rudnick 1, depth: 11,413 ft (3,479 m).

## Compaction and Fractures

Following the methodologies of Wilson and McBride (1988) contact index (CI = average number of contacts per grain) and tight-packing index (TPI = average number of long, interpenetrating, and sutured contacts per grain) data were gathered from the Vedder Sandstones. CI and TPI are highly dependent on sorting and grain size, therefore, only medium-size arenites with less than 15% cement and ductile grains were used. The CI for the Vedder Sandstones ranges from 1.9 to 3.7 and TPI range from 1.3 to 2.2 (Figure 44a, b) (Table 9).

The CI and TPI values suggest that the Vedder Sandstones are moderate to tightly compacted with exception of calcite-cemented samples, and fall within the ranges reported by Horton et al. (2009) for similar depths. Tangential and point contacts are more common in shallower samples (Figure 44a) as well as samples containing abundant carbonate cement. Long, concavo-convex, and sutured contacts were more common in deeper samples (Figure 10). Compaction commonly deformed the grains that were more ductile in nature such as micas (biotite, muscovite), glauconite, and volcanics. The grains most affected by compaction were biotite and volcanics, which often were squashed to form pseudomatrix.

Fracturing of brittle grains is another common result of compaction and all grains were susceptible. Individual fractures (Figure 45) within grains as well as through-going fractures (Figure 46) are common in the Vedder Sandstones. Some through-going fractures contain calcite cement, suggesting that the fracture served as a pathway for migrating pore fluids. SEM-CL analysis indicates that some fractured grains were healed with other authigenic minerals (Figure 39).

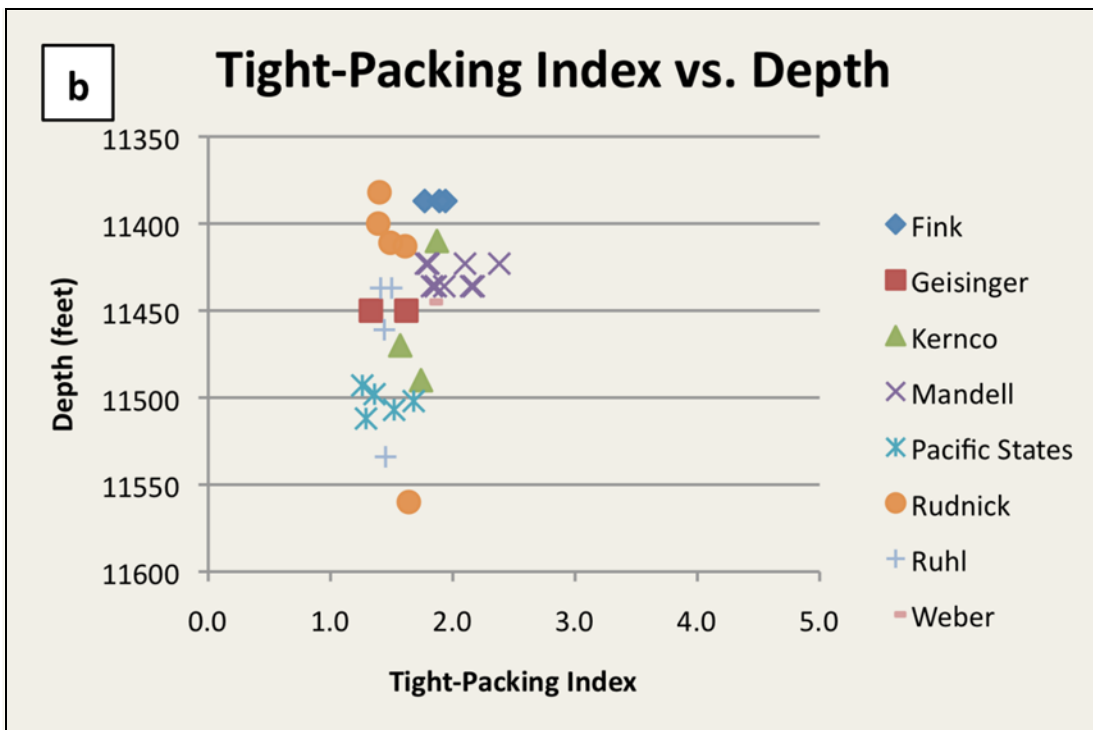
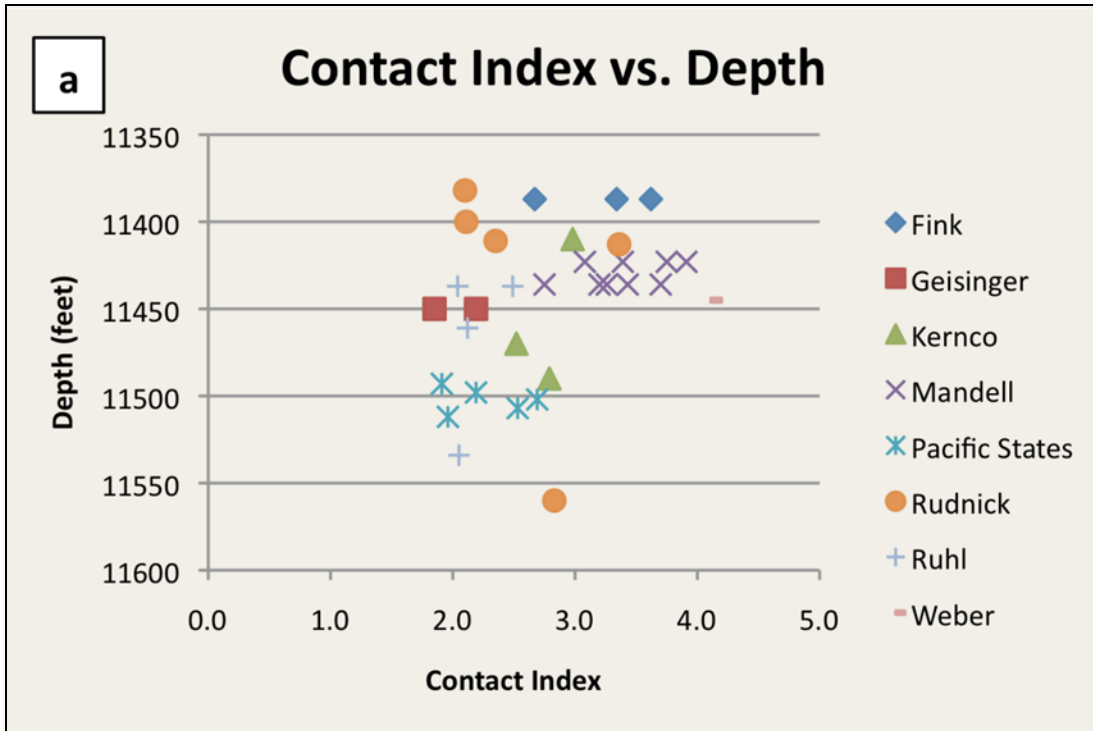


Figure 44: (a) Contact index (b) and tight-packing index of the Vedder Sandstones.

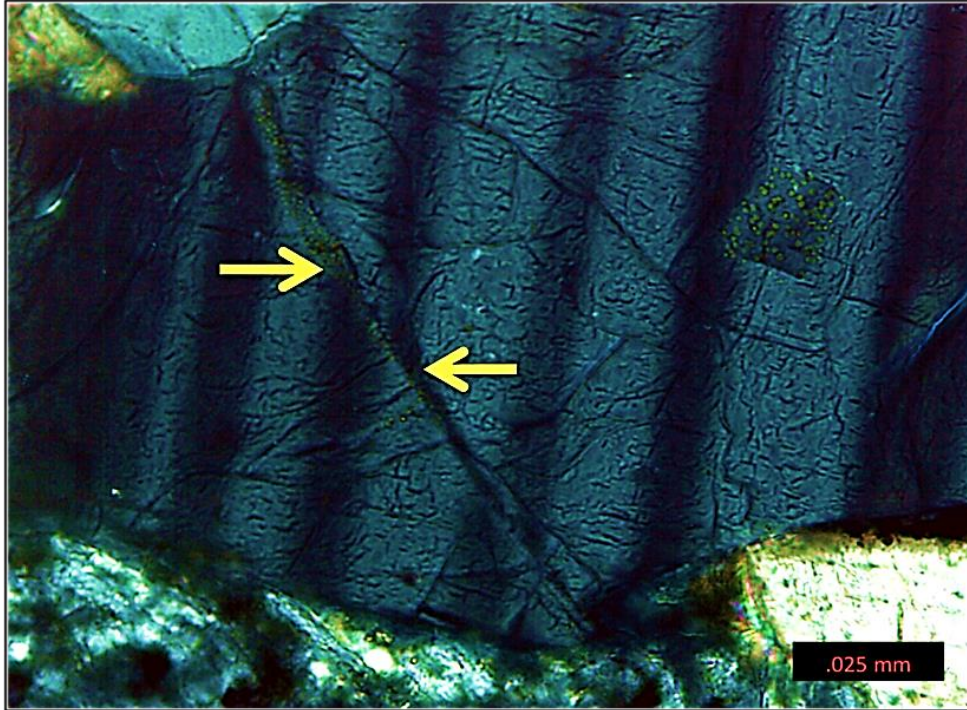


Figure 45: Twin lamellae in plagioclase grain offset along fracture (yellow arrow). Well: Pacific States 21, depth: 11,502 ft (3,505 m).

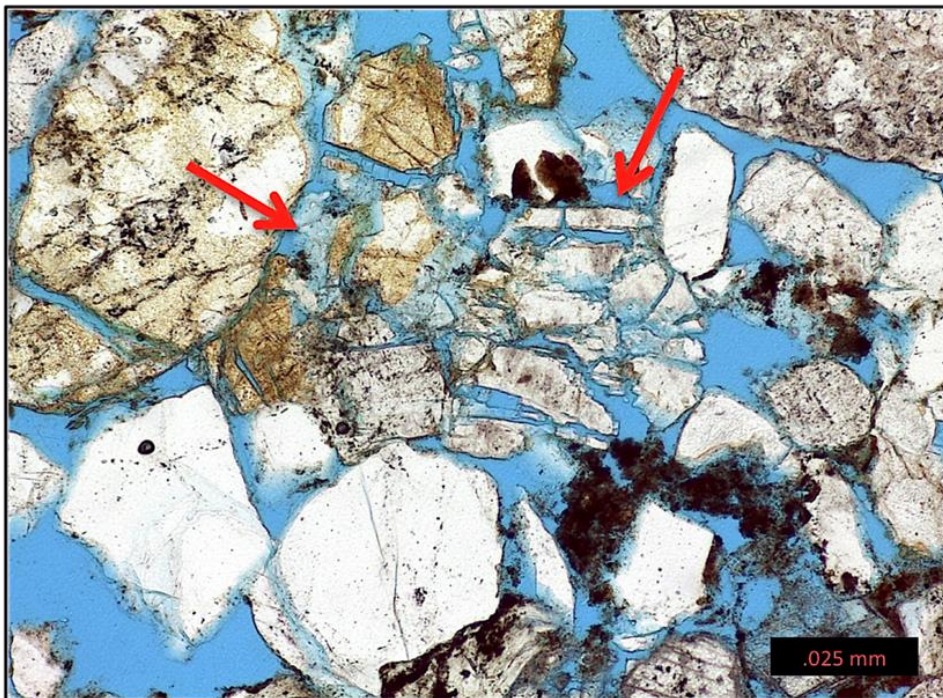


Figure 46: Intensely fractured feldspar grains (red arrows). Well: Kernco 61-34, depth: 11,410 ft (3,478 m).

## Porosity

Thin-section porosity ranges from trace to 31% of the rock volume (Tables 1-8) and shows considerable variation even through very narrow depth intervals (Figure 47). However, there is a general trend of decreasing thin-section porosity with increasing depth (Figure 47). Intragranular porosity averages 1% of the rock volume (Tables 1-8), and intergranular porosity averages close to 12% of the rock volume (Tables 1-8). Porosity is significantly less in carbonate cemented sandstones, matrix rich sandstones such as wackes, and sandstones rich in pseudomatrix (Figure 48).

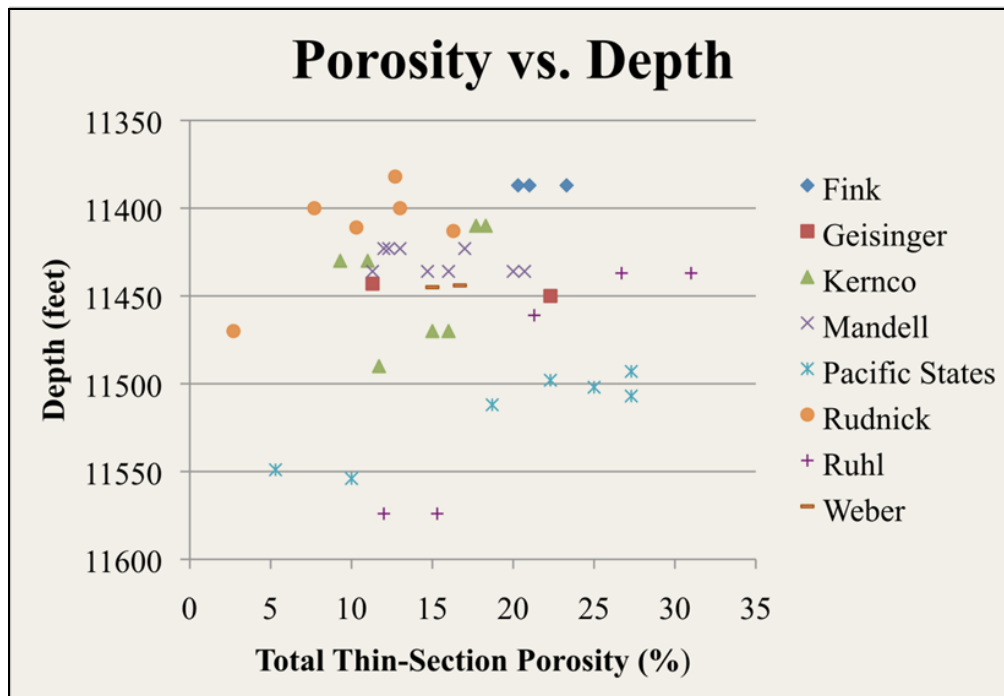


Figure 47: Plot of total porosity vs. depth (feet) for samples with less than a 15% combination of calcite, dolomite, clay, and ductile grains.



thin sections. These calculations are conservative in that unidentified dissolved grains were ignored, no adjustments were made for secondary porosity that may have been destroyed due to subsequent compaction; and no adjustments were made for mobilization of aluminum from albitization of feldspars.

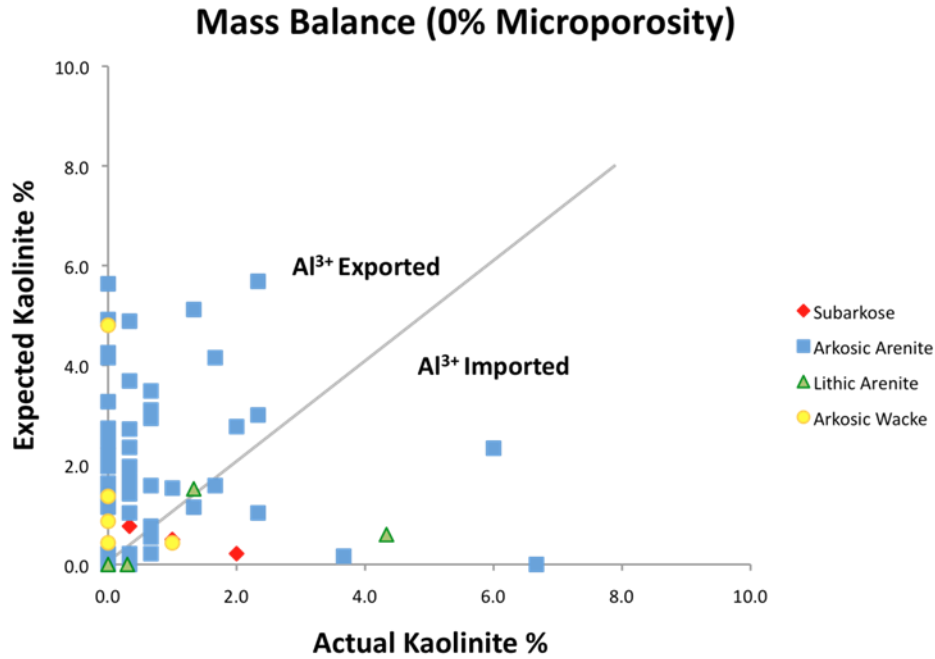


Figure 49: Plot of actual percent kaolinite vs. expected percent kaolinite assuming a microporosity of 0% according to the classification of examined Vedder Sandstones.

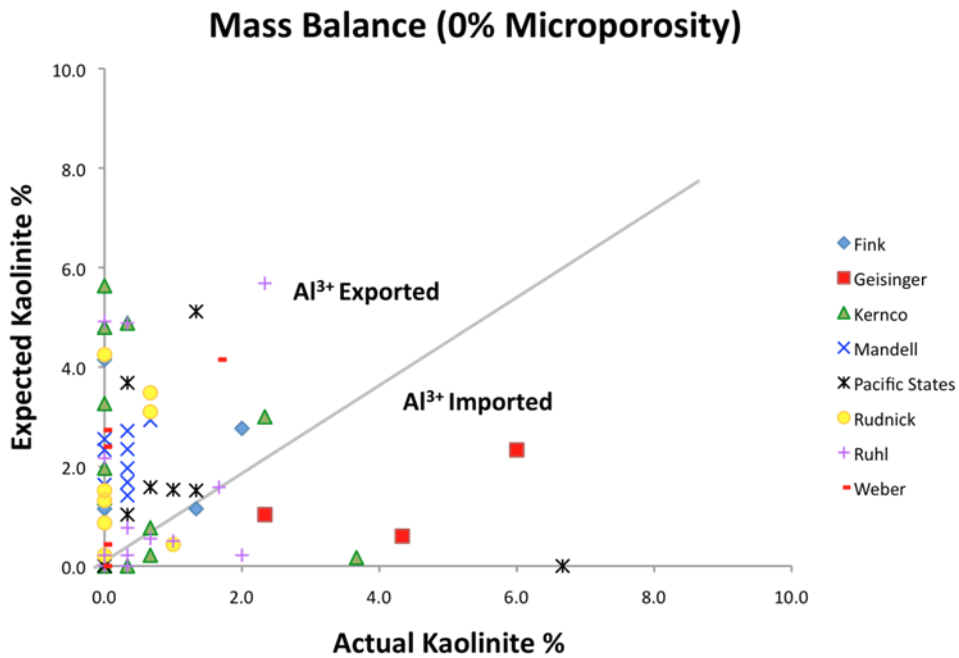


Figure 50: Plot of actual percent kaolinite vs. expected percent kaolinite assuming a microporosity of 0% according to each Rio Bravo well examined.

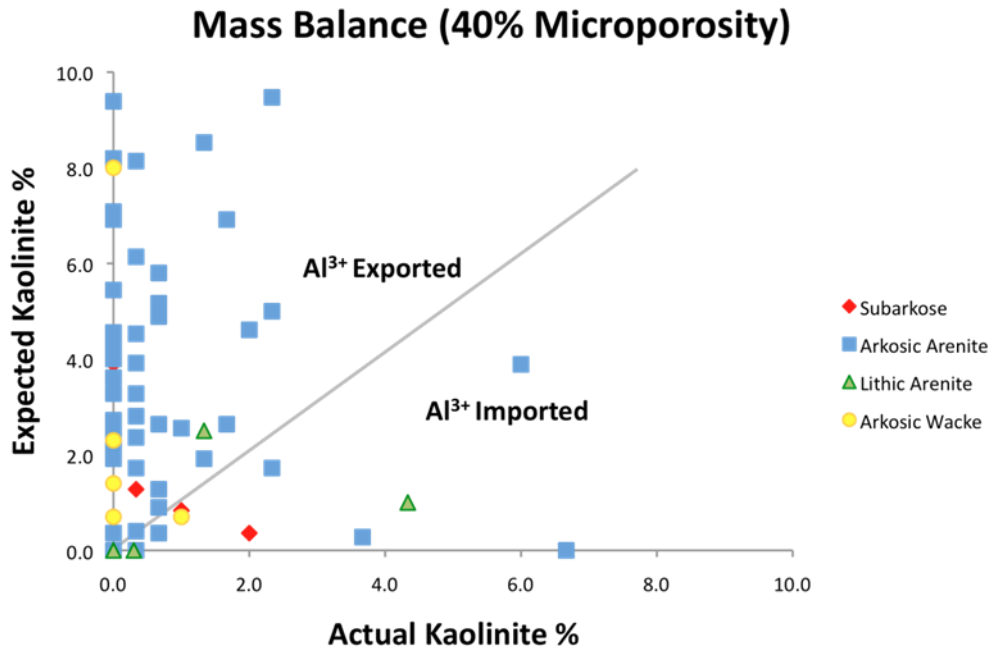


Figure 51: Plot of actual percent kaolinite vs. expected percent kaolinite assuming a microporosity of 40% according to the classification of examined Vedder Sandstones.

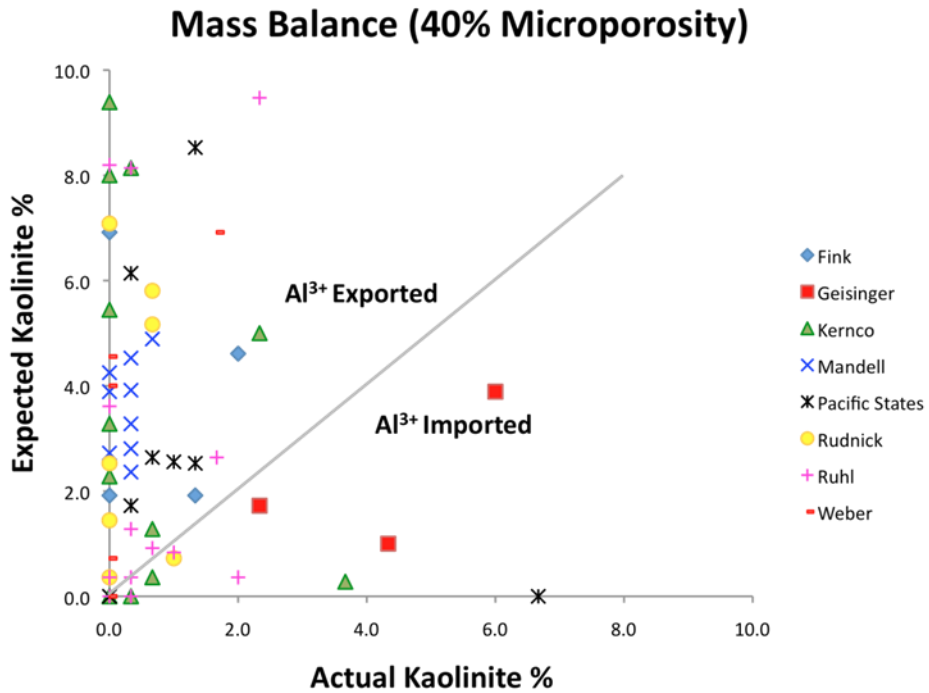


Figure 52: Plot of actual percent kaolinite vs. expected percent kaolinite assuming a microporosity of 40% according to each Rio Bravo well examined.

## DISCUSSION

The Vedder Sandstones at the Rio Bravo oil field were affected by numerous diagenetic processes which include compaction (ductile and brittle grains), cementation (grain coatings, overgrowths, pore-filling cements, clays), alteration (recrystallization of minerals, albitization), and dissolution of grains. These processes are of great importance from the standpoint of the oil reservoir. Each contributes to the destruction or development of porosity, which ultimately determines the reservoir quality and its potential to effectively produce hydrocarbons.

A paragenetic sequence of overlapping diagenetic events was established based on the textural relationships of the minerals (Figure 53). The earliest diagenetic events are shown occurring shortly after deposition and the latest occurring up until present time.

Early diagenesis of the Vedder Sandstones began penecontemporaneously with deposition. For glauconization to occur an abundant supply of potassium and iron must be present (Hower, 1961). This is essentially facilitated by the presence of decaying organic matter in reducing conditions accompanied by a slow rate of detrital influx (Cloud, 1955; Odin 1980; Stonecipher, 1999). These conditions are met in a submarine environment with depths ranging from 328 ft (100 m) to 984 ft (300 m) (Jimenez-Millan et al., 1998). During early diagenesis glauconite may also form from the alteration of micas, volcanic glass, biogenic pellets, and feldspars (Wilson and Pittman, 1977). Although Cloud (1955) suggests glauconite may be transported from its place of origin, reworked, or chemically mobilized and moved after burial, the Vedder Sandstones contained high concentrations of glauconite (Figure 14) suggesting it formed in place and supports the interpretation that the Vedder Sandstones were deposited in a marine shelf environment.

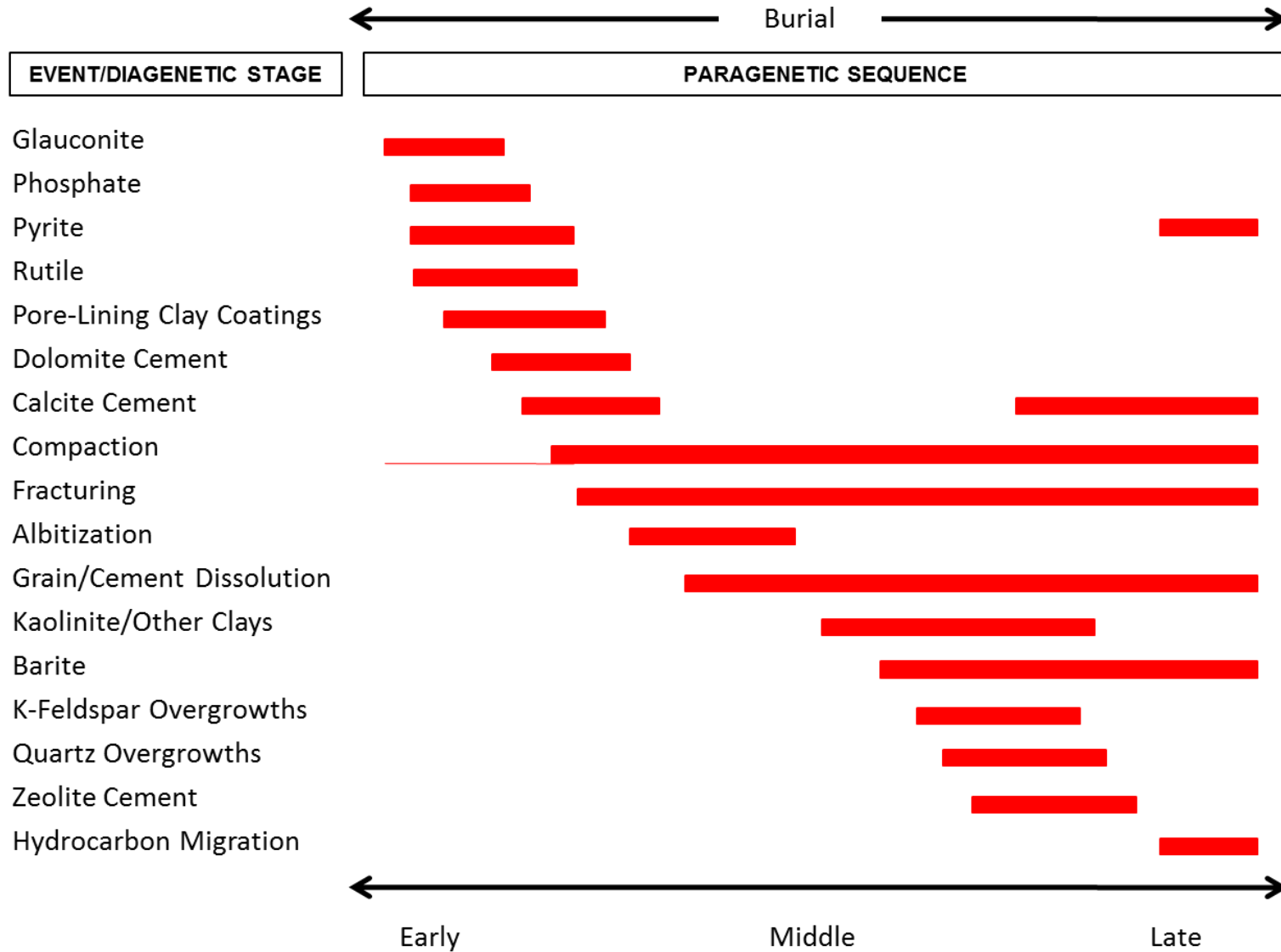


Figure 53: Paragenetic sequence for the Vedder Sandstones.

Phosphate (Figure 15) and glauconite (Figure 14) are often found together in marine sediments. While phosphate is known to be deposited in a wide range of depositional environments (Baturin, 1982), it normally occurs in a low energy marine environment. Phosphorites are linked to microbial decomposition of organic matter within sediments in which the decomposed organic matter releases phosphorous into the pore waters, or phosphate is released from hydrous ferric-oxide minerals (Glenn et al., 1994; Carson & Crowley, 1993). The occurrence of rounded glauconite and phosphate peloids occurring together and replacing silicate minerals is consistent with their formation penecontemporaneous with deposition and continuing through early diagenesis. Nguyen (2014, in press) analyzed the Vedder Sandstones at the Greeley oil field located southeast of the Rio Bravo oil field and observed phosphate nucleated on glauconite grains, further supporting the interpretation that phosphate formed shortly after glauconite.

Authigenic pyrite commonly occurs in association with glauconite grains that have been replaced by phosphate. Like glauconite and phosphate, pyrite formation is also dependent on decomposable organic matter and anoxic environments (Berner, 1970). The early formation of pyrite occurs during shallow burial in organic rich sediments, and is formed by the reaction of sulfide ions with fine-grained iron minerals (Berner, 1970; Morad, 1986a).

Authigenic pyrite also formed between cleavage planes within biotite (Figure 16b). This caused expansion of the biotite fabric thus creating pore space along the cleavage planes. These pores persist in tightly compacted sandstones where expansion of the fabric would have been unlikely; therefore this is an indication that formation of pyrite within biotite occurred during early stages of diagenesis. Textural relationships between pyrite crystals embedded within biotite suggests that alteration may have provided the iron source necessary for pyrite to precipitate as well as potentially providing the iron and potassium necessary for the formation of glauconite (Berner, 1970; Morad, 1986a).

Authigenic pyrite is present as well within chlorite that formed from alteration of biotite (Figure 22). The likely sources of iron for the formation of authigenic chlorite are attributed mostly to detrital biotite and Fe-Ti oxides such as ilmenite (Morad, 1986a). The pyrite observed within chlorite has expanded the fabric of the mineral, thus suggesting the formation of chlorite and pyrite under reducing conditions during early diagenesis.

Chlorite also occurs along fractures within silicate grains (Figure 21a), as thin coatings on detrital grains (Figure 21b), and as cement filling nearby pores (Figure 23). The occurrence along fractures suggests that while the chlorite formed early in the diagenetic history, it continued forming after the initiation of fracturing.

Authigenic rutile is minor and occurs predominantly as clusters of crystals within interstitial cements and on detrital grains. It is associated with pyrite and clays and possibly formed from dissolution of titanium-rich minerals such as ilmenite (Figure 17) (Morad, 1986b).

Carbonate cements observed within the Rio Bravo/Vedder Sandstones consist of dolomite and calcite (Figure 54). Dolomite precipitated as isolated euhedral rhombic (Figure 28) crystals, between biotite cleavage planes (Figure 31), and as pore-filling cement composed of euhedral to subhedral crystals (Figure 28). The expanded fabric shown in Figure 31 indicates a pre-compaction origin for the dolomite. Compositional zoning is common in dolomite crystals where the majority of samples display thin iron-rich zones (Figure 29). The zoning indicates precipitation under evolving geochemical conditions, thus suggesting the possibility of multiple periods of dolomite precipitation. In some rhombs the cores have been dissolved (Figure 29). This suggests that the dolomite contains varying trace element compositions within the crystals (Lee and Boles, 1996). Clay coatings and thin layers of anhydrite (Figure 42) cement are present on the dolomite rhombs. The presence of clay coatings suggest formation during early stages of diagenesis, while the timing of anhydrite precipitation is uncertain. However, dolomite commonly replaced quartz and feldspar grains (Figure 30) within compacted sandstones suggesting a later episode of dolomitic cement as well.

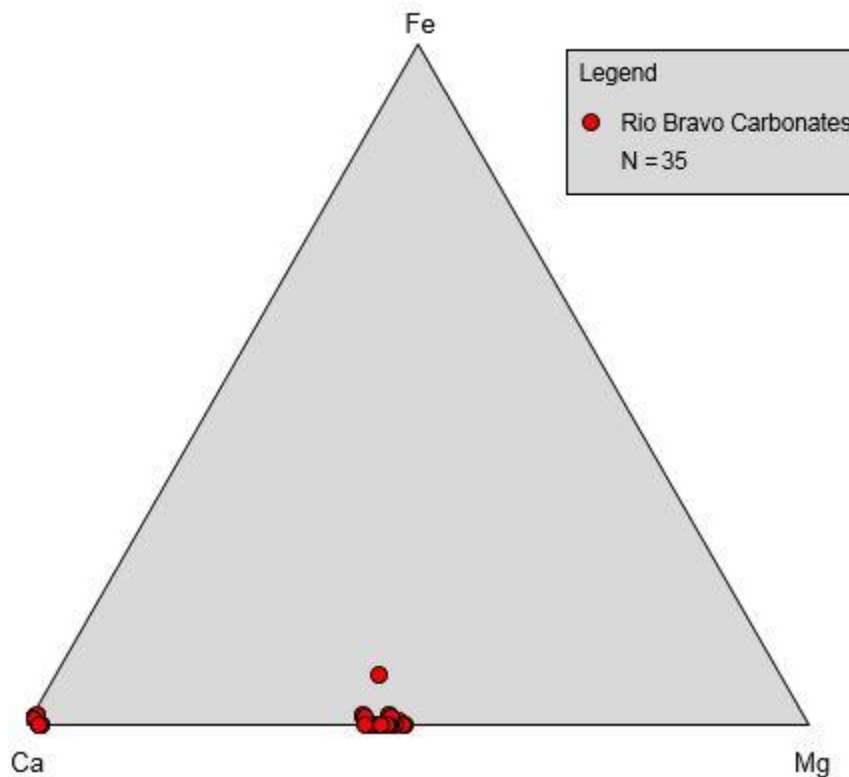


Figure 54: Ternary diagram showing Ca-Mg-Fe composition of carbonate cements (electron microprobe analysis).

The formation of early dolomite is followed by the precipitation of calcite. Early-stage calcite occurs as poikilotopic pore-filling cement in large pore spaces around detrital grains and early dolomite cement crystals. Clay coatings are present on detrital grains prior to the precipitation of early stage calcite (Figure 19). Calcite cementation can inhibit subsequent diagenesis by reducing the permeability to the point that migrating pore-fluids moved only minimally through the sandstone (Eslinger and Pever, 1988).

A second generation of calcite precipitation occurred as a late-stage cement within deeper compacted samples. Late-stage calcite precipitation is common in the San Joaquin basin as the albitization of plagioclase releases calcium ions into the pore fluids (Boles, 1984; Hayes and Boles, 1992; Perez and Boles, 2005). Late-stage calcite replaced quartz and

feldspar grains (Figure 32). In some instances calcite replaced albitized feldspars, indicating a later stage formation. Several through-going fractures are filled with calcite cement (Figure 33) suggesting that the fractures served as a pathway for migrating pore fluids.

Mechanical compaction in the Vedder Sandstones was one of the most important diagenetic processes that affected reservoir quality. Compaction began shortly after deposition causing deformation of labile grains (micas and volcanics) and squeezing them into adjacent pore spaces forming pseudomatrix (Figure 18, Figure 46). Significant volumes of pseudomatrix can clog pores resulting in a loss of usable porosity and connectivity, therefore, decreasing permeability. During early-stage diagenesis grains were also rearranged creating point and tangential contacts. As the sandstones were buried further, compaction increased and caused the grain contacts to evolve from point and tangential to long and concavo-convex as intergranular pressure-induced dissolution caused grains to dissolve into one another (Figure 10).

The frequency of occurrence of long, concavo-convex, and sutured contacts has been used as a measure of intensity of compaction of the sandstones. The detrital Vedder Sandstones contain an average of at least three contacts with adjacent grains (Table 9). No correlation and overall trend could be made in either CI or TPI in the Vedder Sandstones. Using samples from larger depth ranges, Horton et al. (2009) and Taylor (2007) found an increase of CI and TPI with increasing depth in the western San Joaquin Basin. The Rio Bravo/Vedder Sandstones fall within the ranges reported by Horton et al. (2009) for similar depths. The lack of any trend at the Rio Bravo oil field may reflect that the samples taken were from a narrow depth interval and showed considerable variations throughout.

Mixed-layer illite/smectite (I/S) or illite/chlorite (I/C) was formed during two diagenetic episodes, first as pore-lining clay and later as pore-filling cement. The initial clay rims are present as continuous linings of otherwise unfilled pores (Figure 24) and on detrital framework grains within poikilotopic calcite cement (Figure 19). This indicates that the clay rims formed

prior to precipitation of carbonates during early diagenesis. This type of early mixed-layer I/S or I/C is more abundant in shallower samples and may have formed during chloritization of biotite in which potassium was liberated (Morad, 1986a). Authigenic clays occurring as grain coatings, even in small amounts can severely restrict pore throats and thus significantly reduce permeability. In addition, clay coatings have been reported to inhibit quartz cementation by forming a protective coating over the quartz grain, thereby preventing the nucleation of quartz cement (Heald and Larese, 1973; Tillman and Almon, 1979).

Later-stage pore-filling illite/smectite or illite/chlorite is present in deeper samples but is generally absent in carbonate-cemented sands. Figure 24 shows I/S or I/C present as pore-lining cement. The pore linings span gaps created by fractures in feldspar grains suggesting that the clays formed after the initiation of grain fracturing.

Authigenic kaolinite formed during a later-stage of diagenesis after the onset of significant compaction, fracturing, dissolution, and albitization of feldspars. It occurs as well developed booklets that partially to completely fill intergranular pores (Figure 26). Kaolinite is frequently present adjacent to partially dissolved feldspars (Figure 27) suggesting that the silica and aluminum needed for kaolinite precipitation was probably derived from the dissolution and albitization of plagioclase grains (Helmold and Kamp, 1984; Morad et al., 1990; Perez and Boles, 2005).

With an increase in burial depth, and continuation of compaction and fracturing, albitization of plagioclase and potassium feldspars occurred within the Vedder Sandstones (Figure 35, 36, 41). Recognizing the occurrence of diagenetic albitization is important because this process can modify the pore size and influence the porosity and permeability of fluid reservoirs, especially when CO<sub>2</sub> supply is constant (Perez and Boles, 2005).

Albitization has been documented occurring within variable ranges of temperatures during middle-stage diagenesis (Gold, 1987; Boles and Ramseyer, 1988; Boles 1982; Morad et al., 1990). In the San Joaquin basin albite precipitation in open pore spaces has been

documented occurring at temperatures as low as 109° F (43° C), however albitization as a replacement doesn't start until temperatures are higher than 181° F (83° C) (Boles and Ramseyer, 1988). Perez and Boles (2005) proposed that fluid chemistry is important to the formation of authigenic albite, however, temperature is key. Albitization within the Rio Bravo Vedder Sandstones is more extensive in deeper sandstones that are poorly-cemented which suggests that albitization occurred after cementation.

Textural evidence reveals that sometimes albitization is guided by weaknesses in detrital grains like fractures and points of stress. Along the fractured grains pore fluids rich in sodium infiltrated the detrital feldspars and albitized along the fresh surface (Figure 35) (Taylor 2007, Horton et al., 2009;). Pseudomorphic replacement of detrital feldspars is also very common. This type of albitization consists of a gradual replacement of calcium and aluminum by sodium and silicon throughout the detrital grain and appears as a blocky to tabular pattern (Figure 36) (Boles, 1982; Gold, 1987).

Potassium feldspar is a common authigenic component in the Vedder Sandstones of the Rio Bravo oil field. Nearly pure authigenic potassium feldspar occurs within fractures in detrital feldspars and as overgrowths on both plagioclase and potassium feldspars (Figure 37). Cross-cutting relationships of fractures healed by authigenic albite and potassium feldspar indicate that albitization occurred prior to the precipitation of authigenic potassium feldspar (Figure 37). Authigenic feldspars precipitate under moderately high temperatures when sufficient concentrations of dissolved silica, sodium, and potassium are supplied in the pore waters (Kastner and Siever, 1979). It is estimated that precipitation temperatures for late diagenetic potassium feldspar ranges from 158° F (70° C) to 266° F (130°C) (R. Horton, personal communication).

Zeolite cement is present in one well: Kernco 61-34, at the crest of the structure in the Rio Bravo oil field (Figure 4) where chemical mobility may have been greatest. The formation of zeolite cement typically involves dissolution of volcanic grains generating mobilized K<sup>+</sup>, Na<sup>+</sup>,

Ca<sup>+</sup>, and Mg<sup>2+</sup> (Broxton et al., 1987). Aoyagi and Kazama, (1980) suggest that the transformation from volcanic glass to clinoptilolite occurs at a reservoir temperature of 140° F (60° C), and while the mineralogy of zeolite at Rio Bravo oil field was not determined, clinoptilolite is a common zeolite cement elsewhere in the San Joaquin basin (R. Horton, personal communication). Zeolite cement commonly coexists with carbonate cement, and although it has reduced porosity and permeability it appears to have protected the pore structure against compaction (Figure 34). Textural relationships confirm that zeolite cement post-dates carbonates, authigenic albite, and authigenic potassium feldspars (Figure 34). Authigenic quartz was not observed in samples containing abundant zeolite cement suggesting authigenic quartz formed later.

Authigenic quartz cement is not as widespread as authigenic albite and potassium feldspars. It is present as overgrowths and as a fracture filling cement in detrital quartz grains (Figure 39). The fractures produced from early stages of compaction are healed by secondary quartz. Although extensive studies reveal quartz precipitation occurs within a wide range of temperatures, most studies indicate the genesis of quartz cementation at temperatures ranging from 167° F (75° C) to 212° F (100° C) (R. Horton, personal communication).

Barite is present in one sandstone sample (Figure 41). It occurs as cement and replacing detrital grains. Figure 41 illustrates barite replacing an albitized plagioclase grain indicating barite formed after albitization.

The development of secondary porosity through dissolution of framework-grains plays an important role in the diagenesis of sandstones. Dissolution is a special type of alteration that acts to negate the effects of compaction on porosity. It is of great importance to the oil industry because primary migration of hydrocarbons commonly follows closely after the secondary porosity has been formed (Schmidt and McDonald, 1979). The Vedder Sandstones display several episodes of dissolution. An early stage of dissolution occurred prior to the onset of significant compaction as indicated by earlier clay fillings and linings. A later stage of dissolution

occurred after the initiation of compaction and fracturing, dissolving framework-grains and cement. An even later stage of dissolution occurred as evidenced by the dissolution of zeolite cement (Figure 34).

Dissolution affected mostly framework grains, however, dissolution of authigenic-cement (carbonate and zeolite) also occurred. Feldspars (particularly plagioclase) and volcanic grains were the most susceptible to dissolution, however, quartz grains are also significantly dissolved, primarily along grain edges (Figure 55). Dissolution of feldspar grains typically occurred along cleavage traces and broken grains (Figure 56). Figure 57 shows a ternary diagram that has been adjusted for grain dissolution. The arrowheads point to the present compositions and the tail ends represent the reconstructed compositions. The arrowheads with no tails indicate no change in composition. The length of the arrows indicate the magnitude of compositional shift. Preferential dissolution of feldspars, in particular plagioclase, resulted in a shifted composition of sandstones towards the quartz apex on the ternary diagram. Figure 58 shows the amount of secondary porosity that formed by dissolution of plagioclase feldspar plotted against depth and indicates a general trend of plagioclase decreasing with depth. Figure 59 shows the amount of secondary porosity that formed by dissolution of potassium feldspar plotted against depth and indicates that there was no significant change. Figure 7 shows a provenance ternary diagram that has been adjusted for grain dissolution. In determining the provenance of the Vedder Sandstones, pseudomatrix was added to lithic fragments while quartz and feldspars were adjusted for secondary porosity. The arrow heads represent the present composition and the tail ends represent the compositions reconstructed following Harris (1989). Most of the sandstones fall in the field of continental block (basement uplift), suggesting that the Vedder Sandstones are derived from the eastern Sierra Nevada. However, the reconstructed data may not truly represent the original composition of the Vedder Sandstones because there is evidence that secondary porosity may have been destroyed by continued compaction during increasing burial (Horton et al., 2009).

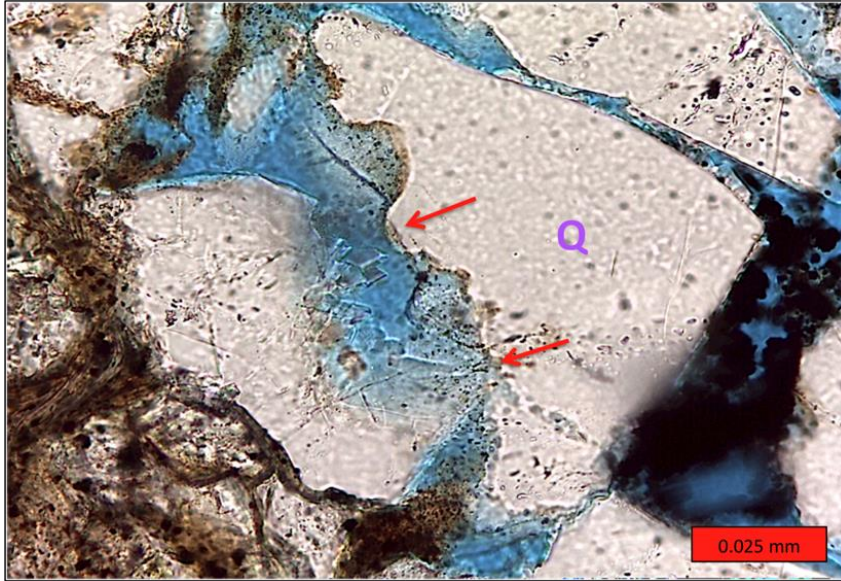


Figure 55: Quartz grain showing effects of dissolution along the grain's edge. Well: Fink 1, depth: 11,387 ft (3,471 m).



Figure 56: Partially dissolved K-feldspar (K) grain. Dissolution occurs parallel to cleavage plains. Well: Pacific States 21, depth: 11,382 ft (3,469 m).

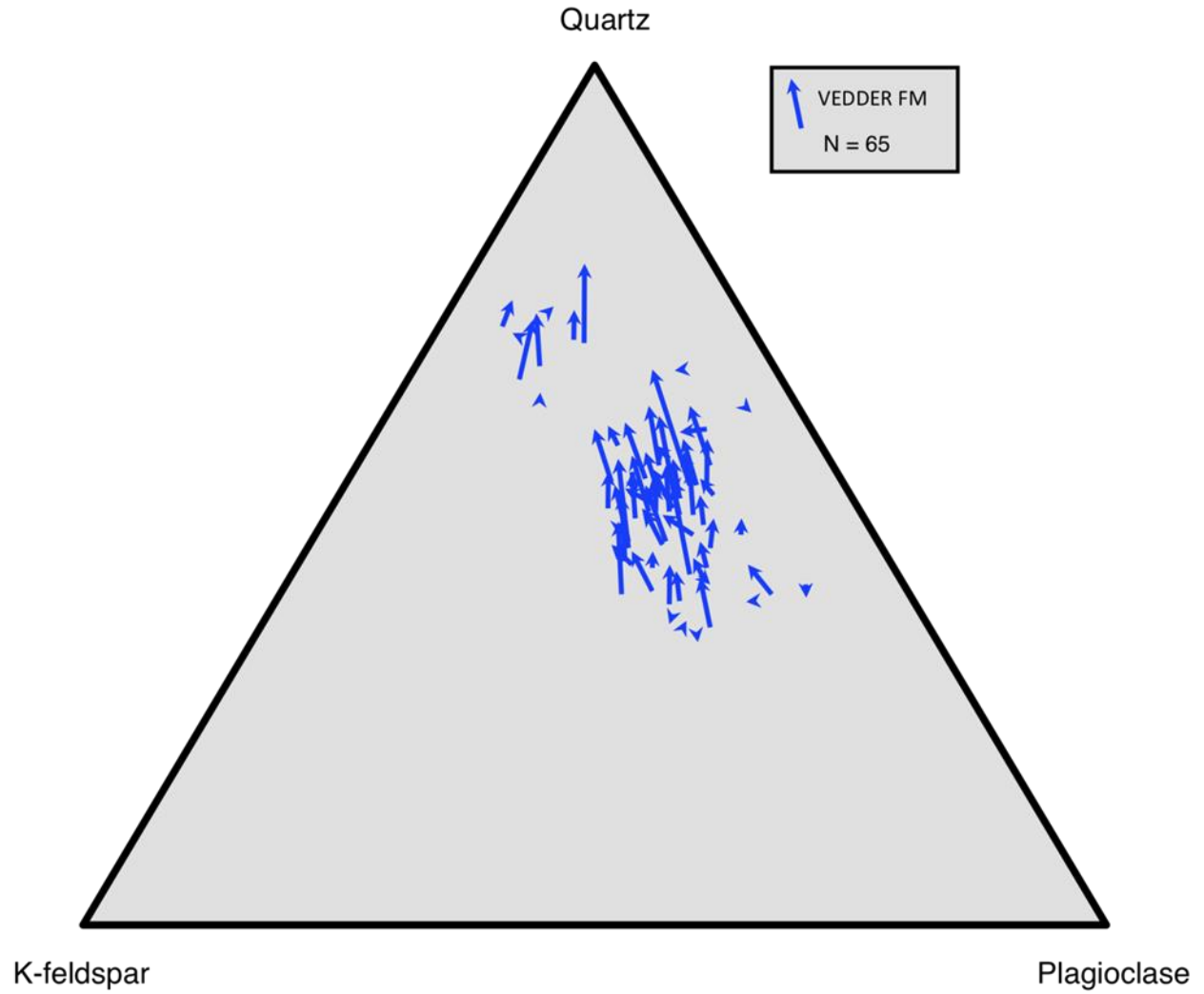


Figure 57: QKP ternary diagram plotted for the Vedder sandstones following the methodology of Harris (1989). The arrow heads indicate the present composition, the arrow tails show the reconstructed compositions.

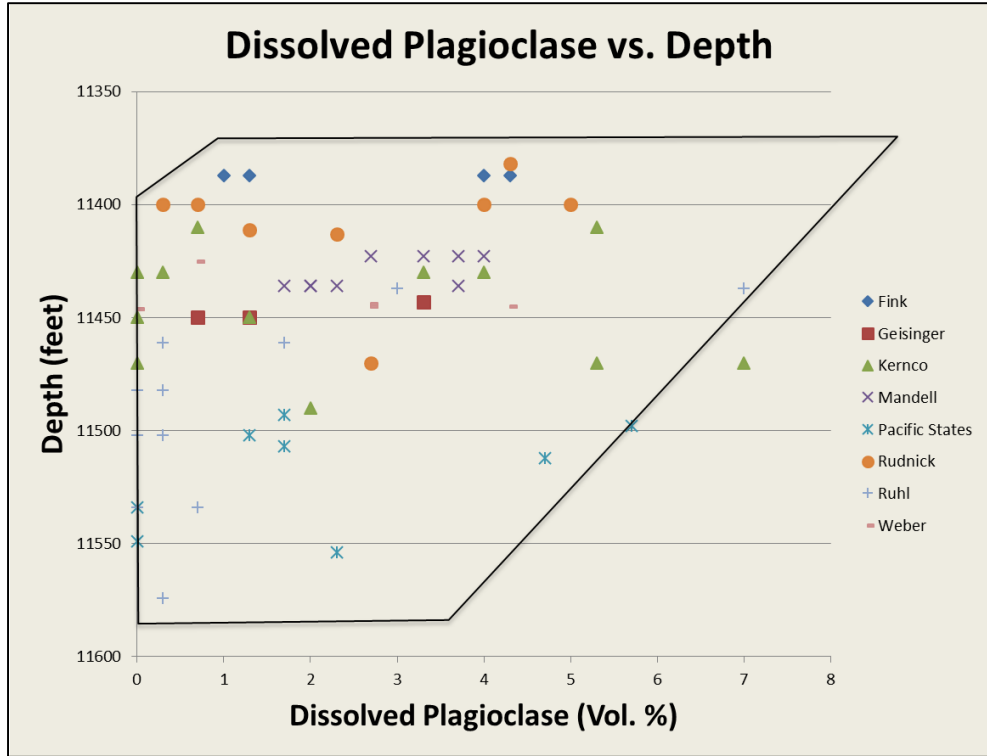


Figure 58: Plot of percent dissolved plagioclase volume vs. depth in feet.

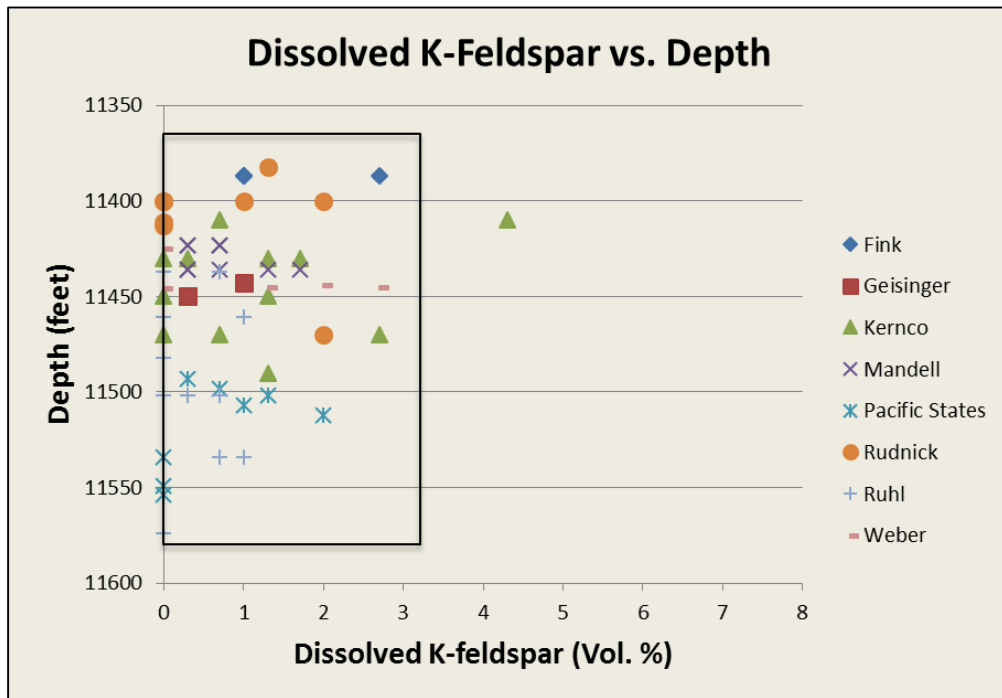


Figure 59: Plot of percent dissolved K-feldspar volume vs. depth in feet.

While the development of secondary porosity through dissolution in sandstones has been well documented (Rowse and de Swardt, 1974; Hayes, 1977, 1979; Schmidt et al, 1977; Schmidt and McDonald, 1979), the overall importance of this process in the development of porosity remains unresolved. Many (e.g. Bjorlykke, 1984, Boles, 1984; Bjorlykke and Jahren 2012; Hayes and Boles, 1991) suggest that marine sandstones porosity development is due to a redistribution of primary porosity, while others (e.g. McBride, 1987; Milliken, 1988; Harris, 1989; Wilkinson et al., 2001) suggest a significant transfer of dissolved material out of the system, especially aluminum. Theoretical models have been developed in order to settle the difference in the development of porosity and suggest that only limited amounts of dissolved materials, especially aluminum, are exported out of the system (Lundegard et al., 1984; Bjorlykke, 1984; Hanor, 1984; Walter, 1986; Giles, 1987; Stoessell, 1987; Bjorlykke et al., 1988; Hutcheon and Abercrombie, 1990; Hayes and Boles, 1991). Thus, these models propose that as the temperature rises during burial, aluminum solubility increases only slightly. In order for aluminum-silicates to dissolve, there must be a nearby aluminum sink or the pore fluids would quickly become supersaturated and dissolution would end. This generally assumes that there is not enough movement of water through the rocks at deep depths to remove aluminum through fluid flow unless large volumes of fresh water, which is not saturated with aluminum, flows through the rocks, as in a fresh water aquifer (Bjorlykke and Jahren, 2012). Experiments on the other hand have produced conflicting results suggesting that deep burial diagenesis rather than meteoric flushing is responsible for export of dissolved material, especially aluminum, out of the system (Crossey et al, 1986; MacGowan and Surdam, 1988; Harris, 1989; Surdam et al., 1989; Fein, 1991; Thyne, 2001; Thyne et al., 2001).

Mass transfer of aluminum in the Rio Bravo Vedder Sandstones was analyzed by comparing the volumes of kaolinite cement present to the volumes of kaolinite cement that would have formed if all aluminum liberated by dissolution of feldspars precipitated as kaolinite. The results suggest an overall export of aluminum from the sandstones (Figure 49 -Figure 52)

as there is less kaolinite present than is predicted from the observed dissolution of feldspar. In addition, the calculations do not take into account albitization of plagioclase, dissolution of other alumino-silicates, secondary porosity for which the precursor mineral could not be determined, or any secondary porosity that may have been destroyed through subsequent compaction (Taylor, 2007; Nguyen, 2014; Nguyen, in press). All of these potentially would have released additional aluminum into the pore fluids. Therefore, export of aluminum from the Vedder Sandstones is likely. These results agree with the work of Harris (1989) and suggest that dissolution can occur without fresh water. The Rio Bravo water is diluted seawater so some fresh water entered the system, however, there was not flushing by large volumes of fresh water either from shale diagenesis or from meteoric input.

Laumontite cement has been documented within a number of reservoirs in the San Joaquin basin (e.g. Bloch et al., 1993; Bloch and Helmond, 1995; Noh and Boles, 1993; Taylor, 2007), however, no laumontite was observed in the Oligocene Vedder Sandstones at the Rio Bravo Oil Field. Studies at the nearby Greeley (Nguyen, 2014; Nguyen, in press) and Wasco (Olabisi, 2015) oil fields suggests that laumontite precipitation occurs between 130 to 135°C on the east side of the basin. The lack of laumontite at the Rio Bravo Oil Field suggests that the sandstones were never buried deeply enough for laumontite to precipitate, thus the Oligocene Vedder Sandstones are currently at or near their maximum burial depth.

Hydrocarbons migrated into available pore space during late diagenesis (Figure 43). Late pyrite cement occurs in association with hydrocarbons in oversize pores and other secondary porosity (Figure 16 c, d). Late pyrite may have formed as iron in the pore waters reacted with sulfur liberated from continuing maturation of the hydrocarbons (Nguyen 2014; Nguyen, in press). This is possible because hydrocarbons do not displace all of the pore water from the reservoir (Syed, 1981).

## SUMMARY

The Oligocene Vedder Sandstones at the Rio Bravo oil field are composed of shallow marine sandstones that are arkosic to lithic arenites. The sandstones contain abundant quartz, plagioclase and potassium feldspars, and minor rock fragments. Common accessory minerals include biotite, muscovite, zircon, hornblende, rutile, garnet, epidote, and magnetite/titanomagnetite. Reservoir quality of the Oligocene Vedder Sandstones at the Rio Bravo oil field has been controlled by several diagenetic features: compaction, cementation, deformation, dissolution, recrystallization, and replacement of minerals. These diagenetic processes significantly altered the reservoir quality by reducing porosity through compaction and cementation or enhancing porosity through dissolution.

Porosity within the Vedder Sandstones ranges from trace amounts to 31% and is controlled by compaction, cementation, and alteration of grains. Mechanical and chemical compaction is evidenced by long and interpenetrating grain contacts, fractured and broken framework grains, sutured quartz grains, deformed ductile grains, and the presence of pseudomatrix. Compaction impacted porosity and permeability through grain rearrangement, fracturing, and deformation of labile grains.

Cementation played a smaller role in affecting reservoir quality. Kaolinite cement is present in the majority of samples and occurs as scattered pore-lining and pore-filling cement, which formed as an alteration product of feldspar grains. Carbonate cement is also present in the majority of samples and forms as poikilotopic pore-filling cement that occurs throughout multiple stages of diagenesis. Zeolite cement is present in small amounts and is common among many of the samples containing significant volcanic grains. Composite images of SEM-BSE and CL images reveals quartz overgrowths present in very minor amounts.

Alteration of detrital grains and cement is widespread throughout the Vedder Sandstones. Illite-smectite or illite-chlorite, and chlorite commonly form from alteration of volcanics and biotite grains. SEM-EDS analysis reveals extensive albitization of both

plagioclase and potassium feldspars grains throughout the majority of uncemented samples. Dissolution of feldspar grains and alteration of rock fragments caused a slight compositional change in the Vedder Sandstones, resulting in more quartz rich sandstone.

Compaction, cementation, and alteration have significantly reduced porosity and permeability in the Vedder Sandstones, however, this reduction was reversed to some extent through the generation of secondary porosity during later diagenesis. The development of secondary porosity through dissolution of framework-grains created an open pore network to facilitate the migration and accumulation of hydrocarbons.

## **ACKNOWLEDGMENTS**

I would like thank Dr. Horton for fueling my passion to become a geologist and taking me under his wings to carry out this research. Thank you for all your guidance, support, knowledge and sense of humor throughout the years.

I would also like to express my gratitude to Dr. Junhua Guo and Brian Taylor for agreeing to be on my committee on such short notice, and for reviewing my work and providing me with great suggestions in such a timely manner.

A huge thank you to Elizabeth Powers for always being there for just about anything I needed to complete my thesis, and for helping to avoid complete meltdowns when my microscope needed fixing. Thank you for always being on top of everything. I thank Charles James and Eric Hierling at the California Well Sample Repository for being so efficient and helpful.

I would like to thank all my amazing friends I met because of this degree. You all (you know who you are) have helped me maintain my sanity and sense of humor throughout this process, and have taught me not to take life so seriously.

Finally, I would like to thank my family for their unconditional love and support throughout my professional career as a student. I thank my parents for always encouraging me to chase my dreams, and to never give up. Thank you to my husband Brady for being my biggest cheerleader in life, and for always being there to get me through the difficult times. I would be lost without you.

## REFERENCES

- Ali, S.A., 1981, Sandstone Diagenesis: Applications to Hydrocarbon Exploration and Production: Pittsburgh, Gulf Science & Technology Company, 221 p.
- Aoyagi, K., and Kazama, T., 1980, Transformational changes of clay minerals, zeolites and silica minerals during diagenesis. *Sedimentology*, v. 27, p. 179-188.
- Atwater, T., and P., Molnar, 1973, Relative motion of the Pacific and North American plates deduced from sea-floor spreading in the Atlantic, Indian, and South Pacific oceans, *in* Proceedings of the Conference on Tectonic Problems of the San Andreas Fault System: vol. 13, pp. 136-148.
- Bartow, J.A. 1991. The Cenozoic evolution of the San Joaquin Valley, California. U.S. Geological Survey Professional Paper 1501.
- Bartow, J.A., and McDougall, K., 1984, Tertiary stratigraphy of southeastern San Joaquin Valley, California: U.S. Geological Survey Bulletin. 1529-J, 41 p.
- Baturin, G.N., 1982. Phosphorites on the sea floor: origin, composition and distribution: New York, Elsevier Scientific Publishing Company, p. 291.
- Bent, J.V., 1988, Paleotectonics and provenance of Tertiary sandstones of the San Joaquin Basin, California: *in* Graham, S.A., ed., 1988, Studies of the Geology of the San Joaquin Basin: Pacific Section Society of Economic Paleontologists and Mineralogists vol. 60, p. 109-127.
- Berner, R.A., 1970, Sedimentary pyrite formation: *American Journal of Science*, v. 268, p. 1-23.
- Bjorlykke, K., 1984, Formation of secondary porosity: How important is it?: *American Association of Petroleum Geologists Memoir* 37, p. 277-286.
- Bjorlykke, K., Mo, A., and Palm, E., 1988, Modelling of thermal convection in sedimentary basins and its relevance to diagenetic reactions: *Marine and Petroleum Geology*, v. 5, p. 338-351.
- Bjorlykke, K., and Jahren J., 2012, Open or closed geochemical systems during diagenesis in sedimentary basins: Constraints on mass transfer during diagenesis and the prediction of porosity in sandstone and carbonate reservoirs. *American Association of Petroleum Geologists Bulletin* 96, p. 2193-2214.
- Bloch, S., Kelley, and S.A., Corrigan, J.D., and Kelton, M.J., 1993, Predictable distribution pattern of laumontite in Paleogene sandstones of the Tejon Block, southern San Joaquin Basin (California) (abs.): *American Association of Petroleum Geologists and Society for Sedimentary Geology Annual Meeting Abstracts*, v. 1993, p. 77.
- Bloch, S., and Helmond, K.P., 1995, Approaches to predicting reservoir quality in sandstones: *American Association of Petroleum Geologists Bulletin*, v. 79, p. 97-115.
- Boggs, S., 1992, *Petrology of Sedimentary Rocks*: New York, Macmillan Publishing Company, p. 353-408.

- Boles, J.R., 1982, Active albitization of Plagioclase, Gulf Coast Tertiary: *American Journal of Science*, v. 282, p. 165-180.
- Boles, J.R., 1984, Secondary porosity reactions in the Stevens sandstone, San Joaquin Valley, California *in* D.A. McDonald and R.C. Surdam, eds., *Clastic Diagenesis: American Association of Petroleum Geologists Memoir 37*, p. 217-224.
- Boles, J.R., and Coombs, D.S., 1977, Zeolite facies alteration of sandstones in the Southland Syncline, New Zealand: *American Journal of Science*, v. 277 p. 982-1012.
- Boles, J.R., and Franks, S.G., 1979, Clay diagenesis in Wilcox sandstones of Southwest Texas: Implications of smectite diagenesis on sandstone cementation: *Journal of Sedimentary Petrology*, v. 49, p. 55-70.
- Boles, J.R., and Ramseyer, K., 1988, Albitization of plagioclase and vitrinite reflectance as paleothermal indicators, San Joaquin basin *in* Graham, S.A., ed., *Studies of the Geology of the San Joaquin basin: Pacific Section Society for Sedimentary Geology*, v. 60, p. 129-139.
- Broxton, D.E., and Bish, D.L., and Warren, R.G., 1987. Distribution and chemistry of diagenetic minerals at Yucca Mountain, Nye County, Nevada. *Clays and Clay Minerals*, v. 35, p. 89-110.
- California Department of Conservation, Division of Oil, Gas, and Geothermal Resources (DOGGR), 1998, *Oil and Gas Fields in California: Sacramento, CD-1*, v. 1, p. 192-193.
- Carson, G.A., and Crowley, S.F., 1993. The glauconite-phosphate association in hardgrounds: examples from the Cenomanian of Devon, southwest England. *Cretaceous Research*, v. 14 p. 69-89.
- Castrano, J.R., and Sparks, D.M., 1974, Interpretation of vitrinite reflectance measurements in sedimentary rocks and determination of burial history using vitrinite reflectance and authigenic minerals, *in* R.R. Dutcher, P.A. Hacquebard, J.M. Schopf, and J.A. Simon, eds., *Carbonaceous materials as indicators of metamorphism: Geological Society of American Special Paper 153*, p. 31-51.
- Cloud Jr. P.E., 1955, Physical limits of glauconite formation: *American Association of Petroleum Geologists Bulletin*, v. 39, no. 4, p. 484-492.
- Crossey, L.J., Surdam, R.C., and Lahann, R., 1986, Application of organic/inorganic diagenesis to porosity prediction in Gautier, D.L., ed., *Roles of organic matter in sediment diagenesis: Society of Economic Mineralogists and Paleontologists Special Publication 38*, p. 147-155.
- Dickinson, W.R., 1970, Interpreting detrital modes of greywacke and arkose: *Journal of Sedimentary Petrology*, v. 40 p. 695-707.
- Dickinson, W.R., 1976, Sedimentary basins developed during evolution of Mesozoic-Cenozoic arc-trench system in western North America: *Canada Journal of Earth Sciences*, v. 13, p. 1268-1287.

- Dickinson, W.R., 1985, Interpreting provenance relations from detrital modes of sandstones, *in* Zuffa, G.G., ed., Provenance of Arenites: Dordrecht, Holland, Reidel, p. 333-361.
- Dickinson, W.R., et. al., 1987, Geohistory analysis of rates of sediment accumulation and subsidence for selected California basins, *in* Ingersol, R.V., and Ernst, W.G., eds., Cenozoic basin development of Coastal California: Prentice Hall, Inc., New Jersey, p. 1-23.
- Dott, R.H., Jr., 1964, Wacke, greywacke and matrix – what approach to immature sandstone classification: *Journal of Sedimentary Petrology*, v, 34, p. 625-632.
- Eslinger, E., and Pevear, E.R., 1988, Clay minerals for petroleum geologists and engineers: *Society of Economic Paleontologists and Mineralogists*, ch. 6, p. 10-29.
- Fein, J.B., 1991, Experimental study of aluminum-oxalate complexing at 80 degrees C; implications for the formation of secondary porosity within sedimentary reservoirs: *Geology*, v. 19, p. 1037-1040.
- Fischer, K.J., Heasler, H.P., and Surdam, R.C., 1988, Hydrocarbon maturation modeling of the San Joaquin basin, California *in* Graham, S.A., ed., 1988, Studies of the Geology of the San Joaquin Basin: Pacific Section Society of Economic Paleontologists and Mineralogists vol. 60, p. 53-64.
- Fischer, K.J., and Surdam, R.C., 1988, Contrasting diagenetic styles in a shelf/turbidite sandstone sequence: The Santa Margarita and Stevens sandstones, southern San Joaquin basin, California *in* Graham, S.A., ed., 1988, Studies of the Geology of the San Joaquin Basin: Pacific Section Society of Economic Paleontologists and Mineralogists vol. 60, p. 233-247.
- Furman U.H., 1941, Rio Bravo oil field. Summary of operations, California oil fields: San Francisco, Annual Report of the State Oil and Gas Supervisor, v. 27, 9-12.
- Gautier, D.L., and Scheirer, A.H., 2007a, Miocene total petroleum system – Lower Bakersfield arch assessment unit of the San Joaquin basin province: U.S. Geological Survey Professional Paper 1713, ch 14, p. [[http://pubs.usgs.gov/pp/pp1713/19/pp1713\\_ch14.pdf](http://pubs.usgs.gov/pp/pp1713/19/pp1713_ch14.pdf)].
- Gautier, D.L., and Scheirer, A.H., 2007b, Eocene composite total petroleum system – North and east of Eocene west side fold belt assessment unit of the San Joaquin basin province: U.S. Geological Survey Professional Paper 1713, ch. 19 p. [[http://pubs.usgs.gov/pp/pp1713/19/pp1713\\_ch19.pdf](http://pubs.usgs.gov/pp/pp1713/19/pp1713_ch19.pdf)].
- Giles, M.R., 1987, Mass transfer and problems of secondary porosity creation in deeply buried hydrocarbon reservoirs: *Marine and Petroleum Geology*, v. 4, p. 188-204.
- Gillespie, J.M., 2011. Potential for carbon capture and storage in Kern County oilfields: California State University, Bakersfield, *Geospatial Review*, v. 9. p. 3.
- Glenn, C.R., 1994. Phosphorous and phosphorites: sedimentology and environments of formation. *Eclogae Gologicae Helveticae* v. 87, no. 3, p. 747-788.

- Gold, P.B., 1987, Textures and geochemistry of authigenic albite from Miocene sandstones, Louisiana Gulf Coast: *Journal of Sedimentary Petrology*, V. 57, p. 353-362.
- Graham, S.A., 1987, Tectonic controls on petroleum occurrence in central California, *in* Ingersol, R.V., and Ernst, W.G., eds., *Cenozoic basin development of Coastal California*: Prentice Hall, Inc., New Jersey, p. 48-63.
- Hanor, J.S., 1984, Variation in the chemical composition of oil-field brines with depth in northern Louisiana and southern Arkansas: implications for mechanisms and rates of mass transport and diagenetic reaction: *Gulf Coast Association Geological Societies Transactions*, v.34, p. 55-61.
- Harding, T.P., 1976, Tectonic significance and hydrocarbon trapping consequences of sequential folding synchronous with San Andreas faulting, San Joaquin Valley, California: *American Association of Petroleum Geologists Bulletin*, v. 60, p. 356-378.
- Harris, N.B., 1989, Diagenetic quartzarenite and destruction of secondary porosity: an example from the Middle Jurassic Brent sandstone of northwest Europe: *Geology*, v. 17, p. 361-364.
- Hayes, M.J., 1977, Sandstone diagenesis the whole truth: *American Association of Petroleum Geologists Bulletin*, v. 61, p. 1380-1381.
- Hayes, J.B., 1979, Sandstone Diagenesis: The Hole Truth, in P.A. Scholle and P.R. Schluger, eds., *Aspects of Diagenesis: Society for Sedimentary Geology Special Publication 26*, p. 127-139.
- Hayes, M.J., and Boles, J.R., 1991, Investigation of aluminum mass-transfer in sandstones, southern San Joaquin basin, California (abs.): *American Association of Petroleum Geologists Bulletin*, v. 75, p. 366-367.
- Hayes, M.J., and Boles, J.R., 1992, Volumetric relations between dissolved plagioclase and kaolinite in sandstones: implications for aluminum mass transfer in the San Joaquin basin, California *in* D.W. Househnecht and E.D. Pittman, eds., *Origin, Diagenesis, and Petrophysics of Clay Minerals in Sandstone: Society for Sedimentary Geology Special Publication 47*, p. 111-123.
- Heald, M.T., and Larse R.E., 1973, The significance of the solution of feldspar in porosity development: *Journal of Sedimentary Petrology*, v. 43, p. 458-460.
- Heald, M.T., and Renton J.J., 1977, Diagenesis of the Mt. Simon and Rose Run Sandstones in western West Virginia and southern Ohio: *Journal of Sedimentary Petrology*, v. 47, p. 66-77.
- Helmold, K.P., and P.C. van de Kamp, 1984, Diagenetic mineralogy and controls on albitization and laumontite formation in Paleogene arkoses, Santa Ynez Mountains, California *in* D.A. McDonald, and R.C. Surdam, eds., 1984, *Clastic Diagenesis: AAPG Memoir 37*, p. 239-276.
- Hiatt, W.N., and Gallagher, J.L., 1975, History of the Rio Bravo Field, *in* *Journal of Petroleum Technology*, SPE 4182, p. 145-158.

- Horbury, A.D., and Robinson, A.G., 1993, Diagenesis, Basin development, and porosity prediction in exploration-An introduction: AAPG Studies in Geology v. 36, p. 1-4.
- Horton, Jr. R.A., McCullough, P.T., & Hanson, D.M., 2009, Grain dissolution, compaction, and development of secondary intergranular porosity, western San Joaquin basin, California. *In* Knauer, L.C., & Britton, A. (eds) Contributions to the Geology of the San Joaquin Basin, California: Pacific Section AAPG, Special Publication, MP48, p. 141-165.
- Hower, J., 1961, Some factors concerning the nature and origin of glauconite: American Mineralogist, v. 46, p. 313-334.
- Hutcheon, I., and Abercrombie, H., 1990, Carbon dioxide in clastic rocks and silicate hydrolysis: Geology, v. 18, p. 541-544.
- Isaacson, K.A., and Blueford, J.R., 1984, Kreyenhagen Formation and related rocks-a history, *in* Blueford, J.R., ed., Kreyenhagen Formation and related rocks: Pacific Section SEPM, v. 37, p. 1-7.
- Ingersoll, R.V., 1979, Evolution of the late Cretaceous forarc basin, northern and central California: Geological Society of America Bulletin, v. 90, p. 813-826.
- Jimenez-Millan, J., Molina, J.M., Nieto, F., L., and Ruiz-Ortiz, P.A., 1998, Glauconite and phosphate peloids in Mesozoic carbonate sediments (Eastern Subbetic Zone, Betic Cordilleras, SE Spain): Clay Minerals, v. 33, p. 547-559.
- Kastner, M., and Siever, R., 1979, Low temperature feldspars in sedimentary rocks: American Journal of Science, v. 279, p. 435-479.
- Kasline, F. E., 1941, Rio Bravo oil field. Summary of operations, California oil fields: San Francisco, Annual Report of the State Oil and Gas Supervisor, v. 27, 9-12.
- Lee, Y.I., and Boles, J.R., 1996. Depositional control on carbonate cement in the San Joaquin basin, California, Society for Sedimentary Geology, v. 55, p. 13-22.
- Lillis, P.G., and Magoon, L.B., 2007, Petroleum systems of the San Joaquin Basin Province, California-Geochemical Characteristics of Oil Types, in Scheirer, A.H., Joaquin Basin Province, California: U.S. Geological Survey Professional Paper 1713, ch. 9, 17 p. [[pubs.usgs.gov/pp/pp1713/09/pp1713\\_ch09.pdf](http://pubs.usgs.gov/pp/pp1713/09/pp1713_ch09.pdf)].
- Loucks, R.G., Dodge, M.M., and Galloway, W.E., 1984, Regional controls on diagenesis and reservoir quality in lower Tertiary sandstones along the Texas Gulf Coast: Part 1. Concepts and principles, p. 15-46.
- Lundegard, P.D., Land, L.S., and Galloway, W.E., 1984, Problem of secondary porosity: Frio Formation (Oligocene), Texas Gulf coast: Geology, v. 12, p. 399-402.
- MacGowan D.B., and Surdam, R.C., 1988, Difunctional carboxylic acid anions in oil-field waters: Organic Geochemistry, v. 12, p. 245-259.
- MacPherson, B.A., 1978, Sedimentation and trapping mechanisms in Upper Miocene Stevens and Older Turbidite Fans of Southeastern San Joaquin Valley: AAPG Bulletin, v. 62, p. 2243-2274.

- McBride, E.F., 1987, Diagenesis of the Maxon Sandstone (Early Cretaceous), Marathon region, Texas: A diagenetic quartzarenite: *Journal Sedimentary Petrology*, v. 57, p. 98-107.
- Merino, E., 1975, Diagenesis in Tertiary sandstones from Kettleman North Dome, California, I, Diagenetic mineralogy: *Journal of Sedimentary Petrology*, V. 45, p. 320-336.
- Milliken, K.L., 1988, Loss of provenance information through subsurface diagenesis in plio-Pleistocene sandstones, northern Gulf of Mexico: *Journal Sedimentary Petrology*, v. 58, p. 992-1002.
- Morad, S., 1986a, Pyrite-chlorite and pyrite-biotite relations in sandstones: *Sedimentary Geology*, v. 49, p. 177-192.
- Morad, S., 1986b, SEM study of authigenic rutile, anatase and brookite in Proterozoic sandstones from Sweden: *Sedimentary Geology*, v. 46, p. 77-89.
- Morad, S., Bergan, M., Knarad, R., and Nystuen, J.P., 1990, Albitization of detrital plagioclase in Triassic reservoir sandstones from the Snorre Field, Norwegian North Sea: *Journal of Sedimentary Petrology*, V. 60, p. 411-425.
- Moxon, I. W., 1988. Sequence Stratigraphy of the Great Valley Basin in the Context of Convergent Margin Tectonics *in* Graham, S.A., ed., 1988, *Studies of the Geology of the San Joaquin Basin: Pacific Section Society of Economic Paleontologists and Mineralogists* vol. 60, p. 3-28.
- Nilsen, T.H., and S.H., Clarke, Jr., 1975, Sedimentation and tectonics in early Tertiary continental borderlands of central California: U.S. Geological Survey Professional Paper 925, p. 64.
- Noh, J.H., and J.R. Boles, 1993, Origin of zeolite cements in the Miocene sandstones, North Tejon oil fields, California: *Journal of Sedimentary Petrology*, V. 63, p. 248-260.
- Nguyen D.T., 2014, Diagenesis of Oligocene and Eocene Sandstones at the Greeley oil field, Southern San Joaquin Basin, California (MS Thesis): Bakersfield, California, California State University, p. 45.
- Nguyen D.T., Horton R.A., and Kaess, A, *in press*, Diagenesis, plagioclase dissolution, and preservation of porosity in Eocene and Oligocene sandstones at the Greeley Oil Field, southern San Joaquin basin, California, USA, *in* Armitage, P.J., Butcher, A.R., Churchill, J.M., Csoma, A.E., Hollis, C., Lander, R.H., Omma, J.E., and Worden, R.H. (eds.), *Reservoir Quality of Clastic and Carbonate Rocks: Analysis, Modelling and Prediction: Geological Society, London, Special Publication*, v. 435.
- Odin, G.S., 1980, Galuconization and phosphatization environments a tentative comparison: *SEPM Special Publications* 29, p. 227-237.
- Olabisi, O.E., 2015, Petrology and Porosity Development in Oligocene and Eocene Sandstones of the Wasco Oil Field, San Joaquin Basin, California, USA (MS Thesis): Bakersfield, California, California State University, p. 62.

- Olson, H.C., 1988, Oligocene-middle Miocene depositional systems north of Bakersfield, California: Eastern basin equivalents of the Temblor Formation, *in* Graham, S.A., ed., 1988, Studies of the geology of the San Joaquin basin, Pacific Section, Society of Economic Paleontologists and Mineralogists, v. 60, p. 189-205.
- Perez J.R., and Boles, J.R., 2005, An empirically derived kinetic model for albitization of detrital plagioclase: *American Journal of Science*, v. 305, p. 312-343.
- Pettijohn, F.J., Potter, P.E., and R. Siever, 1987, *Sand and Sandstone* 2<sup>nd</sup> ed: New York, Springer-Verlag, 553 p.
- Ramseyer, K., J.R. Boles, and P.C. Lichtner, 1992, Mechanism of plagioclase albitization: *Journal of Sedimentary Petrology*, V. 62, p. 349-356.
- Reid, S.A., 1988, Late Cretaceous and Paleogene sedimentation along the east side of the San Joaquin Basin *in* Graham, S.A., ed., 1988, Studies of the Geology of the San Joaquin Basin: Pacific Section Society of Economic Paleontologists and Mineralogists vol. 60, p. 157-171.
- Richardson, E.E., 1966, Structure contours on top of the Vedder sand, southeasterne San Joaquin Valley, California: U.S. Geological Survey, Open-File Report, 15 p.
- Rowell, D.M., and de Swardt, A.M.J., 1974, Secondary leaching porosity in Middle Ecca Sandstones: *Transactions Geological Society South Africa*, V. 77, p. 131-140.
- San Joaquin Valley Geology and The History of Its Oil Industry, 2010, [http://sjvgeology.org/geology/oil\\_geology.html](http://sjvgeology.org/geology/oil_geology.html) (accessed December 12, 2015).
- Scheier, A.H., and Magoon, L.B., 2007, Neogene gas total petroleum system-Neogene nonassociated gas assessment unit of the San Joaquin basin province: U.S. Geological Survey Professional Paper 1713, ch. 22, 14 p. [[http://pubs.usgs.gov/pp/pp1713/14/pp1713\\_ch22.pdf](http://pubs.usgs.gov/pp/pp1713/14/pp1713_ch22.pdf)].
- Schmidt, V., McDonald, D.A., and Platt, R.L., 1977, Pore geometry and reservoir aspects of secondary porosity in sandstones: *Bulletin of Canadian Petroleum Geology*, v. 25, p. 271-290.
- Schmidt, V., and McDonald, D.A., 1979, Texture and recognition of secondary porosity in sandstone, *in* P.A. Scholle and P.R. Schluger, eds., *Aspects of Diagenesis: Society for Sedimentary Geology Special Publication* v. 26, p. 209-225.
- Shanmugam, G., 1985, Significance of secondary porosity in interpreting sandstone composition: *AAPG Bulletin*, v. 69, p.378-384
- Simonson, R. R., 1955, Oil in the San Joaquin Valley, California. *Journal of Sedimentary Research*, 25(2).
- Stoessell, R.K., 1987, Mass transport in sandstones around dissolving plagioclase grains: *Geology*, v. 15, p. 295-298.

- Stonecipher, S.A., 1999, Genetic characteristics of glauconite and siderite: Implications for the origin of ambiguous isolated marine sand bodies, in isolated shallow marine sand bodies: Sequence stratigraphic analysis and sedimentologic interpretation, Society for Sedimentary Geology Special Publication 64, 191-204.
- Sullivan, J.C., and Weddle, J.R., 1960, Rio Bravo oil field, in Summary of operations, California oil fields: San Francisco, Calif., Annual Report of the State Oil and Gas Supervisor, v. no. 1, p. 27-38.
- Surdam R.C., Crossey, L.J., Hagen, E.S., and Heasler, H.P., 1989, Organic-inorganic interactions and sandstone diagenesis: American Association of Petroleum Geologists Bulletin, v. 73, p. 1-23.
- Syed, A.A., 1981, Sandstone diagenesis: Applications to hydrocarbon exploration and production: Gulf Science and Technology Company, Pittsburgh, PA, 203 p.
- Taylor, B.L. 2007, Petrography and diagenesis of the Eocene Point of Rocks Sandstone, McKittrich oil field, Kern County, California. MS Thesis, California State University, Bakersfield, 273 p.
- Tieh, T.T., Berg, R.R., Popp, R.K., Brasher, J.E., and Pike, J.D., 1986, Deposition and diagenesis Upper Miocene arkoses, Yowlumne and Rio Viejo fields; Kern County, California: AAPG Bulletin, V. 70, p. 953-969.
- Tillman, R.W., and W.R. Almon, 1979, Diagenesis of frontier formation offshore bar sandstones, Spearhead Ranch Field, Wyoming, *in* P.A. Scholle and P.R. Schluger eds. Aspects of Diagenesis: SEPM Spec. Plub. No. 26, p. 337-378.
- Thyne, G.D., 2001, A model for diagenetic mass transfer between adjacent sandstone and shale: Marine and Petroleum Geology, v. 18, p. 743-755.
- Thyne, G.D., Boudreau, B., Ramm, M., and Midtbo, R.E., 2001, A reaction-transport model of K-spar dissolution and illitization in the Statfjord Formation, North Sea: American Association of Petroleum Geologists Bulletin, V. 85, p. 621-636.
- Wagoner, J., 2009, 3D Geologic Modeling of the Southern San Joaquin Basin for the Westcarb Kimberlina Demonstration Project – A status report. Lawrence Livermore National Laboratory, LLTNL-TR-410813, Livermore, CA.
- Walter, L.M., 1986, Relative efficiency of carbonate dissolution and precipitation during diagenesis: A progress report on the role of solution chemistry: Society of Economic Mineralogists and Paleontologists Special Publication 38, p. 1-12.
- Wilcox, R.E., Harding, T.P., and Seely, D.R., 1973, Basic wrench tectonics: AAPG Bulletin, v. 57, p. 74-96.
- Wilkinson, M., Milliken, K.L., Haszeldine, R.S., 2001, Systematic destruction of K-feldspar in deeply buried rift and passive margin sandstones: Journal of the Geological Society, v. 158, p. 675-683.

Wilson, J.C., and McBride, E.F., 1988, Compaction and porosity evolution of Pliocene Sandstones, Ventura Basin, California: AAPG Bulletin, v. 72, p. 664-681.

Wilson, M.C., and Pittman, E.D., 1977, Authigenic clays in sandstones: recognition and influence on reservoir properties and paleoenvironment analysis: Journal of Sedimentary Petrology, v. 47, p. 3-31.

Zhu, S., Zhu, X., Wang, X., and Liu, Z., 2012, Zeolite diagenesis and its control on petroleum reservoir quality of Permian in northwestern margin of Junggar Basin, China. Science China Earth Sciences, v. 55, p. 386-396.

## **APPENDIX I – POINT COUNT DATA**

Table 1: Point count data for Well: Fink

Depth (ft)	Qtz	K-spar	Plag	RF	Acc Min	Carb	Matrix	Pseudo	Clay Cem	Sec Inter ø	Inter ø	Intra ø	Total ø
11387	26.3	11.0	18.3	4.3	1.7	1.3	5.3	5.3	2.0	3.3	17.0	0.7	21.0
11388	17.0	13.0	15.7	8.0	0.3	28.7	5.7	2.3	0.0	3.3	2.0	0.0	5.3
11389	30.3	7.7	23.7	10.0	1.7	1.0	1.0	0.0	0.0	9.7	8.0	2.7	20.3
11390	27.3	6.3	17.7	9.0	0.7	3.0	0.7	0.0	4.3	6.3	16.3	0.7	23.3

Table 2: Point count data for Well: Geisinger

Depth (ft)	Qtz	K-spar	Plag	RF	Acc Min	Carb	Matrix	Pseudo	Clay Cem	Sec Inter ø	Inter ø	Intra ø	Total ø
11443	33.0	15.3	15.7	9.0	1.0	0.7	2.7	0.7	6.0	1.7	6.0	3.7	11.3
11450	30.0	7.7	6.7	17.0	0.0	5.0	0.7	0.0	4.3	2.0	20.0	0.3	22.3
11451	30.3	11.3	5.0	9.7	0.0	11.3	0.0	2.3	2.3	2.7	21.7	0.3	24.7

Table 3: Point count data for Well: Kernco

Depth (ft)	Qtz	K-spar	Plag	RF	Acc Min	Carb	Matrix	Pseudo	Clay Cem	Sec Inter ø	Inter ø	Intra ø	Total ø
11410	28.0	13.0	18.0	6.3	1.3	2.7	4.3	5.0	0.7	1.3	15.7	0.7	17.7
11410	19.0	12.7	16.0	9.3	1.0	11.3	2.7	5.3	0.0	9.3	5.0	4.0	18.3
11430	18.7	13.3	23.7	1.3	5.3	4.0	18.3	4.3	3.7	1.3	1.3	0.3	3.0
11430	21.3	13.0	15.7	8.3	1.7	11.0	7.3	6.0	2.3	6.0	2.0	1.3	9.3
11430	18.7	8.3	18.3	2.7	1.3	1.3	3.7	27.0	8.7	0.3	6.7	0.0	7.0
11430	26.7	14.3	20.7	6.0	0.7	1.7	10.0	5.0	1.7	9.3	1.0	0.7	11.0
11450	22.0	14.3	24.3	5.7	0.3	0.7	15.3	6.0	4.0	2.7	0.7	1.0	4.3
11450	21.0	11.0	12.3	5.0	0.0	46.7	0.0	0.0	0.0	0.7	0.0	0.0	0.7
11470	24.0	9.0	18.0	7.7	0.0	0.0	18.3	2.0	0.0	10.7	2.0	2.3	15.0
11470	12.0	7.3	15.3	3.3	0.7	51.7	0.0	0.0	0.0	0.0	2.7	0.0	2.7
11470	25.3	12.7	21.3	5.3	0.7	0.0	8.7	4.0	0.3	4.0	6.0	5.0	16.0
11490	20.3	13.0	23.0	4.7	1.3	0.3	3.3	0.7	18.7	5.0	6.7	1.0	11.7

Table 4: Point count data for Well: Mandell

Depth (ft)	Qtz	K-spar	Plag	RF	Acc Min	Carb	Matrix	Pseudo	Clay Cem	Sec Inter ø	Inter ø	Intra ø	Total ø
11423	31.0	11.7	21.7	3.3	6.0	0.3	2.7	0.0	1.3	5.3	10.0	1.7	17.0
11423	29.7	16.0	23.7	6.7	0.3	0.0	0.7	6.0	0.7	3.0	6.3	3.0	12.3
11423	30.3	9.3	23.7	5.3	1.3	1.7	9.7	0.0	3.0	5.7	6.7	0.7	13.0
11423	29.3	15.0	23.0	10.0	0.3	1.3	1.0	6.0	0.3	3.3	6.7	2.0	12.0
11436	27.0	10.3	19.3	6.7	1.0	1.7	8.7	0.3	0.3	4.7	14.3	1.0	20.0
11436	33.3	14.0	23.3	8.7	1.0	1.7	0.0	2.7	0.0	2.7	6.0	2.7	11.3
11436	27.0	9.3	21.7	7.7	1.7	0.7	8.7	0.3	0.3	4.3	15.0	1.3	20.7
11436	30.7	12.3	20.0	4.0	2.0	2.3	10.3	0.7	0.3	3.3	12.0	0.7	16.0
11436	33.7	13.3	21.0	8.0	0.7	1.7	0.3	4.0	0.0	2.0	11.3	1.3	14.7

Depth in feet; Compositional data in percent; Qtz = Quartz; K-spar = Potassium feldspar; Plag = Plagioclase feldspar; RF = Rock fragments; Acc Min = Accessory minerals; Carb = Carbonate cement; Matrix = Clay matrix; Pseudo = Pseudomatrix; Clay Cem = one or a combination of kaolinite, illite, smectite; Sec ø = Secondary porosity; Inter ø = Intergranular porosity; Intra ø = Intragranular porosity; Total ø = Total porosity.

Table 5: Point count data for Well: Pacific States

Depth (ft)	Qtz	K-spar	Plag	RF	Acc Min	Carb	Matrix	Pseudo	Clay Cem	Sec Inter ø	Inter ø	Intra ø	Total ø
11493	19.7	10.3	21.0	3.7	1.3	4.0	9.0	0.3	0.3	1.7	24.3	1.3	27.3
11498	27.0	13.7	27.7	5.3	1.0	8.0	0.7	0.3	0.3	8.3	12.7	1.3	22.3
11502	25.0	9.0	23.3	4.0	2.3	2.7	2.3	1.3	1.0	2.7	21.7	0.7	25.0
11507	24.0	8.0	19.7	3.7	3.0	4.0	1.7	3.7	1.3	2.3	24.0	1.0	27.3
11512	26.0	12.0	17.0	8.7	0.7	5.3	0.7	6.7	1.3	6.7	9.7	2.3	18.7
11534	25.0	9.3	18.3	3.7	0.0	38.7	0.0	1.7	0.0	0.0	0.0	0.0	0.0
11549	23.3	2.0	14.0	0.3	17.3	7.0	12.7	0.0	6.7	0.7	4.3	0.3	5.3
11554	24.7	8.3	16.3	20.0	0.3	11.0	0.7	3.0	1.3	2.0	6.7	1.3	10.0

Table 6: Point count data for Well: Rudnick

Depth (ft)	Qtz	K-spar	Plag	RF	Acc Min	Carb	Matrix	Pseudo	Clay Cem	Sec Inter ø	Inter ø	Intra ø	Total ø
11382	30.3	12.0	16.3	9.0	0.3	0.0	11.7	4.0	0.7	5.7	5.3	1.7	12.7
11401	16.7	12.0	19.0	5.7	1.0	8.7	25.0	1.7	1.0	1.0	4.0	0.0	5.0
11402	20.7	15.7	18.0	6.3	1.0	9.0	9.0	2.0	3.0	9.7	2.7	0.7	13.0
11404	14.3	6.0	18.0	2.3	0.0	41.0	2.7	5.0	5.7	0.3	1.0	0.0	1.0
11405	20.7	15.3	20.0	5.3	0.7	9.0	7.3	5.3	2.3	3.7	2.0	2.0	7.7
11411	18.7	5.0	23.3	3.0	0.0	0.0	33.7	7.7	1.0	2.0	0.3	0.3	2.7
11413	32.3	10.0	17.7	18.7	2.3	0.7	1.3	4.3	0.0	2.0	7.3	1.0	10.3
11477	28.0	11.7	16.3	6.0	0.0	5.3	5.3	1.7	2.3	7.7	7.3	1.3	16.3

Table 7: Point count data for Well: Ruhl

Depth (ft)	Qtz	K-spar	Plag	RF	Acc Min	Carb	Matrix	Pseudo	Clay Cem	Sec Inter ø	Inter ø	Intra ø	Total ø
11437	16.7	7.3	23.3	10.7	0.7	2.3	7.0	2.3	1.3	3.7	22.0	1.0	26.7
11437	26.7	6.0	14.0	6.0	1.7	4.7	4.7	2.0	0.3	9.3	18.0	3.7	31.0
11461	22.3	6.3	22.0	5.3	1.3	0.7	9.3	0.7	1.7	3.3	17.0	1.0	21.3
11461	21.3	3.0	8.7	2.3	1.3	55.3	0.0	0.0	1.3	0.3	0.3	0.0	0.7
11482	16.7	8.3	16.0	6.3	11.3	30.3	0.0	2.7	3.3	0.0	0.7	0.0	0.7
11482	16.3	6.0	11.0	13.3	0.0	29.3	5.3	1.0	5.0	0.3	8.3	0.0	8.7
11482	23.0	6.7	15.7	11.7	0.7	35.3	0.0	1.0	0.3	0.3	1.0	0.0	1.3
11502	31.0	8.0	4.3	8.0	0.0	33.0	0.3	0.3	2.0	0.3	4.3	0.0	4.7
11502	30.0	9.7	17.0	3.7	0.3	20.7	0.0	0.3	0.7	0.3	10.7	0.0	11.0
11502	32.3	12.7	7.3	8.0	0.0	23.0	0.0	0.0	1.3	0.0	10.7	1.0	11.7
11502	36.7	9.7	7.3	6.3	0.0	27.0	0.3	0.3	2.0	0.0	3.3	0.3	3.7
11534	32.0	11.0	3.7	3.7	2.0	21.0	0.0	0.0	0.7	2.3	15.0	1.0	18.3
11534	43.0	14.3	4.0	5.7	0.0	23.7	0.0	0.0	1.0	0.7	3.3	1.0	5.0
11574	16.7	11.7	21.7	2.0	0.7	19.0	5.7	13.0	0.0	0.0	2.7	0.3	3.0
11574	18.7	11.0	16.7	2.0	0.0	16.0	9.3	5.0	2.3	10.7	0.7	0.7	12.0
11574	27.3	9.3	10.7	7.0	1.7	11.0	0.0	9.7	1.0	11.7	3.7	0.0	15.3

Table 8: Point count data for Well: Weber

Depth (ft)	Qtz	K-spar	Plag	RF	Acc Min	Carb	Matrix	Pseudo	Clay Cem	Sec Inter ø	Inter ø	Intra ø	Total ø
11425	28.3	8.7	19.7	1.0	1.3	0.0	22.7	5.7	0.0	1.3	2.3	0.3	4.0
11444	24.3	13.3	16.0	10.3	0.7	0.0	13.7	3.7	0.0	6.0	10.0	0.7	16.7
11445	24.3	14.3	17.7	3.0	0.3	17.0	0.0	12.7	0.0	5.0	3.0	0.0	8.0
11445	25.0	12.0	26.7	0.7	3.0	0.0	7.0	4.3	1.7	7.3	4.3	3.3	15.0
11446	32.0	13.0	5.7	12.7	0.0	29.7	1.3	0.0	0.0	0.3	0.0	0.0	0.3

Depth in feet; Compositional data in percent; Qtz = Quartz; K-spar = Potassium feldspar; Plag = Plagioclase feldspar; RF = Rock fragments; Acc Min = Accessory minerals; Carb = Carbonate cement; Matrix = Clay matrix; Pseudo = Pseudomatrix; Clay Cem = one or a combination of kaolinite, illite, smectite; Sec ø = Secondary porosity; Inter ø = Intergranular porosity; Intra ø = Intragranular porosity; Total ø = Total porosity.

## **APPENDIX II – CONTACT INDEX AND TIGHT-PACKING INDEX**

Table 9: Contact index and tight-packing index of the Vedder sandstones.

Well	Depth (ft)	CI	TPI	
Fink-1	11,387-1	2.7	1.8	
	11,387-2	N/A	N/A	
	11,387-4	3.3	1.9	
	11,387-5	3.6	1.9	
	11,443-1	N/A	N/A	
Geisinger	11,450-1	2.2	1.6	
	11,450-3	1.9	1.3	
	11,410-2	3.0	1.9	
Kernco 61-34	11,410-6	N/A	N/A	
	11,430-2	N/A	N/A	
	11,430-3	N/A	N/A	
	11,430-7	N/A	N/A	
	11,430-8	N/A	N/A	
	11,450-2	N/A	N/A	
	11,450-5	N/A	N/A	
	11,470-1	N/A	N/A	
	11,470-4	N/A	N/A	
	11,470-5	2.5	1.6	
	11,490-1	2.8	1.7	
	Mandell 3	11,423-1	3.9	2.1
		11,423-2	3.4	1.8
		11,423-4	3.8	2.4
11,423-5		3.1	1.8	
11,436-7		3.2	1.9	
11,436-8		3.3	2.2	
Pacific States	11,436-10	2.8	1.8	
	11,436-13	3.7	2.2	
	11,436-11	3.4	1.9	
	11,493	1.9	1.3	
	11,498	2.2	1.4	
	11,502	2.7	1.7	
	11,507	2.5	1.5	
	11,512	2.0	1.3	
Rudnick	11,534-55	N/A	N/A	
	11,549-55	N/A	N/A	
	11,554-60	2.8	1.6	
	11,382-400	2.1	1.4	
	11,400-1	N/A	N/A	
	11,400-2	N/A	N/A	
	11,400-4	N/A	N/A	
	11,400-5	2.1	1.4	
	11,470-7	N/A	N/A	
	11,411	2.4	1.5	
	11,413	3.4	1.6	

Well	Depth (ft)	CI	TPI
Ruhl-1	11,437-3	2.5	1.5
	11,437-5	2.0	1.4
	11,461-2	2.1	1.4
	11,461-3	N/A	N/A
	11,482-2	N/A	N/A
	11,482-3	N/A	N/A
	11,482-4	N/A	N/A
	11,502-1	N/A	N/A
	11,502-2	N/A	N/A
	11,502-3	N/A	N/A
	11,502-4	N/A	N/A
	11,534-1	2.1	1.5
	11,534-2	N/A	N/A
	11,574-1	N/A	N/A
	11,574-2	N/A	N/A
11,574-3	N/A	N/A	
Weber	11,425-4	N/A	N/A
	11,444-2	N/A	N/A
	11,445-1	N/A	N/A
	11,445-7	4.1	1.8
	11,446-6	N/A	N/A

**CI** = Contact Index

**TPI** = Tight-Packing Index

**N/A** = Not evaluated

## **APPENDIX III – MASS BALANCE DATA**

Table 10: Mass balance data of the Vedder Sandstones

Number of points counted	# of dissolved plagioclase counted (raw)	# of dissolved K-feldspar counted (raw)	# of kaolinite counted (raw)	Actual Kaolinite % (from point counts)	Expected kaolinite % (0% microporosity)	expected kaolinite % (40% microporosity)	Export or Import for 40% microporosity
300	3	3	4	1.3	1.2	1.9	Export
300	3	3	0	0.0	1.2	1.9	Export
300	13	8	0	0.0	4.2	6.9	Export
300	12	1	6	2.0	2.8	4.6	Export
300	10	1	18	6.0	2.3	3.9	Import
300	2	1	13	4.3	0.6	1.0	Import
300	4	1	7	2.3	1.0	1.7	Import
300	2	2	2	0.7	0.8	1.3	Export
300	16	13	0	0.0	5.6	9.4	Export
300	0	1	11	3.7	0.2	0.3	Import
300	10	5	7	2.3	3.0	5.0	Export
300	1	0	2	0.7	0.2	0.4	Import
300	12	4	0	0.0	3.3	5.4	Export
300	4	3	0	0.0	1.4	2.3	Export
300	0	0	1	0.3	0.0	0.0	Import
300	16	8	0	0.0	4.8	8.0	Export
300	0	0	0	0.0	0.0	0.0	Neutral
300	21	2	1	0.3	4.9	8.1	Export
300	6	4	0	0.0	2.0	3.3	Export
300	7	1	1	0.3	1.7	2.8	Export
300	12	2	2	0.7	2.9	4.9	Export
300	10	1	0	0.0	2.3	3.9	Export
300	11	2	1	0.3	2.7	4.5	Export
300	7	5	1	0.3	2.4	3.9	Export
300	11	1	0	0.0	2.6	4.3	Export
300	6	4	1	0.3	2.0	3.3	Export
300	5	2	1	0.3	1.4	2.4	Export
300	6	2	0	0.0	1.6	2.7	Export
300	4	1	1	0.3	1.0	1.7	Export
300	17	0	1	0.3	3.7	6.1	Export
300	4	4	3	1.0	1.5	2.6	Export
300	5	3	2	0.7	1.6	2.6	Export
300	19	6	4	1.3	5.1	8.5	Export
300	0	0	0	0.0	0.0	0.0	Neutral
300	0	0	20	6.7	0.0	0.0	Import
300	7	0	4	1.3	1.5	2.5	Export
300	13	4	2	0.7	3.5	5.8	Export
300	2	0	3	1.0	0.4	0.7	Import
300	15	6	0	0.0	4.3	7.1	Export
300	1	0	0	0.0	0.2	0.4	Export
300	12	3	2	0.7	3.1	5.2	Export
300	4	0	0	0.0	0.9	1.4	Export
300	7	0	0	0.0	1.5	2.5	Export
300	3	4	0	0.0	1.3	2.2	Export
300	10	0	0	0.0	2.2	3.6	Export
300	21	2	1	0.3	4.9	8.1	Export
300	5	3	5	1.7	1.6	2.6	Export
300	1	0	0	0.0	0.2	0.4	Export
300	0	0	0	0.0	0.0	0.0	Neutral
300	0	0	0	0.0	0.0	0.0	Neutral
300	1	0	1	0.3	0.2	0.4	Export
300	0	0	1	0.3	0.0	0.0	Import
300	0	0	0	0.0	0.0	0.0	Neutral
300	1	2	2	0.7	0.6	0.9	Export
300	1	0	6	2.0	0.2	0.4	Import
300	2	2	1	0.3	0.8	1.3	Export
300	0	3	3	1.0	0.5	0.8	Import
300	1	0	0	0.0	0.2	0.4	Export
300	17	12	7	2.3	5.7	9.5	Export
300	15	10	0	0.0	4.9	8.2	Export
300	2	0	0	0.0	0.4	0.7	Export
300	8	6	0	0.0	2.7	4.6	Export
300	8	4	0	0.0	2.4	4.0	Export
300	13	8	5	1.7	4.2	6.9	Export
300	0	0	0	0.0	0.0	0.0	Neutral

## **APPENDIX IV – SANDSTONE PETROGRAPHY DATA**

SANDSTONE PETROGRAPHY DATA

EXAMINED BY: SCL

THIN SECTION: Fink-1 (stained)  
FORMATION (AGE): Vedder  
LOCATION: Rio Bravo  
DEPTH: 11,387-1

PROJECT: Thesis  
ROCK NAME: Arkosic Arenite  
POINT COUNTS: 300

SORTING: very poor  
SIZE: Fine to coarse

COMPACTION: C1: 2.7 TPI: 1.8  
ANGULARITY: Subangular to subround

	SIZE	COMMENTS
1. Quartz (79) 26.33%	Monocrystalline Polycrystalline     Microphanerite   Volcanic Rock Fragment Quartz Arenite Other Sedimentary Metaquartzite Other Metamorphic	
2. K-Feldspar (33) 11%	Microcline      Orthoclase Sanadine Microphanerite   Volcanic Rock Fragment Sedimentary Metamorphic	
3. Plagioclase (55) 18.33%	Microphanerite   Volcanic Rock Fragment Sedimentary Metamorphic	Altering to clay     Mymekite present
4. Volcanics		
5. Microphanerites		
6. Accessory Minerals (5) 1.66%	Glaucophane    Biotite	Chlorite present hornblende present
7. Carbonate Cement (4) 1.33%	Poikilotopic calcite   Blocky calcite	
8. Pseudomatrix (32) 10.66%	Clay-Altered Grains	Matrix:
9. Clay Cement (6) 2%	Kaolinite Cement      ? Illite	
10. Intragranular Porosity (2) .66%	Quartz   K-Feldspar Plagioclase	VRF: Q K P PRF: Q K P
11. Intergranular Porosity (51) 17%	Fractures Fracture-induced dissolution Oversize/elongate pores       Grain-edge dissolution	Primary Porosity Other
12. Other (23) 7.66%	Organics/purite       Chert	

COMMENTS:  
Poikilotopic & blocky calcite present throughout  
lots of  $\phi$  However still clay matrix remains.  
Some areas of high compaction resulting in  
pseudomatrix. Kaolinite cement is present.

PARAGENESIS:  
Biotite  $\rightarrow$  chlorite

SECONDARY INTERGRANULAR POROSITY

FRACTURE-INDUCED DISSOLUTION		
Q	vrfQ	prfQ
K	vrfK	prfK
P	vrfP	prfP
GRAIN-EDGE DISSOLUTION		
Q	vrfQ	prfQ
K	vrfK	prfK
P	vrfP	prfP
OVERSIZE/ELONGATE PORES		
Q	vrfQ	prfQ
K	vrfK	prfK
P	vrfP	prfP
OTHER		

(16) 3.33%

SANDSTONE PETROGRAPHY DATA

EXAMINED BY: Syll

THIN SECTION: Fink-1 11,387-3  
 FORMATION (AGE): Rio Bravo, Miocene  
 LOCATION: Rio Bravo  
 DEPTH: 11,387-2

PROJECT: Thesis  
 ROCK NAME: Arkosic Arenite  
 POINT COUNTS: 300  
 COMPACTION: N/A  
 ANGULARITY: Sub angular

SORTING: Poor  
 SIZE: Fine sand

		SIZE	COMMENTS
1. Quartz	Monocrystalline Polycrystalline     Microphanerite Volcanic Rock Fragment   Quartz Arenite Other Sedimentary Metaquartzite Other Metamorphic		quartz → calcite:      Altered quartz:    Poly Altered:
51			
2. K-Feldspar	Microcline Orthoclase Sanadine Microphanerite   Volcanic Rock Fragment Sedimentary Metamorphic	Altered microcline:	Orthoclase → pseudo:       Orthoclase → calcite:       Altered ortho:
39			
3. Plagioclase	Microphanerite Volcanic Rock Fragment Sedimentary Metamorphic		Plag → Calcite:       plag → pseudo:    Plag Altering:
47			
4. Volcanics			Volcanic → pseudo:      Volcanic → calcite:
11			
5. Microphanerites			
6. Accessory Minerals	<u>biotite</u> <u>muscovite</u> <u>Epidote</u>	<u>Garnet</u>	
1			
7. Carbonate Cement			Muky carbonate:
86			
8. Matrix/Pseudomatrix		clay rim on grain:	
24			Biotite:
7			
9. Clay Cement			
10. Intragranular Porosity	Quartz K-Feldspar Plagioclase	VRF: Q K P	PRF: Q K P
11. Intergranular Porosity	Fractures    Fracture-induced dissolution Oversize/elongate pores    Grain-edge dissolution	Primary Porosity oversize pore from dissolution    Other	
6			
12. Other	<u>organics/pelite</u>       shale:    <u>R.F.</u>	Carbonate shale clast       Chert:	
25			

COMMENTS: Lots of carbonate and clay matrix, fracturing through thin section. Large shale clasts present. Small amounts of glauconite, clay laminations. Volcanics → pseudomatrix. Offset of fracture @ 8, 70.5 of shale clast. Sample was prepared crappy. Hard to distinguish grains.

PARAGENESIS: Calcite deposited first then squashed biotite grain around calcite. @ 36, 76.5  
 Dissolution of grains → clay → carbonate?

Fracturing → carbonate? evidence of this in fracture of CaCO<sub>3</sub> rhomb @ 8, 70.5 between carbonate → oil emplacement?

SECONDARY INTERGRANULAR POROSITY

FRACTURE-INDUCED DISSOLUTION		
Q	vrfQ	prfQ
K	vrfK	prfK
P	vrfP	prfP
GRAIN-EDGE DISSOLUTION		
Q	vrfQ	prfQ
K	vrfK	prfK
P	vrfP	prfP
OVERSIZE/ELONGATE PORES		
Q	vrfQ	prfQ
K	vrfK	prfK
P	vrfP	prfP
OTHER		

Not a lot of clay rims on grains probably diagenetic

SANDSTONE PETROGRAPHY DATA

EXAMINED BY: SZU

THIN SECTION: Fink  
 FORMATION (AGE): Vedder  
 LOCATION: Rio Bravo  
 DEPTH: 11,387-4

PROJECT: Thesis  
 ROCK NAME: Arkosic Arenite  
 POINT COUNTS: 300

SORTING:

COMPACTION: CI: 3.3 TPI: 1.9

SIZE:

ANGULARITY: subangular

	SIZE	COMMENTS
1. Quartz <u>91</u>	Monocrystalline Polycrystalline      Microphanerite Volcanic Rock Fragment    Quartz Arenite Other Sedimentary Metaquartzite Other Metamorphic	Altered to sericite:
2. K-Feldspar <u>23</u>	Microcline      Orthoclase Sanadine Microphanerite Volcanic Rock Fragment Sedimentary Metamorphic	Altered to sericite:    Altered to I/S?:
3. Plagioclase <u>68</u>	Microphanerite Volcanic Rock Fragment     Sedimentary Metamorphic	Altered to sericite:
4. Volcanics <u>13</u>		
5. Microphanerites		
6. Accessory Minerals <u>5</u>	<u>Epidote   </u> <u>Tourmaline</u> <u>biotite    </u>	<u>chlorite</u>
7. Carbonate Cement <u>3</u>		
8. Matrix/Pseudomatrix <u>3</u>	 Biotite → chlorite	
9. Clay Cement		
10. Intragranular Porosity <u>8</u>	Quartz   K-Feldspar      Plagioclase	VRF: Q K P PRF: Q K P
11. Intergranular Porosity <u>24</u>	Fractures Fracture-induced dissolution Oversize/elongate pores       Grain-edge dissolution	Primary Porosity Other
12. Other <u>30</u>	organics / pyrite:      Rock frag:	Phosphate:      Chert:      Hydrate:

COMMENTS:

Lots of  $\phi$ . Hardly any clay compared to previous. Some glauconite and carbonates. Clay rims possibly mixed layer I/S. A lot of plag grains are undergoing sericitization. Zeolite growth? 39, 80ish on plag grain. Lots of good overgrowths on grains. Lots of biotite. Some chlorite.

PARAGENESIS:

Dissolution → clay infiltration I/S?  
 Calcite → squashing of biotite  
 Lots of  $\phi$  due to  $CaCO_3$  dissolution? Some small patches calcite protected grains from high compaction.

SECONDARY INTERGRANULAR POROSITY

FRACTURE-INDUCED DISSOLUTION		
Q	vrfQ	prfQ
K	vrfK	prfK
P	vrfP	prfP
GRAIN-EDGE DISSOLUTION		
Q	vrfQ	prfQ
K	vrfK	prfK
P	vrfP	prfP
OVERSIZE/ELONGATE PORES		
Q	vrfQ	prfQ
K	vrfK	prfK
P	vrfP	prfP
OTHER		

SANDSTONE PETROGRAPHY DATA

EXAMINED BY: SZK

THIN SECTION: Fink-1 (stained)  
 FORMATION (AGE): Vedder  
 LOCATION: Rio Bravo  
 DEPTH: 11, 387-5  
 SORTING: very poorly sorted  
 SIZE: very fine to fine sand

PROJECT: Thesis  
 ROCK NAME: Arkosic Arenite  
 POINT COUNTS: 300  
 COMPACTION: Cl: 3.6 TPI: 1.9  
 ANGULARITY: Angular to subangular

		SIZE	COMMENTS
1. Quartz (60) 27.33%	Monocrystalline Polycrystalline    Microphanerite    Volcanic Rock Fragment    Quartz Arenite Other Sedimentary Metaquartzite Other Metamorphic	.24 mm - .08 mm	Altering to clay
2. K-Feldspar (19) 6.33%	Microcline Orthoclase Sanadine Microphanerite   Volcanic Rock Fragment Sedimentary Metamorphic	.16 - .18 mm	Chalcedony
3. Plagioclase (49) 18.33%	Microphanerite Volcanic Rock Fragment      Sedimentary Metamorphic	.28 - .1 mm	Plag altering to smectite    Altering to calcite   Altering to clay
4. Volcanics (9) 3%			
5. Microphanerites			
6. Accessory Minerals (15) 5%	? Red Muscovite    Glaucophane		Chlorite       Biotite     ? Mica    Muscovite
7. Carbonate Cement (9) 3%	Blocky calcite poikilotopic calcite		Dolomite   Blocky calcite
8. Pseudomatrix			Matrix:
Clay-Altered Grains			
9. Clay Cement (13) 4.3%	 Kaolinite		Illite?
10. Intragranular Porosity (2) .46%	Quartz K-Feldspar   Plagioclase	VRF: Q K P	PRF: Q K P
11. Intergranular Porosity (49) 16.33%	Fractures Fracture-induced dissolution Oversize/elongate pores Grain-edge dissolution		No clay around grains ? Primary Porosity       Other Dissolved clay
12. Other (28) 9.33%	RE       organics/purite		Chert

COMMENTS: Good pic of Kaolinite 11.5, 76.2 Some clay coatings, quartz overgrowths, chlorite is present throughout & is growing over quartz mostly. Lost of muscovite biotite. Some plag highly albified. Dolomite crystals present. Some poikilotopic & blocky calcite.

SECONDARY INTERGRANULAR POROSITY

FRACTURE-INDUCED DISSOLUTION		
Q	vrfQ	prfQ
K	vrfK	prfK
P	vrfP	prfP
GRAIN-EDGE DISSOLUTION		
Q	vrfQ	prfQ
K	vrfK	prfK
P	vrfP	prfP
OVERSIZE/ELONGATE PORES		
Q	vrfQ	prfQ
K	vrfK	prfK
P	vrfP	prfP
OTHER		

PARAGENESIS:  
 Chlorite forming after dissolution of clay?  
 Plag → calcite → late diagenetic?  
 Biotite → chlorite

(19) 6.33%

SANDSTONE PETROGRAPHY DATA

EXAMINED BY: SZL

THIN SECTION: Geisinger  
 FORMATION (AGE): Veader  
 LOCATION: Rio Bravo  
 DEPTH: 11,443-1

PROJECT: Thesis  
 ROCK NAME: Arkosic Arenite  
 POINT COUNTS: 300

SORTING: Moderate

COMPACTION: N/A too big would be bias

SIZE: Conglomerate

ANGULARITY: Subangular - subround

	SIZE	COMMENTS
1. Quartz (99) 33%	Monocrystalline Polycrystalline Microphanerite Volcanic Rock Fragment Quartz Arenite Other Sedimentary Metaquartzite Other Metamorphic	
2. K-Feldspar (46) 15.3%	Microcline Orthoclase Sanadine Microphanerite Volcanic Rock Fragment Sedimentary Metamorphic	Altering: Altering to Kaolinite:
3. Plagioclase (47) 15.6%	Microphanerite Volcanic Rock Fragment Sedimentary Metamorphic	Altering to sericite: Alter to calcite: Altered:
4. Volcanics (3) 1%		
5. Microphanerites		
6. Accessory Minerals (1) .33%	Biotite	
7. Carbonate Cement (2) .66%		
8. Matrix/Pseudomatrix (10) 3.3%		
9. Clay Cement (18) 6%	Kaolinite	
10. Intragranular Porosity (11) 3.6%	Quartz K-Feldspar Plagioclase	VRF: Q K P PRF: Q K P
11. Intergranular Porosity (18) 6%	Fractures Fracture-induced dissolution Oversize/elongate pores Grain-edge dissolution	Primary Porosity Other
12. Other (40) 13.3%	Matrix/organics R.F.	Bone chert Shale

COMMENTS:  
 Very large grains. Sample was prepared very poorly. Hard to distinguish grains. Little cement or clay. Lots of porosity. Very unconsolidated sample. Kaolinite cement throughout (lots)  
 - Part clay has high birefringence possibly chlorite?  
 PARAGENESIS: @ 31.5, 79ish  
 Calcite first then pseudo biotite. good pic

SECONDARY INTERGRANULAR POROSITY

FRACTURE-INDUCED DISSOLUTION		
Q	vrfQ	prfQ
K	vrfK	prfK
P	vrfP	prfP
GRAIN-EDGE DISSOLUTION		
Q	vrfQ	prfQ
K	vrfK	prfK
P	vrfP	prfP
OVERSIZE/ELONGATE PORES		
Q	vrfQ	prfQ
K	vrfK	prfK
P	vrfP	prfP
OTHER		
(5)	1.6%	

SANDSTONE PETROGRAPHY DATA

EXAMINED BY: SK

THIN SECTION: Greisinger-2 (stained)  
 FORMATION (AGE): Vedder  
 LOCATION: Rio Bravo  
 DEPTH: 11,450-1

PROJECT: Thesis  
 ROCK NAME: Lithic Arenite  
 POINT COUNTS: 300  
 COMPACTION: CI: 2.2 TPI: 1.6

SORTING: Poor

ANGULARITY: Subround to Rounded

SIZE: Medium to coarse sand

	SIZE	COMMENTS
1. Quartz (90) 30%	Monocrystalline Polycrystalline       Microphanerite Volcanic Rock Fragment Quartz Arenite Other Sedimentary Metaquartzite Other Metamorphic	
2. K-Feldspar (23) 7.6%	Microcline    Orthoclase Sanadine Microphanerite Volcanic Rock Fragment Sedimentary Metamorphic	
3. Plagioclase (18) 6.6%	Microphanerite    Volcanic Rock Fragment Sedimentary Metamorphic	
4. Volcanics (4) 1.3%		
5. Microphanerites		
6. Accessory Minerals		
7. Carbonate Cement (15) 5%	<u>Blocky Calcite</u>	
8. Pseudomatrix (2) - 4.6%	<u>Matrix</u>	
9. Clay Cement (13) 4.3%	<u>Kaolinite</u>	
10. Intragranular Porosity (1) .33%	Quartz K-Feldspar Plagioclase	VRF: Q K P PRF: Q K P
11. Intergranular Porosity (60) 20.0%	Fractures Fracture-induced dissolution Oversize/elongate pores Grain-edge dissolution	Primary Porosity Other
12. Other (10) 2.2%	<u>Chert</u>       <u>RF</u>	<u>Organics, pyrite</u>

COMMENTS: Good pic of Kaolinite. Lots of Kaolinite. Very unconsolidated, coarse grained, calcite cement patches throughout. Lots of  $\phi$  & rock fragments.

PARAGENESIS:

SECONDARY INTERGRANULAR POROSITY

FRACTURE-INDUCED DISSOLUTION		
Q	vrfQ	prfQ
K	vrfK	prfK
P	vrfP	prfP
GRAIN-EDGE DISSOLUTION		
Q	vrfQ	prfQ
K	vrfK	prfK
P	vrfP	prfP
OVERSIZE/ELONGATE PORES		
Q	vrfQ	prfQ
K	vrfK	prfK
P	vrfP	prfP
OTHER		
(6)	2%	

SANDSTONE PETROGRAPHY DATA

EXAMINED BY SL

THIN SECTION: Geisinger - 2 (stained)  
 FORMATION (AGE): Vedder  
 LOCATION: Rio Bravo  
 DEPTH: 11,450-3

PROJECT: Thesis  
 ROCK NAME: Arkosic Arenite  
 POINT COUNTS: 300

SORTING: Poor

COMPACTION: CI: 1.9 TPI: 1.3

SIZE: Medium to Coarse Sand

ANGULARITY: subround to Round

	SIZE	COMMENTS
1. Quartz (91) 30.3%	Monocrystalline Polycrystalline Microphanerite Volcanic Rock Fragment Quartz Arenite Other Sedimentary Metaquartzite Other Metamorphic	
2. K-Feldspar (34) 11.33%	Microcline Orthoclase Sanadine Microphanerite Volcanic Rock Fragment Sedimentary Metamorphic	
3. Plagioclase (14) 5%	Microphanerite Volcanic Rock Fragment Sedimentary Metamorphic	
4. Volcanics (6) 2%		
5. Microphanerites		
6. Accessory Minerals		
7. Carbonate Cement (24) 11.33%	Blocky Calcite Dolomite	
8. Pseudomatrix (7) 2.33%	Matrix	
9. Clay Cement (7) 2.33%	Kadinite	
10. Intragranular Porosity	Quartz K-Feldspar Plagioclase	VRF: Q K P PRF: Q K P
11. Intergranular Porosity (45) 21.66%	Fractures Fracture-induced dissolution Oversize/elongate pores Grain-edge dissolution	Primary Porosity Other
12. Other (32) 10.66%	clay organics/pyrite	

COMMENTS:  
 Blocky calcite occurring during possibly late diagenesis  
 Lots of  $\beta$ . Little clay matrix. Some matrix  
 turned into Kadinite. Very similar to #8 but  
 less grain contact.

PARAGENESIS:

SECONDARY INTERGRANULAR POROSITY

FRACTURE-INDUCED DISSOLUTION		
Q	vrfQ	prfQ
K	vrfK	prfK
P	vrfP	prfP
GRAIN-EDGE DISSOLUTION		
Q	vrfQ	prfQ
K	vrfK	prfK
P	vrfP	prfP
OVERSIZE/ELONGATE PORES		
Q	vrfQ	prfQ
K	vrfK	prfK
P	vrfP	prfP
OTHER		

SANDSTONE PETROGRAPHY DATA

EXAMINED BY: *SZL*

THIN SECTION: *Kemco 41-34 (stained)*  
FORMATION (AGE): *Vedder*  
LOCATION: *Rio Bravo*  
DEPTH: *11,410-2*

PROJECT: *thesis*  
ROCK NAME: *Arkosic Arenite*  
POINT COUNTS: *300*

SORTING: *Poorly Sorted*

COMPACTION: *C1: 3.0 TPI: 1.9*

SIZE: *Fine to medium Sand w/ Really lg. grains Randomly* ANGULARITY: *Subangular*

	SIZE	COMMENTS
1. Quartz (41) 28%	Monocrystalline Polycrystalline Microphanerite Volcanic Rock Fragment Quartz Arenite Other Sedimentary Metaquartzite Other Metamorphic	<i>Altering to clay  </i>
2. K-Feldspar (39) 13%	Microcline Orthoclase Sanadine Microphanerite Volcanic Rock Fragment Sedimentary Metamorphic	
3. Plagioclase (49) 18%	Microphanerite Volcanic Rock Fragment Sedimentary Metamorphic	<i>Altering to clay   Albitized  </i>
4. Volcanics (5) 1.66%		
5. Microphanerites		
6. Accessory Minerals (4) 1.33%	<i>Hornblende Zeolite Biotite</i>	<i>Zircon Muscovite</i>
7. Carbonate Cement (8) 2.66%	<i>Calcite</i>	
8. Pseudomatrix (28) 9.33%	<i>Matrix</i>	
9. Clay Cement (2) .66%		
10. Intragranular Porosity (2) .66%	Quartz K-Feldspar Plagioclase	<i>Dissolution of clay  </i> VRF: Q K P PRF: Q K P
11. Intergranular Porosity (47) 15.66%	Fractures Fracture-induced dissolution Oversize/elongate pores Grain-edge dissolution	Primary Porosity Other
12. Other (23) 7.66%	<i>Pyrite/Organics RF</i>	<i>phosphate chert   Mymekite  </i>

COMMENTS:

SECONDARY INTERGRANULAR POROSITY

FRACTURE-INDUCED DISSOLUTION		
Q	vrfQ	prfQ
K	vrfK	prfK
P	vrfP	prfP
GRAIN-EDGE DISSOLUTION		
Q	vrfQ	prfQ
K	vrfK	prfK
P	vrfP	prfP
OVERSIZE/ELONGATE PORES		
Q	vrfQ	prfQ
K	vrfK	prfK
P	vrfP	prfP
OTHER		

PARAGENESIS:

(4) 1.33%

SANDSTONE PETROGRAPHY DATA

EXAMINED BY: SZL

THIN SECTION: Kerrco  
 FORMATION (AGE): Uedder  
 LOCATION: Rio Bravo  
 DEPTH: 11,410-6

PROJECT: Thesis  
 ROCK NAME: Arkosic Arenite  
 POINT COUNTS: 300

SORTING: Moderate

COMPACTION: N/A

SIZE: Fine to Med sand

ANGULARITY: subround

	SIZE	COMMENTS
1. Quartz (56) 19.3%	Monocrystalline Polycrystalline      Microphanerite Volcanic Rock Fragment   Quartz Arenite Other Sedimentary Metaquartzite Other Metamorphic	Quartz → calcite
2. K-Feldspar (38) 12.6%	Microcline Orthoclase Sanadine Microphanerite Volcanic Rock Fragment Sedimentary Metamorphic	Altering to clay:      Alte to carbonate:
3. Plagioclase (48) 16%	Microphanerite Volcanic Rock Fragment Sedimentary Metamorphic	Altering to clay:    Alter to carbonate:    Altered:
4. Volcanics (27) 9%	<del>     </del>	Alter to clay: <del>     </del>
5. Microphanerites		
6. Accessory Minerals (3) 1%	<u>Glaucinite</u> <u>Muscovite</u> <u>Chlorite</u>	
7. Carbonate Cement (34) 11.3%	<del>     </del>	
8. Matrix/Pseudomatrix (26) 8.6%	<del>     </del>	pseudo biotite:
9. Clay Cement		
10. Intragranular Porosity (12) 4%	Quartz   K-Feldspar <del>    </del> Plagioclase <del>    </del>	VRF: Q K P PRF: Q K P
11. Intergranular Porosity (15) 5%	Fractures Fracture-induced dissolution Oversize/elongate pores <del>     </del> Grain-edge dissolution	Primary Porosity Other
12. Other (11) 3.6%	<u>phosphate/organics</u> <u>P.F.</u>	Phosphate:

COMMENTS:

Presence of carbonate cement & dolomite  
 rhombs. Porosity is patchy & varies throughout.  
 Dirty sample. Lots of clay.  
 - Glaucinite present growing on phosphate

PARAGENESIS:

Did phosphate or glaucinite come first?

SECONDARY INTERGRANULAR POROSITY

FRACTURE-INDUCED DISSOLUTION		
Q	vrfQ	prfQ
K	vrfK	prfK
P	vrfP	prfP
GRAIN-EDGE DISSOLUTION		
Q	vrfQ	prfQ
K	vrfK	prfK
P	vrfP	prfP
OVERSIZE/ELONGATE PORES		
Q	vrfQ	prfQ
K	vrfK	prfK
P	vrfP	prfP
OTHER		

(28) 9.3%

good! pic.

**SANDSTONE PETROGRAPHY DATA**

EXAMINED BY: Sunnah

THIN SECTION: Kernco 61-34 (stained)  
 FORMATION (AGE): Oligocene  
 LOCATION: Rio Bravo  
 DEPTH: 11,430 - 2

PROJECT: Thesis

ROCK NAME: Arkosic wacke  
 POINT COUNTS: 300

SORTING: Moderate to poorly sorted  
 SIZE: Fine sand to some large grains

COMPACTION: N/A

ANGULARITY: Angular to subangular

	SIZE	COMMENTS
1. Quartz (56) 18.6%	Monocrystalline Polycrystalline   Microphanerite Volcanic Rock Fragment Quartz Arenite Other Sedimentary Metaquartzite Other Metamorphic	Altering to clay
2. K-Feldspar (40) 14%	Microcline   Orthoclase Sanadine Microphanerite Volcanic Rock Fragment Sedimentary Metamorphic	Altered to kaolinite   Altered to clay
3. Plagioclase (67) 24.7%	Microphanerite     Volcanic Rock Fragment   Sedimentary Metamorphic	Altering to dolomite   Altering to clay       Altering to sericite
4. Volcanics .33%		
5. Microphanerites		
6. Accessory Minerals (16) 5.3%	Dolomite Rhomb       Dolomite Altering to clay	Biotite to clay     Biotite
(12) 7. Carbonate Cement 4%	Dolomite	
8. Pseudomatrix		
Clay-Altered Grains		
(79) 9. Clay Matrix 28%	Smectite?       Kaolinite	
10. Intragranular Porosity (1) .33%	Quartz K-Feldspar Plagioclase Clay	VRF: Q K P PRF: Q K P
11. Intergranular Porosity (4) 1.3%	Fractures    Fracture-induced dissolution   Oversize/elongate pores   Grain-edge dissolution	Primary Porosity Other
12. Other (14) 5.3%	Dark minerals       Rock Fragment   Shale clast	

**COMMENTS:**

Oil clusters throughout, P tend to have an affinity to accumulate more on dolomite cement. Dolomite rhombs are growing over clay P detrital minerals. Some sericite cement, kaolinite P possible smectite. Plag → sericite

**PARAGENESIS:**

Dissolution → clay → precipitation dolomite

**SECONDARY INTERGRANULAR POROSITY**

FRACTURE-INDUCED DISSOLUTION		
Q	vrfQ	prfQ
K	vrfK	prfK
P	vrfP	prfP
GRAIN-EDGE DISSOLUTION		
Q	vrfQ	prfQ
K	vrfK	prfK
P	vrfP	prfP
OVERSIZE/ELONGATE PORES		
Q	vrfQ	prfQ
K	vrfK	prfK
P	vrfP	prfP
OTHER (4) = 1.3%		

SANDSTONE PETROGRAPHY DATA

EXAMINED BY: S2L

THIN SECTION: Kernco  
FORMATION (AGE): Vedder  
LOCATION: Rio Bravo  
DEPTH: 11,430-3

PROJECT: Thesis  
ROCK NAME: Arkosic Arenite  
POINT COUNTS: 300

SORTING: Poor

COMPACTION: N/A

SIZE: Fine sand

ANGULARITY: Subangular-subround  
SIZE COMMENTS

1. Quartz (64) 21.3%	Monocrystalline Polycrystalline Microphanerite Volcanic Rock Fragment Quartz Arenite Other Sedimentary Metaquartzite Other Metamorphic	Altering to Matrix: I
2. K-Feldspar (37) 13%	Microcline Orthoclase Sanadine Microphanerite Volcanic Rock Fragment Sedimentary Metamorphic	Altering to calcite: I Altering to clay: III Altering: II
3. Plagioclase (42) 15.6%	Microphanerite Volcanic Rock Fragment Sedimentary Metamorphic	Altering: III Altering to calcite: III
4. Volcanics (15) 5%		Volcanic to Matrix: IIIII
5. Microphanerites		
6. Accessory Minerals (5) 1.6%	Chlorite Biotite Muscovite	Red Mystery II
7. Carbonate Cement (33) 11%		
8. Matrix/Pseudomatrix (40) 13.3%		Biotite pseudo: IIIII
9. Clay Cement Kaolinite? (7) 2.3%		
10. Intragranular Porosity (4) 1.3%	Quartz K-Feldspar Plagioclase	VRF: Q K P PRF: Q K P
11. Intergranular Porosity (6) 2%	Fractures Fracture-induced dissolution Oversize/elongate pores Grain-edge dissolution	Primary Porosity Other
12. Other (22) 7.3%	Dunk/organics R.F.	phosphate: IIII

COMMENTS:  
Clay from dissolution of unstable grains.  
lots of pseudomatrix.  
Sporadic carbonate throughout  
Weird Red Clay (Hematite?) laminations @ 36, 73

PARAGENESIS:  
Biotite -> chlorite  
carbonate/dolomite first then clay/dissolution  
of grains evidence @ 12, 69.5. ~~Its~~ clay  
Also clay coats the carbonates among dolomite sample

SECONDARY INTERGRANULAR POROSITY

FRACTURE-INDUCED DISSOLUTION		
Q	vrfQ	prfQ
K	vrfK	prfK
P	vrfP	prfP
GRAIN-EDGE DISSOLUTION		
Q	vrfQ	prfQ
K	vrfK	prfK
P	vrfP	prfP
OVERSIZE/ELONGATE PORES		
Q	vrfQ	prfQ
K	vrfK	prfK
P	vrfP	prfP
OTHER		
(18)	6%	

SEM to see what auth. clays are produced?

SANDSTONE PETROGRAPHY DATA

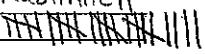
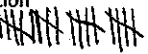
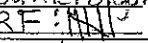
EXAMINED BY: SW

THIN SECTION: Kemco 61-34 (stained)  
FORMATION (AGE): Uedder  
LOCATION: Rio Bravo  
DEPTH: 11,430-7

PROJECT: Thesis  
ROCK NAME: Arkosic Arenite  
POINT COUNTS: 300

SORTING: Poor  
SIZE: Very fine Sand

COMPACTION: N/A  
ANGULARITY: Subangular to Round

	SIZE	COMMENTS
1. Quartz (56) 18.66%	Monocrystalline Polycrystalline    Microphanerite Volcanic Rock Fragment Quartz Arenite Other Sedimentary Metaquartzite Other Metamorphic	
2. K-Feldspar (25) 8.33%	Microcline Orthoclase Sanadine Microphanerite   Volcanic Rock Fragment Sedimentary Metamorphic	
3. Plagioclase (55) 18.33%	Microphanerite Volcanic Rock Fragment Sedimentary Metamorphic	
4. Volcanics (2) .66%		
5. Microphanerites		
6. Accessory Minerals (4) 1.33%	<u>Biotite</u>    _____ _____ _____	<u>Muscovite</u> _____ _____
7. Carbonate Cement (4) 1.33%	<u>Calcite</u>      _____	
8. Pseudomatrix (92)	Matrix: 	
Clay-Altered Grains		
9. Clay Cement (26) 30.66%	<u>Kaolinite</u>    <u>?</u> 	
10. Intragranular Porosity	Quartz K-Feldspar Plagioclase	VRF: Q K P PRF: Q K P
11. Intergranular Porosity (20) 6.66%	Fractures Fracture-induced dissolution Oversize/elongate pores  Grain-edge dissolution	Primary Porosity Other
12. Other (15) 5%	<u>pyrite/organics</u> :  <u>RF</u> : 	

COMMENTS: the only  $\phi$  porosity is through microfrazures that run throughout. lots of clay matrix, some that is very iron rich.

PARAGENESIS:

SECONDARY INTERGRANULAR POROSITY

FRACTURE-INDUCED DISSOLUTION		
Q	vrfQ	prfQ
K	vrfK	prfK
P	vrfP	prfP
GRAIN-EDGE DISSOLUTION		
Q	vrfQ	prfQ
K	vrfK	prfK
P	vrfP	prfP
OVERSIZE/ELONGATE PORES		
Q	vrfQ	prfQ
K	vrfK	prfK
P	vrfP	prfP
OTHER		
(1)	.33%	

SANDSTONE PETROGRAPHY DATA

EXAMINED BY: SZL

THIN SECTION: Kemco  
 FORMATION (AGE): Udden  
 LOCATION: Rio Bravo  
 DEPTH: 11,430-8

PROJECT: Thesis  
 ROCK NAME: Arkosic Arenite  
 POINT COUNTS: 300

SORTING: poor  
 SIZE: Med - Fine sand

COMPACTION: N/A  
 ANGULARITY: sub rounded

	SIZE	COMMENTS
1. Quartz (70) 26.6%	Monocrystalline Polycrystalline <del>     </del> Microphanerite <del>     </del> Volcanic Rock Fragment <del>     </del> Quartz Arenite Other Sedimentary Metaquartzite Other Metamorphic <del>  </del>	Altering: <del>  </del> Poly Altering: <del>  </del>
2. K-Feldspar (43) 14.3%	Microcline <del>  </del> Orthoclase Sanadine Microphanerite Volcanic Rock Fragment Sedimentary Metamorphic	Altering to clay: <del>     </del> Altered: <del>  </del>
3. Plagioclase (62) 26.6%	Microphanerite Volcanic Rock Fragment Sedimentary Metamorphic	Altering to clay: <del>  </del> Altered: <del>     </del>
4. Volcanics (10) 3.3%		Altering: <del>  </del> Altered to sericite: <del>  </del>
5. Microphanerites		
6. Accessory Minerals (2) .66%	<u>Hornblende: <del>  </del></u> <u>Red Muscovite: <del>  </del></u>	
7. Carbonate Cement (5) 1.6%	<del>     </del>	
8. Matrix/ Pseudomatrix (48) 16%	<del>     </del> <del>     </del>	Pseudo Biotite: <del>  </del>
9. Clay Cement (2) .66%	<del>  </del>	
10. Intragranular Porosity (2) .66%	Quartz K-Feldspar <del>  </del> Plagioclase	VRF: Q K P PRF: Q K P
11. Intergranular Porosity (3) 1%	Fractures Fracture-induced dissolution Oversize/elongate pores <del>  </del> Grain-edge dissolution	Primary Porosity Other Dissolution of clay: <del>  </del>
12. Other (13) 5%	<u>quartz/organics: <del>     </del></u> <u>R.F. <del>     </del></u>	<u>chert: <del>  </del></u> <u>Shale: <del>  </del></u>

COMMENTS:  
 Lots of detrital & authigenic clays. A lot of dissolution of feldspar grains. Some porosity due to grain plucking. Other due to shrinkage & dissolution of matrix. Some small amounts of carbonate. Some dolomite rhombs present.

PARAGENESIS:  
 Dissolution → Pyrite/organics

SECONDARY INTERGRANULAR POROSITY

FRACTURE-INDUCED DISSOLUTION		
Q	vrfQ	prfQ
K	vrfK	prfK
P	vrfP	prfP
GRAIN-EDGE DISSOLUTION		
Q	vrfQ	prfQ
K	vrfK	prfK
P	vrfP	prfP
OVERSIZE/ELONGATE PORES		
Q	vrfQ	prfQ
K	vrfK	prfK
P	vrfP	prfP
OTHER		
(28)	9.3%	

SANDSTONE PETROGRAPHY DATA

EXAMINED BY: SL

THIN SECTION: KOYKO 6134  
 FORMATION (AGE): Veeder  
 LOCATION: Rio Bravo  
 DEPTH: 11,450-2  
 SORTING: poorly  
 SIZE: Fine Sand

PROJECT: Thesis  
 ROCK NAME: Arkosic wacke  
 POINT COUNTS: 300  
 COMPACTION: N/A  
 ANGULARITY: sub angular - sub round

	SIZE	COMMENTS
1. Quartz (63) 22%	Monocrystalline Polycrystalline <del>    </del> Microphanerite <u>granitic    </u> Volcanic Rock Fragment Quartz Arenite Other Sedimentary Metaquartzite Other Metamorphic <u>  </u>	
2. K-Feldspar (43) 14.3	Microcline <u>  </u> Orthoclase Sanadine Microphanerite Volcanic Rock Fragment Sedimentary Metamorphic	ortho altered: <del>     </del>
3. Plagioclase (73) 24.3	Microphanerite <u> </u> Volcanic Rock Fragment Sedimentary Metamorphic	Altering to clay: <u>   </u> Altered to clay: <u>   </u>
4. Volcanics (10) 3.3%	<del>     </del>	
5. Microphanerites		
6. Accessory Minerals (1) .33%	<u>Muscovite  </u>	
7. Carbonate Cement (2) .16%	<u>  </u>	
8. Matrix/Pseudomatrix (64) 21.3%	<del>     </del>	pseudo biotite: <u>   </u>
9. Clay Cement (12) 4%	? <del>     </del>	
10. Intragranular Porosity (3) 1%	Quartz K-Feldspar <u>  </u> Plagioclase <u> </u>	VRF: Q K P PRF: Q K P
11. Intergranular Porosity (2) .66%	Fractures <u> </u> Fracture-induced dissolution Oversize/elongate pores Grain-edge dissolution <u> </u>	Primary Porosity  Other
12. Other (16) 5.3%	<u>pink/organics:    </u> <u>RF:    </u>	Chert: <u>  </u>

COMMENTS:  
 Very dirty sample. Some fracturing throughout  
 porosity is patchy throughout.  
 Some phosphate bodies throughout.  
 Some areas are highly compacted.

PARAGENESIS:

Dissolution of f grain → clay

SECONDARY INTERGRANULAR POROSITY

FRACTURE-INDUCED DISSOLUTION		
Q	vrfQ	prfQ
K	vrfK	prfK
P	vrfP	prfP
GRAIN-EDGE DISSOLUTION		
Q <u>   </u>	vrfQ	prfQ
K <u>   </u>	vrfK	prfK
P <u>   </u>	vrfP	prfP
OVERSIZE/ELONGATE PORES		
Q	vrfQ	prfQ
K	vrfK	prfK
P	vrfP	prfP
OTHER		

(8) 2.16%

SANDSTONE PETROGRAPHY DATA

EXAMINED BY: SZE

THIN SECTION: Kemco  
FORMATION (AGE): Vedder  
LOCATION: Rio Bravo  
DEPTH: 11,450-5

PROJECT: Thesis  
ROCK NAME: Arkosic Arkonite  
POINT COUNTS: 300

SORTING: Poor

COMPACTION: NA

SIZE: Medium Sand

ANGULARITY: Angular - Subround

	SIZE	COMMENTS
1. Quartz 62 (20.6%)	Monocrystalline Polycrystalline Microphanerite Volcanic Rock Fragment Quartz Arenite Other Sedimentary Metaquartzite Other Metamorphic	quartz → dolomite:
2. K-Feldspar 32 (10.6%)	Microcline Orthoclase Sanadine Microphanerite Volcanic Rock Fragment Sedimentary Metamorphic	ortho → dolomite:
3. Plagioclase 30 (12%)	Microphanerite Volcanic Rock Fragment Sedimentary Metamorphic	plag → dol:
4. Volcanics 8 (2.6%)		
5. Microphanerites		
6. Accessory Minerals		
7. Carbonate Cement 140 (46.6%)	Dolomite:	
8. Matrix/Pseudomatrix		
9. Clay Cement 1.33%	Kaolinite:	
10. Intragranular Porosity	Quartz K-Feldspar Plagioclase	VRF: Q K P PRF: Q K P
11. Intergranular Porosity	Fractures Fracture-induced dissolution Oversize/elongate pores Grain-edge dissolution	Primary Porosity Other
12. Other 14 (4.6%)	Dolomite/organics:       R.F.:       chert:	

COMMENTS: Dolomite throughout whole sample.

SECONDARY INTERGRANULAR POROSITY

FRACTURE-INDUCED DISSOLUTION		
Q	vrfQ	prfQ
K	vrfK	prfK
P	vrfP	prfP
GRAIN-EDGE DISSOLUTION		
Q	vrfQ	prfQ
K	vrfK	prfK
P	vrfP	prfP
OVERSIZE/ELONGATE PORES		
Q	vrfQ	prfQ
K	vrfK	prfK
P	vrfP	prfP
OTHER		

PARAGENESIS: Calcite → dolomite?

2 (6.6%)

SANDSTONE PETROGRAPHY DATA

EXAMINED BY: SZE

THIN SECTION: Kenico  
FORMATION (AGE): Wedder  
LOCATION: Rio Bravo  
DEPTH: 11,470-1

PROJECT: Thesis  
ROCK NAME: Arkosic wacke  
POINT COUNTS: 300

SORTING: Poorly sorted

COMPACTION: N/A

SIZE: Fine sand

ANGULARITY: Angular - subround

	SIZE	COMMENTS
1. Quartz (72) 24%	Monocrystalline Polycrystalline Microphanerite Volcanic Rock Fragment Quartz Arenite Other Sedimentary Metaquartzite Other Metamorphic	Altered to clay:
2. K-Feldspar (67) 8.3%	Microcline Orthoclase Sanadine Microphanerite Volcanic Rock Fragment Sedimentary Metamorphic	ortho altered to clay:
3. Plagioclase (54) 18%	Microphanerite Volcanic Rock Fragment Sedimentary Metamorphic	Altered to clay:
4. Volcanics (22) 7.3%		Altered to clay:
5. Microphanerites		
6. Accessory Minerals	<u>Muscovite:</u>	
7. Carbonate Cement		
8. Matrix/ Pseudomatrix (62) 20.6% Clay-Altered Grains		pseudo biotite:     chlorite pseudo:   shale pseudo:
9. Clay Cement		
10. Intragranular Porosity (7) 2.3%	Quartz K-Feldspar Plagioclase	VRF: Q K P PRF: Q K P
11. Intergranular Porosity (6) 2%	Fractures Fracture-induced dissolution Oversize/elongate pores Grain-edge dissolution	Primary Porosity Other
12. Other (20) 6.6%	<u>pyrite/organics:</u> <u>R.F.T.</u>	chert:     Phosphate:   Fossil:

COMMENTS:  
lots of volcanics, very dirty sample. zoned  
Plagioclase  
Phosphates present. sporadic porosity in sample  
Lot of volcanics have altered to clay matrix

PARAGENESIS:  
Biotite → chlorite

SECONDARY INTERGRANULAR POROSITY

FRACTURE-INDUCED DISSOLUTION		
Q	vrfQ	prfQ
K	vrfK	prfK
P	vrfP	prfP
GRAIN-EDGE DISSOLUTION		
Q	vrfQ	prfQ
K	vrfK	prfK
P	vrfP	prfP
OVERSIZE/ELONGATE PORES		
Q	vrfQ	prfQ
K	vrfK	prfK
P	vrfP	prfP
OTHER		
(22)	10.6%	

THIN SECTION: Kernco 61-34 (stained)  
FORMATION (AGE): Uedder  
LOCATION: Rio Bravo  
DEPTH: 11,470-4

SANDSTONE PETROGRAPHY DATA

EXAMINED BY: SU

PROJECT: Thesis  
ROCK NAME: Arkosic Arenite  
POINT COUNTS: 300  
COMPACTION: N/A  
ANGULARITY: Subround to Round

SORTING: Poor  
SIZE: Very Fine Sand

	SIZE	COMMENTS
1. Quartz (36) 12%	Monocrystalline Polycrystalline      Microphanerite Volcanic Rock Fragment Quartz Arenite Other Sedimentary Metaquartzite Other Metamorphic	
2. K-Feldspar (22) 7.33%	Microcline Orthoclase Sanadine Microphanerite Volcanic Rock Fragment Sedimentary Metamorphic	
3. Plagioclase (46) 15.33%	Microphanerite Volcanic Rock Fragment Sedimentary Metamorphic	
4. Volcanics (4) 1.33%		
5. Microphanerites		
6. Accessory Minerals (2) .66%	<u>Trondolite</u> _____ _____ <u>Muscovite</u> _____ _____	
7. Carbonate Cement (155) 51.66%	<u>Dolomite</u>       _____ _____	
8. Pseudomatrix		
Clay-Altered Grains		
9. Clay Cement		
10. Intragranular Porosity	Quartz K-Feldspar Plagioclase	VRF: Q K P PRF: Q K P
11. Intergranular Porosity (8) 2.66%	Fractures Fracture-induced dissolution Oversize/elongate pores       Grain-edge dissolution	Primary Porosity Other
12. Other (27) 9%	<u>quartz/arenite</u>       <u>RF</u>	

COMMENTS:

SECONDARY INTERGRANULAR POROSITY

FRACTURE-INDUCED DISSOLUTION		
Q	vrfQ	prfQ
K	vrfK	prfK
P	vrfP	prfP
GRAIN-EDGE DISSOLUTION		
Q	vrfQ	prfQ
K	vrfK	prfK
P	vrfP	prfP
OVERSIZE/ELONGATE PORES		
Q	vrfQ	prfQ
K	vrfK	prfK
P	vrfP	prfP
OTHER		

PARAGENESIS:

SANDSTONE PETROGRAPHY DATA

EXAMINED BY: SZL

THIN SECTION: Kemco  
FORMATION (AGE): Vedder  
LOCATION: Rio Bravo  
DEPTH: 11,470-5

PROJECT: Thesis  
ROCK NAME: Arkosic Arenite  
POINT COUNTS: 300

SORTING: Moderate  
SIZE: Medium sand

COMPACTION: C: 2.5 TPI: 1.6  
ANGULARITY: Subangular-Subround

	SIZE	COMMENTS
1. Quartz 76	Monocrystalline Polycrystalline Microphanerite Volcanic Rock Fragment   Quartz Arenite Other Sedimentary Metaquartzite Other Metamorphic	
2. K-Feldspar 30	Microcline   Orthoclase Sanadine Microphanerite Volcanic Rock Fragment Sedimentary Metamorphic	Altering to clay:
3. Plagioclase 64	Microphanerite Volcanic Rock Fragment   Sedimentary Metamorphic	Altering:      Altered to clay:
4. Volcanics 5		Altering:
5. Microphanerites		
6. Accessory Minerals 2	Muscovite:   Biotite:	
7. Carbonate Cement		
8. Matrix/ Pseudomatrix 12 Clay-Altered Grains	26 12 	Pseudo Biotite:      Pseudo muscovite:   Pseudo Shale:
9. Clay Cement 1	Kaolinite:	
10. Intragranular Porosity 15	Quartz    K-Feldspar   Plagioclase	VRF: Q K P PRF: Q K P
11. Intergranular Porosity 18	Fractures Fracture-induced dissolution Oversize/elongate pores Grain-edge dissolution	Primary Porosity Other
12. Other 14 10	Point counts:       R.F.:	Chert:   Shale:   Phosphate:

COMMENTS:  
Dirty sample but clean enough to try compaction.  
Lots of dissolution of all grains.

PARAGENESIS:  
Possible siderite clay in sample?  
Clay first then kaolinite. @ 33, 75

SECONDARY INTERGRANULAR POROSITY

FRACTURE-INDUCED DISSOLUTION		
Q	vrfQ	prfQ
K	vrfK	prfK
P	vrfP	prfP
GRAIN-EDGE DISSOLUTION		
Q	vrfQ	prfQ
K	vrfK	prfK
P	vrfP	prfP
OVERSIZE/ELONGATE PORES		
Q	vrfQ	prfQ
K	vrfK	prfK
P	vrfP	prfP
OTHER		
15		

SANDSTONE PETROGRAPHY DATA

EXAMINED BY: SZL

THIN SECTION: Kern 061-34  
 FORMATION (AGE): Vedder  
 LOCATION: Rio Bravo  
 DEPTH: 11,490-1

PROJECT: Thesis

ROCK NAME: Arkosic Arenite  
 POINT COUNTS: 300

SORTING: Very Poor

COMPACTION: C1:2.8 TPI:1.7

SIZE: Fine Sand

ANGULARITY: Subangular - Subrounded

	SIZE	COMMENTS
1. Quartz (61) 20.33%	Monocrystalline Polycrystalline     Microphanerite Volcanic Rock Fragment Quartz Arenite Other Sedimentary Metaquartzite Other Metamorphic	
2. K-Feldspar (39) 13%	Microcline   Orthoclase Sanadine Microphanerite Volcanic Rock Fragment Sedimentary Metamorphic	
3. Plagioclase (65) 23%	Microphanerite      - granitic Volcanic Rock Fragment Sedimentary Metamorphic	
4. Volcanics (2) .66%		
5. Microphanerites		
6. Accessory Minerals (4) 1.33%	Biotite    Muscovite	hornblende
7. Carbonate Cement (1) .33%		
8. Pseudomatrix (12) 4%		Matrix:
9. Clay Cement (56) 18.66%		
10. Intragranular Porosity (3) 1%	Quartz K-Feldspar   Plagioclase	clay   VRF: Q K P PRF: Q K P
11. Intergranular Porosity (20) 6.66%	Fractures Fracture-induced dissolution Oversize/elongate pores       Grain-edge dissolution	Primary Porosity Other
12. Other (21) 7%	RF:       puncte/organics:	Chert

COMMENTS:

Lots of clay Altered grains that are squashed between grains protecting from compaction & touching of Fwg, some Calcite cement throughout. Grains w/ no clay protection show high amounts of fracturing. Lots of grain dissolution.

PARAGENESIS:

SECONDARY INTERGRANULAR POROSITY

FRACTURE-INDUCED DISSOLUTION		
Q	vrfQ	prfQ
K	vrfK	prfK
P	vrfP	prfP
GRAIN-EDGE DISSOLUTION		
Q	vrfQ	prfQ
K	vrfK	prfK
P	vrfP	prfP
OVERSIZE/ELONGATE PORES		
Q	vrfQ	prfQ
K	vrfK	prfK
P	vrfP	prfP
OTHER		

(12) 4%

SANDSTONE PETROGRAPHY DATA

EXAMINED BY: SZL

THIN SECTION: Mandell-3 (stained)  
 FORMATION (AGE): Vedder  
 LOCATION: Rio Bravo  
 DEPTH: 11,423-1

PROJECT: Thesis  
 ROCK NAME: Arkosic Arenite  
 POINT COUNTS: 300

SORTING: Very Poor  
 SIZE: Medium Sand

COMPACTION: CI: 3.9 TPI: 2.1  
 ANGULARITY: Angular to subround

	SIZE	COMMENTS
1. Quartz (89)	Monocrystalline Polycrystalline    Microphanerite      Volcanic Rock Fragment Quartz Arenite Other Sedimentary Metaquartzite Other Metamorphic	Altering to Muscovite   Altering to clay
2. K-Feldspar (35)	Microcline   Orthoclase Sanadine Microphanerite Volcanic Rock Fragment Sedimentary Metamorphic	Altering to clay
3. Plagioclase (60)	Microphanerite     Volcanic Rock Fragment Sedimentary Metamorphic	Altering to clay
4. Volcanics (9)		
5. Microphanerites		
6. Accessory Minerals (18)	Chlorite     Muscovite      Dolomite	Biotite w/ organics      Glauconite → clay   Biotite → clay    Zircon
7. Carbonate Cement (1)		
8. Pseudomatrix		
9. Clay Cement Matrix (12)	Dark clay?	smectite?     Kaolinite?
10. Intragranular Porosity (5)	Quartz    K-Feldspar   Plagioclase	VRF: Q K P PRF: Q K P
11. Intergranular Porosity (30)	Fractures   Fracture-induced dissolution Oversize/elongate pores       Grain-edge dissolution	Primary Porosity       Other Dissolution of clay
12. Other (16)	organics, fomite       phosphate	RF = 1

COMMENTS:  $\phi$  porosity has been formed by dissolution of clays as well as dissolution of FWG's. Lots of clay rims around FWG's. Some biotite deformed & altered to pseudomatrix. Lots of. Biotite is altering to chlorite. Biotite altering to clay is squeezing b/w FWG. Glauconite is present

PARAGENESIS:

compaction → fracturing → clays → dissolution  
 Fracturing → albitization  
 chlorite → dissolution → clay → oil

SECONDARY INTERGRANULAR POROSITY

FRACTURE-INDUCED DISSOLUTION		
Q	vrfQ	prfQ
K	vrfK	prfK
P	vrfP	prfP
GRAIN-EDGE DISSOLUTION		
Q	vrfQ	prfQ
K	vrfK	prfK
P	vrfP	prfP
OVERSIZE/ELONGATE PORES		
Q	vrfQ	prfQ
K	vrfK	prfK
P	vrfP	prfP
OTHER		
(16)		

SANDSTONE PETROGRAPHY DATA

EXAMINED BY: SZU

THIN SECTION: Mardell  
FORMATION (AGE): Jedder  
LOCATION: Rio Bravo  
DEPTH: 11,423-2

PROJECT: Thesis  
ROCK NAME: Arkosic Arenite  
POINT COUNTS: 300

SORTING: Poor

COMPACTION: C1:3.4 TPI:1.8

SIZE: upper fine to lower medium sand

ANGULARITY: subangular-subround  
SIZE COMMENTS

1. Quartz <u>85</u>	Monocrystalline Polycrystalline <del>     </del> Microphanerite <del>     </del> Volcanic Rock Fragment Quartz Arenite Other Sedimentary Metaquartzite Other Metamorphic		
2. K-Feldspar <u>47</u>	Microcline <del>     </del> Orthoclase Sanadine Microphanerite <del> </del> Volcanic Rock Fragment Sedimentary Metamorphic		Altered:
3. Plagioclase <u>69</u>	Microphanerite <del>  </del> Volcanic Rock Fragment Sedimentary Metamorphic		Altered:
4. Volcanics <u>5</u>	<del>   </del>		
5. Microphanerites			
6. Accessory Minerals <u>1</u>	<u>glaucophane</u>		
7. Carbonate Cement			
8. Matrix/ Pseudomatrix <u>2</u> <u>18</u>	<del>     </del>		Biotite pseudo:    Muscovite pseudo:
9. Clay Cement <u>2</u>	<u>Kalinite</u>		
10. Intragranular Porosity <u>9</u>	Quartz   K-Feldspar <del>  </del> Plagioclase <del>     </del>	VRF: Q K P	PRF: Q K P
11. Intergranular Porosity <u>9</u>	Fractures Fracture-induced dissolution Oversize/elongate pores <del>     </del> Grain-edge dissolution		Primary Porosity Other
12. Other <u>9</u> <u>15</u>	<u>white organics</u> : <del>     </del> <u>R.F.</u> : <del>     </del>		Phosphate:   Chert:

COMMENTS:  
This is a poorly made sample had to distinguish a lot of grains. Zoned of pseudomatrix, some residual oil left. Lots of rock fragments

PARAGENESIS:

SECONDARY INTERGRANULAR POROSITY

FRACTURE-INDUCED DISSOLUTION		
Q	vrfQ	prfQ
K	vrfK	prfK
P	vrfP	prfP
GRAIN-EDGE DISSOLUTION		
Q	vrfQ	prfQ
K	vrfK	prfK
P	vrfP	prfP
OVERSIZE/ELONGATE PORES		
Q	vrfQ	prfQ
K	vrfK	prfK
P	vrfP	prfP
OTHER		
		<u>9</u>

SANDSTONE PETROGRAPHY DATA

EXAMINED BY: SZL

THIN SECTION: Mandell-3  
 FORMATION (AGE): Jedder  
 LOCATION: Rio Bravo  
 DEPTH: 11,423-4

PROJECT: Thesis

ROCK NAME: Sub Arkose Arenite  
 POINT COUNTS: 300

SORTING: Moderately Sorted

COMPACTION: C1: 3.8 TPI: 2.4

SIZE: Medium sand

ANGULARITY: Sub-angular - Sub-round

	SIZE	COMMENTS
1. Quartz <u>92</u>	Monocrystalline Polycrystalline <u>###</u> Microphanerite Volcanic Rock Fragment Quartz Arenite Other Sedimentary Metaquartzite Other Metamorphic <u>  </u>	Quartz w/ chlorite   @ 74, 11
2. K-Feldspar <u>28</u>	Microcline   Orthoclase Sanadine Microphanerite   Volcanic Rock Fragment Sedimentary Metamorphic	
3. Plagioclase <u>71</u>	Microphanerite <u>  </u> Volcanic Rock Fragment Sedimentary Metamorphic	Plag → sericite <u>###</u>
4. Volcanics <u>6</u>	<u>###</u>	
5. Microphanerites		
6. Accessory Minerals <u>4</u>	<u>Muscovite   </u> <u>glauconite   </u>	
7. Carbonate Cement <u>5</u>	<u>###</u>	
8. Matrix/ Pseudomatrix <u>29</u>	<u>     </u>	
9. Clay Cement <u>9</u>	<u>     </u>	
10. Intragranular Porosity <u>2</u>	Quartz K-Feldspar   Plagioclase	VRF: Q K P PRF: Q K P
11. Intergranular Porosity <u>20</u>	Fractures Fracture-induced dissolution Oversize/elongate pores <u>     </u> Grain-edge dissolution	Primary Porosity Other <u>###</u>
12. Other <u>8</u>	<u>organics/inite:      </u> <u>10 RP:      </u>	Chert:

COMMENTS:  
 sporadic carbonate throughout. Lots of dissolution  
 volcanic.  
 - plag grain w/ inclusion 72, 12

SECONDARY INTERGRANULAR POROSITY

FRACTURE-INDUCED DISSOLUTION		
Q	vrfQ	prfQ
K	vrfK	prfK
P	vrfP	prfP
GRAIN-EDGE DISSOLUTION		
Q <u>     </u>	vrfQ	prfQ
K	vrfK	prfK
P <u>     </u>	vrfP	prfP
OVERSIZE/ELONGATE PORES		
Q	vrfQ	prfQ
K	vrfK	prfK
P	vrfP	prfP
OTHER		

PARAGENESIS:

SANDSTONE PETROGRAPHY DATA

EXAMINED BY: SZU

THIN SECTION: Mandell  
FORMATION (AGE): Veeder  
LOCATION: Rio Bravo  
DEPTH: 11,423-5

PROJECT: Thesis  
ROCK NAME: Arkosic Arenite  
POINT COUNTS: 300

SORTING: Poor

COMPACTION: 01:3.1 TPI:1.8

SIZE: Fine sand

ANGULARITY: Subangular

	SIZE	COMMENTS
1. Quartz 88	Monocrystalline Polycrystalline      Microphanerite Volcanic Rock Fragment Quartz Arenite Other Sedimentary Metaquartzite Other Metamorphic	
2. K-Feldspar 45	Microcline    Orthoclase Sanadine Microphanerite Volcanic Rock Fragment Sedimentary Metamorphic	Altered:
3. Plagioclase 69	Microphanerite Volcanic Rock Fragment Sedimentary Metamorphic	Altered:    Alter to sericite:    Alter to calcite:
4. Volcanics 13		Altered:
5. Microphanerites		
6. Accessory Minerals 1	Biotite:   Hornblende	
7. Carbonate Cement 4		
8. Matrix/ Pseudomatrix 3 18 Clay-Altered Grains	 	pseudo Biotite:       Biotite → chlorite:
9. Clay Cement 1	Kaolinite:	
10. Intragranular Porosity 6	Quartz K-Feldspar Plagioclase	VRF: Q K P PRF: Q K P
11. Intergranular Porosity 20	Fractures Fracture-induced dissolution Oversize/elongate pores       Grain-edge dissolution	Primary Porosity Other
12. Other 17	1 Dark organics:   R.F.:	Phosphate:   Chert:    Bone:

COMMENTS:  
Most chlorite out of all samples present.  
Small amounts of carbonate. Tons of biotite in this sample.

SECONDARY INTERGRANULAR POROSITY

FRACTURE-INDUCED DISSOLUTION		
Q	vrfQ	prfQ
K	vrfK	prfK
P	vrfP	prfP
GRAIN-EDGE DISSOLUTION		
Q	vrfQ	prfQ
K	vrfK	prfK
P	vrfP	prfP
OVERSIZE/ELONGATE PORES		
Q	vrfQ	prfQ
K	vrfK	prfK
P	vrfP	prfP
OTHER		
10		

PARAGENESIS:

THIN SECTION: Mandell-3 (stained)  
 FORMATION (AGE): Vedder  
 LOCATION: Rio Bravo  
 DEPTH: 11,436-7

SANDSTONE PETROGRAPHY DATA

EXAMINED BY: SZL

PROJECT: Thesis  
 ROCK NAME: Arkosic Arenite  
 POINT COUNTS: 300  
 COMPACTION: CI: 3.2 TPI: 1.9

SORTING:

SIZE: fine sand

ANGULARITY: Subangular to subround  
 SIZE COMMENTS

	SIZE	COMMENTS
1. Quartz (29) 27%	Monocrystalline Polycrystalline Microphanerite Volcanic Rock Fragment Quartz Arenite Other Sedimentary Metaquartzite Other Metamorphic	Altered
2. K-Feldspar (31) 10.33%	Microcline Orthoclase Sanadine Microphanerite    Volcanic Rock Fragment Sedimentary Metamorphic	
3. Plagioclase (58) 19.33%	Microphanerite Volcanic Rock Fragment Sedimentary Metamorphic	Altered         Altered to sericite
4. Volcanics (1) .33%		
5. Microphanerites		
6. Accessory Minerals (3) 1%	Biotite   Glauconite   Chlorite	
7. Carbonate Cement (5) 1.66%		
8. Pseudomatrix (1) .33%		
Clay-Altered Grains		
9. Clay Cement (27) 9%	Kaolinite   	
10. Intragranular Porosity (8) 1%	Quartz K-Feldspar    Plagioclase	VRF: Q K P PRF: Q K P
11. Intergranular Porosity (43) 14.33%	Fractures   Fracture-induced dissolution Oversize/elongate pores     Grain-edge dissolution	Primary Porosity Other
12. Other (33) 11%	RF:     pyrite/organics:	Chert     Altered chert

COMMENTS:  
 Plagioclase grains are highly altered and some highly fractured. Some fractured plg grains have been healed over. Lots of clay altered shale? fragments. Some CaCO<sub>3</sub> in slide

PARAGENESIS:

SECONDARY INTERGRANULAR POROSITY

FRACTURE-INDUCED DISSOLUTION		
Q	vrfQ	prfQ
K	vrfK	prfK
P	vrfP	prfP
GRAIN-EDGE DISSOLUTION		
Q	vrfQ	prfQ
K	vrfK	prfK
P	vrfP	prfP
OVERSIZE/ELONGATE PORES		
Q	vrfQ	prfQ
K	vrfK	prfK
P	vrfP	prfP
OTHER		
(14)	4.66%	

SANDSTONE PETROGRAPHY DATA

EXAMINED BY: SZL

THIN SECTION: Mandell  
FORMATION (AGE): Veeder  
LOCATION: Rio Bravo  
DEPTH: 11,436-8

PROJECT: Thesis  
ROCK NAME: Arkosic Arenite  
POINT COUNTS: 300  
COMPACTION: 01; 3.3 TPI; 2.2  
ANGULARITY: Subangular

SORTING: Moderate  
SIZE: fine to medium sand

	SIZE	COMMENTS
1. Quartz (100)	Monocrystalline Polycrystalline <u>     </u> Microphanerite <u>     </u> Volcanic Rock Fragment Quartz Arenite Other Sedimentary Metaquartzite Other Metamorphic <u> </u>	
2. K-Feldspar (42)	Microcline <u>   </u> Orthoclase Sanadine Microphanerite <u> </u> Volcanic Rock Fragment Sedimentary Metamorphic	<u>Altered:   </u>
3. Plagioclase (70)	Microphanerite <u>    </u> Volcanic Rock Fragment Sedimentary Metamorphic	<u>Altered to suicite:   </u> <u>Altering:  </u>
4. Volcanics (4)	<u>     </u>	
5. Microphanerites		
6. Accessory Minerals (3)	<u>Biotite:    </u>	
7. Carbonate Cement (5)	<u>   </u>	
8. Matrix/Pseudomatrix (8)	<u>   </u>	<u>pseudo Biotite:   </u> <u>pseudo Chlorite:  </u>
9. Clay Cement		
10. Intragranular Porosity (8)	Quartz K-Feldspar Plagioclase <u>     </u>	VRF: Q K P PRF: Q K P
11. Intergranular Porosity (18)	Fractures <u> </u> Fracture-induced dissolution Oversize/elongate pores <u>     </u> Grain-edge dissolution	Primary Porosity  Other
12. Other (24)	<u>Dark organics:     </u> <u>R.F.:      </u>	<u>Phosphate:     </u> <u>Chert:     </u>

COMMENTS: Some glauconite, muscovite

PARAGENESIS:

SECONDARY INTERGRANULAR POROSITY

FRACTURE-INDUCED DISSOLUTION		
Q	vrfQ	prfQ
K	vrfK	prfK
P	vrfP	prfP
GRAIN-EDGE DISSOLUTION		
Q <u>   </u>	vrfQ	prfQ
K	vrfK	prfK
P <u>   </u>	vrfP	prfP
OVERSIZE/ELONGATE PORES		
Q	vrfQ	prfQ
K	vrfK	prfK
P	vrfP	prfP
OTHER		

(8)

THIN SECTION: Mandell-3 (stained)  
FORMATION (AGE): Vedder  
LOCATION: Rio Bravo  
DEPTH: 11,436-10

SANDSTONE PETROGRAPHY DATA

EXAMINED BY: SL

PROJECT: Thesis  
ROCK NAME: Arkosic Arenite  
POINT COUNTS: 300  
COMPACTION: C1: 2.8 TPI: 1.8  
ANGULARITY: Subangular - Subround

SORTING: Moderate  
SIZE: Fine to Medium Sand

	SIZE	COMMENTS
1. Quartz (81) (27%)	Monocrystalline Polycrystalline Microphanerite Volcanic Rock Fragment Quartz Arenite Other Sedimentary Metaquartzite Other Metamorphic	Altered
2. K-Feldspar (25) (9.33%)	Microcline Orthoclase Sanadine Microphanerite Volcanic Rock Fragment Sedimentary Metamorphic	
3. Plagioclase (65) 21.66%	Microphanerite Volcanic Rock Fragment Sedimentary Metamorphic	Altered Albitized
4. Volcanics (9) 3%		
5. Microphanerites		
6. Accessory Minerals (5) 1.66%	Biotite Chlorite Glaucophane	Muscovite
7. Carbonate (2) Cement .66%	Dolomite	
8. Pseudomatrix (2) .66%		Matrix:
Clay-Altered Grains		
9. Clay (26) Cement 8.66%	Kaolinite	
10. Intragranular Porosity (4) 1.33%	Quartz K-Feldspar Plagioclase	VRF: Q K P PRF: Q K P
11. Intergranular Porosity (45) 15%	Fractures Fracture-induced dissolution Oversize/elongate pores Grain-edge dissolution	Primary Porosity Other
12. Other (20) 6.66%	Phosphate Organics	Phosphate Chert

COMMENTS:

SECONDARY INTERGRANULAR POROSITY

FRACTURE-INDUCED DISSOLUTION		
Q	vrfQ	prfQ
K	vrfK	prfK
P	vrfP	prfP
GRAIN-EDGE DISSOLUTION		
Q	vrfQ	prfQ
K	vrfK	prfK
P	vrfP	prfP
OVERSIZE/ELONGATE PORES		
Q	vrfQ	prfQ
K	vrfK	prfK
P	vrfP	prfP
OTHER		

PARAGENESIS:

(13) 4.33%

THIN SECTION: Mandell-3 (stained)  
 FORMATION (AGE): Vedder  
 LOCATION: Rio Bravo  
 DEPTH: 11,436-13  
 SORTING: Moderate to poorly sorted  
 SIZE: Fine sand

SANDSTONE PETROGRAPHY DATA

EXAMINED BY: S2L

PROJECT: Thesis  
 ROCK NAME: Arkosic Arenite  
 POINT COUNTS: 300  
 COMPACTION: C1: 3.7-TPI: 2.2  
 ANGULARITY: Subangular to subround

	SIZE	COMMENTS
1. Quartz (92) 30.46%	Monocrystalline Polycrystalline       Microphanerite Volcanic Rock Fragment Quartz Arenite Other Sedimentary Metaquartzite Other Metamorphic	
2. K-Feldspar (37) 12.33%	Microcline Orthoclase Sanadine Microphanerite    Volcanic Rock Fragment Sedimentary Metamorphic	
3. Plagioclase (60) 26%	Microphanerite Volcanic Rock Fragment Sedimentary Metamorphic	Altered       Altering to sericite
4. Volcanics (2) .46%		
5. Microphanerites		
6. Accessory Minerals (6) 2%	Chlorite Biotite Epidote	Muscovite
7. Carbonate (7) Cement 2.33%	Dolomite	
8. Pseudomatrix (2) .46%		
9. Clay (32) Cement 10.46%	 Kaolinite	
10. Intragranular Porosity (2) .46%	Quartz K-Feldspar Plagioclase	VRF: Q K P PRF: Q K P
11. Intergranular Porosity (36) 12%	Fractures Fracture-induced dissolution Oversize/elongate pores Grain-edge dissolution	Primary Porosity Other
12. Other (14) 4.46%	RF       Dumite/organics	Chert

COMMENTS:

SECONDARY INTERGRANULAR POROSITY

FRACTURE-INDUCED DISSOLUTION		
Q	vrfQ	prfQ
K	vrfK	prfK
P	vrfP	prfP
GRAIN-EDGE DISSOLUTION		
Q	vrfQ	prfQ
K	vrfK	prfK
P	vrfP	prfP
OVERSIZE/ELONGATE PORES		
Q	vrfQ	prfQ
K	vrfK	prfK
P	vrfP	prfP
OTHER		

PARAGENESIS:

(10) 3.33%

SANDSTONE PETROGRAPHY DATA

EXAMINED BY: SZL

THIN SECTION: Mandell  
FORMATION (AGE): Vedder  
LOCATION: Rio Bravo  
DEPTH: 11,436-11  
SORTING: Moderate  
SIZE: Medium Sand

PROJECT: Thesis  
ROCK NAME: Arkosic Arenite  
POINT COUNTS: 300  
COMPACTION: Cl: 3.4 TPI: 1.9  
ANGULARITY: Subangular

	SIZE	COMMENTS
1. Quartz (101) 33.6%	Monocrystalline Polycrystalline <u>    </u> Microphanerite Volcanic Rock Fragment Quartz Arenite Other Sedimentary Metaquartzite Other Metamorphic <u> </u>	
2. K-Feldspar (40) 13.3%	Microcline <u>    </u> Orthoclase Sanadine Microphanerite <u> </u> Volcanic Rock Fragment Sedimentary Metamorphic	<u>Altering to Kaolinite:  </u>
3. Plagioclase (63) 2%	Microphanerite <u> </u> Volcanic Rock Fragment Sedimentary Metamorphic	
4. Volcanics (10) 3.3%	<u>    </u>	<u>pseudo:    </u>
5. Microphanerites		
6. Accessory Minerals (2) .66%	<u>Biotite:  </u> <u>Muscovite:  </u>	
7. Carbonate Cement (5) 1.6%	<u>    </u>	
8. Matrix/Pseudomatrix (13) 4.3%	<u>    </u>	<u>pseudo Biotite:    </u>
9. Clay Cement		
10. Intragranular Porosity (4) 1.3%	Quartz K-Feldspar Plagioclase <u>    </u>	VRF: Q K P PRF: Q K P
11. Intergranular Porosity (34) 11.3%	Fractures Fracture-induced dissolution Oversize/elongate pores <u>                </u> Grain-edge dissolution	Primary Porosity  Other
12. Other (22) 7.3%	<u>pyrite (organics):</u> <u>R.F.:    </u>	<u>phosphates:    </u> <u>chert:   </u>

COMMENTS:  
small amounts of chlorite, kaolinite & biotite,  
lots of porosity w/ little clay.

PARAGENESIS:

SECONDARY INTERGRANULAR POROSITY

FRACTURE-INDUCED DISSOLUTION		
Q	vrfQ	prfQ
K	vrfK	prfK
P	vrfP	prfP
GRAIN-EDGE DISSOLUTION		
Q <u>   </u>	vrfQ	prfQ
K <u> </u>	vrfK	prfK
P <u>  </u>	vrfP	prfP
OVERSIZE/ELONGATE PORES		
Q	vrfQ	prfQ
K	vrfK	prfK
P	vrfP	prfP
OTHER		
(6) 2%		

SANDSTONE PETROGRAPHY DATA

EXAMINED BY: SU

THIN SECTION: PS-21 (Stained)  
 FORMATION (AGE): Vedder  
 LOCATION: Rio Bravo  
 DEPTH: 11,493

PROJECT: Thesis  
 ROCK NAME: Arkosic Arenite  
 POINT COUNTS: 300

SORTING: Moderate

COMPACTION: C1: 1.9, TPI: 1.3

SIZE: Very Fine sand w/ some larger coarse grains

ANGULARITY: Angular - Subangular

	SIZE	COMMENTS
1. Quartz (59) 19.66%	Monocrystalline Polycrystalline     Microphanerite Volcanic Rock Fragment Quartz Arenite Other Sedimentary Metaquartzite Other Metamorphic	
2. K-Feldspar (31) 10.33%	Microcline    Orthoclase Sanadine Microphanerite    Volcanic Rock Fragment Sedimentary Metamorphic	
3. Plagioclase (63) 21%	Microphanerite     Volcanic Rock Fragment Sedimentary Metamorphic	Altered
4. Volcanics (2) .66%		
5. Microphanerites		
6. Accessory Minerals (3) 1%	<u>Muscovite</u>    <u>Biotite</u>	<u>Glauconite present</u> <u>Hornblende present</u>
7. Carbonate Cement (2) 4%	<u>Dolo.</u>	
8. Pseudomatrix (1) .33%		Matrix
9. Clay Cement (27) 9%	?       <u>Kaolinite</u>	
10. Intragranular Porosity (4) 1.33%	Quartz K-Feldspar   Plagioclase	VRF: Q K P PRF: Q K P
11. Intergranular Porosity (73) 24.33%	Fractures Fracture-induced dissolution Oversize/elongate pores       Grain-edge dissolution	Primary Porosity Other
12. Other (20) 6.66%	<u>RF</u>       <u>pyrite/organics</u>	<u>Chert</u>    <u>MurMekite</u>

COMMENTS:

SECONDARY INTERGRANULAR POROSITY

FRACTURE-INDUCED DISSOLUTION		
Q	vrfQ	prfQ
K	vrfK	prfK
P	vrfP	prfP
GRAIN-EDGE DISSOLUTION		
Q	vrfQ	prfQ
K	vrfK	prfK
P	vrfP	prfP
OVERSIZE/ELONGATE PORES		
Q	vrfQ	prfQ
K	vrfK	prfK
P	vrfP	prfP
OTHER		

PARAGENESIS:

clay → shrinkage of FWG, dissolution

(5) 1.66%

SANDSTONE PETROGRAPHY DATA

EXAMINED BY: SU

THIN SECTION: PS  
 FORMATION (AGE): Jedder  
 LOCATION: Rio Bravo  
 DEPTH: 11,498

PROJECT: Thesis  
 ROCK NAME: Arkosic Arenite  
 POINT COUNTS: 300

SORTING:

COMPACTION: CI: 2.2 TPI: 64

SIZE:

ANGULARITY:

	SIZE	COMMENTS
1. Quartz 81	Monocrystalline Polycrystalline <del>     </del> Microphanerite Volcanic Rock Fragment Quartz Arenite Other Sedimentary Metaquartzite Other Metamorphic <del>    </del>	
2. K-Feldspar 41	Microcline <del>    </del> Orthoclase Sanadine Microphanerite Volcanic Rock Fragment Sedimentary Metamorphic	Altered:
3. Plagioclase 53	Microphanerite Volcanic Rock Fragment Sedimentary Metamorphic	Altering to carbonate:     Altered to seicite:
4. Volcanics 5	<del>     </del>	
5. Microphanerites		
6. Accessory Minerals 3	<u>Chlorite:   </u> <u>Muscovite:  </u>	
7. Carbonate Cement 23	<del>     </del>	
8. Matrix/Pseudomatrix 1		pseudo Biotite → chlorite:
9. Clay Cement	<u>Kaolinite:  </u>	
10. Intragranular Porosity	Quartz K-Feldspar Plagioclase <del>    </del>	VRF: Q K P PRF: Q K P
11. Intergranular Porosity 38	Fractures Fracture-induced dissolution Oversize/elongate pores <del>     </del> Grain-edge dissolution	Primary Porosity Other
12. Other 10	+ <u>zinc organics:    </u> <del>Fe:    </del>	Bone:   Chert:

COMMENTS:  
 carbonates & clays are mostly dissolved.  
 lots of porosity, kaolinite present  
 chlorite present in small amounts

SECONDARY INTERGRANULAR POROSITY

FRACTURE-INDUCED DISSOLUTION		
Q	vrfQ	prfQ
K	vrfK	prfK
P	vrfP	prfP
GRAIN-EDGE DISSOLUTION		
Q	vrfQ	prfQ
K	vrfK	prfK
P	vrfP	prfP
OVERSIZE/ELONGATE PORES		
Q	vrfQ	prfQ
K	vrfK	prfK
P	vrfP	prfP
OTHER		
		25

PARAGENESIS:

carbonate → chlorite 28, 78  
 chlorite → CaCO<sub>3</sub>? 9, 70

\* Albitization → chlorite healing fracture?  
 PIC @ 40, 69

Which one first?

SANDSTONE PETROGRAPHY DATA

EXAMINED BY: SU

THIN SECTION: Pacific Section 21 (stained)  
FORMATION (AGE):  
LOCATION:  
DEPTH: 11, 502

PROJECT: Thesis  
ROCK NAME: Alkalic Arenite  
POINT COUNTS: 300

SORTING: Poorly sorted

COMPACTION: C1: 2.7 TPI: 1.7

SIZE: fine to Medium Sand

ANGULARITY: Subangular to subrounded  
SIZE COMMENTS

1. Quartz (75) 25%	Monocrystalline Polycrystalline Microphanerite Volcanic Rock Fragment Quartz Arenite Other Sedimentary Metaquartzite Other Metamorphic		
2. K-Feldspar (27) 9%	Microcline Orthoclase Sanadine Microphanerite Volcanic Rock Fragment Sedimentary Metamorphic		
3. Plagioclase (70) 23.33%	Microphanerite Volcanic Rock Fragment Sedimentary Metamorphic		<u>Altering to clay</u>
4. Volcanics (2) .66%			
5. Microphanerites			
6. Accessory Minerals (7) 2.31%	<u>Muscovite</u> <u>Hornblende</u> <u>Biotite</u>	<u>Glaucanite</u> <u>Brown Manganese</u>	<u>33, 68</u>
7. Carbonate Cement (8) 2.66%	<u>Calcite</u> <u>Poikilotopic</u>		
8. Pseudomatrix (1) 3.66%		<u>Matrix</u>	
9. Clay Cement (3) 1%	<u>Kaolinite</u>		
10. Intragranular Porosity (2) .66%	Quartz K-Feldspar Plagioclase	VRF: Q K P	PRF: Q K P
11. Intergranular Porosity (65) 21.66%	Fractures Fracture-induced dissolution Oversize/elongate pores Grain-edge dissolution		Primary Porosity Other
12. Other (22) 7.33%	<u>pyrite/organics</u>	<u>Chert</u>	

COMMENTS:  
Albitized plag. grains, Abundant Kaolinite cement present throughout. Some pseudomatrix. Some blocky P poikilotopic carbonate cement throughout.

PARAGENESIS:

SECONDARY INTERGRANULAR POROSITY

FRACTURE-INDUCED DISSOLUTION		
Q	vrfQ	prfQ
K	vrfK	prfK
P	vrfP	prfP
GRAIN-EDGE DISSOLUTION		
Q	vrfQ	prfQ
K	vrfK	prfK
P	vrfP	prfP
OVERSIZE/ELONGATE PORES		
Q	vrfQ	prfQ
K	vrfK	prfK
P	vrfP	prfP
OTHER		
(8)	2.66%	

SANDSTONE PETROGRAPHY DATA

EXAMINED BY SZL

THIN SECTION: PS-21 11,507 (stained)  
 FORMATION (AGE): Vedder  
 LOCATION: Rio Bravo  
 DEPTH: 11,507

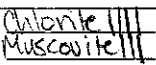
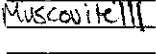
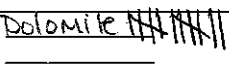
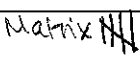
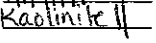
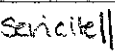
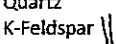
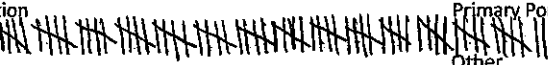
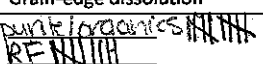
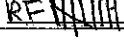
PROJECT: Thesis

ROCK NAME: Arkosic Arenite  
 POINT COUNTS: 300

SORTING: Moderate Sorting  
 SIZE: Fine to Medium Sand

COMPACTION: 0.25 TPI: 1.5

ANGULARITY: Subangular to Rounded

	SIZE	COMMENTS
1. Quartz (72) 24%	Monocrystalline Polycrystalline  Microphanerite Volcanic Rock Fragment Quartz Arenite Other Sedimentary Metaquartzite Other Metamorphic	
2. K-Feldspar (24) 8%	Microcline Orthoclase Sanadine Microphanerite  Volcanic Rock Fragment Sedimentary Metamorphic	
3. Plagioclase (59) 19.66%	Microphanerite   Volcanic Rock Fragment Sedimentary Metamorphic	Altering to clay
4. Volcanics (2) .66%		
5. Microphanerites		
6. Accessory Minerals (8) 2.66%	<u>Chalcite</u>  <u>Muscovite</u> 	<u>Biotite</u>
7. Carbonate Cement (12) 4%	<u>Dolomite</u> 	
8. Pseudomatrix (5) 1.66% Clay-Altered Grains	<u>Matrix</u> 	
9. Clay Cement (15) 5%	 <u>Kaolinite</u> 	<u>sericite</u> 
10. Intragranular Porosity (3) 1%	Quartz K-Feldspar  Plagioclase	VRF: Q K P PRF: Q K P
11. Intergranular Porosity (72) 24%	Fractures Fracture-induced dissolution Oversize/elongate pores  Grain-edge dissolution	Primary Porosity Other
12. Other (2) 7%	<u>pyrite/organics</u>  <u>RE</u> 	<u>Myrmecite</u> <u>chert</u>

COMMENTS:  
 Kaolinite cement is patches throughout. Clay Matrix prims remain on majority of grains.

PARAGENESIS:

SECONDARY INTERGRANULAR POROSITY

FRACTURE-INDUCED DISSOLUTION		
Q	vrfQ	prfQ
K	vrfK	prfK
P	vrfP	prfP
GRAIN-EDGE DISSOLUTION		
Q 	vrfQ	prfQ
K 	vrfK	prfK
P 	vrfP	prfP
OVERSIZE/ELONGATE PORES		
Q	vrfQ	prfQ
K	vrfK	prfK
P	vrfP	prfP
OTHER		
(7)	2.33%	

SANDSTONE PETROGRAPHY DATA

EXAMINED BY: SZK

THIN SECTION: Pacific States  
 FORMATION (AGE): Vedder  
 LOCATION: Rio Bravo  
 DEPTH: 11,512

PROJECT: Thesis  
 ROCK NAME: Arkosic Arenite  
 POINT COUNTS: 300

SORTING: moderate  
 SIZE: Upper fine to Medium sand

\*COMPACTION: lots of  $\phi$ , CaCO<sub>3</sub> & pseudo CI: 2.0 TPI: 1.3  
 ANGULARITY: Subround

	SIZE	COMMENTS
1. Quartz (78) 26%	Monocrystalline Polycrystalline Microphanerite Volcanic Rock Fragment Quartz Arenite Other Sedimentary Metaquartzite Other Metamorphic	Altered: 1
2. K-Feldspar (36) 12%	Microcline Orthoclase Sanadine Microphanerite Volcanic Rock Fragment Sedimentary Metamorphic	Altering: 1
3. Plagioclase (51) 17%	Microphanerite Volcanic Rock Fragment Sedimentary Metamorphic	Altered: 1
4. Volcanics (10) 3.3%		Altered: 1
5. Microphanerites		
6. Accessory Minerals (2) .66%	Biotite Muscovite	
7. Carbonate Cement (16) 5.3%		
8. Matrix/Pseudomatrix (22) 7.3%		Biotite pseudo: 1
9. Clay Cement (4) 1.3%	Kaolinite	
10. Intragranular Porosity (7) 2.3%	Quartz K-Feldspar Plagioclase	VRF: Q K P PRF: Q K P
11. Intergranular Porosity (29) 9.6%	Fractures Fracture-induced dissolution Oversize/elongate pores Grain-edge dissolution	Primary Porosity Other
12. Other (25) 8.3%	pyrite/grain coats R.F.	chert: 1

COMMENTS:  
 Small amounts of carbonate. Sedimentary Rock fragments throughout. Lots of  $\phi$ . Lots of shale fragments deformed into pseudomatrix. Residual oil left behind.  
 Small amounts of chlorite, & kaolinite clay coats & calcite protect grain compaction.

PARAGENESIS:  
 Phosphate  $\rightarrow$  Kaolinite  
 chlorite glauc  $\rightarrow$  Biotite  
 SRF  $\rightarrow$  chlorite?  
 Dolomite  $\rightarrow$  pseudo?

SECONDARY INTERGRANULAR POROSITY

FRACTURE-INDUCED DISSOLUTION		
Q	vrfQ	prfQ
K	vrfK	prfK
P	vrfP	prfP
GRAIN-EDGE DISSOLUTION		
Q	vrfQ	prfQ
K	vrfK	prfK
P	vrfP	prfP
OVERSIZE/ELONGATE PORES		
Q	vrfQ	prfQ
K	vrfK	prfK
P	vrfP	prfP
OTHER		
(20)	6.6%	



SANDSTONE PETROGRAPHY DATA

EXAMINED BY: Sunnih

THIN SECTION: Pacific States 21 (stained)  
 FORMATION (AGE): Oligocene  
 LOCATION: Rio Bravo  
 DEPTH: 11,549 - 11,555

PROJECT: Thesis

ROCK NAME: Arkosic Arenite  
 POINT COUNTS: 300

SORTING: very poorly sorted

COMPACTION: N/A

SIZE: Fine to Medium silt w/ some larger grains in Matrix

ANGULARITY: Angular to subangular

	SIZE	COMMENTS
1. Quartz (70) 23.9%	Monocrystalline 53 Polycrystalline <u>     </u> Microphanerite Volcanic Rock Fragment   Quartz Arenite Other Sedimentary Metaquartzite   Other Metamorphic	Chert <u>    </u> Altering to clay
2. K-Feldspar (6) 1.9%	Microcline 5 Orthoclase   Sanadine Microphanerite Volcanic Rock Fragment Sedimentary Metamorphic	
3. Plagioclase (42)	Microphanerite    Volcanic Rock Fragment Sedimentary Metamorphic	Alter to Illite/Smectite <u>     </u> Alter to chlorite   Alter to Dolomite     Alter to clay?
4. Volcanics 32% (1)		
5. Microphanerites		
6. Accessory Minerals 12	<u>chlorite</u> <u>     </u> <u>Muscovite</u>	<u>Biotite</u>   <u>Hornblende</u> <u>Apatite</u>    <u>Glauconite</u> - present
7. Carbonate Cement (11) 3.55%	<u>Dolomite</u> <u>     </u>	
8. Pseudomatrix		
Clay-Altered Grains		
9. Clay Matrix Cement (77) 24.9%	<u>Illite/Smectite</u> : 38 <u>chlorite</u> : 19	<u>Koolinite</u> : 20
10. Intragranular Porosity (1) 32%	Quartz   K-Feldspar Plagioclase	VRF: Q K P PRF: Q K P
11. Intergranular Porosity (13) 4.2%	Fractures    Fracture-induced dissolution    Oversize/elongate pores Grain-edge dissolution	Primary Porosity Other Shrinking: <u>    </u>
12. Other 17.8% (55)	<u>Glauconite</u> : <u>     </u> <u>pyrite/organics</u> : 32	<u>Phosphate</u> :

COMMENTS:

Quartz grains are floating in a detrital clay matrix. Partial dolomitization occurring + shrinking of grains which is creating porosity around the grains. Clays within the sample are carbonate. Chlorite is infilling fractures among grains. Rutile crystals in some quartz grains. Microfractures are also present among sample. Lots of glauconite. Quartz looks healed over shrinkage in fractures.

PARAGENESIS:

clay → Fracturing → chlorite infilling fractures of mostly quartz grains → Dolomitization → Migration of oil. Good Pic of this process #

Oil on dolomite # 23, 79 Dolomitization possibly before... of detrital quartz grain.

SECONDARY INTERGRANULAR POROSITY

FRACTURE-INDUCED DISSOLUTION		
Q	vrfQ	prfQ
K	vrfK	prfK
P	vrfP	prfP
GRAIN-EDGE DISSOLUTION		
Q	vrfQ	prfQ
K	vrfK	prfK
P	vrfP	prfP
OVERSIZE/ELONGATE PORES		
Q	vrfQ	prfQ
K	vrfK	prfK
P	vrfP	prfP
OTHER		

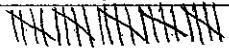
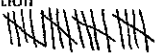
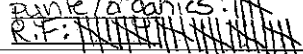
(2) .64%

SANDSTONE PETROGRAPHY DATA

EXAMINED BY: SZL

THIN SECTION: Pacific States  
FORMATION (AGE): vedder  
LOCATION: Rio Bravo  
DEPTH: 11,554 - 11,560  
SORTING: Poor  
SIZE: Medium sand

PROJECT: Thesis  
ROCK NAME: Lithic Arenite  
POINT COUNTS: 300  
COMPACTION: Cl: 2.8 TPI: 1.6  
ANGULARITY: Subround

	SIZE	COMMENTS
1. Quartz (74)	Monocrystalline Polycrystalline  Microphanerite Volcanic Rock Fragment Quartz Arenite Other Sedimentary Metaquartzite Other Metamorphic	
2. K-Feldspar (25)	Microcline Orthoclase Sanadine Microphanerite Volcanic Rock Fragment Sedimentary Metamorphic	
3. Plagioclase (49)	Microphanerite Volcanic Rock Fragment Sedimentary Metamorphic	Altering to calcite:    Altering:
4. Volcanics (29)		Altering:
5. Microphanerites		
6. Accessory Minerals (1)	<u>Biotite:  </u> _____ _____	_____ _____
7. Carbonate Cement (33)		
8. Matrix/Pseudomatrix (10)	 	Biotite pseudo:
9. Clay Cement (4)	<u>kaolinite:     </u>	
10. Intragranular Porosity (4)	Quartz K-Feldspar Plagioclase 	VRF: Q K P PRF: Q K P
11. Intergranular Porosity (20)	Fractures Fracture-induced dissolution Oversize/elongate pores  Grain-edge dissolution	Primary Porosity  Other
12. Other (44)	<u>pyrite/organics:     </u> <u>R.F.: </u>	Phosphate:      Chert:      Shale:

COMMENTS:  
Lots of porosity. Some carbonates in minor amounts  
Kaolinite cement. Lots of rock fragments.  
Volcanics are altering to pseudo zcolite

\*Maybe too many r.f., carbonate, & pseudo for CE. P.T.P.I to be valuable?

PARAGENESIS:

SECONDARY INTERGRANULAR POROSITY

FRACTURE-INDUCED DISSOLUTION		
Q	vrfQ	prfQ
K	vrfK	prfK
P	vrfP	prfP
GRAIN-EDGE DISSOLUTION		
Q	vrfQ	prfQ
K	vrfK	prfK
P	vrfP	prfP
OVERSIZE/ELONGATE PORES		
Q	vrfQ	prfQ
K	vrfK	prfK
P	vrfP	prfP
OTHER		

(6)

SANDSTONE PETROGRAPHY DATA

EXAMINED BY: *SZC*

THIN SECTION: *Rudnick*  
FORMATION (AGE): *Veeder*  
LOCATION: *Rio Bravo*  
DEPTH: *11,382 - 11,400*

PROJECT: *Thesis*  
ROCK NAME: *Arkosic Arenite*  
POINT COUNTS: *300*  
COMPACTION: *CI: 2.1 TPI: 1.4*  
ANGULARITY: *Subround*

SORTING: *Poorly sorted*  
SIZE: *Medium Sand*

	SIZE	COMMENTS
1. Quartz (91) 30.9%	Monocrystalline Polycrystalline Microphanerite Volcanic Rock Fragment Quartz Arenite Other Sedimentary Metaquartzite Other Metamorphic	
2. K-Feldspar (36) 11.8%	Microcline Orthoclase Sanadine Microphanerite Volcanic Rock Fragment Sedimentary Metamorphic	<i>Altering to sericite: 1</i> <i>Altering: 1</i>
3. Plagioclase (49) 16.1%	Microphanerite Volcanic Rock Fragment Sedimentary Metamorphic	
4. Volcanics (17) 5.5%		
5. Microphanerites		
6. Accessory Minerals (1) 3.2%	<i>Muscovite: 1</i>	
7. Carbonate Cement		
8. Matrix/Pseudomatrix (48)		<i>Shale pseudo: 1</i>
9. Clay Cement (2)	<i>Kaolinite: 1</i>	
10. Intragranular Porosity (5) 6.5%	Quartz K-Feldspar Plagioclase	VRF: Q K P PRF: Q K P
11. Intergranular Porosity (6) 5.2%	Fractures Fracture-induced dissolution Oversize/elongate pores Grain-edge dissolution	Primary Porosity Other
12. Other (9) 6.2%	<i>Punk organics: 1</i> <i>RF: 1</i>	<i>Chert: 1</i> <i>Phosphate: 1</i>

\*Plag overgrowth @ 8, 73.2

COMMENTS:  
*Plag overgrowth observed zots of  $\phi$  w/ clay left behind.*  
*Zots of volcanics.*  
*Kaolinite present.*  
*clay protected grains from compaction P after dissolution TPI is very low, or grains are too big and would create a bias.*  
PARAGENESIS:  
*Zots of plag & Qtz overgrowths.*

SECONDARY INTERGRANULAR POROSITY

FRACTURE-INDUCED DISSOLUTION		
Q	vrfQ	prfQ
K	vrfK	prfK
P	vrfP	prfP
GRAIN-EDGE DISSOLUTION		
Q	vrfQ	prfQ
K	vrfK	prfK
P	vrfP	prfP
OVERSIZE/ELONGATE PORES		
Q	vrfQ	prfQ
K	vrfK	prfK
P	vrfP	prfP
OTHER		

(17) 5.5%

Total: 300

THIN SECTION: Rud-1 (stained)  
FORMATION (AGE): Vedder  
LOCATION: Rio Bravo  
DEPTH: 11,400-1

SANDSTONE PETROGRAPHY DATA

EXAMINED BY: S2L

PROJECT: Thesis

ROCK NAME: Arkosic Wacke  
POINT COUNTS: 300

SORTING: Poor

COMPACTION: N/A

SIZE: Fine Sand

ANGULARITY: Angular to subangular

	SIZE	COMMENTS
1. Quartz (50) 16.66%	Monocrystalline Polycrystalline Microphanerite Volcanic Rock Fragment Quartz Arenite Other Sedimentary Metaquartzite Other Metamorphic	
2. K-Feldspar (36) 12%	Microcline Orthoclase Sanadine Microphanerite Volcanic Rock Fragment Sedimentary Metamorphic	
3. Plagioclase (57) 19%	Microphanerite Volcanic Rock Fragment Sedimentary Metamorphic	Altering to clay
4. Volcanics (5) 1.66%		
5. Microphanerites		
6. Accessory Minerals (1) .33%	Biotite _____ _____ _____	
7. Carbonate Cement (26) 8.66%	Calcrete Dolomite	
8. Pseudomatrix 26.66%	Matrix:	
9. Clay Cement (3) 1%	Kaolinite	
10. Intragranular Porosity	Quartz K-Feldspar Plagioclase	VRF: Q K P PRF: Q K P
11. Intergranular Porosity (12) 4%	Fractures Fracture-induced dissolution Oversize/elongate pores Grain-edge dissolution	Primary Porosity Other
12. Other (27) 9%	Punk/organics RE	Chert

COMMENTS:  
Lots of matrix, poorly sorted. Nothing special about this one.

PARAGENESIS:

SECONDARY INTERGRANULAR POROSITY

FRACTURE-INDUCED DISSOLUTION		
Q	vrfQ	prfQ
K	vrfK	prfK
P	vrfP	prfP
GRAIN-EDGE DISSOLUTION		
Q	vrfQ	prfQ
K	vrfK	prfK
P	vrfP	prfP
OVERSIZE/ELONGATE PORES		
Q	vrfQ	prfQ
K	vrfK	prfK
P	vrfP	prfP
OTHER		

(3) 1%

SANDSTONE PETROGRAPHY DATA

EXAMINED BY: SZL

THIN SECTION: Rudnick  
FORMATION (AGE): Veeder  
LOCATION: Rio Bravo  
DEPTH: 11,400-2

PROJECT: Thesis  
ROCK NAME: Arkosic Arenite  
POINT COUNTS: 300

SORTING: Poor

COMPACTION: N/A

SIZE: Fine sand

ANGULARITY: Subangular

	SIZE	COMMENTS
1. Quartz 62	Monocrystalline Polycrystalline Microphanerite Volcanic Rock Fragment Quartz Arenite Other Sedimentary Metaquartzite Other Metamorphic	Altered to calcite:
2. K-Feldspar 47	Microcline   Orthoclase Sanadine Microphanerite   Volcanic Rock Fragment Sedimentary Metamorphic	Altering:
3. Plagioclase 54	Microphanerite Volcanic Rock Fragment Sedimentary Metamorphic	Altering:    Altered to calcite:
4. Volcanics 10		
5. Microphanerites		
6. Accessory Minerals		
7. Carbonate Cement 27		
8. Matrix/Pseudomatrix 61		Biotite pseudo:
9. Clay Cement 9		
10. Intragranular Porosity 2	Quartz K-Feldspar Plagioclase	VRF: Q K P PRF: Q K P
11. Intergranular Porosity 8	Fractures    Fracture-induced dissolution Oversize/elongate pores     Grain-edge dissolution	Primary Porosity Other
12. Other 9	+ dune/organics:     R.E.:	3 chert:

COMMENTS:  
Dirty sample. Some CaCO<sub>3</sub> clasts, clay coatings on grains. Some kaolinite throughout.

PARAGENESIS:  
Feldspar → kaolinite

SECONDARY INTERGRANULAR POROSITY

FRACTURE-INDUCED DISSOLUTION		
Q	vrfQ	prfQ
K	vrfK	prfK
P	vrfP	prfP
GRAIN-EDGE DISSOLUTION		
Q	vrfQ	prfQ
K	vrfK	prfK
P	vrfP	prfP
OVERSIZE/ELONGATE PORES		
Q	vrfQ	prfQ
K	vrfK	prfK
P	vrfP	prfP
OTHER		

THIN SECTION: Rudnick-1 (stained)  
FORMATION (AGE): Vedder  
LOCATION: Rio Bravo  
DEPTH: 11,400-4

SANDSTONE PETROGRAPHY DATA

EXAMINED BY: SZL

PROJECT: Thesis  
ROCK NAME: Arkosic Arenite  
POINT COUNTS: 300

SORTING: Very Poor  
SIZE: Very fine sand

COMPACTION: N/A  
ANGULARITY: Subangular to subround

	SIZE	COMMENTS
1. Quartz (43) 14.33%	Monocrystalline Polycrystalline Microphanerite Volcanic Rock Fragment Quartz Arenite Other Sedimentary Metaquartzite Other Metamorphic	
2. K-Feldspar (18) 6%	Microcline Orthoclase Sanadine Microphanerite    Volcanic Rock Fragment Sedimentary Metamorphic	
3. Plagioclase (54) 18%	Microphanerite    Volcanic Rock Fragment Sedimentary Metamorphic	
4. Volcanics (3)		
5. Microphanerites		
6. Accessory Minerals		
(123) 7. Carbonate Cement 41%		
(23) 8. Pseudomatrix 7.66% Clay-Altered Grains	 Matrix:	
(17) 9. Clay Cement 5.66%		
10. Intragranular Porosity	Quartz K-Feldspar Plagioclase	VRF: Q K P PRF: Q K P
(3) 11. Intergranular Porosity 1%	Fractures Fracture-induced dissolution Oversize/elongate pores     Grain-edge dissolution	Primary Porosity Other
12. Other (15) 5%	RF     pyrite/organics	

COMMENTS:

Band of carbonate running through. Very cool

PARAGENESIS:

SECONDARY INTERGRANULAR POROSITY

FRACTURE-INDUCED DISSOLUTION		
Q	vrfQ	prfQ
K	vrfK	prfK
P	vrfP	prfP
GRAIN-EDGE DISSOLUTION		
Q	vrfQ	prfQ
K	vrfK	prfK
P	vrfP	prfP
OVERSIZE/ELONGATE PORES		
Q	vrfQ	prfQ
K	vrfK	prfK
P	vrfP	prfP
OTHER		

(1) .33%

SANDSTONE PETROGRAPHY DATA

EXAMINED BY: Sze

THIN SECTION: Rudnick  
FORMATION (AGE): Vedder  
LOCATION: Rio Bravo  
DEPTH: 11,400-5  
SORTING: Poor  
SIZE:

PROJECT: thesis  
ROCK NAME: Arkosic Arenite  
POINT COUNTS: 300  
COMPACTION: Lots of clay, may not be able to use?  
CI: 2.1 TP: 1.4  
ANGULARITY: Subangular

	SIZE	COMMENTS
1. Quartz <u>62</u>	Monocrystalline Polycrystalline Microphanerite Volcanic Rock Fragment Quartz Arenite Other Sedimentary Metaquartzite Other Metamorphic	Altering:
2. K-Feldspar <u>46</u>	Microcline Orthoclase Sanadine Microphanerite Volcanic Rock Fragment Sedimentary Metamorphic	Altering to clay:
3. Plagioclase <u>60</u>	Microphanerite Volcanic Rock Fragment Sedimentary Metamorphic	Altering:      Altering 2 calcite:
4. Volcanics <u>8</u>		Altered:
5. Microphanerites		
6. Accessory Minerals <u>1</u>	Biotite:	
7. Carbonate Cement <u>27</u>		
8. Matrix/Pseudomatrix <u>22</u> <u>16</u> Clay-Altered Grains	 	Biotite pseudo:      Biotite → chlorite pseudo:
9. Clay Cement <u>7</u>	 Kaolinite:	
10. Intragranular Porosity <u>6</u>	Quartz K-Feldspar Plagioclase	VRF: Q K P PRF: Q K P
11. Intergranular Porosity <u>6</u>	Fractures Fracture-induced dissolution Oversize/elongate pores Grain-edge dissolution	Primary Porosity Other
12. Other <u>16</u>	Dark Organics:       S.R.F.:	Bone:    Chert:

COMMENTS:  
lots of dissolution, matrix, pseudo, carbonate  
may not have good compaction index?

PARAGENESIS:  
Fracturing → pyrite 40, 78

SECONDARY INTERGRANULAR POROSITY

FRACTURE-INDUCED DISSOLUTION		
Q	vrfQ	prfQ
K	vrfK	prfK
P	vrfP	prfP
GRAIN-EDGE DISSOLUTION		
Q	vrfQ	prfQ
K	vrfK	prfK
P	vrfP	prfP
OVERSIZE/ELONGATE PORES		
Q	vrfQ	prfQ
K	vrfK	prfK
P	vrfP	prfP
OTHER		

SANDSTONE PETROGRAPHY DATA

EXAMINED BY: *SLH*

THIN SECTION: Rudnick - 1 (stained)  
 FORMATION (AGE): Vedder  
 LOCATION: Rio Bravo  
 DEPTH: 11,400 - 7

PROJECT: Thesis  
 ROCK NAME: Arkosic wacke  
 POINT COUNTS: 300

SORTING: Very Poor  
 SIZE: Very fine sand

COMPACTION: N/A  
 ANGULARITY: Subangular - Subrounded

	SIZE	COMMENTS
1. Quartz (56) 18.66%	Monocrystalline Polycrystalline Microphanerite Volcanic Rock Fragment Quartz Arenite Other Sedimentary Metaquartzite Other Metamorphic	Altraing 1
2. K-Feldspar (15) 5%	Microcline Orthoclase Sanadine Microphanerite Volcanic Rock Fragment Sedimentary Metamorphic	
3. Plagioclase (76) 25.33%	Microphanerite Volcanic Rock Fragment Sedimentary Metamorphic	
4. Volcanics (2) .66%		
5. Microphanerites		
6. Accessory Minerals (3) 1%	hornblende Muscovite Biotite	
7. Carbonate Cement		
8. Pseudomatrix (24) 41.33% Clay-Altered Grains	Matrix:       101	(20)
9. Clay Cement (3) 1%		
10. Intragranular Porosity (1) .33%	Quartz K-Feldspar Plagioclase clay	VRF: Q K P PRF: Q K P
11. Intergranular Porosity (1) .33%	Fractures Fracture-induced dissolution Oversize/elongate pores Grain-edge dissolution	Primary Porosity Other
12. Other (13) 4.33%	pink organics RF:	

COMMENTS:  
 Lots of matrix, pseudomatrix. little K-spar. Probably dissolved & crushed into pseudo p clay

PARAGENESIS:

SECONDARY INTERGRANULAR POROSITY

FRACTURE-INDUCED DISSOLUTION		
Q	vrfQ	prfQ
K	vrfK	prfK
P	vrfP	prfP
GRAIN-EDGE DISSOLUTION		
Q	vrfQ	prfQ
K	vrfK	prfK
P	vrfP	prfP
OVERSIZE/ELONGATE PORES		
Q	vrfQ	prfQ
K	vrfK	prfK
P	vrfP	prfP

OTHER  
 (6) 21.

SANDSTONE PETROGRAPHY DATA

EXAMINED BY: SZL

THIN SECTION: Rudnick  
FORMATION (AGE): Vedder  
LOCATION: Rio Bravo  
DEPTH: 11,411  
SORTING: Poor  
SIZE:

PROJECT: Thesis  
ROCK NAME: Arkosic Arenite  
POINT COUNTS: 300  
COMPACTION: CI: 2.4 TPI: 1.5  
ANGULARITY: subangular - subround  
SIZE COMMENTS

1. Quartz 97	Monocrystalline Polycrystalline Microphanerite Volcanic Rock Fragment Quartz Arenite Other Sedimentary Metaquartzite Other Metamorphic				Poly at tang:
2. K-Feldspar 30	Microcline Orthoclase Sanadine Microphanerite Volcanic Rock Fragment Sedimentary Metamorphic				Altering to clay:   Altered:
3. Plagioclase 53	Microphanerite Volcanic Rock Fragment Sedimentary Metamorphic				Altering:
4. Volcanics 35					Altered:
5. Microphanerites					
6. Accessory Minerals 1	Biotite Garnet				
7. Carbonate Cement 2	Dolomite				
8. Matrix/Pseudomatrix 13					Biotite pseudo:
9. Clay Cement					
10. Intragranular Porosity 3	Quartz K-Feldspar Plagioclase		VRF: Q K P	PRF: Q K P	
11. Intergranular Porosity 22	Fractures Fracture-induced dissolution Oversize/elongate pores Grain-edge dissolution			Primary Porosity Other	
12. Other 21	4 Dunite/organics R.F.			Phosphato: Chert:	Bone:

COMMENTS:  
Lots of volcanics, possible bauxite?  
lots of deformed shale clasts forming a clay matrix. Dolomite rhombs in @ starting to grow or leftover from dissolution?

PARAGENESIS:  
Dolomite filling in @ @ 38, 71

SECONDARY INTERGRANULAR POROSITY

FRACTURE-INDUCED DISSOLUTION		
Q	vrfQ	prfQ
K	vrfK	prfK
P	vrfP	prfP
GRAIN-EDGE DISSOLUTION		
Q	vrfQ	prfQ
K	vrfK	prfK
P	vrfP	prfP
OVERSIZE/ELONGATE PORES		
Q	vrfQ	prfQ
K	vrfK	prfK
P	vrfP	prfP
OTHER		

**SANDSTONE PETROGRAPHY DATA**

EXAMINED BY: S. Unruh

THIN SECTION: Rud-1 11,413 stained  
 FORMATION (AGE): Oligocene  
 LOCATION: Rio Bravo  
 DEPTH: 11,413

PROJECT: Thesis

ROCK NAME: Arkosic Arenite  
 POINT COUNTS: 300

SORTING: Moderate to poorly sorted

COMPACTION: C1: 3.4 TPI: 1.6

SIZE: Medium to coarse sand  
 .32 - .44

ANGULARITY: subround to subangular

	SIZE	COMMENTS
1. Quartz (94)	Monocrystalline 71 Polycrystalline IIII Microphanerite Volcanic Rock Fragment   Quartz Arenite Other Sedimentary Metaquartzite Other Metamorphic	Quartz overgrowth   chert IIII
2. K-Feldspar (35)	Microcline Orthoclase II Sanadine Microphanerite Volcanic Rock Fragment Sedimentary Metamorphic	Altering to clay IIII Altering to calcite IIII
3. Plagioclase (49)	Microphanerite   Volcanic Rock Fragment Sedimentary 36 Metamorphic	Altering to seafite III Altering to kaolinite IIII Altering to calcite
4. Volcanics 5.3% (16)	III III III I	
5. Microphanerites		
6. Accessory Minerals .6% (2)	Biotite II	
7. Carbonate Cement 5.3% (16)	Calcite: III III III I	
8. Pseudomatrix 1.6% (5)	III	
9. Clay Cement 6% (18)	Biotite Altering to clay: II III III III I	clay coatings very common
10. Intragranular Porosity 1.3% (4)	Quartz II K-Feldspar   Plagioclase	Dissolved grain can't tell: I VRF: Q K P PRF: Q K P
11. Intergranular Porosity 7.3% (22)	Fractures Fracture-induced dissolution Oversize/elongate pores IIII Grain-edge dissolution	Primary Porosity III III IIII Other Dissolved clay: II
12. Other 7% (21)	Shale II hydrated carbon/pyrite III III II	phosphate pellets/Bone III II

**COMMENTS:**

Compaction & calcite bands run throughout. Calcite is cement replacing grains mostly plagioclase. Lots of clay coatings & volcanics w/ possible zeolites. Porosity is mostly primary throughout thin section. Sorting varies throughout as well as  $\phi$  & perm. due to cement & compaction bands.

**PARAGENESIS:**

Feldspar grains partially replaced by calcite. Calcite cement band goes throughout slide

\* Also possible zeolites in sample.

**SECONDARY INTERGRANULAR POROSITY**

FRACTURE-INDUCED DISSOLUTION		
Q I	vrfQ	prfQ
K II	vrfK	prfK
P	vrfP	prfP
GRAIN-EDGE DISSOLUTION		
Q IIII	vrfQ	prfQ
K III	vrfK	prfK
P III	vrfP	prfP
OVERSIZE/ELONGATE PORES		
Q	vrfQ	prfQ
K	vrfK	prfK
P IIII	vrfP	prfP
OTHER		

(23)

7.6%

SANDSTONE PETROGRAPHY DATA

EXAMINED BY: SU

THIN SECTION: Ruhl-1 (stained)  
FORMATION (AGE): Vedder  
LOCATION: Rio Poroso  
DEPTH: 11,437-3

PROJECT: Thesis  
ROCK NAME: Arkosic Arenite  
POINT COUNTS: 300

SORTING: Modulate Sorting  
SIZE: Very fine - fine sand

COMPACTION: C1; 2.5 TA: 1.5  
ANGULARITY: Subround to Rounded

	SIZE	COMMENTS
1. Quartz (50) 16.66%	Monocrystalline Polycrystalline     Microphanerite Volcanic Rock Fragment Quartz Arenite Other Sedimentary Metaquartzite Other Metamorphic	
2. K-Feldspar (22) 7.33%	Microcline   Orthoclase Sanadine Microphanerite     Volcanic Rock Fragment Sedimentary Metamorphic	
3. Plagioclase (70) 23.33%	Microphanerite    Volcanic Rock Fragment Sedimentary Metamorphic	Altering to clay
4. Volcanics (7) 2.33%		
5. Microphanerites		
6. Accessory Minerals (2) .66%	<u>Biotite:  </u> <u>Muscovite:  </u>	
7. Carbonate Cement (7) 2.33%	<u>Calcite Blocky    </u> <u>Dolomite  </u>	
8. Pseudomatrix (28) 9.33%		Matrix:
9. Clay Cement (4) 1.33%		
10. Intragranular Porosity (3) .1%	Quartz    K-Feldspar Plagioclase	VRF: Q K P PRF: Q K P
11. Intergranular Porosity (46) 22%	Fractures Fracture-induced dissolution Oversize/elongate pores       Grain-edge dissolution	Primary Porosity Other
12. Other (30) 10%	<u>RF:      </u> <u>pyrite/organics    </u>	<u>phosphate  </u>

COMMENTS:

Noticing that carbonates either calcite or dolomite have an affinity for oil to cluster around. Squashed grains in some areas of tighter packing, clay rims on fwg.

PARAGENESIS:

SECONDARY INTERGRANULAR POROSITY

FRACTURE-INDUCED DISSOLUTION		
Q	vrfQ	prfQ
K	vrfK	prfK
P	vrfP	prfP
GRAIN-EDGE DISSOLUTION		
Q	vrfQ	prfQ
K	vrfK	prfK
P	vrfP	prfP
OVERSIZE/ELONGATE PORES		
Q	vrfQ	prfQ
K	vrfK	prfK
P	vrfP	prfP
OTHER		

(11)  
3.66%

SANDSTONE PETROGRAPHY DATA

EXAMINED BY: SZL

(33)

THIN SECTION: Ruhl-1  
 FORMATION (AGE): Wedder  
 LOCATION: Rio Bravo  
 DEPTH: 11,437-5

PROJECT: Thesis  
 ROCK NAME: Arkosic Arenite  
 POINT COUNTS: 300

SORTING: Poorly sorted  
 SIZE: fine to medium sand

COMPACTION: Cl:2.0 TPI: 1.4  
 ANGULARITY: Subangular

	SIZE	COMMENTS
1. Quartz 80	Monocrystalline Polycrystalline     Microphanerite Volcanic Rock Fragment Quartz Arenite Other Sedimentary Metaquartzite Other Metamorphic	
2. K-Feldspar 18	Microcline Orthoclase Sanadine Microphanerite Volcanic Rock Fragment Sedimentary Metamorphic	
3. Plagioclase 42	Microphanerite Volcanic Rock Fragment Sedimentary Metamorphic	Plag → sericite
4. Volcanics 3		
5. Microphanerites		
6. Accessory Minerals 5	<u>Biotite</u>     <u>Muscovite</u>	
7. Carbonate Cement 14	<del>     </del>	
8. Matrix/ Pseudomatrix Clay-Altered Grains	14 <del>     </del> 6 <del>    </del>	
9. Clay Cement 1		
10. Intragranular Porosity dissolved grain	Quartz   K-Feldspar Plagioclase other: <del>    </del>	VRF: Q K P PRF: Q K P
11. Intergranular Porosity 54	Fractures Fracture-induced dissolution Oversize/elongate pores <del>     </del> Grain-edge dissolution	Primary Porosity Other
12. Other 5 15	<u>organics/pink</u> :     <u>R.F.</u> <del>     </del>	Phosphate   Chert

COMMENTS:  
 Clay coatings on all grains.  
 Some glauconite/diatomite.  
 Kaolinite present.  
 Fracturing of quartz grain w/ muscovite in between grain  
 Sporadic CaCO<sub>3</sub> in sample  
 Rutile needles

PARAGENESIS:

SECONDARY INTERGRANULAR POROSITY

FRACTURE-INDUCED DISSOLUTION		
Q	vrfQ	prfQ
K	vrfK	prfK
P	vrfP	prfP
GRAIN-EDGE DISSOLUTION		
Q <del>     </del>	vrfQ	prfQ
K	vrfK	prfK
P <del>     </del>	vrfP	prfP
OVERSIZE/ELONGATE PORES		
Q	vrfQ	prfQ
K	vrfK	prfK
P	vrfP	prfP
OTHER		

72.2 25

SANDSTONE PETROGRAPHY DATA

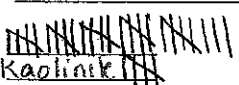
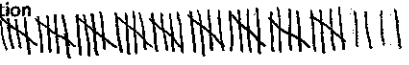
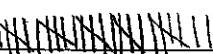
EXAMINED BY: SZL

THIN SECTION: Ruhl-1 (stained)  
 FORMATION (AGE): Vedder  
 LOCATION: Rio Bravo  
 DEPTH: 11,461-2  
 SORTING: Moderate  
 SIZE: Medium Sand

PROJECT: Thesis  
 ROCK NAME: Arkosic Arenite  
 POINT COUNTS: 300

COMPACTION: CI: 2.1 TPI: 1.4

ANGULARITY: Subangular to Subround

	SIZE	COMMENTS
1. Quartz <u>67</u>	Monocrystalline Polycrystalline  Microphanerite Volcanic Rock Fragment Quartz Arenite Other Sedimentary Metaquartzite Other Metamorphic	Altered poly I Altered I
2. K-Feldspar <u>19</u>	Microcline Orthoclase Sanadine Microphanerite Volcanic Rock Fragment Sedimentary Metamorphic	
3. Plagioclase <u>66</u>	Microphanerite Volcanic Rock Fragment Sedimentary Metamorphic	Altered III Altered to smectite
4. Volcanics <u>(3)</u> <u>1%</u>		
5. Microphanerites		
6. Accessory Minerals <u>(4)</u> <u>1.33%</u>	<u>Chlorite</u> <u>Muscovite</u>	<u>Glaucophane</u> <u>Hornblende</u> <u>Biotite</u>
7. Carbonate Cement <u>(2)</u> <u>66%</u>	<u>Dolomite</u>	
8. Pseudomatrix <u>(2)</u> <u>66%</u>	Matrix:	
9. Clay Cement <u>(33)</u> <u>11%</u>	 <u>Kaolinite</u>	
10. Intragranular Porosity <u>(2)</u> <u>1%</u>	Quartz K-Feldspar Plagioclase <u>U</u>	VRF: Q K P PRF: Q K P
11. Intergranular Porosity <u>(51)</u> <u>17%</u>	Fractures Fracture-induced dissolution Oversize/elongate pores  Grain-edge dissolution	Primary Porosity Other
12. Other <u>(4)</u> <u>13.33%</u>	<u>RF</u> <u>Punct. organics</u> 	

COMMENTS:  
 Lots of residual oil. Lots of porosity. Lots of clay altered grains w/ oil covering deformed biotite grains

PARAGENESIS:

SECONDARY INTERGRANULAR POROSITY

FRACTURE-INDUCED DISSOLUTION		
Q	vrfQ	prfQ
K	vrfK	prfK
P	vrfP	prfP
GRAIN-EDGE DISSOLUTION		
Q 	vrfQ	prfQ
K 	vrfK	prfK
P 	vrfP	prfP
OVERSIZE/ELONGATE PORES		
Q	vrfQ	prfQ
K	vrfK	prfK
P	vrfP	prfP
OTHER		

(10) 3.33%

SANDSTONE PETROGRAPHY DATA

EXAMINED BY: SZL

THIN SECTION: Ruhl-1  
 FORMATION (AGE): Vedder  
 LOCATION: Rio Bravo  
 DEPTH: 11,461.5

PROJECT: Thesis  
 ROCK NAME: Arkosic Arenite  
 POINT COUNTS: 300

SORTING: Poor

COMPACTION: N/A  
 ANGULARITY: Subangular to subround

SIZE	COMMENTS
1. Quartz <u>64</u>	Monocrystalline Polycrystalline <u>    </u> Microphanerite Volcanic Rock Fragment <u>  </u> Quartz Arenite Other Sedimentary Metaquartzite Other Metamorphic <u> </u>
2. K-Feldspar <u>9</u>	Microcline Orthoclase Sanadine Microphanerite Volcanic Rock Fragment Sedimentary Metamorphic
3. Plagioclase <u>26</u>	Microphanerite Volcanic Rock Fragment Sedimentary Metamorphic
4. Volcanics	<u> </u>
5. Microphanerites	
6. Accessory Minerals <u>4</u>	<u>Muscovite:  </u> <u>Biotite:  </u> <u>Glaucophane:   </u>
7. Carbonate Cement <u>66</u>	<u>     </u>
8. Pseudomatrix	
9. Clay Cement <u>4</u>	<u>    </u>
10. Intragranular Porosity	Quartz VRF: Q PRF: Q K-Feldspar K K Plagioclase P P
11. Intergranular Porosity <u>1</u>	Fractures Fracture-induced dissolution Primary Porosity Oversize/elongate pores Grain-edge dissolution Other
12. Other <u>6</u>	<u>14 organics / calcite:      </u> <u>6 RF:      </u> <u>3 chert:  </u> <u>3 fossil:    </u>

COMMENTS:

- Carbonate cement throughout Both calcite & Dolomite.  
 - Dolomite & calcite are partially replacing f.w. grains.  
 - Zircon present @ 63.5, 34.5

PARAGENESIS:

SECONDARY INTERGRANULAR POROSITY

FRACTURE-INDUCED DISSOLUTION		
Q	vrfQ	prfQ
K	vrfK	prfK
P	vrfP	prfP
GRAIN-EDGE DISSOLUTION		
Q	vrfQ	prfQ
K	vrfK	prfK
P	vrfP	prfP
OVERSIZE/ELONGATE PORES		
Q	vrfQ	prfQ
K	vrfK	prfK
P	vrfP	prfP
OTHER		

SANDSTONE PETROGRAPHY DATA

EXAMINED BY: SJL

THIN SECTION: Ruhl  
 FORMATION (AGE): Wedder  
 LOCATION: Rio Bravo  
 DEPTH: 11,482-2

PROJECT: Thesis  
 ROCK NAME: Arkosic Arenite  
 POINT COUNTS: 300

SORTING: Poor

COMPACTION: N/A

SIZE: fine to conglomerate

ANGULARITY: subround

	SIZE	COMMENTS
1. Quartz (50) 16.6%	Monocrystalline Polycrystalline <del>    </del> Microphanerite Volcanic Rock Fragment Quartz Arenite Other Sedimentary   Metaquartzite Other Metamorphic	
2. K-Feldspar (25) 8.3%	Microcline Orthoclase Sanadine Microphanerite Volcanic Rock Fragment Sedimentary Metamorphic	Altering to CaCO <sub>3</sub> :
3. Plagioclase (48) 16%	Microphanerite    Volcanic Rock Fragment   Sedimentary Metamorphic	Altering to CaCO <sub>3</sub> : <del>    </del>      Altering:
4. Volcanics (7) 2.3%		Volcanic → chlorite:     Altering:
5. Microphanerites		
6. Accessory Minerals (34) 11.3%	Glaucanite: <del>     </del> Chlorite: <del>     </del>	Hornblende:   Glauc to chlorite:
7. Carbonate Cement (9) 30.3%	<del>     </del>	
8. Matrix/ Pseudomatrix (8) 2.6%	<del>    </del>	pseudoglauc:
9. Clay Cement (10) 3.3%	<del>    </del>	
10. Intragranular Porosity	Quartz K-Feldspar Plagioclase	VRF: Q K P PRF: Q K P
11. Intergranular Porosity (2) .66%	Fractures   Fracture-induced dissolution Oversize/elongate pores   Grain-edge dissolution	Primary Porosity Other
12. Other (20) 8.3%	organics/quinite: <del>    </del> R.F.: <del>    </del>	chert: <del>    </del>

COMMENTS:  
 Lots of glauconite, dolomite cement, chlorite filling in fractured grains.

SECONDARY INTERGRANULAR POROSITY

FRACTURE-INDUCED DISSOLUTION		
Q	vrfQ	prfQ
K	vrfK	prfK
P	vrfP	prfP
GRAIN-EDGE DISSOLUTION		
Q	vrfQ	prfQ
K	vrfK	prfK
P	vrfP	prfP
OVERSIZE/ELONGATE PORES		
Q	vrfQ	prfQ
K	vrfK	prfK
P	vrfP	prfP
OTHER		

PARAGENESIS:  
 Glaucanite → chlorite  
 fracturing → infilling of chlorite in fractures  
 Glaucanite → organics/quinite

SANDSTONE PETROGRAPHY DATA

EXAMINED BY: *SJL*

THIN SECTION: *Ruhl-1 (stained)*  
FORMATION (AGE): *Vedder*  
LOCATION: *Rio Bravo*  
DEPTH: *11, 482-3*

PROJECT: *Thesis*  
ROCK NAME: *Lithic Arenite*  
POINT COUNTS: *300*  
COMPACTION: *N/A*  
ANGULARITY: *Subrounded*

SORTING: *Very Poor*  
SIZE: *Fine to Medium Sand*

	SIZE	COMMENTS
1. Quartz (49) 16.33% Monocrystalline Polycrystalline <i>     </i> Microphanerite Volcanic Rock Fragment Quartz Arenite Other Sedimentary Metaquartzite Other Metamorphic	<i>.12 - .40 mm</i>	
2. K-Feldspar (18) 6% Microcline Orthoclase Sanadine Microphanerite <i>  </i> Volcanic Rock Fragment Sedimentary Metamorphic	<i>.04 - .26 mm</i>	
3. Plagioclase (33) 11% Microphanerite <i>    </i> Volcanic Rock Fragment Sedimentary Metamorphic	<i>.12 - .32 mm</i>	
4. Volcanics (14) <i>     </i> 4.66%		
5. Microphanerites		
6. Accessory Minerals		
7. Carbonate Cement <i>     </i> 29.33%		
8. Pseudomatrix (19) <i>     </i> 6.33% Clay-Altered Grains Matrix <i>     </i>		
9. Clay Cement (15) <i>     </i> 5%		
10. Intragranular Porosity	Quartz K-Feldspar Plagioclase	VRF: Q K P PRF: Q K P
11. Intergranular Porosity (25) 8.33%	Fractures Fracture-induced dissolution Oversize/elongate pores <i>     </i> Grain-edge dissolution	Primary Porosity Other
12. Other (38) 12.66%	<i>phosphate</i> <i>    </i> <i>pyrite/organics</i> <i>     </i>	<i>Chert</i> <i>    </i>

COMMENTS:  
*lots of carbonate cement along w/ clay altered grains throughout. Dolomitization occurring on numerous grains lots of dissolution of grains.*

PARAGENESIS:

SECONDARY INTERGRANULAR POROSITY

FRACTURE-INDUCED DISSOLUTION		
Q	vrfQ	prfQ
K	vrfK	prfK
P	vrfP	prfP
GRAIN-EDGE DISSOLUTION		
Q	vrfQ	prfQ
K	vrfK	prfK
P	vrfP	prfP
OVERSIZE/ELONGATE PORES		
Q	vrfQ	prfQ
K	vrfK	prfK
P	vrfP	prfP
OTHER		
(1) 1%		

SANDSTONE PETROGRAPHY DATA

EXAMINED BY: SZL

THIN SECTION: Ruhl-1  
FORMATION (AGE): Vedder  
LOCATION: Rio Bravo  
DEPTH: 11,482-4

PROJECT: Thesis  
ROCK NAME: A/Kosic Arenite  
POINT COUNTS: 300

SORTING: Poor  
SIZE: Medium sand

COMPACTION:  
ANGULARITY: Sub angular - sub round

	SIZE	COMMENTS
1. Quartz 69	Monocrystalline Polycrystalline <del>     </del> Microphanerite Volcanic Rock Fragment Quartz Arenite Other Sedimentary Metaquartzite <del>     </del> Other Metamorphic	
2. K-Feldspar 20	Microcline Orthoclase Sanadine Microphanerite Volcanic Rock Fragment Sedimentary Metamorphic	
3. Plagioclase 47	Microphanerite   Volcanic Rock Fragment   Sedimentary Metamorphic	
4. Volcanics 14	<del>     </del>	
5. Microphanerites		
6. Accessory Minerals 2	<u>Biotite</u> <u>Muscovite</u>	
7. Carbonate Cement 106	<del>     </del>	
8. Matrix/ Pseudomatrix 3	<del>     </del>	
Clay-Altered Grains		
9. Clay Cement 1		
10. Intragranular Porosity	Quartz K-Feldspar Plagioclase	VRF: Q K P PRF: Q K P
11. Intergranular Porosity	Fractures Fracture-induced dissolution Oversize/elongate pores Grain-edge dissolution <del>     </del>	Primary Porosity Other
12. Other	<u>4 Organics/Purite -      </u> <u>2) R.F. <del>     </del></u>	<u>9 chert <del>     </del></u>

COMMENTS:  
- RF are most affected by calcification. They seem to be the least stable  
- Lots of zoned plagioclase grains

PARAGENESIS:

SECONDARY INTERGRANULAR POROSITY

FRACTURE-INDUCED DISSOLUTION		
Q	vrfQ	prfQ
K	vrfK	prfK
P	vrfP	prfP
GRAIN-EDGE DISSOLUTION		
Q	vrfQ	prfQ
K	vrfK	prfK
P	vrfP	prfP
OVERSIZE/ELONGATE PORES		
Q	vrfQ	prfQ
K	vrfK	prfK
P	vrfP	prfP
OTHER		

SANDSTONE PETROGRAPHY DATA

EXAMINED BY: S2L

THIN SECTION: Ruhl-1 (stained)  
FORMATION (AGE): Vedder  
LOCATION: Rio Bravo  
DEPTH: 11,502-1

PROJECT: Thesis  
ROCK NAME: Lithic Arenite  
POINT COUNTS: 300

SORTING: Poorly Sorted

COMPACTION: N/A

SIZE: Coarse Sand

ANGULARITY: Subround to Rounded

	SIZE	COMMENTS
1. Quartz 93 31%	Monocrystalline Polycrystalline Microphanerite Volcanic Rock Fragment Quartz Arenite Other Sedimentary Metaquartzite Other Metamorphic	weird quartz? 24, 77?
2. K-Feldspar (24) 8%	Microcline Orthoclase Sanadine Microphanerite Volcanic Rock Fragment Sedimentary Metamorphic	
3. Plagioclase (13) 4.33%	Microphanerite Volcanic Rock Fragment Sedimentary Metamorphic	Altering to calcite 1
4. Volcanics (3) 1%		
5. Microphanerites		
6. Accessory Minerals		
7. Carbonate Cement (99) 33%		
8. Pseudomatrix (1) 1%		Matrix: 1
9. Clay (6) Cement 2%		Kalinite 1
10. Intragranular Porosity	Quartz K-Feldspar Plagioclase	VRF: Q K P PRF: Q K P
11. Intergranular Porosity (13) 4.33%	Fractures Fracture-induced dissolution Oversize/elongate pores Grain-edge dissolution	Primary Porosity Other
12. Other (46) 15.33%	RF pyrite/organics	chert

COMMENTS:

SECONDARY INTERGRANULAR POROSITY

FRACTURE-INDUCED DISSOLUTION

Q	vrfQ	prfQ
K	vrfK	prfK
P	vrfP	prfP

GRAIN-EDGE DISSOLUTION

Q	vrfQ	prfQ
K	vrfK	prfK
P	vrfP	prfP

OVERSIZE/ELONGATE PORES

Q	vrfQ	prfQ
K	vrfK	prfK
P	vrfP	prfP

OTHER

(1) 1%

PARAGENESIS:

SANDSTONE PETROGRAPHY DATA

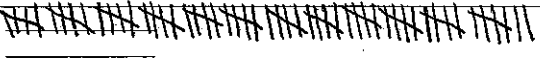
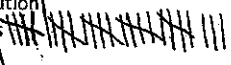
EXAMINED BY: SZL

THIN SECTION: Ruh-1  
 FORMATION (AGE): Vedder  
 LOCATION: Rio Bravo  
 DEPTH: 11,502-2

PROJECT: Thesis  
 ROCK NAME: Arkosic Arenite  
 POINT COUNTS: 300

SORTING: Poorly sorted  
 SIZE: Medium sand - Coarse

COMPACTION: N/A  
 ANGULARITY: Sub-rounded

	SIZE	COMMENTS
1. Quartz 90	Monocrystalline Polycrystalline  Microphanerite  Volcanic Rock Fragment Quartz Arenite Other Sedimentary Metaquartzite Other Metamorphic	calcedony 1
2. K-Feldspar 29	Microcline Orthoclase Sanadine Microphanerite   Volcanic Rock Fragment Sedimentary Metamorphic	
3. Plagioclase 51	Microphanerite   Volcanic Rock Fragment Sedimentary Metamorphic	Plag → sericite
4. Volcanics 4		
5. Microphanerites		
6. Accessory Minerals	<u>Biotite 1</u>	
7. Carbonate Cement 62		
8. Matrix/Pseudomatrix		
9. Clay Cement	<u>  </u>	
10. Intragranular Porosity	Quartz K-Feldspar Plagioclase	VRF: Q K P PRF: Q K P
11. Intergranular Porosity 32	Fractures   Fracture-induced dissolution Oversize/elongate pores  Grain-edge dissolution 	Primary Porosity Other
12. Other	<u>15 organics/ovrite</u>  <u>7 R.F.</u> 	<u>9 Chert</u>  <u>Phosphate</u>

COMMENTS:  
 More  $\phi$  than 11,482-21  
 - Quartz grains are highly fractured  
 - Myrmekitic present  
 - Some zoned plagioclase grains present

PARAGENESIS:

SECONDARY INTERGRANULAR POROSITY

FRACTURE-INDUCED DISSOLUTION		
Q	vrfQ	prfQ
K	vrfK	prfK
P	vrfP	prfP
GRAIN-EDGE DISSOLUTION		
Q	vrfQ	prfQ
K	vrfK	prfK
P	vrfP	prfP
OVERSIZE/ELONGATE PORES		
Q	vrfQ	prfQ
K	vrfK	prfK
P	vrfP	prfP
OTHER		

SANDSTONE PETROGRAPHY DATA

EXAMINED BY: SZL

THIN SECTION: Ruh1-1 (stained)  
FORMATION (AGE): Vedder  
LOCATION: Rio Bravo  
DEPTH: 11,502-3

PROJECT: Thesis  
ROCK NAME: Arkosic Arenite  
POINT COUNTS: 300

SORTING: well sorted Fwg w/ CaCO<sub>3</sub> cement

COMPACTION: N/A

SIZE: Coarse to Very Coarse

ANGULARITY: Subround to Round

	SIZE	COMMENTS
1. Quartz (97) 32.33%	Monocrystalline Polycrystalline Microphanerite Volcanic Rock Fragment Quartz Arenite Other Sedimentary Metaquartzite Other Metamorphic	
2. K-Feldspar (38) 12.66%	Microcline Orthoclase Sanadine Microphanerite Volcanic Rock Fragment Sedimentary Metamorphic	
3. Plagioclase (22) 7.33%	Microphanerite Volcanic Rock Fragment Sedimentary Metamorphic	Altering w/ muscovite flakes 19, 71 Altering to sericite
4. Volcanics (5) 1.66%		
5. Microphanerites		
6. Accessory Minerals		FeO <sub>2</sub> min. present 14, 74
7. Carbonate Cement (69) 23%	Dolomite	
8. Pseudomatrix		
9. Clay Cement (4) 1.33%	Kaolinite	
10. Intragranular Porosity (3) 1%	Quartz K-Feldspar Plagioclase	VRF: Q K P PRF: Q K P
11. Intergranular Porosity (32) 10.66%	Fractures Fracture-induced dissolution Oversize/elongate pores Grain-edge dissolution	Primary Porosity Other
12. Other (30) 10%	phosphate chert unkelorganics	

COMMENTS:

Sample is full of dolomite cement along w/ some Fe rich matrix? Very orange/reddish. Very coarse grained sample.

PARAGENESIS:

SECONDARY INTERGRANULAR POROSITY

FRACTURE-INDUCED DISSOLUTION		
Q	vrfQ	prfQ
K	vrfK	prfK
P	vrfP	prfP
GRAIN-EDGE DISSOLUTION		
Q	vrfQ	prfQ
K	vrfK	prfK
P	vrfP	prfP
OVERSIZE/ELONGATE PORES		
Q	vrfQ	prfQ
K	vrfK	prfK
P	vrfP	prfP
OTHER		

SANDSTONE PETROGRAPHY DATA

EXAMINED BY: SL

THIN SECTION: Ruhl-1  
FORMATION (AGE): Vedder  
LOCATION: Rio Bravo  
DEPTH: 11,502-4

PROJECT: Thesis  
ROCK NAME: Subarkosic Arenite  
POINT COUNTS: 300

SORTING: Moderate

COMPACTION: N/A

SIZE: Medium to coarse grained

ANGULARITY: Subrounded

	SIZE	COMMENTS
1. Quartz (110) 36.6%	Monocrystalline Polycrystalline <del>     </del> Microphanerite Volcanic Rock Fragment Quartz Arenite Other Sedimentary Metaquartzite Other Metamorphic <del>     </del>	Altering to calcite: <del>     </del> cheat → kaolinite: 1
2. K-Feldspar (29) 9.6%	Microcline    Orthoclase Sanadine Microphanerite Volcanic Rock Fragment Sedimentary Metamorphic	Altering to calcite: 1
3. Plagioclase 22 7.7%	Microphanerite    Volcanic Rock Fragment Sedimentary Metamorphic	Altering to calcite: 1 Altering to calcite: 1
4. Volcanics (5) 1.6%	<del>     </del>	
5. Microphanerites		
6. Accessory Minerals	=====	
7. Carbonate Cement (81) 27%	<del>     </del>	
8. Matrix/Pseudomatrix (3) 1%		pseudo chlorite: 1
9. Clay Cement (6) 2%	kaolinite: <del>     </del>	
10. Intragranular Porosity (1) .33%	Quartz K-Feldspar Plagioclase	VRF: Q K P PRF: Q K P
11. Intergranular Porosity (10) 3.3%	Fractures Fracture-induced dissolution Oversize/elongate pores <del>     </del> Grain-edge dissolution	Primary Porosity  Other
12. Other (34) 11.3%	pyrite/organics:    RF: <del>     </del>	Phosphate: <del>     </del> cheat: <del>     </del>

COMMENTS: Poikiloblastic carbonate cement. Small amounts of kaolinite.

SECONDARY INTERGRANULAR POROSITY

FRACTURE-INDUCED DISSOLUTION		
Q	vrfQ	prfQ
K	vrfK	prfK
P	vrfP	prfP
GRAIN-EDGE DISSOLUTION		
Q	vrfQ	prfQ
K	vrfK	prfK
P	vrfP	prfP
OVERSIZE/ELONGATE PORES		
Q	vrfQ	prfQ
K	vrfK	prfK
P	vrfP	prfP
OTHER		

PARAGENESIS: Phosphate first then carbonate. Good pic.

SANDSTONE PETROGRAPHY DATA

EXAMINED BY: S. Unnik

THIN SECTION: Ruh-1 (Stained)  
 FORMATION (AGE): Oligocene  
 LOCATION: Rio Bravo Field  
 DEPTH: 11,534 -1

PROJECT: Thesis

ROCK NAME: Sub Arkosic Arenite  
 POINT COUNTS: 300

SORTING: Moderate to well sorted

COMPACTION: C1: 2.1 TPI: 1.5

SIZE: Coarse to very coarse sand

ANGULARITY: Round to well Rounded

	SIZE	COMMENTS
1. Quartz (96) 32%	Monocrystalline Polycrystalline <del>    </del> Microphanerite   Volcanic Rock Fragment Quartz Arenite Other Sedimentary Metaquartzite Other Metamorphic	Quartz w/ dolomite rims   remnant
2. K-Feldspar (33) 11%	Microcline Orthoclase <del>    </del> Sanadine Microphanerite   Volcanic Rock Fragment Sedimentary Metamorphic	
3. Plagioclase (11) 3.66%	Microphanerite Volcanic Rock Fragment   Sedimentary Metamorphic	Altered to sericite
4. Volcanics (6) 2%	<del>    </del>	
5. Microphanerites		
6. Accessory Minerals (6) 2%	Muscovite   Chlorite    Claucaonite	Apatite
7. Carbonate Cement (63) 21%	Dolomite <del>     </del>	
8. Pseudomatrix		
Clay-Altered Grains		
9. Clay Cement (2) .66%	kaolinite   sericite	
10. Intragranular Porosity (3) 1%	Quartz   K-Feldspar    Plagioclase	VRF: Q K P PRF: Q K P
11. Intergranular Porosity (45) 15%	Fractures Fracture-induced dissolution Oversize/elongate pores <del>     </del> Grain-edge dissolution	Primary Porosity <del>     </del> Other Shrinkage
12. Other (28) 9.3%	phosphate <del>     </del> hydrocarbon/pyrite	Rock fragment/shale <del>     </del> chert <del>     </del>

COMMENTS:

Lots of carbonate cement w/ Dolomite Rhombs. cement occluding pore space. Texture is mainly of floating grains & point contacts  
 Lots of primary porosity & oversize pores. K-spars show dissolution w/ intragranular porosity the most. Dolomite rhombs floating. Small amounts of oil shows present.  
 Chlorite is healing over on some quartz grains.

PARAGENESIS:

Fracturing → Dolomite precip. → dissolution → secondary ∅ → oil migration.

Chlorite? not sure on timing

SECONDARY INTERGRANULAR POROSITY

FRACTURE-INDUCED DISSOLUTION		
Q	vrfQ	prfQ
K	vrfK	prfK
P	vrfP	prfP
GRAIN-EDGE DISSOLUTION		
Q	vrfQ	prfQ
K	vrfK	prfK
P	vrfP	prfP
OVERSIZE/ELONGATE PORES		
Q	vrfQ	prfQ
K	vrfK	prfK
P	vrfP	prfP
OTHER		

(7) 2.33%

SANDSTONE PETROGRAPHY DATA

EXAMINED BY: SZL

THIN SECTION: Ruhl  
 FORMATION (AGE): Nadder  
 LOCATION: Rio Bravo  
 DEPTH: 11,534-2

PROJECT: Thesis  
 ROCK NAME: Subarkosic Arenite  
 POINT COUNTS: 300

SORTING: Well

COMPACTION: N/A

SIZE: Medium

ANGULARITY: Sub rounded

	SIZE	COMMENTS
1. Quartz (129) 43%	Monocrystalline Polycrystalline <del>     </del> Microphanerite Volcanic Rock Fragment Quartz Arenite Other Sedimentary Metaquartzite Other Metamorphic	Poly quartz → calcite:
2. K-Feldspar (43) 14.3%	Microcline <del>     </del> Orthoclase Sanadine Microphanerite   Volcanic Rock Fragment Sedimentary Metamorphic	
3. Plagioclase (12) 4%	Microphanerite      Volcanic Rock Fragment Sedimentary Metamorphic	
4. Volcanics (4) 1.3%		
5. Microphanerites		
6. Accessory Minerals		
7. Carbonate Cement (71) 23.6%	<del>     </del>	
8. Matrix/Pseudomatrix		
Clay-Altered Grains		
9. Clay Cement (3) 1%	Kaolinite:	
10. Intragranular Porosity (3) 1%	Quartz K-Feldspar      Plagioclase	VRF: Q K P PRF: Q K P
11. Intergranular Porosity (10) 3.3%	Fractures Fracture-induced dissolution Oversize/elongate pores <del>     </del> Grain-edge dissolution	Primary Porosity Other
12. Other (23) 7.6%	Quartz/organics R.F. <del>     </del>	Shell:   Chert: <del>     </del> Phosphate:

COMMENTS:  
 Poikilotopic calcite cement.  
 Chert + R.F. tend to alter to Kaolinite.  
 Most microcline I've had yet in a thin section

PARAGENESIS:  
 Fracture → calcite  
 ? chlorite or phosphate? what came first?  
 calcite → dissolution

SECONDARY INTERGRANULAR POROSITY

FRACTURE-INDUCED DISSOLUTION		
Q	vrfQ	prfQ
K	vrfK	prfK
P	vrfP	prfP
GRAIN-EDGE DISSOLUTION		
Q	vrfQ	prfQ
K	vrfK	prfK
P	vrfP	prfP
OVERSIZE/ELONGATE PORES		
Q	vrfQ	prfQ
K	vrfK	prfK
P	vrfP	prfP
OTHER		

(2) .6%

SANDSTONE PETROGRAPHY DATA

EXAMINED BY: SU

THIN SECTION: Ruhl-1 (stained)  
 FORMATION (AGE): Vedder  
 LOCATION: Rio Bravo  
 DEPTH: 11, 574-1

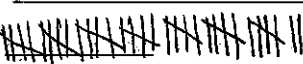
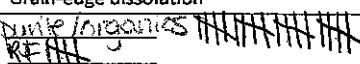
PROJECT: Thesis  
 ROCK NAME: Arkosic Arenite  
 POINT COUNTS: 300

SORTING: Poor

COMPACTION: N/A

SIZE: Very fine grained sand

ANGULARITY: Angular to sub angular

	SIZE	COMMENTS
1. Quartz (50) 14.66%	Monocrystalline Polycrystalline    Microphanerite Volcanic Rock Fragment Quartz Arenite Other Sedimentary Metaquartzite Other Metamorphic	
2. K-Feldspar (35) 11.66%	Microcline Orthoclase Sanadine Microphanerite   Volcanic Rock Fragment Sedimentary Metamorphic	
3. Plagioclase (65) 21.66%	Microphanerite     Volcanic Rock Fragment Sedimentary Metamorphic	
4. Volcanics (1) .33%		
5. Microphanerites		
6. Accessory Minerals (2) .66%	<u>Glaucophane</u> → <u>Chionite</u> <u>Hornblende</u>	<u>Zircon</u> <u>Muscovite present</u>
(57) 7. Carbonate Cement .19%	<del>Dolomite</del> 	
8. Pseudomatrix (9) 	<u>Matrix</u> 	
Clay-Altered Grains		
9. Clay Cement (37) 6.33%		
10. Intragranular Porosity (1) .33%	Quartz K-Feldspar Plagioclase	VRF: Q K P PRF: Q K P
11. Intergranular Porosity (8) 2.66%	Fractures Fracture-induced dissolution Oversize/elongate pores  Grain-edge dissolution	Primary Porosity Other
12. Other (25) 8.33%	<del>None</del> <u>Organics</u> 	

COMMENTS:

Lots of clay-Altered grains along w/ dolomite cement. Some altered biotite grains that altered to clay.

PARAGENESIS:

SECONDARY INTERGRANULAR POROSITY

FRACTURE-INDUCED DISSOLUTION		
Q	vrfQ	prfQ
K	vrfK	prfK
P	vrfP	prfP
GRAIN-EDGE DISSOLUTION		
Q	vrfQ	prfQ
K	vrfK	prfK
P	vrfP	prfP
OVERSIZE/ELONGATE PORES		
Q	vrfQ	prfQ
K	vrfK	prfK
P	vrfP	prfP
OTHER		

SANDSTONE PETROGRAPHY DATA

EXAMINED BY: SZL

THIN SECTION: Ruhl  
FORMATION (AGE): Uedder  
LOCATION: Rio Bravo  
DEPTH: 11, 574-2

PROJECT: Thesis

ROCK NAME: Arkosic Arenite  
POINT COUNTS: 300

SORTING: Poor

COMPACTION: N/A

SIZE: fine sand

ANGULARITY: sub angular

	SIZE	COMMENTS
1. Quartz (56) 18.6%	Monocrystalline Polycrystalline      Microphanerite Volcanic Rock Fragment Quartz Arenite Other Sedimentary Metaquartzite Other Metamorphic	Poly to calcite:   Quartz → calcite:
2. K-Feldspar (33) 11%	Microcline Orthoclase Sanadine Microphanerite Volcanic Rock Fragment Sedimentary Metamorphic	Altkung:      Altkung to calcite:      Microcline to calcite:
3. Plagioclase (50) 16.6%	Microphanerite Volcanic Rock Fragment Sedimentary Metamorphic	Altkung:      Altkung to calcite:
4. Volcanics		
5. Microphanerites		
6. Accessory Minerals	Zircon	
7. Carbonate Cement (48) 16.1%	<del>     </del> Dirty carbonate cement	
8. Matrix/Pseudomatrix (43) 14.3%	<del>     </del> Clay-Altered Grains	Biotite pseudo:
9. Clay Cement (7) 2.3%	Kaolinite:	
10. Intragranular Porosity (2) .6%	Quartz K-Feldspar   Plagioclase	VRF: Q      PRF: Q K            K P            P
11. Intergranular Porosity (2) .6%	Fractures    Fracture-induced dissolution Oversize/elongate pores Grain-edge dissolution	Primary Porosity  Other
12. Other (27) 9%	pyrite/organics:      R.F.:	Shale:   Chert:         Phosphate:

COMMENTS:  
Lots of matrix, dissolution of grains, carbonate cement. Calcite → dolomite.

PARAGENESIS:

Biotite → chlorite → carbonate?

SECONDARY INTERGRANULAR POROSITY

FRACTURE-INDUCED DISSOLUTION

Q	vrfQ	prfQ
K	vrfK	prfK
P	vrfP	prfP

GRAIN-EDGE DISSOLUTION

Q	vrfQ	prfQ
K	vrfK	prfK
P	vrfP	prfP

OVERSIZE/ELONGATE PORES

Q	vrfQ	prfQ
K	vrfK	prfK
P	vrfP	prfP

OTHER

(32) 10.6%

SANDSTONE PETROGRAPHY DATA

EXAMINED BY: RL

THIN SECTION: Ruhl-1  
 FORMATION (AGE): Vedder Oligocene  
 LOCATION: Rio Bravo  
 DEPTH: 11,574-T3  
 SORTING: Poor  
 SIZE: Fine Sand

PROJECT: Thesis  
 ROCK NAME: Arkosic Arenite  
 POINT COUNTS: 300  
 COMPACTION: N/A  
 ANGULARITY: Sub angular

	SIZE	COMMENTS
1. Quartz <u>82</u>	Monocrystalline Polycrystalline <u>    </u> Microphanerite Volcanic Rock Fragment Quartz Arenite Other Sedimentary Metaquartzite <u>  </u> Other Metamorphic	
2. K-Feldspar <u>28</u>	Microcline Orthoclase Sanadine Microphanerite <u> </u> Volcanic Rock Fragment Sedimentary Metamorphic	
3. Plagioclase <u>32</u>	Microphanerite <u>  </u> Volcanic Rock Fragment <u> </u> Sedimentary Metamorphic	<u>Skeletal remains of plag 1</u>
4. Volcanics <u>5</u>	<u>    </u>	
5. Microphanerites		
6. Accessory Minerals <u>5</u>	<u>Muscovite   </u> <u>Zircon  </u> <u>Glauconite  </u>	<u>Hornblende</u> <u>Biotite  </u>
7. Carbonate Cement <u>33</u>	<u>     </u>	
8. Matrix/Pseudomatrix <u>29</u>	<u>     </u>	
9. Clay Cement <u>3</u>	<u>   </u>	
10. Intragranular Porosity	Quartz K-Feldspar Plagioclase	VRF: Q K P PRF: Q K P
11. Intergranular Porosity	Fractures <u>    </u> Fracture-induced dissolution <u> </u> Oversize/elongate pores <u>    </u> Grain-edge dissolution	Primary Porosity Other <u> </u>
12. Other <u>19</u>	<u>organics / quartz</u> <u>1 c.R.F.    </u>	<u>fossil-1</u> <u>chert-1</u>

COMMENTS:  
 Carbonate replacing some grains.  
 Poikiloblastic cement throughout. Some dolomite  
 rhombs throughout & in shale clasts  
 Feldspar grains are highly altered

PARAGENESIS:

75, 27

SECONDARY INTERGRANULAR POROSITY

FRACTURE-INDUCED DISSOLUTION		
Q	vrfQ	prfQ
K	vrfK	prfK
P	vrfP	prfP
GRAIN-EDGE DISSOLUTION		
Q	vrfQ	prfQ
K	vrfK	prfK
P	vrfP	prfP
OVERSIZE/ELONGATE PORES		
Q	vrfQ	prfQ
K	vrfK	prfK
P	vrfP	prfP
OTHER		
<u>35</u>		

**SANDSTONE PETROGRAPHY DATA**

EXAMINED BY: S Unruh

THIN SECTION: Weber (stained)  
 FORMATION (AGE): Oligocene  
 LOCATION: Rio Bravo  
 DEPTH: 11,425-4

PROJECT: Thesis  
 ROCK NAME: Arkosic Wacke  
 POINT COUNTS: 300

SORTING: Partly Sorted

COMPACTION: N/A

SIZE: Fine sand with some larger medium sand grains

ANGULARITY: Angular to Subangular

	SIZE	COMMENTS
1. Quartz <u>95</u>	Monocrystalline <u>69</u> Polycrystalline <u>111</u> Microphanerite Volcanic Rock Fragment Quartz Arenite Other Sedimentary Metaquartzite Other Metamorphic <u>11</u>	<u>Quartz to clay III IIII</u>
2. K-Feldspar <u>26</u>	Microcline Orthoclase Sanadine Microphanerite Volcanic Rock Fragment Sedimentary Metamorphic	<u>K-spar to clay IIII</u>
3. Plagioclase <u>59</u>	Microphanerite Volcanic Rock Fragment Sedimentary Metamorphic	<u>Altered to sericite I</u> <u>Altered to clay III IIII</u> <u>mymakite I</u>
17% 4. Volcanics <u>III</u> <u>(3)</u>		
5. Microphanerites		
6. Accessory Minerals <u>1.3% (4)</u>	<u>muscovite III</u> <u>zircon I</u>	
7. Carbonate Cement		
31% 8. Pseudomatrix <u>93</u> <u>IIII</u> <u>(93)</u> Clay-Altered Grains	<u>Matrix: 87</u>	<u>Biotite to clay I</u> <u>Muscovite to clay I</u>
9. Clay Cement		
33% 10. Intragranular Porosity <u>(1)</u>	Quartz K-Feldspar Plagioclase <u>I</u>	VRF: Q K P PRF: Q K P
2.3% 11. Intergranular Porosity <u>(7)</u>	Fractures Fracture-induced dissolution Oversize/elongate pores Grain-edge dissolution <u>III II</u>	Primary Porosity Other
8.3% 12. Other <u>(25)</u>	<u>pyrite / organics III III III III III</u> <u>chert I</u>	

COMMENTS:  
 Lots of clay virtually no porosity, primary or secondary. all shows w/ in sample. Tight compaction. Small amounts of K-spar grains exist. clay taking over all sample. Coarse grains are mixed w/ fine sand grains

PARAGENESIS:  
 The quartz is not forming a framework which implies that the clays were introduced at the same time as the quartz possibly.

**SECONDARY INTERGRANULAR POROSITY**

FRACTURE-INDUCED DISSOLUTION		
Q	vrfQ	prfQ
K	vrfK	prfK
P	vrfP	prfP
GRAIN-EDGE DISSOLUTION		
Q IIII	vrfQ	prfQ
K	vrfK	prfK
P I	vrfP	prfP
OVERSIZE/ELONGATE PORES		
Q	vrfQ	prfQ
K	vrfK	prfK
P	vrfP	prfP
OTHER		

1.3% (4)

SANDSTONE PETROGRAPHY DATA

EXAMINED BY: SLC

THIN SECTION: Weber  
 FORMATION (AGE): Vedder  
 LOCATION: Rio Bravo  
 DEPTH: 11,444-2

PROJECT: Thesis  
 ROCK NAME: Arkosic Arenite  
 POINT COUNTS: 300

SORTING: poor  
 SIZE: Fine sand

COMPACTION: N/A  
 ANGULARITY: subangular-subround

	SIZE	COMMENTS
1. Quartz <u>73</u>	Monocrystalline Polycrystalline      Microphanerite Volcanic Rock Fragment Quartz Arenite Other Sedimentary Metaquartzite Other Metamorphic	Polycrystalline → clay   Altered to clay
2. K-Feldspar <u>40</u>	Microcline Orthoclase Sanadine Microphanerite Volcanic Rock Fragment Sedimentary Metamorphic	Altered to clay
3. Plagioclase <u>48</u>	Microphanerite    Volcanic Rock Fragment Sedimentary Metamorphic	Altered to clay
4. Volcanics <u>29</u>		Altered to clay
5. Microphanerites		
6. Accessory Minerals <u>2</u>	<u>Biotite  </u> <u>Epidote</u> <u>Muscovite  </u>	
7. Carbonate Cement		
8. Matrix/Pseudomatrix <u>41</u> <u>  </u> <u>   </u> Clay-Altered Grains		Pseudo Biotite:
9. Clay Cement		
10. Intragranular Porosity <u>2</u>	Quartz   K-Feldspar Plagioclase	VRF: Q K P PRF: Q K P
11. Intergranular Porosity <u>30</u>	Fractures       Fracture-induced dissolution Oversize/elongate pores Grain-edge dissolution	Primary Porosity Other
12. Other	<u>with Inorganics:   </u> <u>RF:   </u>	fossil:

**COMMENTS:** Lots of clay & dissolved feldspar grains. Residual oil left over. Volcanics present. Lots of fractures throughout (possibly from thin section making)? Small amounts of kaolinite. Clay coats over grains which indicates not authigenic clay?  
**PARAGENESIS:**  
 Lots of crush & slipped or rotated grains. Lots of altered biotite & wavy clay laminations. Detrital clay throughout looks like dis-aggregated clay clasts & biotite. Clay has high birefringence.

**SECONDARY INTERGRANULAR POROSITY**

FRACTURE-INDUCED DISSOLUTION		
Q	vrfQ	prfQ
K	vrfK	prfK
P	vrfP	prfP
GRAIN-EDGE DISSOLUTION		
Q	vrfQ	prfQ
K	vrfK	prfK
P	vrfP	prfP
OVERSIZE/ELONGATE PORES		
Q	vrfQ	prfQ
K	vrfK	prfK
P	vrfP	prfP
OTHER		

18

SANDSTONE PETROGRAPHY DATA

EXAMINED BY: SZL

THIN SECTION: Weber  
FORMATION (AGE): Vedder  
LOCATION: Rio Bravo  
DEPTH: 11,445-1

PROJECT: Thesis  
ROCK NAME: Arkosic Arenite  
POINT COUNTS: 300

SORTING: Poor

COMPACTION: N/A

SIZE: Very fine to fine sand

ANGULARITY: Angular to subangular

	SIZE	COMMENTS
1. Quartz (73) 24%	Monocrystalline Polycrystalline Microphanerite   Volcanic Rock Fragment   Quartz Arenite Other Sedimentary Metaquartzite Other Metamorphic	Altered to clay:
2. K-Feldspar (43) 14%	Microcline Orthoclase Sanadine Microphanerite Volcanic Rock Fragment Sedimentary Metamorphic	ortho alter to clay:       ortho to calcite:
3. Plagioclase (53) 17.6%	Microphanerite Volcanic Rock Fragment Sedimentary Metamorphic	Altering to clay:       Plag → Calcite:
4. Volcanics (8) 2.6%		Volcanic → clay:
5. Microphanerites		
6. Accessory Minerals (1) .3%	Muscovite   _____ _____	
7. Carbonate Cement (5) 1.6%	Dolomite Rhombo:       Calcite:	Carbonate clay/matrix? :
8. Matrix/ Pseudomatrix (36) 12.6%	Volcanic pseudo:   	Biotite pseudo:       ortho → clay:       plag → clay:       Muscovite:
9. Clay-Altered Grains Cement 15.3%	Clay → (46)? Not sure where to put b/c its a CaCO <sub>3</sub> clay cement.	
10. Intragranular Porosity	Quartz K-Feldspar Plagioclase	VRF: Q K P PRF: Q K P
11. Intergranular Porosity (9) 3%	Fractures       Fracture-induced dissolution Oversize/elongate pores Grain-edge dissolution	Primary Porosity Other
12. Other (9) 3%	Dark organics       RE:	Chert:

COMMENTS:

Some patches of calcite throughout. Lots of matrix possibly detrital & authigenic. Grains are very dissolved. Very dirty sample. Uneven distribution of  $\phi$ . Lots of clay matrix. Even quartz grains are altered. Some dolomite Rhombs.

PARAGENESIS:

Dissolution → calcite → dolomite

Grains are crushed & rotated quite a bit throughout sample.

SECONDARY INTERGRANULAR POROSITY

FRACTURE-INDUCED DISSOLUTION		
Q	vrfQ	prfQ
K	vrfK	prfK
P	vrfP	prfP
GRAIN-EDGE DISSOLUTION		
Q	vrfQ	prfQ
K	vrfK	prfK
P	vrfP	prfP
OVERSIZE/ELONGATE PORES		
Q	vrfQ	prfQ
K	vrfK	prfK
P	vrfP	prfP

OTHER  
(15)  
5%

SANDSTONE PETROGRAPHY DATA

EXAMINED BY: S. Unruh

THIN SECTION: Weber 11,445-7 (stained)  
 FORMATION (AGE): Vedder, Oligocene  
 LOCATION: Rio Bravo  
 DEPTH: 11,445-7

PROJECT: Thesis

ROCK NAME: Arkosic Arenite  
 POINT COUNTS: 300

SORTING: Moderate to poor

COMPACTION: CI: 4.1 TPI: 1.8

SIZE: Medium to coarse sand

ANGULARITY: Angular to subangular

	SIZE	COMMENTS
1. Quartz (75)	Monocrystalline Polycrystalline     Microphanerite Volcanic Rock Fragment Quartz Arenite Other Sedimentary Metaquartzite Other Metamorphic .7 x .6 mm	Altered to illite:     Quartz healed fractures: 1 Quartz Altered to clay: 1
2. K-Feldspar (36) 11.5%	Microcline Orthoclase Sanadine Microphanerite Volcanic Rock Fragment Sedimentary Metamorphic 1 mm x .4 mm	Altered to illite?    Altered to kaolinite:
3. Plagioclase (80)	Microphanerite Volcanic Rock Fragment Sedimentary Metamorphic .8 x .5 mm	Altered to kaolinite:       Altered to illite:       Altered to sericite:       Albite: 1
4. Volcanics .32% (1)	1	
5. Microphanerites		
6. Accessory Minerals .29% (9)	Biotite:     Muscovite:	phosphate:
7. Carbonate Cement		
8. Pseudomatrix .22% (7)	 Clay-Altered Grains	
9. Clay matrix cement 10.9% (34)	Illite:       Kaolinite:       sericite: 1	Biotite Altered to clay:       Muscovite Altered to clay: 1
10. Intragranular Porosity 3.2% (10)	Quartz K-Feldspar       Plagioclase	VRF: Q K P PRF: Q K P
11. Intergranular Porosity 4.2% (13)	Fractures    Fracture-induced dissolution Oversize/elongate pores     Grain-edge dissolution	Primary Porosity       Dissolution of clay:       Other Shrinkage:
12. Other 6.4% (26)	pyrite/hydrocarbons:       shale: P	

COMMENTS:

Lots of clay. clay preserved grains from compaction. Areas w/ no or little clay have higher compaction + pseudomatrix. Plag. grains show healing of fractures w/ albite. Lots of secondary porosity. Clay matrix is CaCO<sub>3</sub>. Very bright

PARAGENESIS:

clay → grain shrinking → fracturing → dissolution → secondary φ → migration of oil

SECONDARY INTERGRANULAR POROSITY

FRACTURE-INDUCED DISSOLUTION		
Q	vrfQ	prfQ
K	vrfK	prfK
P	vrfP	prfP
GRAIN-EDGE DISSOLUTION		
Q	vrfQ	prfQ
K	vrfK	prfK
P	vrfP	prfP
OVERSIZE/ELONGATE PORES		
Q	vrfQ	prfQ
K	vrfK	prfK
P	vrfP	prfP
OTHER		

7.0% (22)

33 point counts

SANDSTONE PETROGRAPHY DATA

EXAMINED BY: SZL

THIN SECTION: Weber  
 FORMATION (AGE): Uedder  
 LOCATION: Rio Bravo  
 DEPTH: 11,446-6

PROJECT: Thesis  
 ROCK NAME: Arkosic Arenite  
 POINT COUNTS: 300

SORTING: Moderate

COMPACTION: N/A

SIZE: Medium to fine sand

ANGULARITY: Subrounded

	SIZE	COMMENTS
1. Quartz (96) 32%	Monocrystalline Polycrystalline Microphanerite Volcanic Rock Fragment Quartz Arenite Other Sedimentary Metaquartzite Other Metamorphic	Poly → calcite:    Qtz → calcite:
2. K-Feldspar (39) 13%	Microcline Orthoclase Sanadine Microphanerite Volcanic Rock Fragment Sedimentary Metamorphic	ortho → sericite:   Altered → calcite:
3. Plagioclase (17) 5.6%	Microphanerite Volcanic Rock Fragment Sedimentary Metamorphic	Plag → calcite:
4. Volcanics (30) 10%		Altered:   Volcanic → calcite:
5. Microphanerites		
6. Accessory Minerals		
7. Carbonate Cement (89) 29.6%	Calcite:	
8. Matrix/Pseudomatrix (4) 1.3%		
9. Clay Cement		
10. Intragranular Porosity	Quartz K-Feldspar Plagioclase	VRF: Q K P PRF: Q K P
11. Intergranular Porosity	Fractures Fracture-induced dissolution Oversize/elongate pores Grain-edge dissolution	Primary Porosity Other
12. Other (24) 8%	Quartz/organics RF	chert:      Phosphate:

COMMENTS:  
 Coarser grained than previous sample. All calcite cement throughout. Better sorting of grains than previous.

Possible quartz cement @ 16.5, 78  
 Toxikilopic cement throughout  
 small amounts of matrix left behind

PARAGENESIS:

Dissolution → calcite  
 Floating grains w/ calcite surrounding showing  
 dissolution → calcite @ 23, 76

SECONDARY INTERGRANULAR POROSITY

FRACTURE-INDUCED DISSOLUTION		
Q	vrfQ	prfQ
K	vrfK	prfK
P	vrfP	prfP
GRAIN-EDGE DISSOLUTION		
Q	vrfQ	prfQ
K	vrfK	prfK
P	vrfP	prfP
OVERSIZE/ELONGATE PORES		
Q	vrfQ	prfQ
K	vrfK	prfK
P	vrfP	prfP
OTHER		
(1)	3%	

Toxikilopic ←

Good for CL for overgrowths?